

# **GEOLOGY FOR SOCIETY**

SINCE 1858



**GEOLOGICAL  
SURVEY OF  
NORWAY**

· NGU ·



**Nordland**  
FYLKESKOMMUNE



GEOLOGICAL  
SURVEY OF  
NORWAY  
- NGU -



<b>Report no.:</b> 2018.011		<b>ISSN: 0800-3416 (print)</b> <b>ISSN: 2387-3515 (online)</b>	<b>Grading:</b> Open
<b>Title:</b> Geophysical and geological investigations of graphite occurrences in Vesterålen and Lofoten, Northern Norway 2017			
<b>Authors:</b> J.S. Rønning, H. Gautneb, B.E. Larsen, J. Knežević, V.C. Baranwal, H. Elvebakk, J. Gellein, F. Ofstad & M. Brønner.		<b>Client:</b> Nordland fylkeskommune / NGU	
<b>County:</b> Nordland		<b>Commune:</b> Hadsel, Bø, Sortland and Øksnes	
<b>Map-sheet name (M=1:250,000)</b> Svolvær		<b>Map-sheet no. and -name (M=1:50,000)</b> 1131 I Austvågøya 1132 I Nykvåg, 1132 II Stokmarknes 1232 III Sortland, 1232 IV Myre	
<b>Deposit name and grid-reference: WGS 84 UTM 33</b> Several, see report text for details.		<b>Number of pages:</b> 180	<b>Price (NOK):</b> NOK 500,- <b>Map enclosures:</b>
<b>Fieldwork carried out:</b> June and August 2017	<b>Date of report:</b> 30.04.2018	<b>Project no.:</b> 371100	<b>Person responsible:</b> <i>Marco Brønner</i>
<b>Summary:</b> <p>As a part of the MINN project (Minerals in Northern Norway), a helicopter-borne geophysical survey was performed in Lofoten and Vesterålen in 2013. Electromagnetic data from this survey showed up anomalies that may be caused by large graphite mineralisation. With financial support from Nordland County, NGU has performed geophysical and geological follow-up work to 1) confirm the existence of graphite and 2) Briefly evaluate the quantity and quality of graphite structures.</p> <p>The project started in 2015 and the results from the first two years are reported by Gautneb et al. (2017) and Rønning et al. (2017). Follow-up work performed in 2017 is reported in this report. 15 locations have been investigated in total in 2017. The degree of detail in these studies varies from just a few lines of simple electromagnetic measurements (EM31) to electric measurements such as Self Potential (SP), Charged Potential (CP) and Electric Resistivity Traversing (ERT) in combination with Induced Polarisation (IP). In two areas, Sommarland and Haugsnes in Bø municipality, two short core drilling bore holes were made. The selection of follow-up objects was based on both magnetic and electromagnetic data from helicopter-borne measurements.</p> <p>All results from the 2017 work are reported here. Where possible, the volume of graphite is estimated based on the total strike length, the width of individual zones (from drilling, observations and width of EM31 measurements) and an assumed depth extent of 100 m. In these areas, an estimation of graphite tonnage is also given.</p>			
<b>Keywords:</b> Graphite	Geology	Geophysics	
Electromagnetic	Electrical	Magnetic	
Mapping	Analytical methods	Scientific report	

## ***Executive summary***

### **Aim:**

To increase the knowledge of known and unknown graphite occurrences in the Vesterålen and Lofoten areas and to make these occurrences interesting for prospecting companies. This report is regarded as a follow up of the recommendations given in 2017 (Gautneb et al. 2017 & and Rønning et al. 2017).

### **Methods:**

- Ground geophysical follow-up methods (EM31/Magnetic, CP/SP electric and ERT/IP electric), of the mineralised areas.
- Representative sampling of outcropping graphite bearing rocks.
- Shallow core drilling, sampling and analyses. Petrographical characterisation of the graphite bearing rock units.

### **Areas/localities investigated:**

1. Sommarland/Kråkberget and adjacent areas
2. Haugsnes
3. Husvågen - Rise
4. Møkland, (southern part)
5. Smines
6. Myre & Raudhammaren
7. Brenna
8. Vikeid
9. Morfjord and adjacent localities
10. In addition, some other minor areas and localities.

### **Results:**

#### **Sommarland/Kråkberget:**

Several graphite bodies are identified, individual mineralised zones are up to ca. 300 metres in length (in total ca. 1000 m). Total carbon (TC) analysis of various sub-localities indicate a graphite content that varies between 7.7 and 18 %. Two shallow drill-holes show ca. 4 m thick graphite with an average TC of 7.4 % and 8.5 %.

#### **Haugsnæs**

At least 11 steeply dipping and sub-parallel mineralised zones are identified over a length of ca. 2.5 km and over a width of ca. 100 m. Surface samples show an average TC of 19.3 %. Two shallow drill holes show individual relatively thin graphite lenses (1 – 2 m) with an average TC of < 5 %.

#### **Møkland** (southern part)

A mineralised area was described earlier in 2017. In the southern part of Møkland, possible graphite zones can be identified for at least a length of 1.5 km towards the south west. There are no surface exposures.

### **Smines**

A mineralised area was traced over 2 km in strike length. Very few exposures were located. Single samples have a TC (Total Carbon) up to 17.3 % with an average of 8.3 % TC.

### **Myre and Raudhammaren area.**

Several highly conductive areas (<10  $\Omega$ m) are identified with helicopter-borne electromagnetic measurements. These are covered by a layer of up to ca. 10 m thick peat/moraine. Raudhammaren shows indications of 4 sub-parallel mineralised zones. Available samples (loose boulders) show a TC content of up to 25.9 % with an average of 14.2%.

### **Brenna (Previously called Frøskeland)**

A mineralised area of 250 m strike length is indicated, which probably comprises of several zones. Graphite is exposed and samples show an average TC content of 11.4 % and a maximum value of 30.4 %.

### **Vikeid**

Three resistivity profiles and helicopter-borne EM indicate mineralised zones over a 2 km strike length. Several highly conductive areas are identified with resistivity < 3  $\Omega$ m. This area has previously been investigated in the 1990's and shows an average TC of ca. 14 %.

### **Morfjord**

The abandoned mine at Morfjord is part of a mineralised area that is comprised of four sub-parallel highly conductive zones. The mineralised area is probably continuous under the sea to Sommarhus, one km to the north and to Sellåter 1.5 km to the north east. Average TC contents are: Morfjord 18.4 %, Sellåter 6.3 % and Sommarhus 24.1 %.

### **Recommendations**

The nature of the highly conductive areas in the Myre area should be positively identified using core drilling.

The dimensions of the mineralised area at Smines should be investigated using CP/SP methods.

Additional profiling using resistivity and/or EM31 and possibly core drilling should be done at Rise, Husvågen, Møkland, Romsetfjord and in the Morfjord area.

## **Sammendrag på norsk.**

Som en del av prosjektet *Mineralressurser i Nord-Norge* (MINN) ble det i 2013 foretatt geofysiske målinger fra helikopter over hele Langøya og deler av Austvågøya i Vesterålen/Lofoten. Disse målingene viste flere markerte elektromagnetiske anomalier, delvis knyttet til kjente grafittforekomster og delvis på mulige nye hittil ukjente forekomster. For å øke kunnskapen om de enkelte mineraliseringene foreslo NGU i 2016 et oppfølgingsprosjekt der en ser nærmere på størrelse og kvalitet av de forskjellige forekomstene. Prosjektet har fått støtte fra Nordland fylkeskommune både i 2015, 2016 og 2017. Undersøkelser gjennomført i 2015 og 2016 ble rapportert vinteren 2017 (Rønning et al. 2017, Gautneb et al. 2017). Undersøkelsene utført i 2017 rapporteres i denne rapport. Nordland fylkeskommune støtter undersøkelsene også i 2018 som da blir det siste året med undersøkelser i NGU-regi.

For å gjøre dataene tilgjengelig for internasjonale selskaper er alle rapportene skrevet på engelsk og på et faglig nivå som krever kompetanse innenfor geologi og geofysikk. Bruksområder og marked for grafitt er ikke omtalt.

I 2017 ble det foretatt undersøkelser på følgende lokaliteter:

1. Sommarland/Kråkberg og omliggende områder, Bø kommune
2. Haugsnes, Bø kommune
3. Husvågen and Rise, Bø kommune
4. Møkland, (sydlige del), Bø kommune
5. Smines, Øksnes kommune
6. Myre & Raudhammaren, Øksnes kommune
7. Brenna (kalt Frøskeland I tidligere rapporter), Sortland kommune
8. Vikeid, Sortland kommune
9. Morfjord og omkringliggende områder (Sommarhus og Sellåter), Hadsel kommune
10. I tillegg noen mindre områder og lokaliteter.

## **Hovedresultater:**

### **Sommarland/Kråkberget:**

Flere kropper av grafitt er indentifisert med en samlet lengde på ca. 1000 m. Analyse av Total carbon (TC) indikerer et grafittinnhold som varierer fra 7,7 til 18 %. To borehull med lengde 49 og 35 m har skjæring med grafittskifer på opptil 4 meter med gjennomsnittlig TC på fra 7,4 til 8,5 %.

### **Haugsnnes**

Minst 11 tynne, tilnærmet parallelle og steiltstående grafittførende soner er lokalisert over en lengde på 2,5 km. Total bredde på mineralisert område er ca. 100 m. Overflateprøver har en gjennomsnittlig TC på 19,3 %. To korte borehull skjærer flere

tynne grafittskifre med 1-2 meters mektighet og gjennomsnittlig grafittinnhold på mindre enn 5%.

### **Møkland** (sydlige del)

De grafittførende sone som ble beskrevet i 2017 fortsetter minst 1,5 km mot sydvest. Dette området har ingen blotninger av grafittførende bergart.

### **Smines**

Et mineralisert området på ca. 2 km lengde er identifisert, det er svært få blotninger av grafittskifer, enkelt analyser kan ha opp til 17,3 % grafitt.

### **Myre/Raudhammaren area.**

Flere området med elektrisk godt ledende materiale er identifisert. De fleste er imidlertid overdekket med opp mot ca. 10 meter med myr/morene. Raudhammaren har sannsynligvis 4 parallelle soner med grafitt, men ingen er synlig i fastfjell. Tilgjengelige analyser har et gjennomsnittlig grafittinnhold på 14,2 %.

### **Brenna (tidligere omtalt som Frøskeland)**

Et mineralisert området på 250 m lengde er lokalisert. Dette består sannsynligvis av flere individuelle grafittførende soner. Tilgjengelige prøver har et gjennomsnittlig grafittinnhold på 11,4 %.

### **Vikeid**

Flere profiler med resistivitet og EM indikerer en mineralisert sone på mer enn 2 km lengde, innenfor denne er det lokalisert individuelle soner med god elektrisk ledningsevne som indikerer grafitt. Området er svært overdekket. Prøvetaking på 1990 tallet ga et gjennomsnittlig grafittinnhold på ca. 14 %.

### **Morfjord**

Den nedlagte grafittgruva I Morfjord er del av et mineralisert området med 4 sub-parallele soner med høy ledningsevne. Det er sannsynlig at disse sonene fortsetter under sjøen mot nord til Sommarhus og mot nordøst til Sellåter. Gjennomsnittlig TC gehalt er: Morfjord 18,4 %, Sellåter 6,3 % og Sommarhus 24,1 %.

### **Anbefalinger.**

Hva som er årsaken til det store området med høy elektrisk ledningsevne øst for Myre må klarlegges ved hjelp av boring. Kvaliteten av grafitten i andre områder bør også evalueres der dette er mulig.

Størrelse og form av påvist grafittmineralisering ved Smines må kartlegges ved CP/SP målinger.

Utfyllende profilering med resistivitet og EM31 og om mulig kjerneboring bør gjøres ved: Rise, Husvågen, Møkland, Romsetfjord og i Morfjordområdet.

## Contents

1. INTRODUCTION.....	11
1.1 Physiography and landownership.....	12
2. GEOLOGICAL SETTING .....	13
3. HISTORICAL BACKGROUND AND PREVIOUS INVESTIGATIONS .....	15
4. GEOPHYSICAL AND GEOLOGICAL METHODS.....	16
4.1 Geophysical methods.....	16
4.1.1 Helicopter-borne electromagnetic measurements.....	16
4.1.2 Ground EM and magnetic methods (Modified EM31) .....	18
4.1.3 Charged Potential and Self Potential methods .....	19
4.1.4 2D resistivity and Induced Polarisation (IP) .....	21
4.2 Geological methods.....	23
4.2.1 Core drilling, sampling and analyses .....	23
4.2.2 Analytical methods.....	24
5. SELECTION OF FOLLOW-UP OCCURRENCES.....	25
5.1 Petrophysical properties of graphite .....	25
5.2 Data from helicopter-borne measurements at Langøya, Vesterålen .....	26
5.3 Data from helicopter-borne measurements at Austvågøya, Lofoten .....	32
5.4 Selected areas for follow-up work .....	35
6. RESULTS OF FOLLOW-UP WORK AT SOMMARLAND, BØ MUNICIPALITY	36
6.1 Geophysics Central Sommarland.....	36
6.1.1 Geophysical measurements performed in 2017.....	36
6.1.2 Example of an integrated interpretation of geophysical methods.....	40
6.2 Geological observations, sampling and analyses .....	42
6.3 Core drilling Central Sommarland.....	43
6.3.1 Geological core logging .....	43
6.3.2 Mineralogy from thin sections .....	48
6.3.3 Quality of the graphite at Sommarland.....	51
6.4 Geophysics Kråkberget, Sommarland East and Sommarland South .....	53
6.5 Sommarland summary .....	57
7. RESULTS OF FOLLOW-UP WORK AT HAUGSNES, BØ MUNICIPALITY.....	59
7.1 Geophysics Haugsnes.....	59
7.2 Core drilling at Haugsnes .....	64
7.2.1 Geological core logging .....	65
7.2.2 Mineralogy from thin sections .....	68
7.2.3 Quality of graphite at Haugsnes.....	70
7.3 Haugsnes summary.....	71

8. RESULTS OF THE FOLLOW-UP WORK IN OTHER AREAS, BØ MUNICIPALITY .....	74
8.1 Husvågen – Rise .....	74
8.2 Møkland south .....	76
9. RESULTS FROM THE FOLLOW-UP WORK AT ØKSNES MUNICIPALITY ....	78
9.1 Follow-up work at Smines .....	78
9.1.1 Geophysical measurements.....	78
9.1.2 Geological update on outcrops and analysis .....	80
9.2 Geophysics at Myre east .....	81
9.3 Geophysics and sampling at Raudhammaren.....	84
10. RESULTS OF FOLLOW-UP WORK, SORTLAND MUNICIPALITY .....	87
10.1 Geophysics and geology at Romsetfjord.....	87
10.2 Geophysics and geology at Vikeid .....	89
10.3 Geophysics and geology at Brenna .....	95
11. RESULTS OF THE FOLLOW-UP WORK IN HADSEL MUNICIPALITY .....	100
11.1 Morfjord south (abandoned old mine) .....	100
11.2 Geophysics and geology at Sommarhus and Sellåter.....	103
12. ADDITIONAL OBSERVATIONS AND DATA .....	105
12.1 Petrography of the graphite schist and associated rocks .....	105
12.1.1 Examples of thin sections .....	105
12.1.2 Particle analysis of graphite crystals .....	109
12.2 Petrophysical data from the drill cores .....	111
13. SUMMARY AND CONCLUSIONS.....	117
13.1 Summary of geometric information .....	117
13.2 Summary of tonnage estimates.....	118
13.3 Summary of carbon analysis, updated table .....	118
14. REFERENCES .....	121

## **APPENDIX**

Appendix 1: List of thin sections from drill cores.....	123
Appendix 2: TS and TC analysis of drill cores.....	124
Appendix 3: Pictures of drill cores.....	127
Appendix 4: Portable XRF analysis of drill cores.....	145
Appendix 5: Complete list of analysed samples for TS, TC and TOC.....	159
Appendix 6: Samples analysed for total carbon, total sulphur and petrophysics....	172
Appendix 7: Petrophysics of drill core samples.....	178



## 1. INTRODUCTION

Norway has been a major producer of graphite for more than 100 years and in many places in the country the geology favours the formation of flake graphite deposits. Graphite is a common mineral in Norwegian rocks, however it is rare to find it enriched in economically interesting amounts. There are more than 70 registered graphite occurrences in Norway. They are located at four graphite provinces (Figure 1.1). In all these provinces there has been historic graphite mining. Today only one deposit, the Skaland graphite mine on the island of Senja, is in operation, producing ca. 10,000 tons of concentrate per year. The Lofoten-Vesterålen area and island of Senja has a number of other graphite occurrences.

In this report we will present the data and results from recent graphite exploration in ten potentially important graphite occurrences in Vesterålen and Lofoten. We will also give a brief review of the earlier work carried out in the area. In every chapter we will limit our descriptions to what is regarded relevant for the graphite mineralisation. More academic studies of the general geology and metamorphic petrology are reported by others elsewhere (Engvik et al. 2016, Griffin et al. 1978).

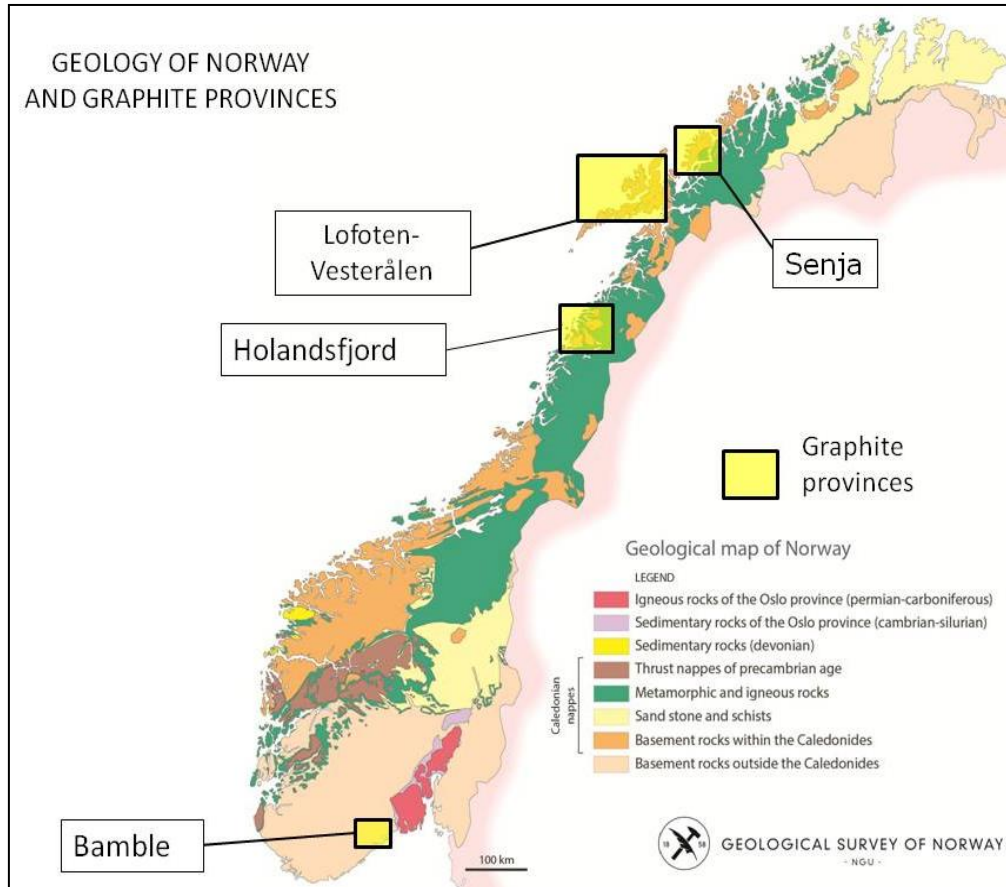


Figure 1.1: Geology and graphite provinces of Norway.

The investigations, which were planned for three years, are financially supported by Nordland County Administration. In this second year, the investigations were concentrated at (easting and northing, WGS84 UTM Zone 33 N):

- Morfjord, Hadsel Municipality, 487000 - 7587000
- Sommarhus, Hadsel municipality, 487000 - 7589000
- Husvågen, Bø Municipality, 480700 - 7622400
- Rise, Bø Municipality, 483200 - 7623000
- Møkland, Bø Municipality, 485900 - 7627000
- Kråkberget, Bø municipality, 488000 - 7627800
- Sommarland, Bø Municipality, 487600 - 7626400
- Sommarland east, Bø Municipality, 488500 - 7624500
- Sommarland south, Bø Municipality, 486500 - 7624600
- Haugsnes in Bø Municipality, 488300 - 7618800
- Smines, Øksnes Municipality, 499000 - 7639000
- Myre, Øksnes Municipality, 506500 - 7643800
- Romsetfjord, Sortland Municipality, 500600 - 7634700
- Vikeid, Sortland Municipality, 511000 - 7628500
- Brenna, Sortland Municipality, 502200 - 7628800

During the work the following people have contributed with their different areas of expertise:

- Vikas C. Baranwal: Interpretation of airborne magnetic and EM data.
- Harald Elvebakk: Ground follow-up geophysics.
- Håvard Gautneb: Graphite geology, core logging, analysis and petrography, responsible field geologist.
- Jomar Gellein: Ground follow-up geophysics.
- Janja Knezevic: Graphite geology, core logging, ground geophysics, sample preparation, petrography, GIS.
- Janusz Koziel: Instrumentation.
- Bjørn Eskil Larsen: Ground follow-up geophysics, processing of data, GIS.
- Frode Ofstad: Airborne and ground follow-up geophysics, electronics.
- Geir Viken: Core drilling.
- Jan Steinar Rønning: Responsible geophysicist, reporting, report editing and project leader.

The authors like to thank Iain Henderson and Marco Brönnner (both NGU) for improving the English language.

## 1.1 Physiography and landownership

The cadastral map of the area can be seen at [www.seiendom.no](http://www.seiendom.no). During normal annual snow conditions all parts of the investigated area can be accessed from the middle of May to the end of October. Snow can be expected at the mountain tops from mid-October. Prospectors interested in this area should check the web sites of the Norwegian Directorate of Mining ([www.dirmin.no](http://www.dirmin.no)) for Norwegian mining regulations and possible rights to the graphite mineralisation.

## 2. GEOLOGICAL SETTING

The Lofoten-Vesterålen area in northern Norway is normally considered to be a part of the Baltic Shield. The graphite-bearing rocks in Vesterålen occur in sequences belonging to a Precambrian domain comprising Lofoten, Vesterålen and the western islands of Troms County (see Figure 2.1).

The general outline of the geology was established in the 1960s and 1970s, following work by Heier (1960) and Griffin et al. (1978, and references therein). In broad terms, the area is composed of an Archaean to possibly Early Proterozoic basement of magmatic and metasedimentary rocks, intruded by an Early Proterozoic magmatic suite composed of anorthosite-mangerite-charnockite-granite (AMCG) rocks. Subsequent radiometric dating has confirmed the presence of Archaean and Early Proterozoic rocks (Corfu 2004 and 2007, Davidsen & Skår 2004). Most of the AMCG suite was intruded into the basement within a relatively narrow time interval from 1800 to 1790 Ma (Corfu 2004).

The supracrustal sequences are distributed as patches intermingled with the Archaean domains, with graphite-bearing rocks occurring with marbles, quartzites, banded iron formations and presumed felsic and mafic volcanic rocks. Polyphase high-grade metamorphism and deformation have obliterated most of the primary supracrustal features, and the sequence is now represented by various schists, gneisses and migmatites (Griffin et al. 1978, and references therein). The metamorphic event(s) reached peak conditions at  $P = 0.8\text{--}0.9$  GPa and  $T = 860\text{--}880$  °C (Engvik et al. 2016). The metasedimentary rocks and associated graphitic schists were thought to be of Early Proterozoic age (Griffin et al. 1978), but results from ongoing studies are less conclusive and hold open the possibility of an Archaean age for this sequence. The mapping resulted in the publication of the 1:250,000 map sheet Svolvær, covering the Lofoten and Vesterålen area (Tveten 1978).

NGU has, subsequent to the studies of W. L. Griffin and co-workers, continued local mapping activities, leading to the publication of the preliminary 1:50,000 map sheet Sortland (Tveten 1990) and the 1:250,000 map sheet Andøy (Tveten and Henningsen, 1998). In 1988 most of the island of Langøya was measured with airborne geophysics (Mogaard et al. 1988).

Some of these activities have been conducted as a part of the exploration for graphite resources in Vesterålen (Gautneb & Tveten 1992, Gautneb 1992, 1993 & 1995). This work was reviewed by Gautneb & Tveten (2000).

Renewed activities in the Vesterålen area started in 2011 under the MINN program at NGU (**M**ineral resources **I**n **N**orthern **N**orway), comprising general bedrock mapping and studies, airborne geophysics (Rodionov et al. 2013 a & b), and targeted mineral exploration. These activities have led to the discovery of several new graphite occurrences.

The units containing the graphite-bearing rocks are thus believed to be intermingled with Archaean rocks. This relationship is, however, not easy to observe in the field. Polyphasal deformation combined with granulite-facies metamorphism locally with anatexis, have obscured most primary contacts. The supracrustal units containing the

graphite schists are also often intruded by younger intrusions. These field relationships are important as they have the consequence that the graphite layers and lenses in Lofoten – Vesterålen, even though airborne geophysical data can indicate a considerable size, are commonly cut by later intrusions and folds into segments with a limited size (areal extent). However, aggregated areas commonly represent economically interesting dimensions and conditions such as metamorphic grade are favourable for high quality graphite formation.

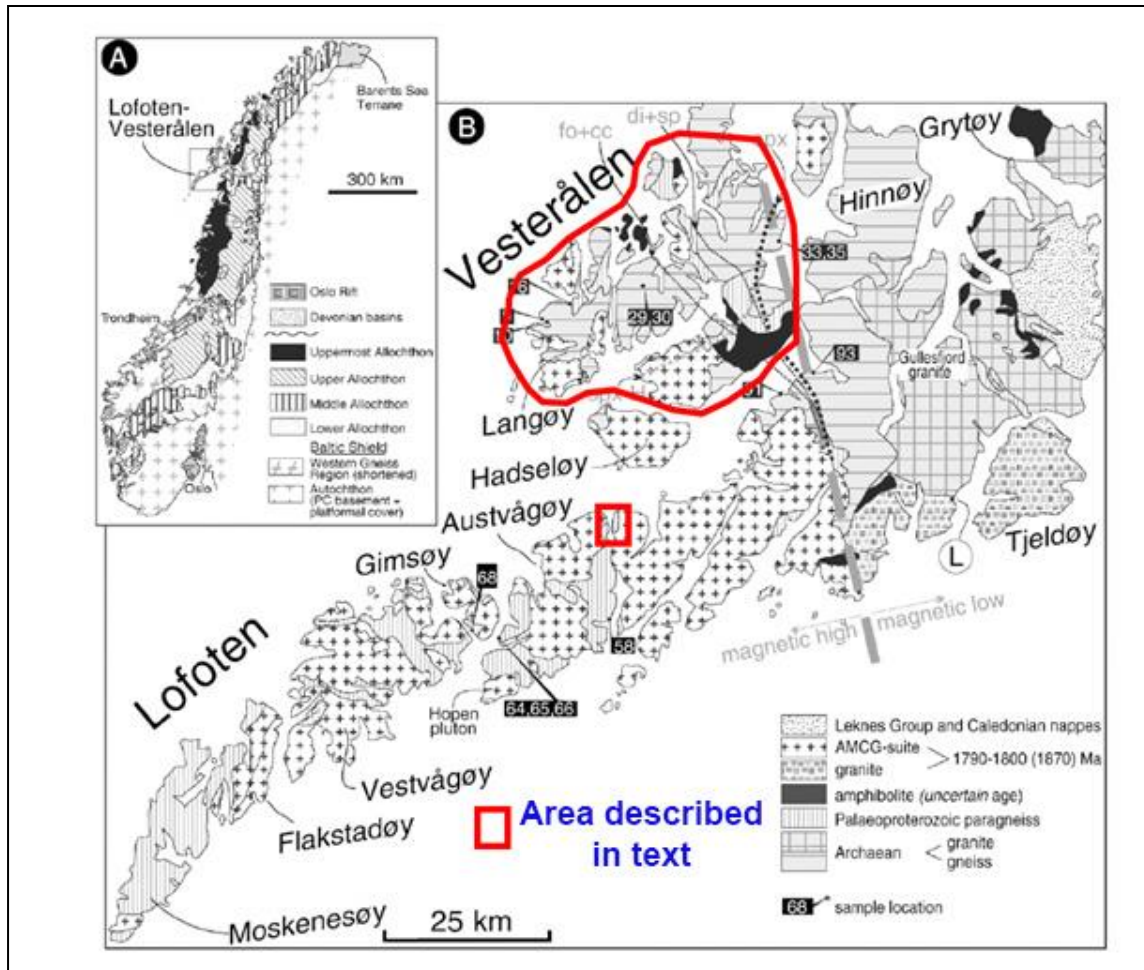


Figure 2.1: Simplified geological map of the Lofoten-Vesterålen islands (modified from Corfu 2007).

### 3. HISTORICAL BACKGROUND AND PREVIOUS INVESTIGATIONS

The graphite deposits of Vesterålen were among the first to be described by geologists in Norway. Keilhau (1844) and Helland (1887) described several graphite deposits in Lofoten and Vesterålen. These occurrences had probably been known for some time. The British company, Anglo-Norwegian Mining, started mining in the Jennestad area around 1890 and the mine was in operation until 1914. During the same period several other occurrences were explored and subjected to test mining. The Møkland, Sommarland and Morfjord occurrences were trenched and put into small-scale test production in this period.

All known graphite occurrences in Northern Norway were investigated in the early 1950s with respect to the co-occurrence of uranium with graphite. The results were negative for most of the uranium occurrences (Neumann 1952).

The Jennestad graphite mine were in operation again from 1949 to 1960. Approximately 700 m of tunnels were mined out during this period. Unpublished reports describe the geology in the mines and their surroundings (Skjeseth 1952, Vokes 1954) and Heier (1960) describes the regional geology.

In the 1970s, W.L. Griffin et al. (1978) investigated the crustal evolution of the Lofoten-Vesterålen rocks. They concluded that the graphite-bearing rocks were part of a supracrustal sequence comprising marbles, acid and basic volcanic rocks, banded iron formations and graphite schist. Polyphasal high grade (up to granulite facies) metamorphism and deformation have obscured most of the characteristics of the primary supracrustals and they are today mapped as various types of gneisses and migmatites (Griffin et al. 1978 and references therein).

Part of Langøya was measured with airborne geophysics in 1988 (Mogaard et al. 1988). Only a part of this survey included electromagnetic measurements. Graphite occurrences in the Jennestad area were reinvestigated with sampling, drilling and ground geophysics in the period 1990 - 1994. At total, 1100 m of drilling was performed on 15 different drill holes. At the Hornvann sub-locality proven reserves of 240,000 tons with a grade of 25 % graphitic carbon were mapped (Gautneb & Tveten 1992, Dalsegg 1994, Gautneb 1993 & 1995, Rønning 1991 & 1993). This work was reviewed by Gautneb & Tveten (2000).

Corfu (2004 & 2007) performed radiometric dating, reviewed earlier work and studied the metamorphic evolution of selected rocks units from the Lofoten-Vesterålen area.

In 2012, the junior mining company *Norwegian graphite* re-investigated the Jennestad area, by mapping and drilling. Their reports are available from NGU (Håvard Gautneb) upon request. The company found indicated reserves of 3.66 Mt with 10 % graphitic carbon. The thickness of the graphite-bearing units is reported to be up to 34 metres. *Norwegian graphite* was liquidated in 2016.

NGU, as part of the MINN program (<http://www.ngu.no/prosjekter/minn>), carried out a new airborne geophysical survey, including electromagnetic measurements over the whole of Langøya and parts of Austvågøya in 2013 (Rodionov et al. 2013a and 2013b). These surveys resulted in a large extension of the area with potential graphite

deposits, with a number of new geophysical anomalies, and is the basis for the investigations in this report. The airborne geophysical survey is reviewed in more detail in Chapter 4.1.1.

Based on the helicopter-borne geophysics, ground based graphite investigations were performed in the area during 2015 and 2016 (Gautneb et al. 2017, Rønning et al. 2017).

## 4. GEOPHYSICAL AND GEOLOGICAL METHODS

The resolution of helicopter-borne electromagnetic measurements is low and detailed ground measurements were necessary to achieve a good knowledge of the graphite deposits. Here we describe the geophysical and geological methods used in the graphite investigations in 2017.

### 4.1 Geophysical methods

In the graphite investigations in Lofoten and Vesterålen, we have used the following geophysical methods: Helicopter-borne electromagnetic (HEM), ground-based electromagnetic EM31 in combination with magnetic measurements, Charged Potential (CP), Self Potential (SP), 2D Resistivity (also called ERT) and 2D Induced Polarisation (IP).

#### 4.1.1 Helicopter-borne electromagnetic measurements

New helicopter-borne geophysical survey was performed in 2013 both at Langøya and at parts of Austvågøya. In total, 5650 line-km data (1050 km<sup>2</sup>) were acquired at Langøya, and 1956 line-km (390 km<sup>2</sup>) at Austvågøya. The full technical description, including details of processing of the data collected was reported by Rodionov et al. (2013a and 2013b). The survey included the instrumentation listed in Table. 4.1

**Table 4.1: Instrumentations used in helicopter-borne geophysical survey.**

Instrument	Producer/Model	Accuracy	Sampling frequency
Magnetometer	Scintrex Cs-2	0,002 nT	5 Hz
Base magnetometer	GEM GSM-19	0.1 nT	0.33 Hz
Electromagnetic	Geotech Hummingbird	1 – 2 ppm	10 Hz
Gamma spectrometer	Radiation Solutions RSX-5	1024 channels, 16 liters down, 4 liters up	1 Hz
Radar altimeter	Bendix/King KRA 405B	± 3 % 0 – 500 feet ± 5 % 500 –2500 feet	1 Hz
Pressure/temperature	Honeywell PPT	± 0,03 % FS	1 Hz
Navigation	Topcon GPS-receiver	± 5 m	1 Hz
Acquisition system	NGU in house software		

The electromagnetic (EM) instrumentation, modified Geotech Hummingbird (Geotech 1997), can map variations in electric conductivity in the ground and is the most useful

method in graphite exploration. Details about frequencies, coil orientations and coil separation are shown in Table 4.2.

**Table 4.2: Configuration and frequencies of the Hummingbird EM recorder.**

Coils:	Frequency	Orientation	Coil separation
A	7000 Hz	Coaxial	6.20 m
B	6600 Hz	Coplanar	6.20 m
C	980 Hz	Coaxial	6.025 m
D	880 Hz	Coplanar	6.025 m
E	34000 Hz	Coplanar	4.87 m



**Figure 4.1: The equipment used in the helicopter-borne geophysical survey in Vesterålen and Lofoten.**

The apparent resistivity for each frequency was calculated based on "In phase" and "Out of phase" components of the EM data, using a half-space model of the earth (Geosoft 1997). Data can also be presented as profile maps, on which "In Phase" and "Out of phase" components for each frequency are plotted along the flight path.

Inverted resistivity sections can be produced based on the measured "In phase" and "Out of phase" components for each frequency. Available software is EM1DFM (Electromagnetic 1D Frequency Measurements, UBC (2000)) and AarhusInv, formerly called em1Dinv, AarhusInv (2013). These inversion codes create 2D images based on 1D inversion and with vertical conducting structures, misleading images may be constructed. For this reason, inversions of EM data from Lofoten and Vesterålen were performed but are not presented here. NGU are considering 2D or 3D inversion of EM data from the area.

The main result from this geophysical survey was a large extension of the area with potential for new graphite mineralisation, and a better definition of the areal extent of known occurrences. This was the basis for defining new graphite targets to be followed up by ground investigations. Most of the occurrences described in this report were previously known, but the total mineralised area is larger than previous known. Several new objects are derived from the interpretation of the new airborne geophysical data.

All the data from the helicopter survey can be downloaded from [www.ngu.no](http://www.ngu.no) as jpg-maps or geo-referenced data sets (geotiff-files).

#### 4.1.2 Ground EM and magnetic methods (Modified EM31)

Electromagnetic measurements from helicopter in the Vesterålen and Lofoten area (Rodionov et al. 2013 a & b) show many anomalies that might be caused by graphite. Some of these coincide with known graphite showings, others do not. The area is largely covered by soil and vegetation, so detailed geophysical measurements were necessary to locate possible new graphite mineralisation. In the first attempt to map known and possibly unknown graphite deposits, a ground conductivity meter Geonics EM31 (Geonics, 1984) was used. This instrument is calibrated such that it measures the apparent electric conductivity directly in mS/m down to 6 – 7 m. The instrument has normally horizontal coplanar coils separated by 3.8 m and working at a frequency of 9,800Hz.

NGU modified this instrument during the winter of 2017, including a GPS positioning system, magnetic sensor and a data logger. This has made measurements more effective and the quality of data are improved by continuous sampling and simultaneous registration of the magnetic field. Normal operation of the instrument produces one reading of apparent electric conductivity for each metre. Apparent resistivity can be calculated as the inverse value of apparent conductivity.



Figure 4.2: Geonics EM31 used in graphite investigations in Vesterålen.

The EM31 is a very effective instrument for locating unexposed graphite deposits: we experienced a success rate of almost 100 % when excavating targets indicated by the instrument. Trenches were excavated based on the EM31 data and the underlying graphite deposits were revealed. Exposed graphite deposits in trenches like this were later used as grounding points for CP measurements. The instrument cannot discriminate between sulphides and graphite.

Measurements with EM31 may, in some cases, show a negative apparent conductivity. This may happen when there is a vertical structure that is thinner than the coil separation of 3.8 m. In these cases, the apparent conductivity is read as -99 mS/m and given a special colour in the data presentation.

#### 4.1.3 Charged Potential and Self Potential methods

**Charged Potential (CP)** measurements are acquired by connecting a current electrode directly to the conductive body and locating the other remote electrode at a considerable distance to ensure that its effect is virtually non-existent in the survey area. The current can be injected through a surface outcrop or a bore hole if no outcrops are available. The potential between two non-polarizable electrodes is then measured on the surface around the conductive body in a sequence of connected measurement-points. When the electric conductivity of the mineralisation is more than 1000 times higher than that in the surrounding host rock, the electrical potential will, in practice, stay constant above the mineralisation, and then drop down when the measurements are outside the ore-body (Figure 4.3). By measuring the potential around a known graphite ore-body, the body's length, dip and size can be mapped. In addition, an outline of unknown ore-bodies in the neighbourhood can be mapped.

A practical way of interpreting depth extent of nearly vertical electric conductive bodies from CP data is presented by Kihle & Eidsvig (1978).

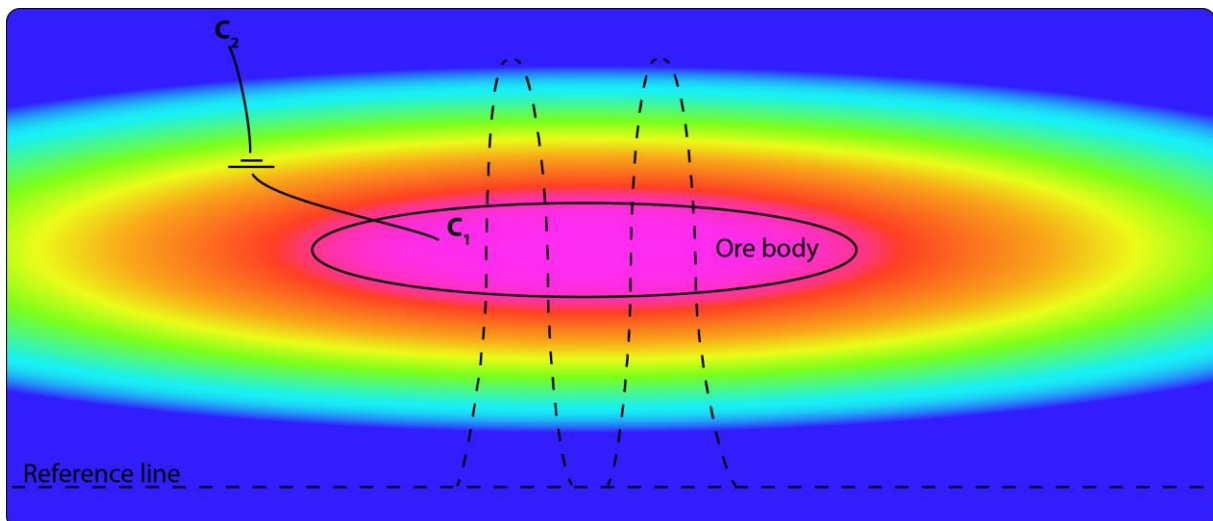


Figure 4.3: Conceptual illustration of the CP- method. The current electrode ( $C_1$ ) is connected to the ore body and the remote electrode ( $C_2$ ) is placed far outside the survey area. The colour indicates the strength of the charged potential above an ore-body. The dashed line shows the survey path which will the entire body.

**Self Potential (SP)** is measured simultaneously with CP. SP is a natural potential in the ground created by electrochemical processes in the surrounding of electronically conducting minerals as graphite, sulphides and oxides (Sato & Mooney 1960). SP is

not dependent on exposed graphite for current injection and can be a useful tool if there are several conductive bodies in the investigated area.

SP may give negative potential values of 1000 mV or even more above a graphite mineralisation. Measured SP signals less than 50 mV are not regarded as anomalies in mineral prospecting.

The equipment used for **combined CP and SP** measurements was developed at NGU in 2014. It consists of an immobile current transmitter and a mobile receiver (Voltmeter). The transmitter sends current between the ore electrode ( $C_1$  in Figure 4.3) and the remote electrode ( $C_2$  in Figure 4.3) and charges the ore body. The current is transmitted in pulses of two seconds on and two seconds off. The pulses are synchronized through GPS-time enabling the receiver to "know" when the ore body is charged. SP is measured when the current is switched off and CP+SP is measured with the current on, and then, to get the pure CP, SP is subtracted from the CP+SP measurement. All of this is done automatically during the measuring procedure. Each measurement is the potential between the two mobile electrodes and individual measurements must be summarised consecutively to a total potential sum.

The position of each measured point is given by a GPS recorder at the position of the receiver. The accuracy of the positioning is +/- 5 m.



Figure 4.4: Establishing CP ore grounding point and data acquisition in combined CP and SP measurements.

#### 4.1.4 2D resistivity and Induced Polarisation (IP)

Detailed 2D resistivity and Induced Polarisation (IP) sections give valuable information in the evaluation of possible graphite mineralisation.

##### Data acquisition

The 2D resistivity and IP methods are carried out by injecting current into the ground with the use of two electrodes and by measuring the voltage between two separate electrodes. Based on measured resistance (measured voltage / injected current) and a geometrical factor dependent on the electrode positions, the apparent resistivity and IP effect can then be calculated.

The 2D resistivity/IP measurements were performed using the Lund cable system (Dahlin 1993) and the instrument ABEM Terrameter LS (ABEM, 2012) was used to acquire the data. As seen in Figure 4.4, four multi-electrode cables can be used, and for the surveys presented in this report, a Multiple Gradient electrode configuration (Dahlin & Zhou, 2006) was applied. Once the electrodes are connected to the ground and the measuring instrument, an automatic measuring procedure starts transmitting current at one electrode pair and measures electric potential at up to four electrode pairs simultaneously. Resistivity is measured when current is on while IP-effect is measured shortly after current cut. An electrode separation of 5 m was used for the profiles giving a maximum depth range of about 60 m. The resolution decreases with depth and resistivity data deeper than ca. 40 m are, by experience, of low reliability.

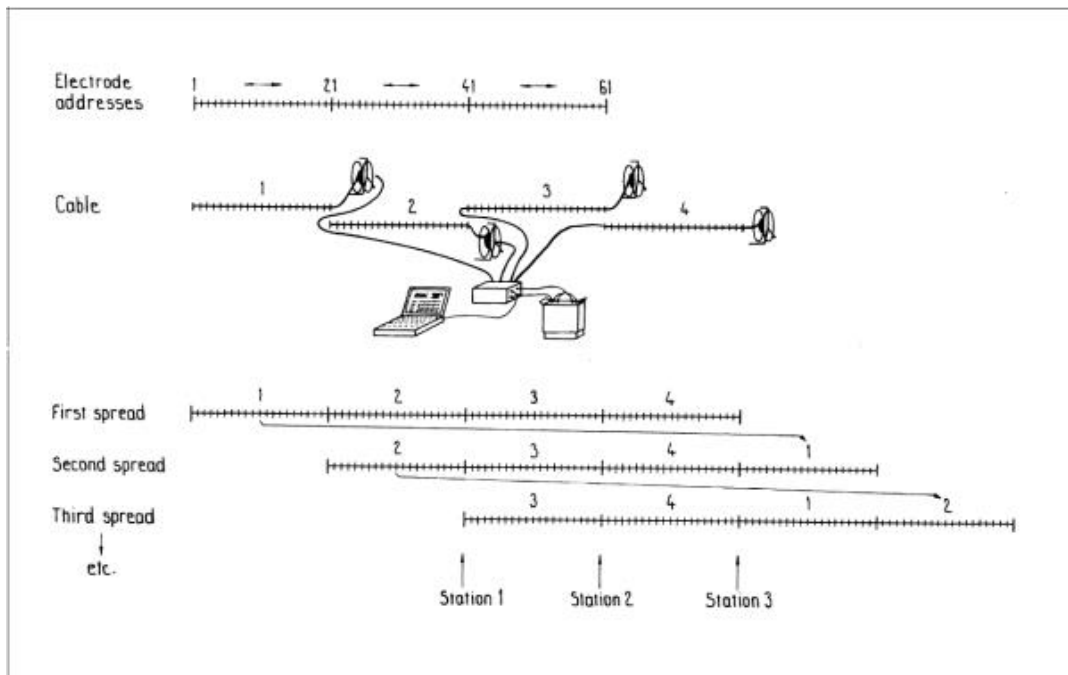


Figure 4.5: Diagram of measuring procedure illustrating the setup of the Lund System and the roll-along method for performing as many measurements as required. From (ABEM, 2012).

##### Quality of the data

The quality of 2D resistivity/IP data is dependent on current strength, resistivity in the ground and noise level in the area. In general, we conclude that the quality is good, but some data have a higher than desirable standard deviation during inversion according to the software's guidelines (Loke 2014). These data points were removed from the dataset before the inversion. Table 4.3 describes the number of deleted data points and remaining points for the final inversion. An alternative method to evaluate data quality is by looking at the absolute error in the inverted sections. Absolute error of less than 5 % is very good; 5 – 10 % is good; between 10 and 30 % is not that good but acceptable.

**Table 4.3: 2D resistivity/IP. Number of measured, removed and remaining data points for inversion.**

Name	Start:	End	Measured data points	Removed data points	Final data points
2017 - Profile 1	X: 509838 Y: 7627980	X: 509927 Y: 7627594	1164	160	1004
2017 - Profile 2	X: 510838 Y: 7628678	X: 511126 Y: 7628428	1168	124	1044
2017 - Profile 3	X: 502084 Y: 7628766	X: 502343 Y: 7628932	676	91	585
2017 - Profile 4	X: 507290 Y: 7643881	X: 507225 Y: 7644279	1168	72	1096
2017 - Profile 5	X: 505862 Y: 7643673	X: 505921 Y: 7644069	1136	4	1132
2017 - Profile 6	X: 502059 Y: 7628976	X: 502196 Y: 7628714	676	218	458
2017 - Profile 7	X: 511819 Y: 7629428	X: 512021 Y: 7629204	676	27	649

## Data inversion

Almost all resistivity and IP measurements give an apparent resistivity and IP value. The apparent resistivity values represent a weighted average resistivity which results from resistivity of each heterogeneous volume in the surroundings of the measurement points. To find the specific resistivity of each part of the heterogeneous investigated volume, the data are inverted. This is done by dividing the profile into blocks each characterised by specific resistivity values. These are adjusted following an iterative procedure until a theoretical model fits the measured data. The same procedure is used to find the true IP effect in the sub-surface.

Resistivity/IP measurements were inverted using the computer program RES2DINV (Loke 2014) with robust data constraint.

## Interpretation

Graphite is an electronically conducting mineral, and the resistivity in massive graphite ore bodies is commonly less than 2  $\Omega$ m, with conductivity higher than 500 mS/m, (Dalsegg 1994, Rønning et al. 2012, Rønning et al. 2014). This can be used to distinguish between resistivity anomalies caused by graphite mineralisation and other ionic conducting geological materials such as porous rock filled with saline water,

marine clay deposits and even sulphide deposits (resistivity less than 10  $\Omega\text{m}$ ). Unfortunately, 2D resistivity/IP measurement may be disturbed by artificial conductivity effects interfering with responses from two or more sub-vertical conducting graphite structures (Rønning, et al., 2014).

Induced Polarization (IP) responds to electronic conducting minerals which are not in electrical contact. This means that massive graphite deposits should not give an IP effect with the exception at the surface of the mineralisation. IP effects are often seen in the contacts between graphite bodies and surrounding host rock where graphite grains are not connected (disseminated graphite).

## 4.2 Geological methods

The investigated areas are partly soil covered, but there are numerous outcrops. The graphite schist was sampled when found in these areas and coordinates for each sampling point was recorded, taking care to obtain as representative samples as possible and from an as large area as possible. Normal sample size was approximately 1-2 kg. The samples were sent for further analysis to the NGU laboratory.

### 4.2.1 Core drilling, sampling and analyses

NGU has a truck mounted drilling rig as shown in Figure 4.5. When the 4x4 wheel drive truck can drive into an area, core drilling can be performed. The core diameter is 36 mm. The core length is limited to ca. 50 m.



Figure 4.6: NGUs truck mounted drilling gear in operation.

Two localities were chosen for core drilling:

- 1) The Sommarland area with drill hole Som1701 and Som1702
- 2) The Haugsnes area with drill hole Haug1701 and Haug1702.

The purpose of the drilling was as follows:

- 1) To obtain a continuous section through the graphite bearing units and their country rock.
- 2) To obtain information on the thickness and grade of graphite schists, on localities where there exists detailed ground geophysical information on the surface.

The drilling undertaken is not detailed enough to estimate a meaningful resource tonnage. Drilling was limited to localities accessible with the truck and with a depth limitation of ca. 50 m.

The drill core was logged, described, sampled and analysed in the following manner (The corresponding section of this report are shown in parentheses):

- a) Lithological logs and descriptions of cores (Chapters 6.3 and 7.2)
- b) All drill cores were photographed dry and wet (Appendix 3)
- c) Measurements with Portable XRF, one point per 0.25 meter (Appendix 4)
- d) Splitting of core in 3 parts, one half and 2 quarter cuts of the core
- e) At selected intervals, where visual logging shows the occurrence of graphite, sampling at each 0.5 metre were made.
- f) The most graphite rich intervals were analysed for TC and TS (Appendix 2)
- g) Selected thin sections were made from representative intervals (Sommarland in chapter 6.3, Haugsnes chapter 7.2 and general observations chapter 12.1)
- h) Areas of high electric conductivity were identified using simple Ohm-meter measurements (Chapters 6.3 and 7.2).
- i) Petrophysical measurements (NGU-lab) were performed on selected samples at the same intervals as the thin section (Chapter 12.1).

#### 4.2.2 Analytical methods

Samples from different outcrops and drill cores were crushed using standard methods. The powders were analysed for total carbon (TC) and total sulphur (TS) using a Leco SC-632 analyser. The detection limits are 0.06 % and 0.02 % for carbon and sulphur respectively. The analytical uncertainty at 2  $\sigma$  level is +/-15 % relative. The aggregate results for all surface samples are shown in Appendix 5 while Appendix 2 show the data from the drill-cores.

The graphite industry uses the term "graphitic carbon" (Cg) when reporting graphite occurrences. This type of analysis is essentially the same as "total organic carbon" (TOC) but includes an extra step in which inorganic carbonate minerals and organic matter are removed by use of acid and by roasting the sample before using a Leco carbon analyser. In rock types with little or no carbonate minerals and organic matter, analyses of total carbon (TC) are similar or close to TOC and graphitic carbon (Cg) but the former is much cheaper and faster. An overview of TC and TOC can be seen on selected samples in Appendix 5. The commercial laboratory procedures for TC, TOC and Cg analyses are described by [www.alsglobal.com](http://www.alsglobal.com).

Several standard thin sections were made from the drill-cores. An overview of these are shown in Appendix 1 and described in chapters 6.3, 7.2 and 12.1.

## 5. SELECTION OF FOLLOW-UP OCCURRENCES

The selection of follow-up graphite occurrences was based on results from the helicopter-borne geophysics performed in 2013. This was dominantly Electro-Magnetic data, but also based on the magnetic data. Data acquisition, processing and visualisation was described by Rodionov et al. (2013a and 2013b).

### 5.1 Petrophysical properties of graphite

The electronic conductivity of pure graphite is reported to be ca.  $10^{-3}$   $\Omega\text{m}$  (Telford et al. 1976). In most cases, graphite appears together with other minerals, and our experience demonstrates that the resistivity of graphite mineralisation may be ca. 1  $\Omega\text{m}$  (see chapter 4.1.4 for details).

Graphite is reported to be a diamagnetic mineral which means that graphite has a negative magnetic susceptibility and may reduce the earth's magnetic field (Reynolds 2011). Within this project, NGU has tested laboratory measurements of magnetic susceptibility on 125 graphite samples (see Appendix 6 and 7). However, the method employed here for measuring magnetic susceptibility is an electromagnetic method which will fail on electronically good conductive graphite. Due to this, the measured results cannot be treated with confidence.

Sulphur occurring as the magnetic mineral Pyrrhotite can have the opposite effect since this mineral normally has a higher magnetic susceptibility. This means that low magnetic field in an area may indicate a lack of pyrrhotite in the bedrock.

Apparent resistivity and magnetic anomaly fields have been studied empirically from helicopter-borne measurements in a graphite bearing area west of the town of Sortland (Figure 5.1). Areas which show up with low resistivity and exposed graphite mineralisation also display a low magnetic field. At the moment, it is unclear whether the latter is caused by the diamagnetic effect of graphite, nonmagnetic host-rock or even remnant magnetisation of the host-rock. This will be studied later in a separate research project. If it is found that the diamagnetic effect that is indeed causing the low magnetic field, this would suggest the presence of extensive amounts of graphite.

A low magnetic field coinciding with low resistivity may be an indicator of good quality graphite. NGU has therefore developed a method to identify areas with low resistivity and low magnetic field from helicopter-borne geophysical measurements. In this study we use this method to identify potentially good quality graphite, both for the Langøya area in Vesterålen and parts of the Austvågøya area in Lofoten.

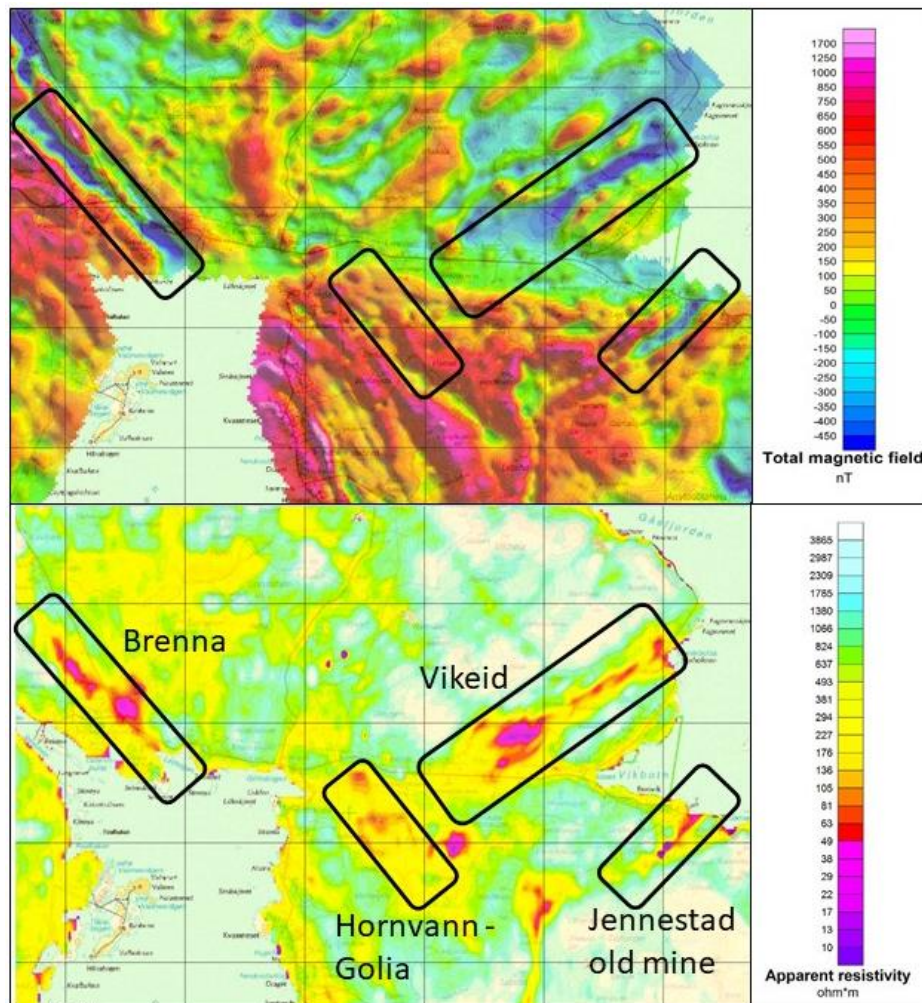


Figure 5.1: Magnetic anomaly field and apparent resistivity (7000 Hz coaxial coils) from helicopter-borne measurements in the Jennestad area, west of Sortland town (Modified from Rodionov et al. 2013a).

## 5.2 Data from helicopter-borne measurements at Langøya, Vesterålen

Helicopter-borne geophysical measurements produce data of magnetic anomaly field, electromagnetic data at five frequencies and the concentrations of uranium, thorium and potassium. All of these data are relevant for graphite prospecting.

Electromagnetic data can pinpoint potential graphite deposits directly since the electric conductivity of graphite is quite low (high resistivity).

As described in the previous section, low magnetic field and low resistivity can be a good indicator of good quality graphite. However, in combination with iron-rich minerals, this effect can be cancelled out by magnetic minerals (iron oxides, pyrrhotite and others).

In graphite exploration radioactive elements such as uranium and thorium can be an environmental problem during graphite extraction and therefore the acquisition of radiometric data from the helicopter-borne measurements is important.

Based on this we present examples of electromagnetic data, magnetic data and radiometric data as a basis for selecting ground follow-up investigations on potential graphite objects.

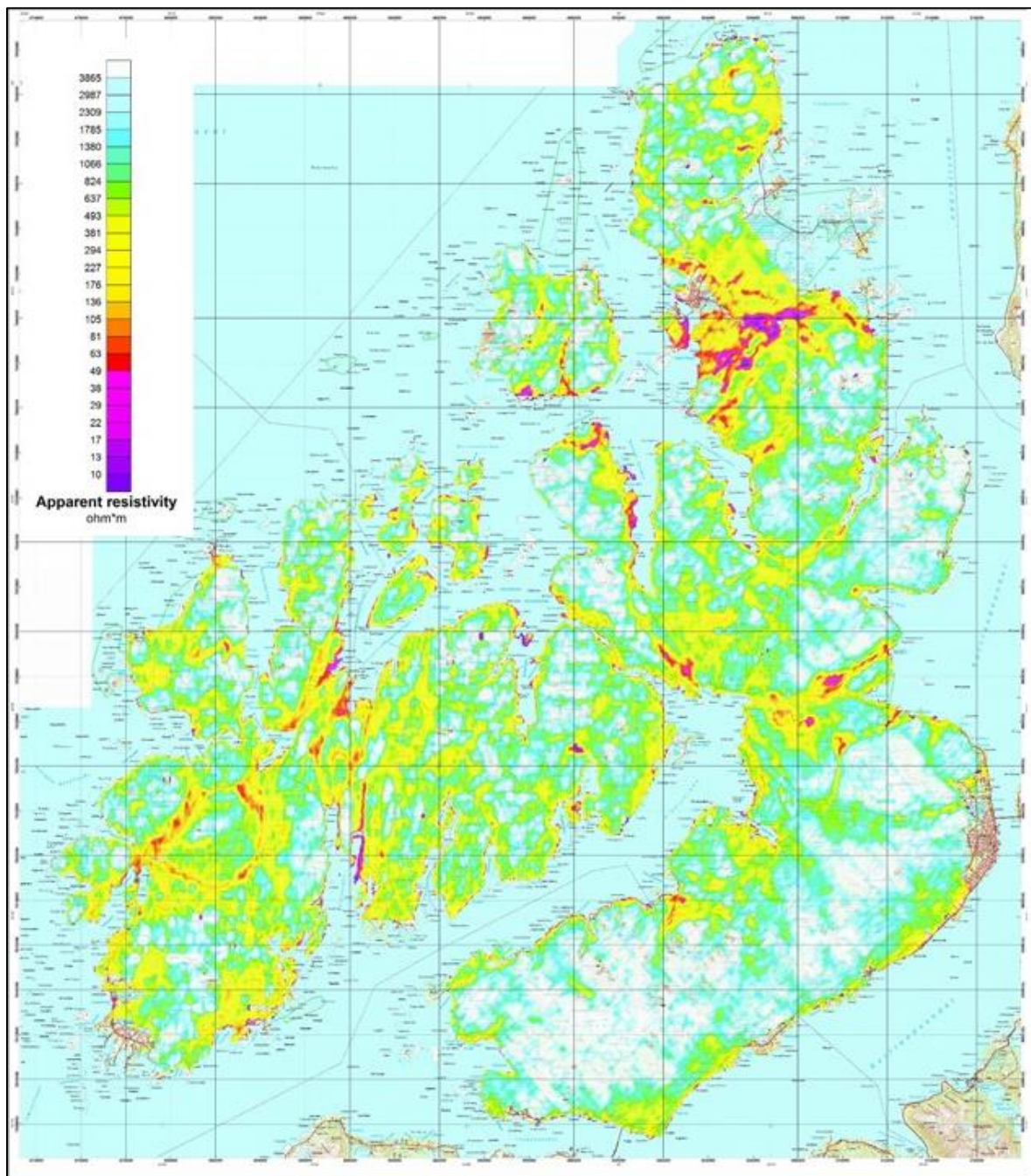


Figure 5.2: Apparent resistivity calculated from EM 7000 Hz Coaxial coil configuration at Langøya in Vesterålen.

An example of the electromagnetic data from Langøya is presented in Figure 5.2. Yellow colours represent moderate anomalous low apparent resistivity. Orange, red and violet colours represent low apparent resistivity ( $< 100 \Omega\text{m}$ , high apparent conductivity). Note that these apparent values represent an average of a greater volume, and that smaller structures inside this volume might have lower resistivities (higher conductivities). The cause of the low resistivity may be graphite, sulphides, iron oxides and salt water in porous soil and rocks.

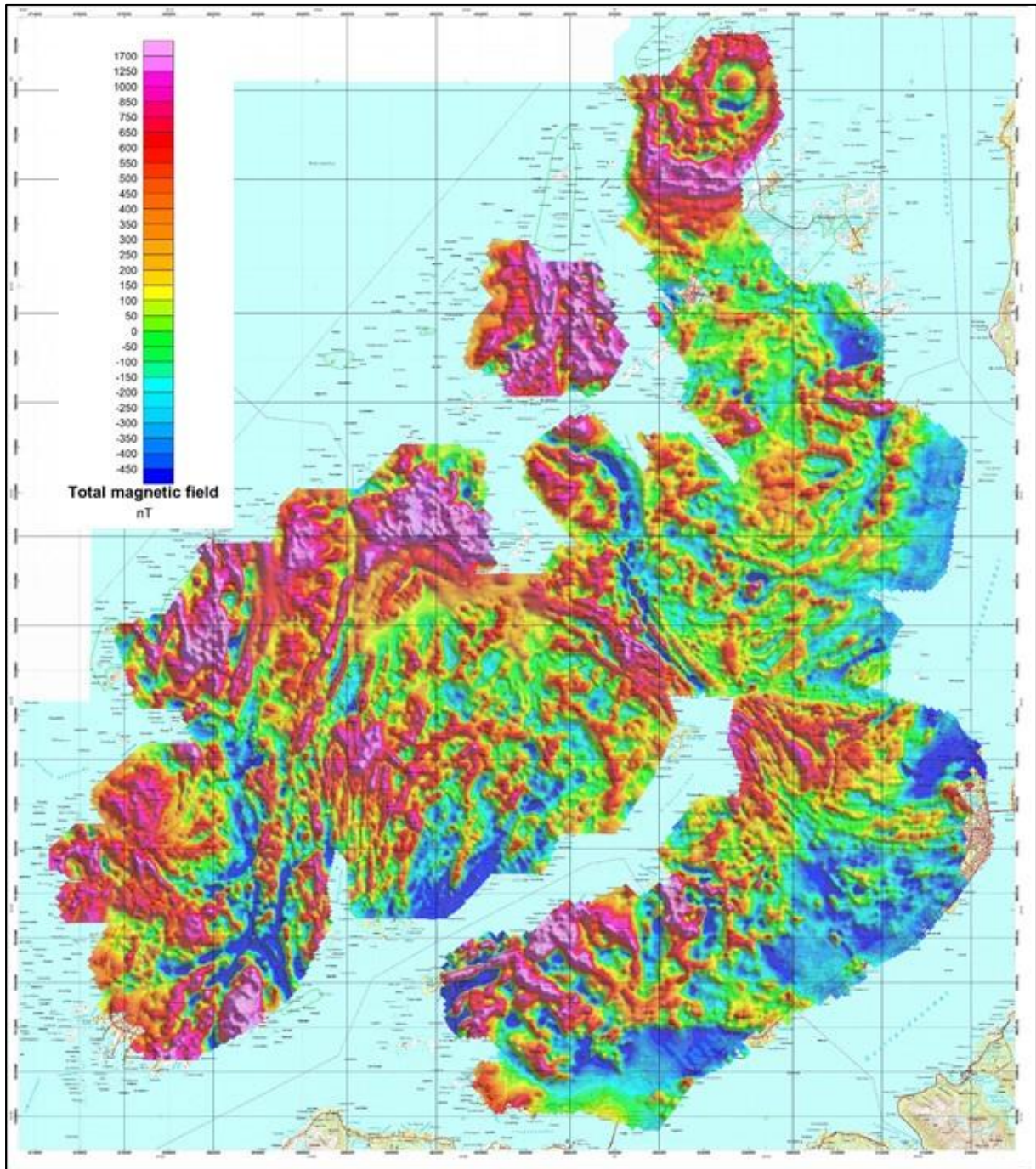


Figure 5.3: Magnetic anomaly field at Langøya, Vesterålen.

The magnetic anomaly field at Langøya (Figure 5.3) is produced by subtracting the International Geomagnetic Reference Field (IGRF 2015) for the year of acquisition (2013) from the diurnal corrected magnetic total field. The magnetic anomaly field shows strong positive anomalies ( $> 1700$  nT) but also areas where the magnetic field is very low ( $< -300$  nT, blue colours). Low magnetic field may indicate, as discussed above, good quality graphite, but also bedrock with low iron content (low magnetic susceptibility) and rocks with remanent (permanent) magnetisation.

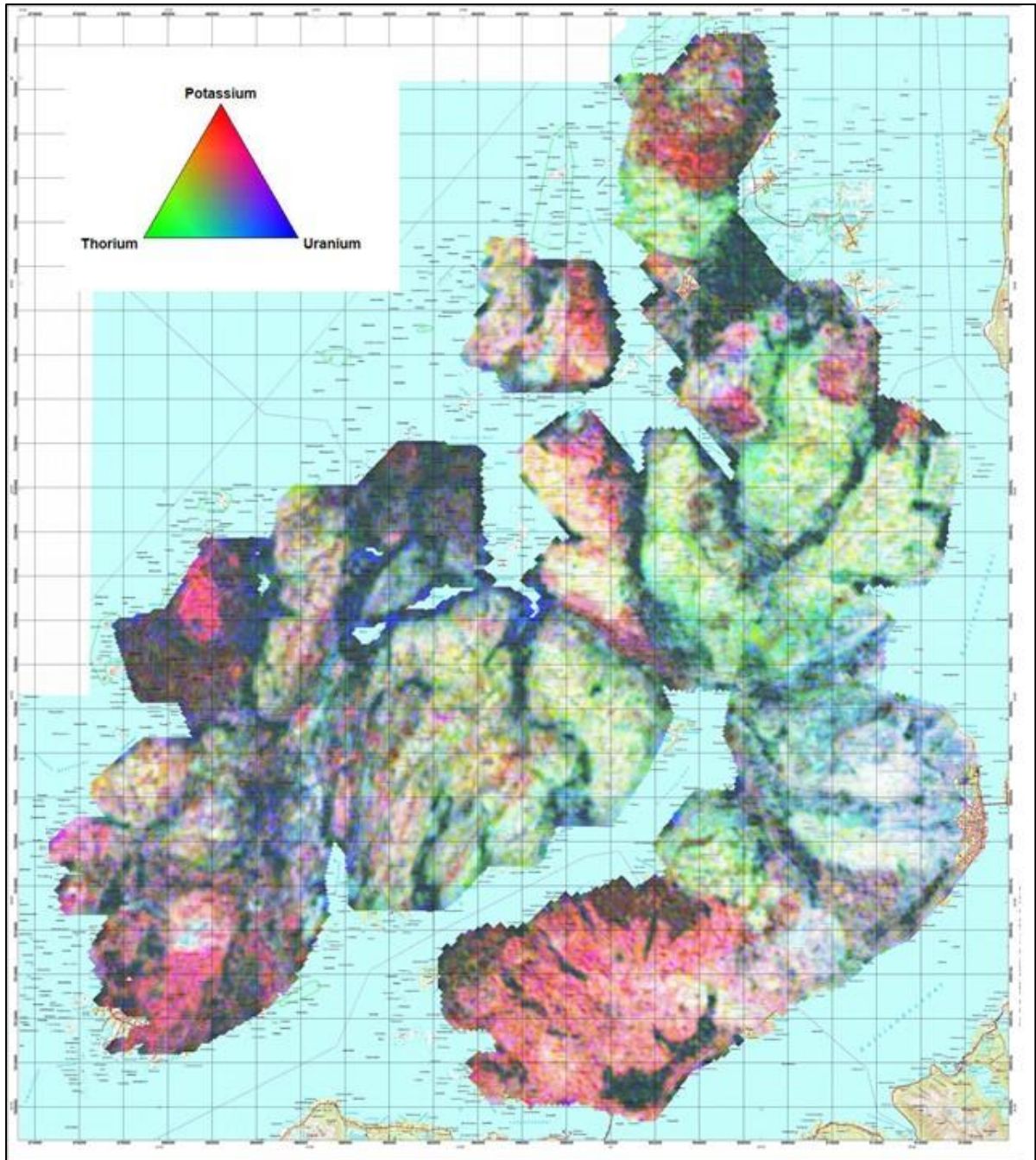


Figure 5.4: Radiometric ternary map (combined eU, eTh and K) from Langøya in Vesterålen.

The concentration of the radioactive elements uranium and thorium are generally low at Langøya. The helicopter-borne measurements show a uranium concentration < 2 ppm and a thorium concentration < 10 ppm. These values must be looked upon as apparent values since they represent a weighted average value over a footprint of ca. 150 m x 180 m. Inside each footprint the values may be higher. For element concentrations (U, Th and K), see processing report (Rodionov et al. 2013a).

In the ternary map (Figure 5.4), red colour represents potassium, green represents thorium and blue represents uranium. Dark colours are low in all three elements whereas white indicates high values in all three elements. As can be seen, few areas are dominated by uranium and thorium.

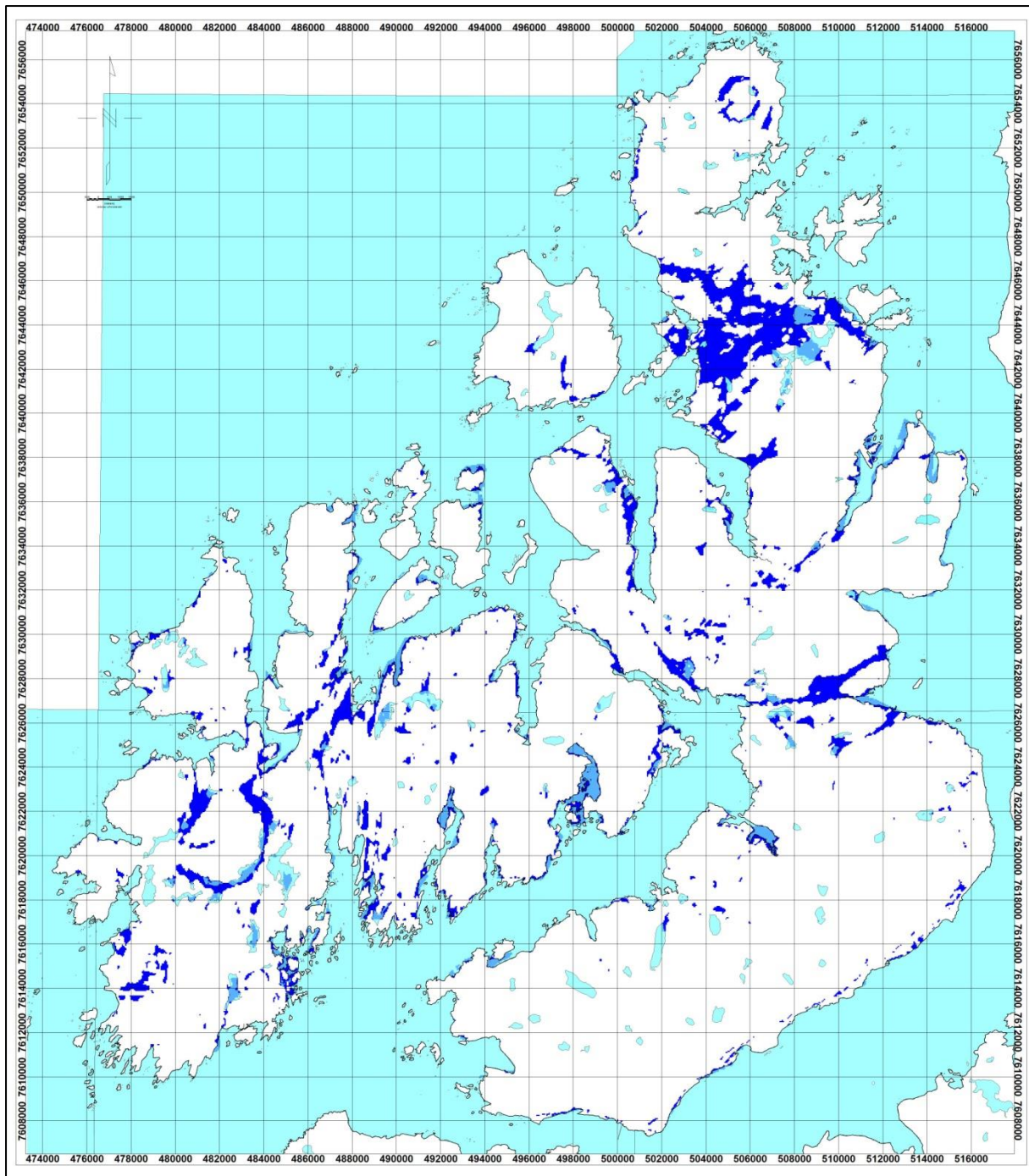


Figure 5.5: Blue colour show areas at Langøya where apparent resistivity from EM 7000 Hz coaxial coils is  $< 300 \Omega\text{m}$  and magnetic total field is  $< \text{IGRF} + 300 \text{ nT}$ .

NGU has developed a new method for integrated interpretation of magnetic and electro-magnetic methods. In Figure 5.5, blue colours show areas where the apparent resistivity is  $< 300 \Omega\text{m}$  and the magnetic anomaly field is  $< 300 \text{ nT}$  (total field minus IGRF  $< 300 \text{ nT}$ ). According to the assumptions presented here, these are potential areas for extensive volumes of high quality graphite. Figure 5.6 shows the locations of sampled graphite schists.

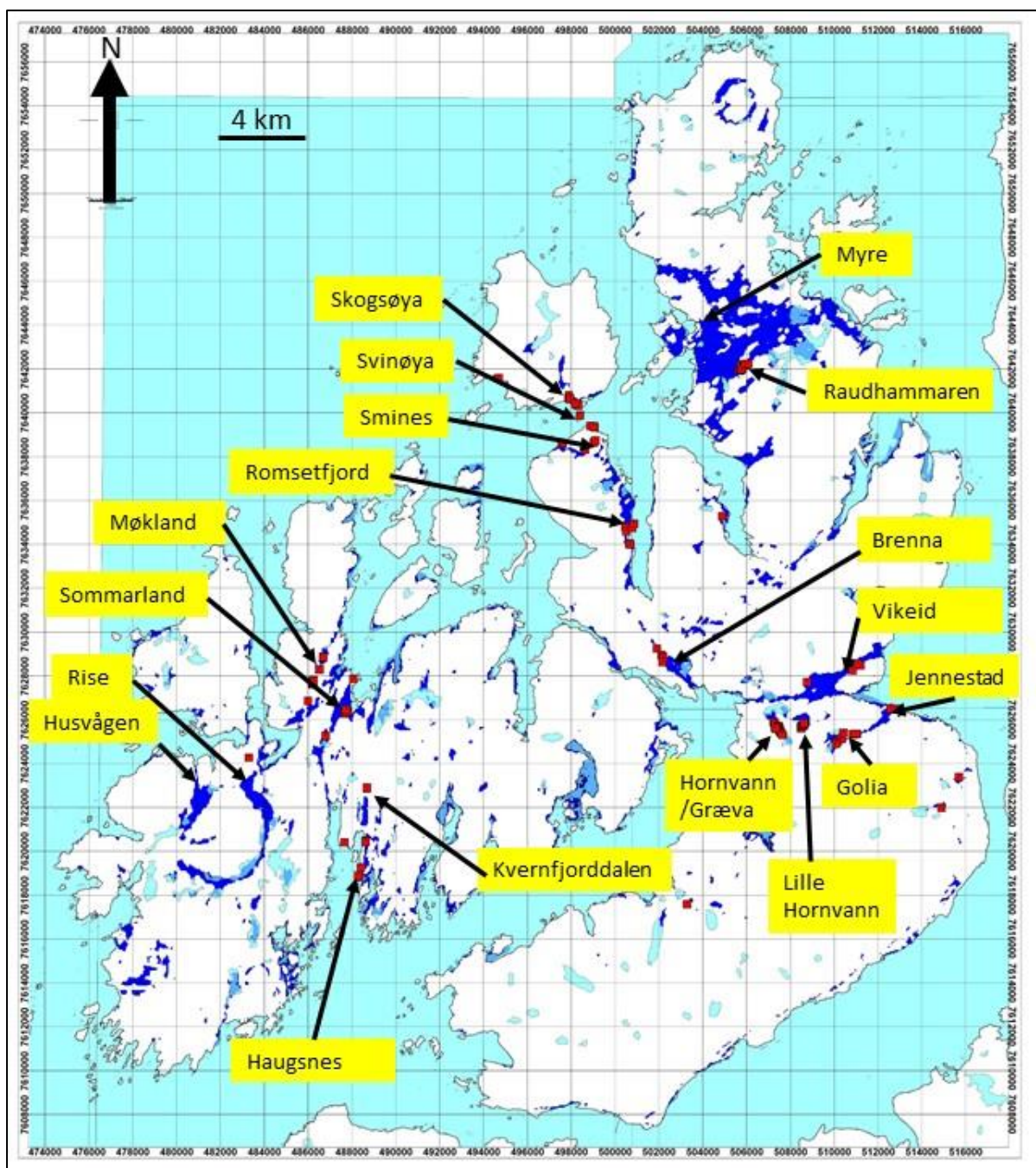


Figure 5.6: Blue colour show areas at Langøya where apparent resistivity from EM 7000 Hz coaxial coils is  $< 300 \Omega\text{m}$  and magnetic anomaly field is  $< 300 \text{ nT}$ . Red squares are samples of graphite bearing rock.

The areas called Hornvann, Græva, Lille Hornvann, Golia, Jennestad and Viketid were investigated in the 1990's (see chapter 3). Some follow-up work was performed at Møkland, Skogsøya, Svinøya, Smines during 2013-2014. In 2015 and 2016 NGU carried out investigations at Møkland, Sommarland, Kvern fjorddalen, Haugsnes, Smines and Raudhammaren (Gautneb et al. 2017, Rønning et al. 2017). During the field season of 2017, NGU carried out additional work at Husvågen – Rise, Møkland south, Sommarland, Haugsnes, Brenna, Viketid, Raudhammaren and east of Myre. These investigations are reported here.

### 5.3 Data from helicopter-borne measurements at Austvågøya, Lofoten

The same helicopter-borne geophysical measurements that were performed at Langøya (Rodionov et al. 2013b) were also undertaken at Austvågøya. The processed data are presented in Figures 5.7, 5.8 and 5.9.

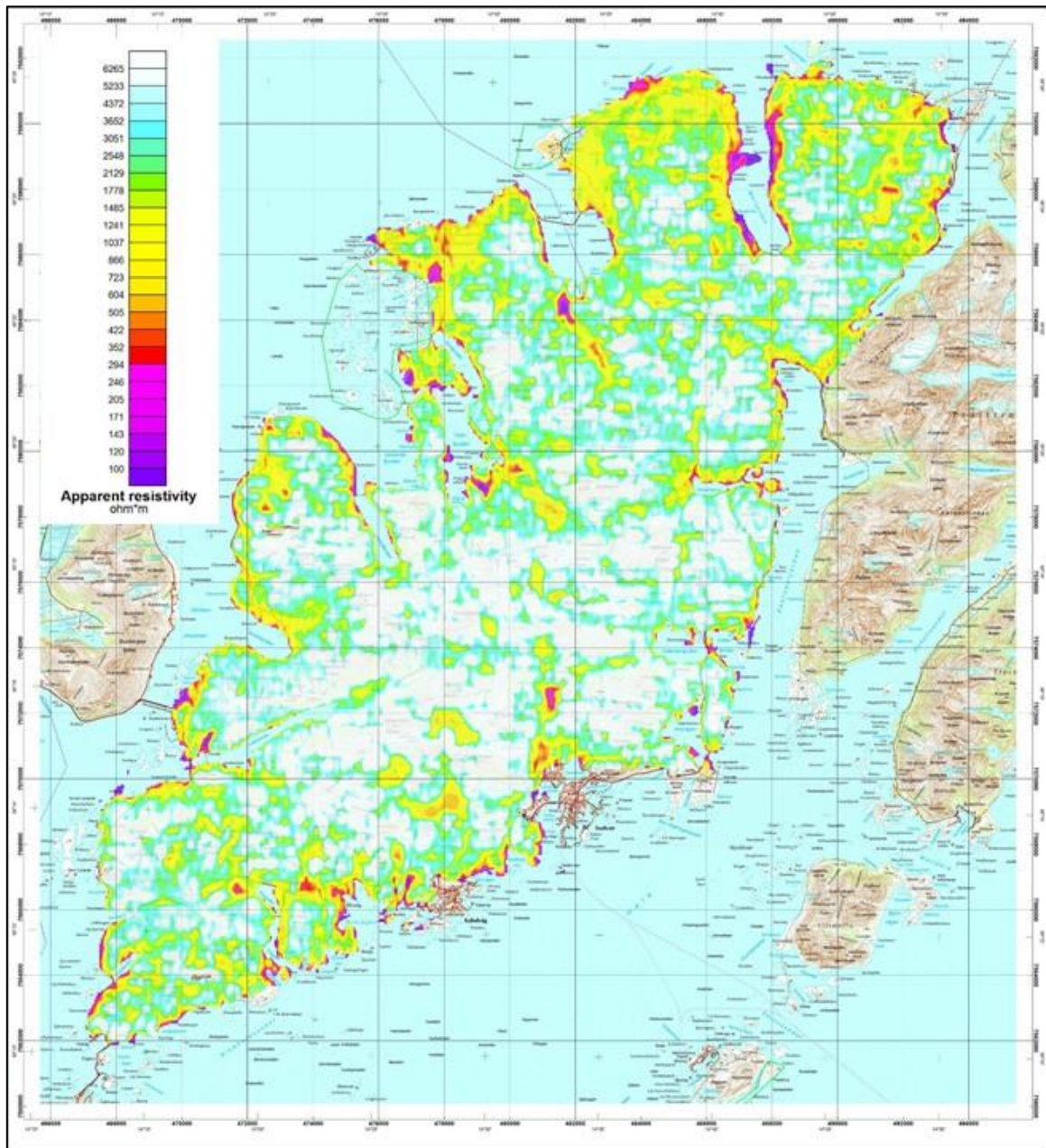


Figure 5.7: Apparent resistivity calculated from EM 7000 Hz Coaxial coil configuration at parts of Austvågøya, Lofoten.

An example of the electromagnetic data from Austvågøya is presented in Figure 5.7. Yellow colours represent moderate anomalously low apparent resistivity. Orange, red and violet colours represent low apparent resistivity (high apparent conductivity). Note that these apparent values represent an average of a greater volume, and that smaller structures inside this volume may have lower resistivities (higher conductivities). The cause of low resistivity may be graphite, sulphides, iron oxides and salt water in porous soils and rocks.

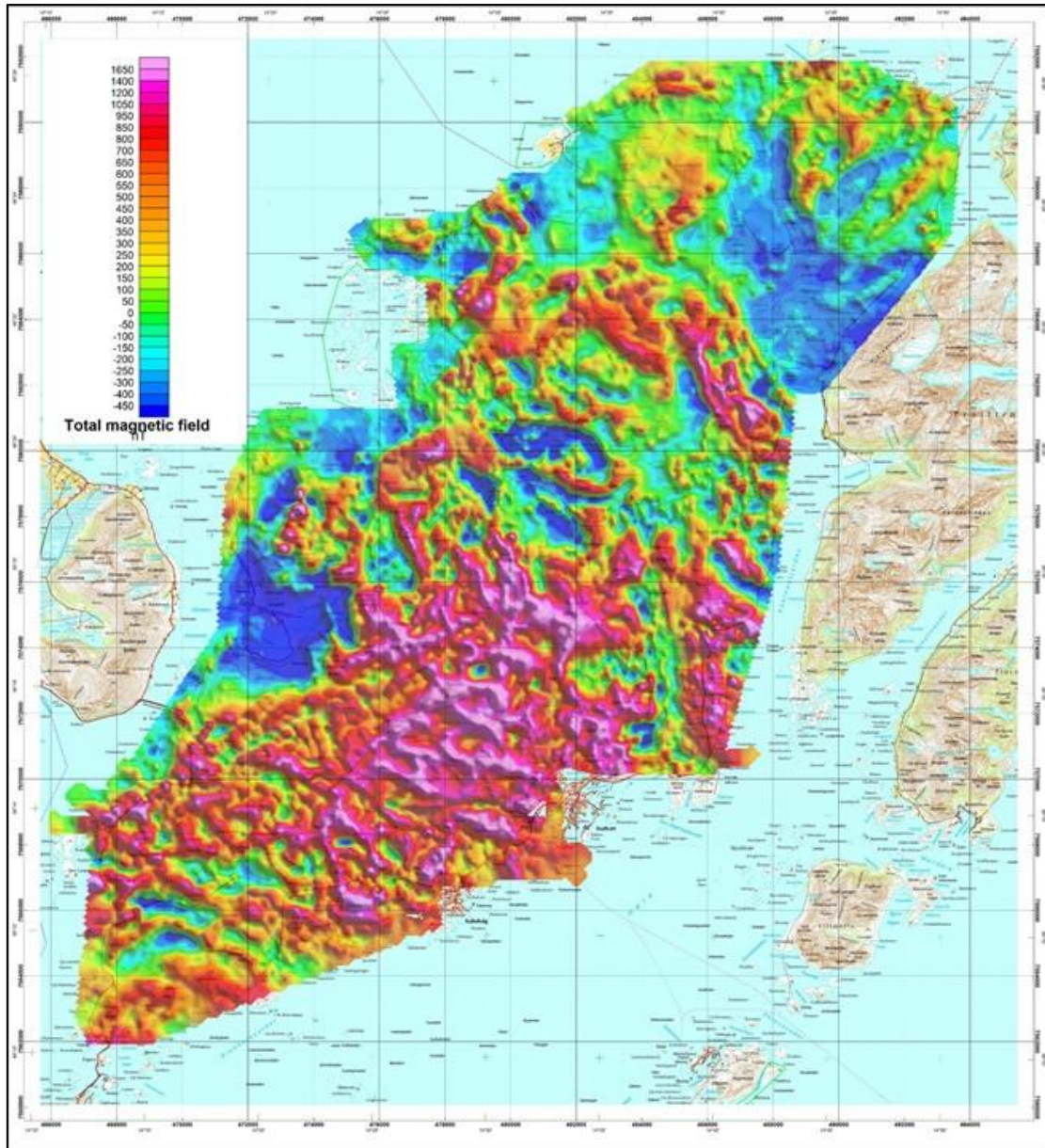


Figure 5.8: Magnetic anomaly field at parts of Austvågøya, Lofoten.

The magnetic anomaly field in parts of Austvågøya (Figure 5.8) is produced by subtracting the International Geomagnetic Reference Field (IGRF 2015) from the diurnal corrected magnetic total field. The magnetic anomaly field shows strong positive anomalies ( $> 1600$  nT) but also areas where the magnetic field is very low ( $< -300$  nT, blue colours). As discussed, these areas potentially have graphite of good quality.

The concentration of the radioactive elements uranium and thorium are also generally low at Austvågøya. The helicopter-borne measurements (Rodionov et al. 2013b) show a uranium concentration of  $< 3$  ppm and a thorium concentration of  $< 11$  ppm. These values must be considered as apparent values since they represent a weighted average value over a footprint of ca.  $150\text{ m} \times 180\text{ m}$ . Inside each footprint individual values may be higher. For element concentrations (U, Th and K), see the processing report (Rodionov et al. 2013b).

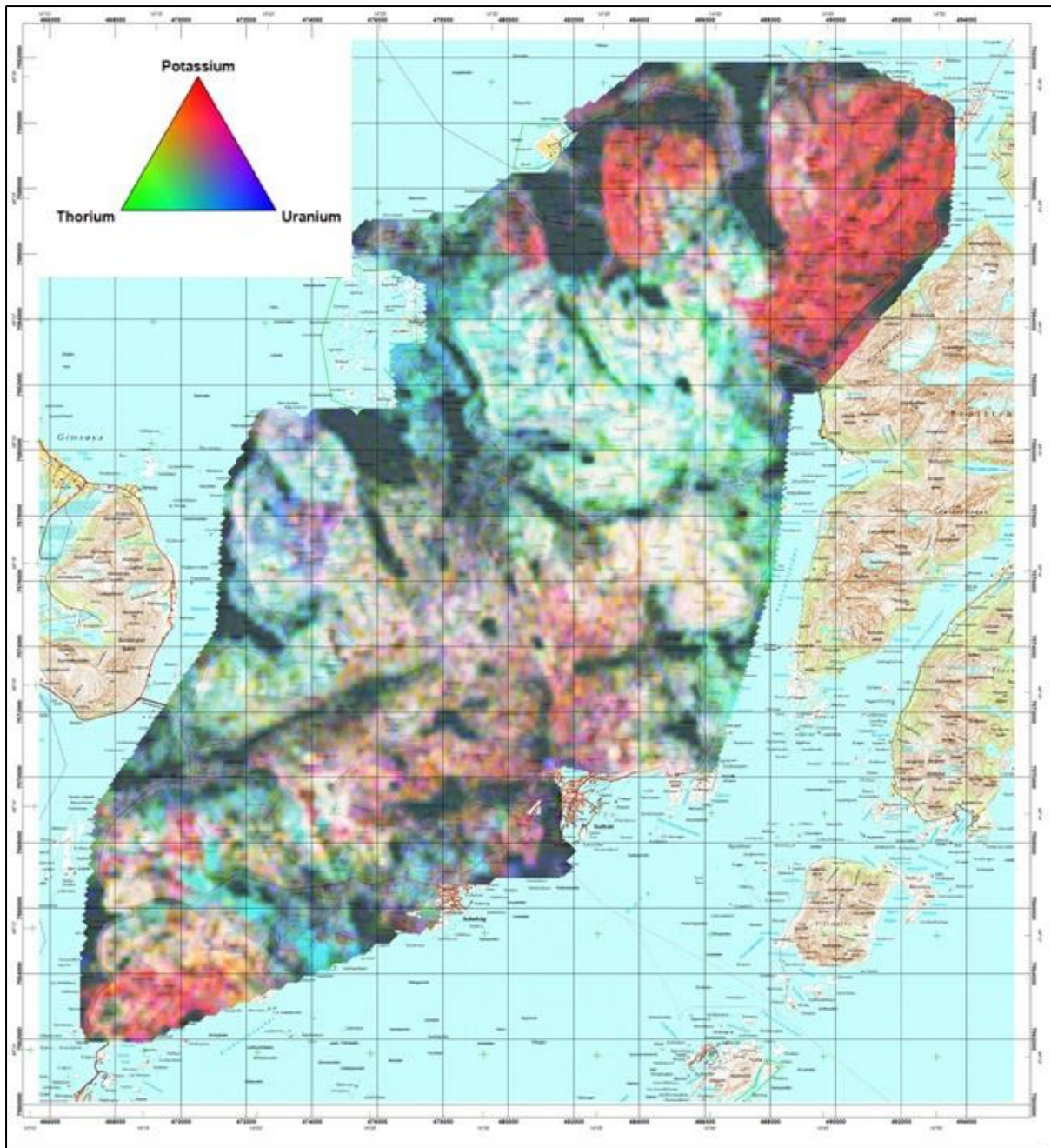


Figure 5.9: Radiometric ternary map (eU, eTh and K) from Austvågøya, Lofoten.

The ternary map (Figure 5.9) shows potassium (red), thorium (green) and uranium (blue). Dark colours are low in all three elements while white indicates high values in all three elements. Few areas are dominated by uranium.

NGU has developed a new method for joint interpretation of magnetic and electromagnetic methods. In Figure 5.10 blue colours show areas where the apparent resistivity is  $< 300 \Omega\text{m}$  and the magnetic total field is  $< 300 \text{ nT}$ . According to this new method, these are areas with potentially extensive volumes of high quality graphite.

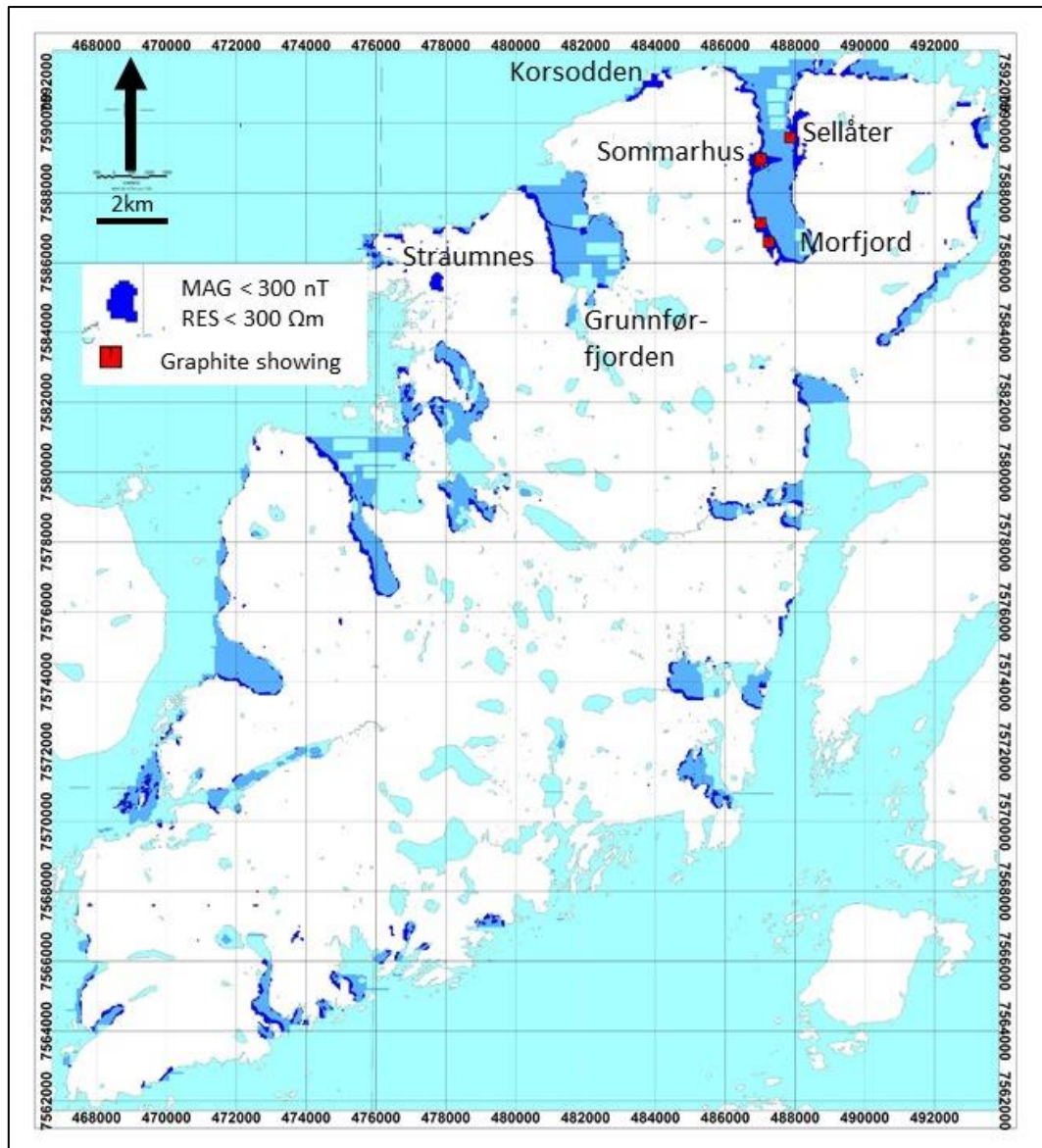


Figure 5.10: The blue colour shows areas at Austvågøya where apparent resistivity from EM 7000 Hz coaxial coils are  $< 300 \Omega\text{m}$  and magnetic total field is  $< \text{IGRF} + 300 \text{ nT}$ . The red squares are samples of graphite bearing rock.

The most pronounced areas where there is a potential for graphite of high quality are at Morfjord (abandoned mine), Sommarhus, Sellåter and Korsodden. Follow-up work has been performed in three of these areas and graphite mineralisation were located. The area Korsodden is not relevant for follow up work due to its infrastructure. The areas of Straumsnes and Grunnfjørden are less interesting due to their small size and their geological environment (see figure 5.8). Follow-up work at Morfjord, Sommarhus and Sellåter are presented in this report.

#### 5.4 Selected areas for follow-up work

In 2017, ground geophysical and geological investigations were performed at

- Sommarland, Haugsnes, Husvågen – Rise and Møkland in Bø Municipality,
- Smines, Raudhammaren and Myre in Øksnes Municipality,
- Romsetfjord, Brenna and Vikeid in Sortland Municipality,
- Morfjord and adjacent areas in Hadsel Municipality.

## 6. RESULTS OF FOLLOW-UP WORK AT SOMMARLAND, BØ MUNICIPALITY

The area called Sommarland is divided into 4 localities, Central Sommarland, Kråkberget, Sommarland east and Sommarland south. These areas were followed up with ground geophysics and in the central Sommarland area, two boreholes were drilled (core drilling).

### 6.1 Geophysics Central Sommarland

In the central part of the Sommarland area in Bø municipality some previous geological and geophysical studies exist (Neumann 1952, Gautneb et al. 2017 and Rønning et al. 2017). The field investigations at Sommarland in 2016 (Rønning et al. 2017) can be summarised thus.

*Chemical analyses of five samples from the known graphite mineralisation at Sommarland show an average graphitic carbon content of 7.7 % with a maximum value of 17.1 % (Gautneb, et al., 2017). One 2D resistivity/IP profile was measured next to the showing. The showing itself does not give an impressive signature. West of the showing, however, there is a more pronounced resistivity anomaly, and this should be investigated further with ground EM profiling (EM31), core drilling if possible and combined CP/SP measurements. The area should be investigated all the way from the old abandoned graphite mine at Kråkberget where the apparent resistivity from helicopter-borne EM measurements is very good ( $< 10 \Omega\text{m}$ ).*

#### 6.1.1 Geophysical measurements performed in 2017

In 2017, NGU performed extensive measurements with EM31, Self Potential (SP) and Charged potential (CP) with one grounding electrode. In addition, core drilling of two bore holes was undertaken.

**EM31** measurements in the central part of Sommarland area are shown in Figure 6.1 together with apparent resistivity from helicopter-borne EM results. A large amount of high apparent conductivity readings ( $> 50 \text{ mS/m}$ , apparent resistivity  $< 20 \Omega\text{m}$ ) are observed, and these are related to graphite showings (see Figure 6.1). The potential graphite mineralisation appears to be located along at least three linear structures, of which one is ca. 400 m long. The conductive structure from the helicopter-borne EM measurements appears to terminate towards the south, as is also suggested by the EM31 measurements. However, one of these lineaments is open towards the south. New EM31 measurements further towards the south-west, do not show electric conductivity that can be associated with graphite. This may be caused by the presence of thicker sediment cover.

The half peak value width of the EM31 anomalies (see section 6.2.1) at the Central Sommarland vary from ca. 2 m up to 22 m, which indicate that graphite may have a considerably thickness.

The **Self Potential (SP)** shown in figure 6.2 covers a more extensive area from central Sommarland and to the north to the old abandoned graphite mine at Kråkberget. Only a few points show SP anomalies greater than 500 mV, possibly indicating graphite. Two of these points coincide with high conductivity (low resistivity) from EM31 measurements indicating a ca. 400 m long graphite structure. Some small anomalies (100 – 200 mV) are observed south of these but the SP also indicates a termination of the graphite mineralisation towards the south. The third high SP anomaly lies south-west of the old abandoned Kråkberget mine. This anomaly is observed at only one location.

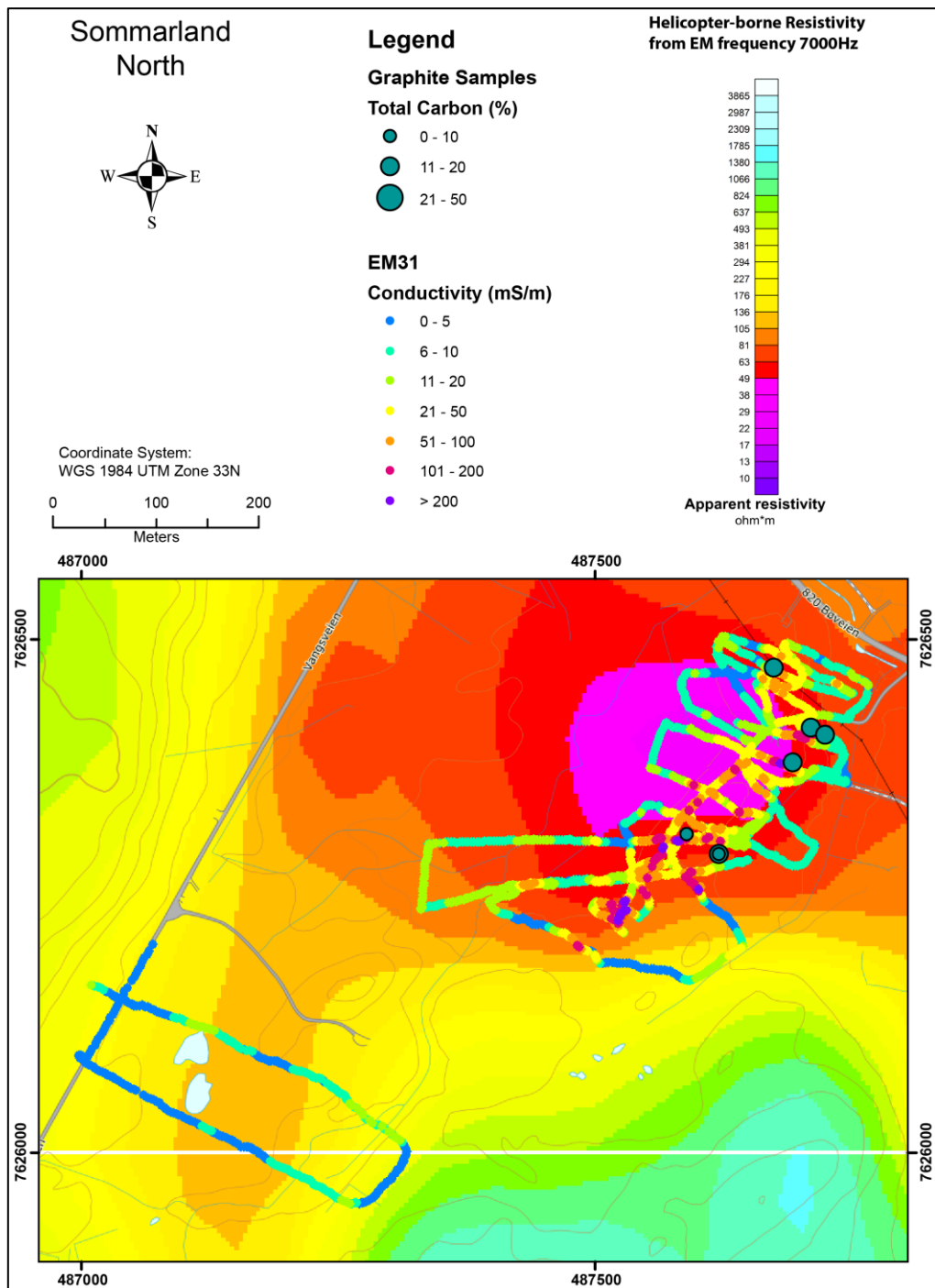


Figure 6.1: The central part of the Sommarland area. The results from EM31 measurements overlay on top of helicopter-borne measurements of apparent resistivity from EM 7000 Hz coaxial coil configuration.

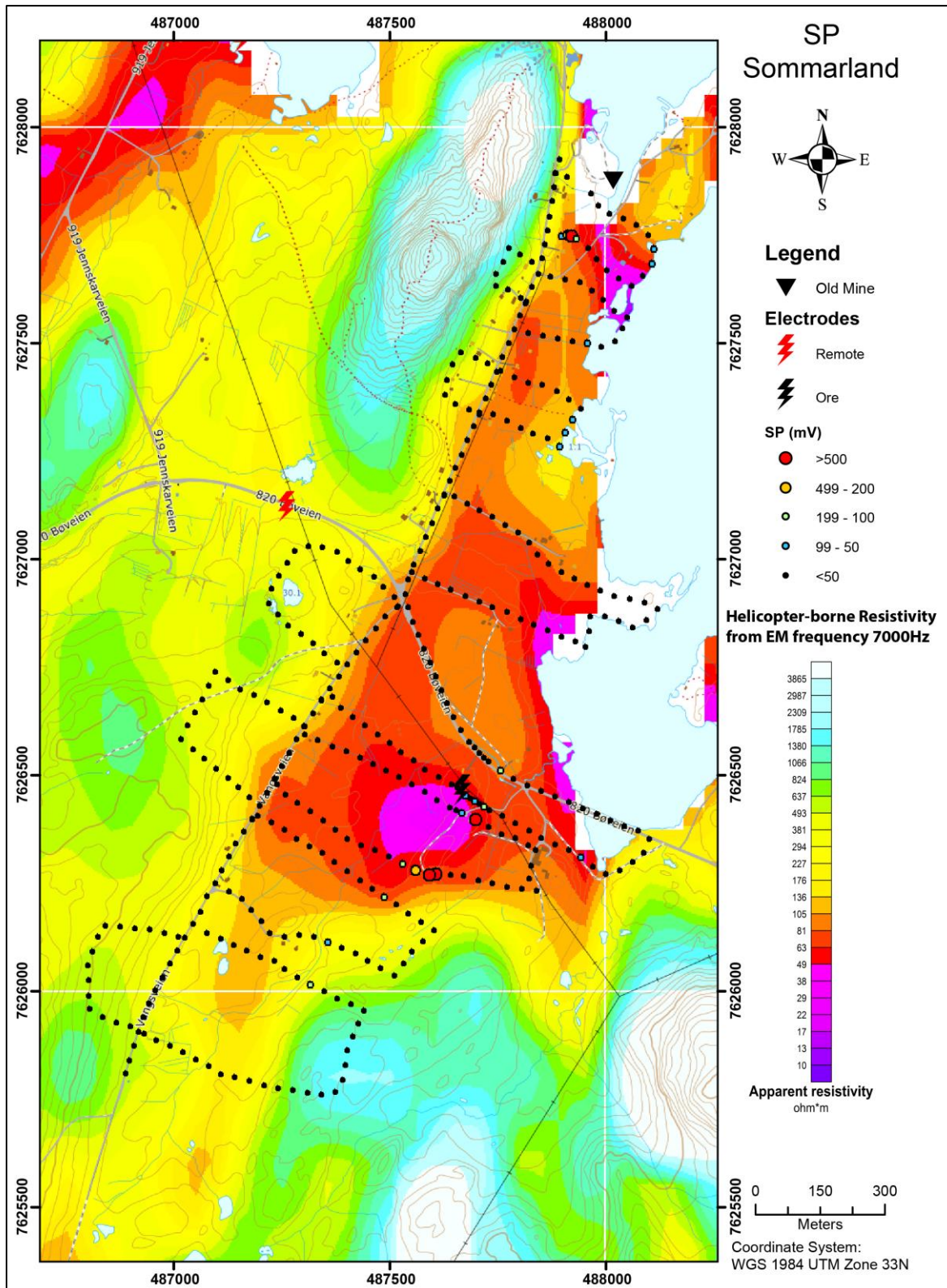


Figure 6.2: SP measurements in the central part of the Sommarland area and towards the Kråkberget abandoned mine in the north. The coloured background is apparent resistivity from helicopter-borne EM measurements with EM 7000 Hz coaxial coil configuration.

The results of the **CP measurements** in the central Sommarland area, are shown in figure 6.3. The contact with the graphite is established in a showing at coordinate 487667 – 7626466 and the remote current electrode was placed at coordinate 487260 – 7627123 (UTM Zone 33). The far-away electrode is located a bit too close, ca. 800 m

towards north-west. The CP anomaly here indicates a mineralisation (red top CP value) with a total strike length that is less than 100 m. This body has no electric contact with the ca. 400 m long mineralisation giving an anomaly at both EM31 and SP.

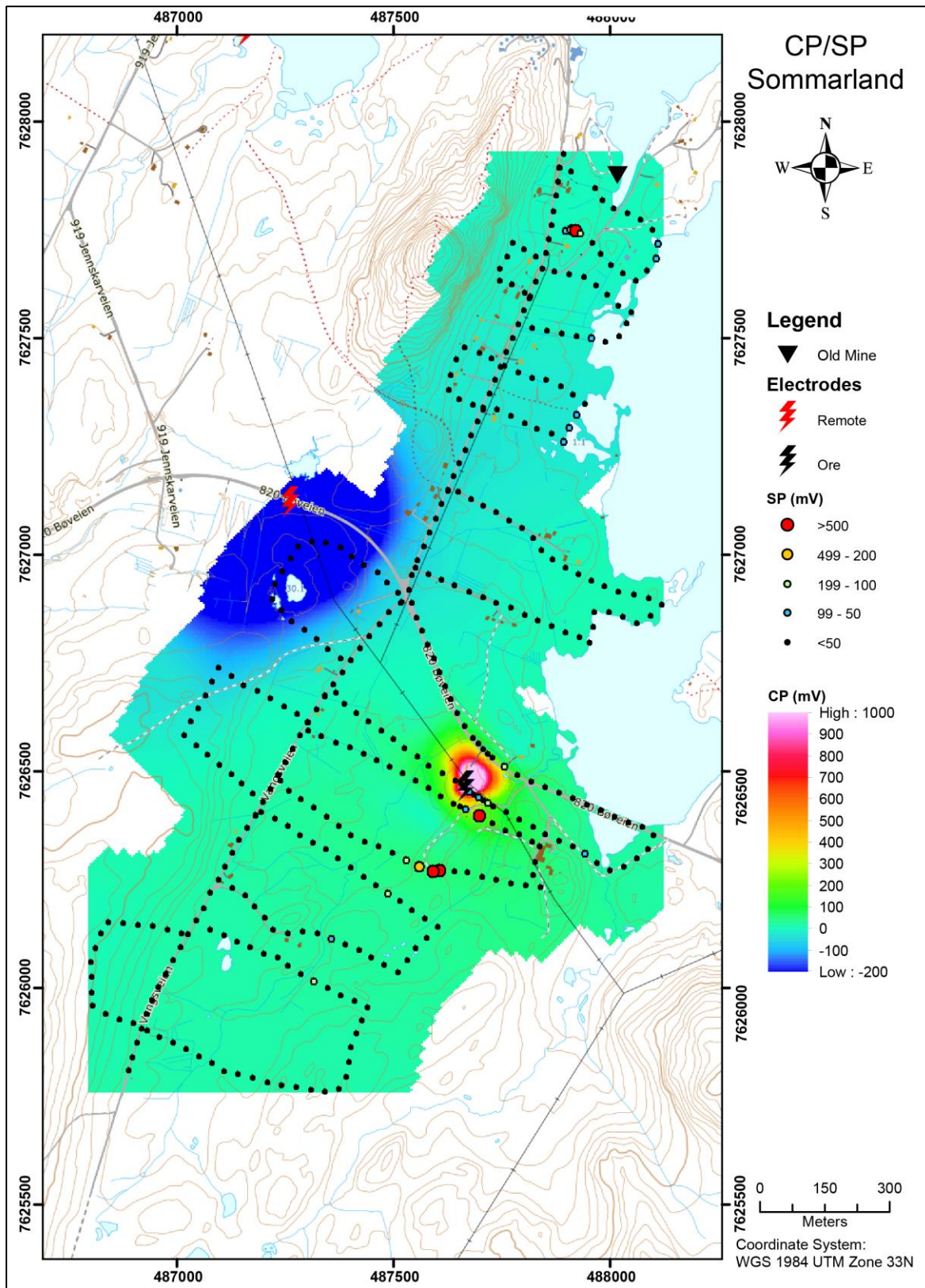


Figure 6.3: CP measurements with grounding point in the central part of the Sommarland area and SP data from the same area.

### 6.1.2 Example of an integrated interpretation of geophysical methods

The location of a line measured with EM31 (apparent conductivity and anomaly magnetic field) and inverted 2D resistivity and Induced Polarisation is shown in figure 6.4.

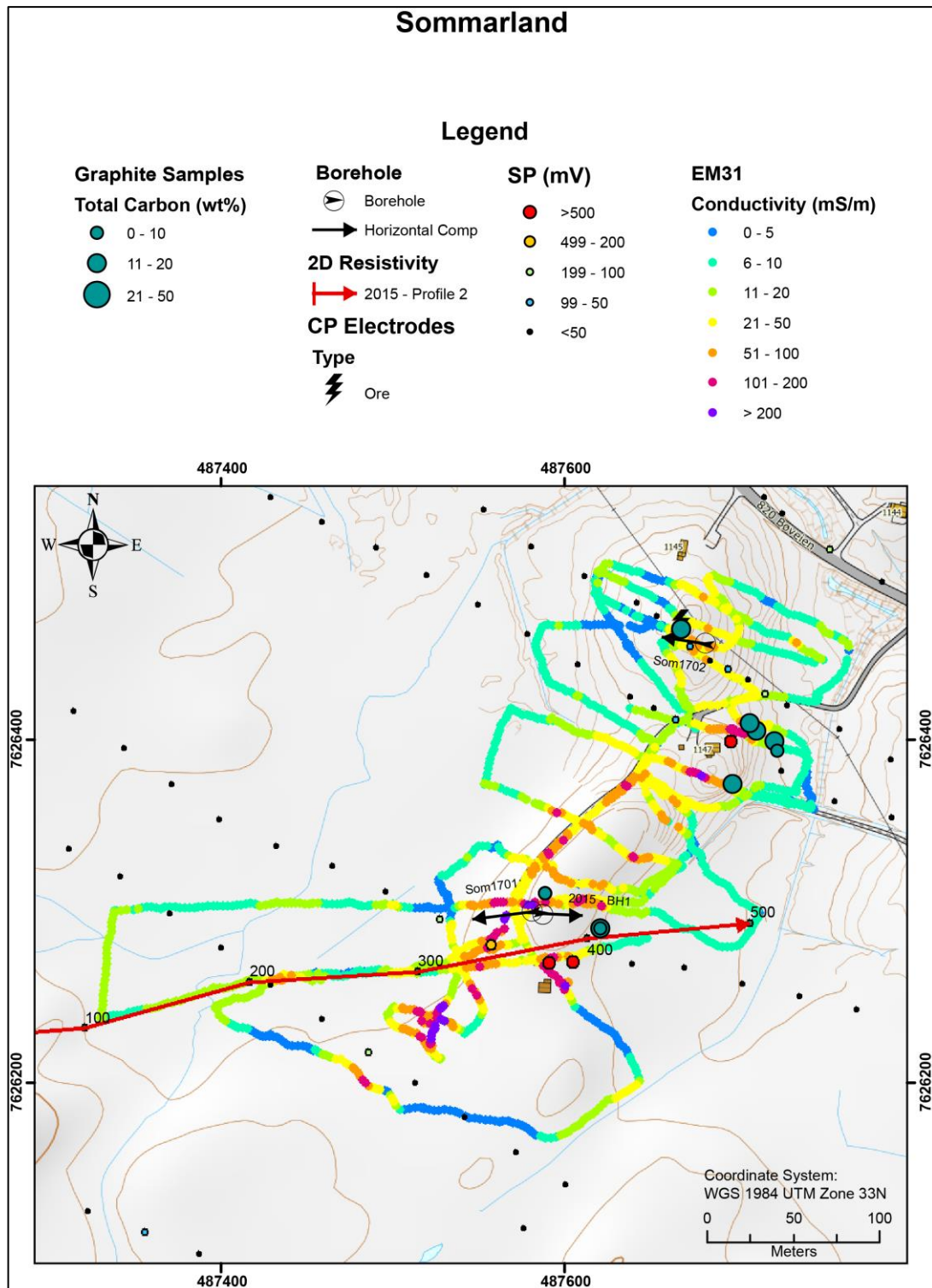


Figure 6.4: Location of the bore-holes in Sommarland (2015 Bh 1, Som1701 and Som1702), 2D Resistivity/IP profile from 2015 and graphite showings overlain on top of EM31 and SP anomalies.

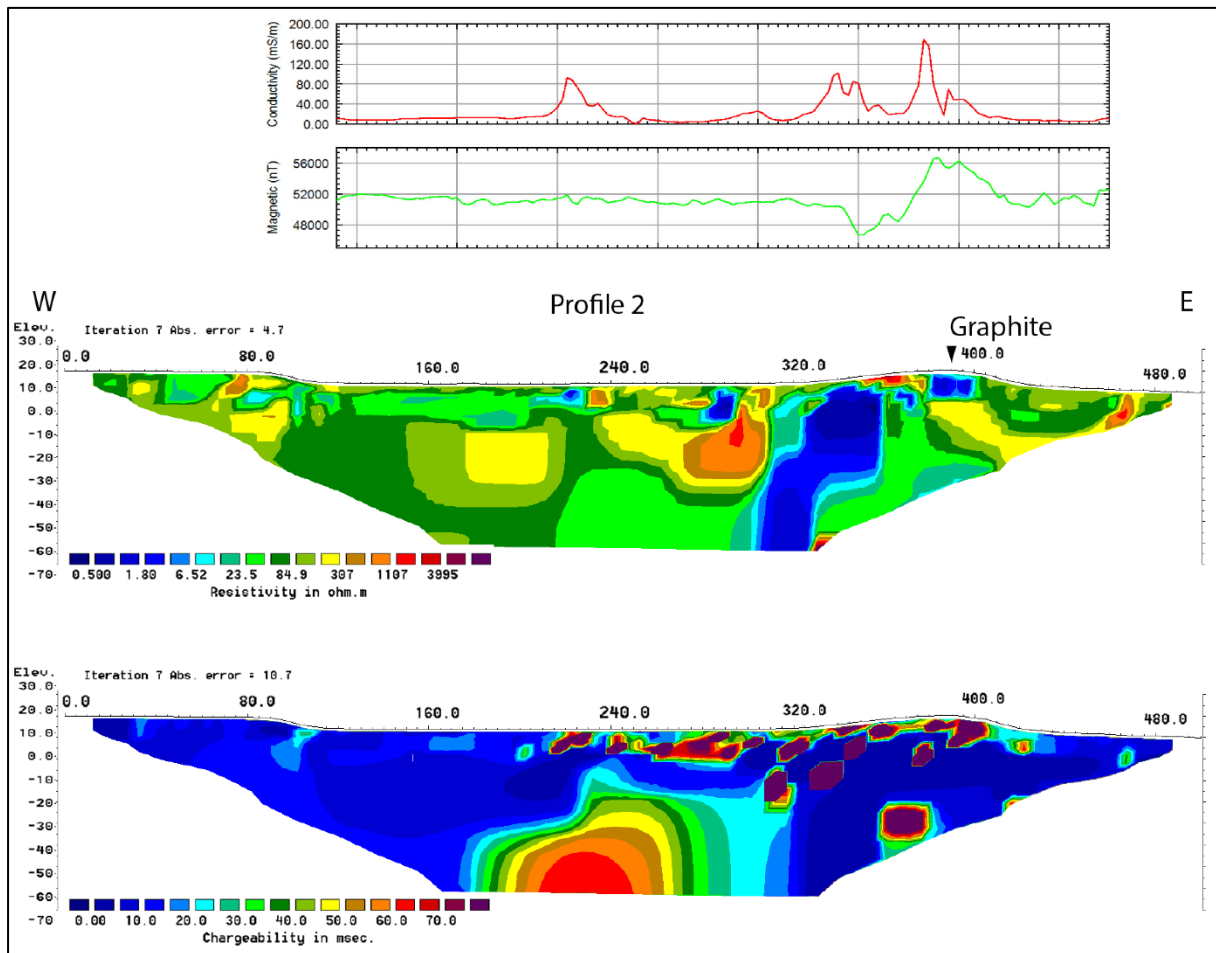


Figure 6.5: Apparent electric conductivity, magnetic total field measured with EM31, 2D Resistivity and 2D Induced Polarisation along almost the same line at Sommarland (see figure 6.4).

The apparent electric conductivity, measured with EM31 (upper part of figure 6.5), shows four anomalous conductive zones. Peak apparent conductivity ranges from ca. 80 to 160 mS/m (resistivity ca. 12 to 6  $\Omega$ m). This may represent graphite as graphite is exposed at position 400 in the resistivity profile. In detail, this may consist of two or more individual zones. In the interpretation of the anomalous zone thickness we use the full width half maximum (FWHM).

The total magnetic field, measured with the modified EM31 equipment, shows a decreased field in a width of ca. 25 m and an increased magnetic field in ca. 25 m. This may indicate an inhomogeneous graphite mineralisation. Low magnetic field coincides partly with elevated electric conductivity and may be an indicator of good graphite quality. Higher magnetic field is caused by magnetic minerals (pyrrhotite and iron oxides) and may be an indicator of a lowered graphite quality. However, this effect should be investigated further.

In the 2D resistivity profile measured in 2015 and first presented in Rønning et al. (2017), four low resistivity structures appear which coincide with the EM31 anomalies. Three of these anomalies appear to be shallow while the ca. 60 m wide structure from ca. position 300 to ca. position 360 go deeper than the penetration depth of this investigation method (70 m). The comparison of apparent conductivity measured with

EM31 and the 2D inverted resistivity profile demonstrates the effect of limited depth penetration for the EM31 instrument. The highest EM31 response (160 mS/m) coincides with outcropping graphite that appears as a shallow but good conducting (low resistivity) zone. The most pronounced resistivity zone, located between position 300 and 360 with a depth extend deeper than the penetrating depth of the resistivity method, gives a moderate peak apparent resistivity value (80 – 100 mS/m). This is probably due to the overburden thickness and the limited depth penetration of the EM31 instrument. Good conducting graphite mineralisation located deeper than ca. 10 m may not be located using the EM31 method.

Partly high IP effect (Chargeability in lower part of figure 6.5) indicates disseminated graphite with probable low quality. Massive graphite will not give an IP effect. Total absence of IP effect and low resistivity indicates conductive soil (clay and silt) or porous rock saturated with saline water.

In the majority of the profile, the resistivity in the area is less than 200  $\Omega$ m and the IP effect is absent. It appears that the graphite mineralisation at Sommarland is hosted in a porous rock with saline water and is probably the same kind as detected in the Møkland area (Rønning et al. 2017).

## 6.2 Geological observations, sampling and analyses

Just a few metres north of the houses at Sommarland, an old and partly overgrown exploration trench was investigated. The trench is ca.3 x 5 metres with a depth of 1.5 m from which rich graphite samples of apparently good quality were collected. These have an average of 15.2 % TC. Drill hole Som1702 was planned to penetrate this graphite lens at depth (see chapter 6.3 for details). In addition, loose boulders of rich graphite ore were found in several places. It is likely that during the period of mining at Kråkberget (ca. 1900-1918) exploration and test mining took place at Sommarland. Compiled TC analyses from all surface samples at Sommarland are shown in table 6.1.

**Table 6.1: Total Carbon (TC) data from 13 surface samples from the central Sommarland area.**

Locality	N	Average TC (%)	Max TC (%)	Min TC (%)	STdv TC
Central Sommarland	13	12.10	18.20	2.83	5.53

The data demonstrates that good carbon contents can be found at Sommarland. However, with the present degree of poor exposure, sampling and drilling alone are not sufficient to determine the graphite content with a high degree of confidence due to the geological complexity.

### 6.3 Core drilling Central Sommarland

Based on geological and geophysical data (Gautneb et al. 2017 and Rønning et al. 2017), NGU carried out core drilling in 2017 using the truck mounted equipment (Figure 4.5). Technical details of these two drill holes and the drill hole from 2015, are given in table 6.2. Figure 6.4 shows all anomalies from EM31 and SP measurements in addition to the locations of the drill holes and the graphite showings.

**Table 6.2: Technical data for the core drilling at Sommarland.**

Borehole	UTM Easting	UTM Northing	Azimuth (°)	Dip (°)	Length (m)
Bh 2015	487587	7626298	090	- 60	50,0
Som1701	487581	7626300	260	-45	49,1
Som1702	487682	7626456	276	-45	34,4

The drill hole Bh 2015 did not intersect graphite mineralisation, and therefore no data from this hole is presented. Petrophysical data from the Sommarland drill holes are discussed in chapter 12.2.

#### 6.3.1 Geological core logging

Figures 6.6, 6.7 and 6.8 show an EW section of lithological logs from the 2017 drill holes as well as portable XRF analyses (of among others Fe-S-Ni), Leco analysis of total carbon (TC) and total sulphur (TS). Figure 6.9 shows the location of the graphite schist in the field and its footwall host rock. Drill cores images are presented in Appendix 3.

The host rock to the graphite schists is strongly metamorphosed during two granulite facies episodes, and the effect of this metamorphism combined with compositional inhomogeneity, result in a very variable rock. Variations in average content of pyroxene and feldspar minerals are visible along drill cores as well as different degrees of metamorphism and recrystallisation. In addition to standard core observations, the geological core logging was undertaken with an added focus on iron and graphite content to obtain a better integration with the geophysical observations.

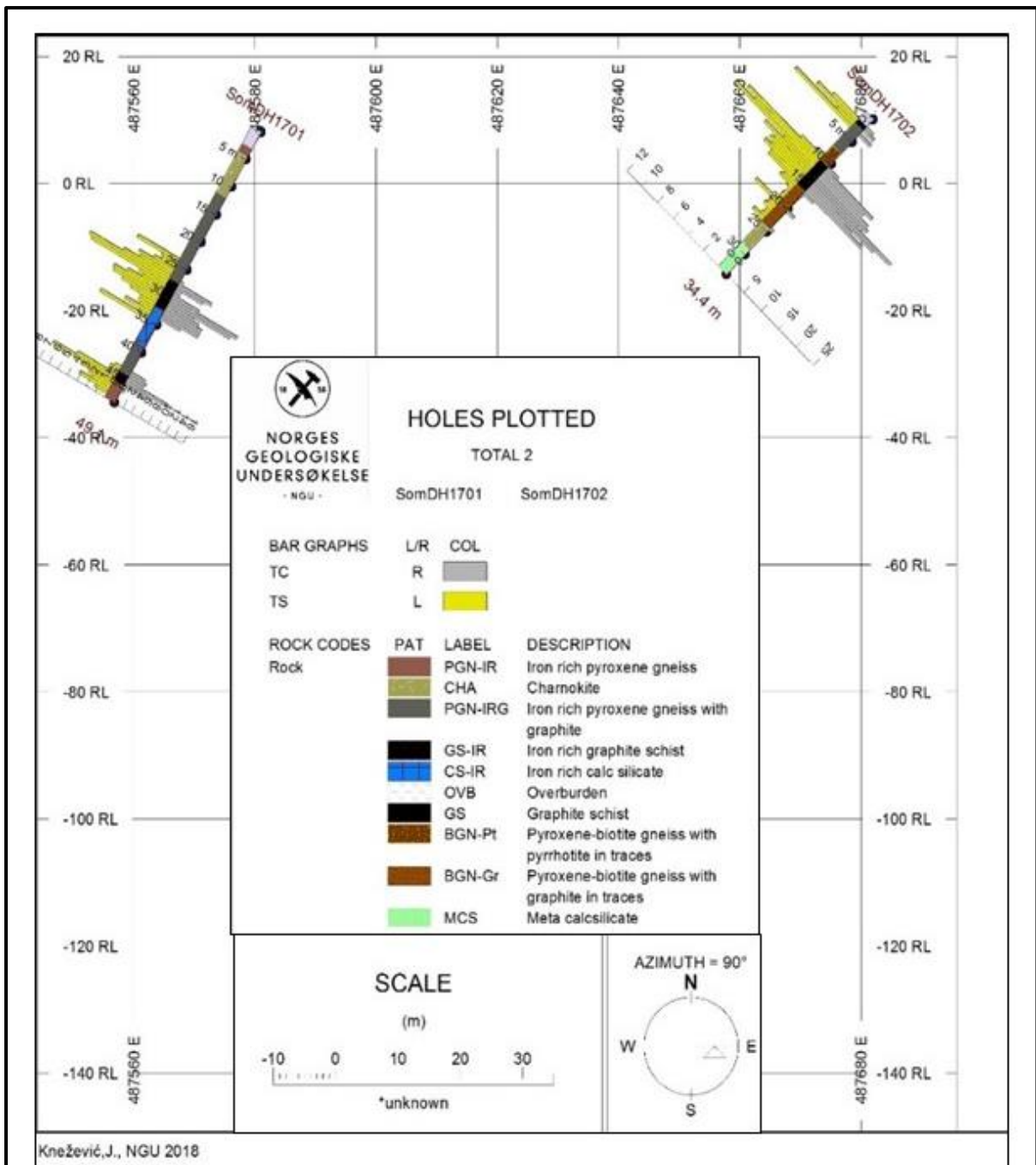


Figure 6.6: Lithological log and a graphical display of Total Carbon (TC in %) and Total Sulphur (TS in %) for the two drill holes at Sommarland acquired in 2017 (Som1701 and Som1702) seen from the south.

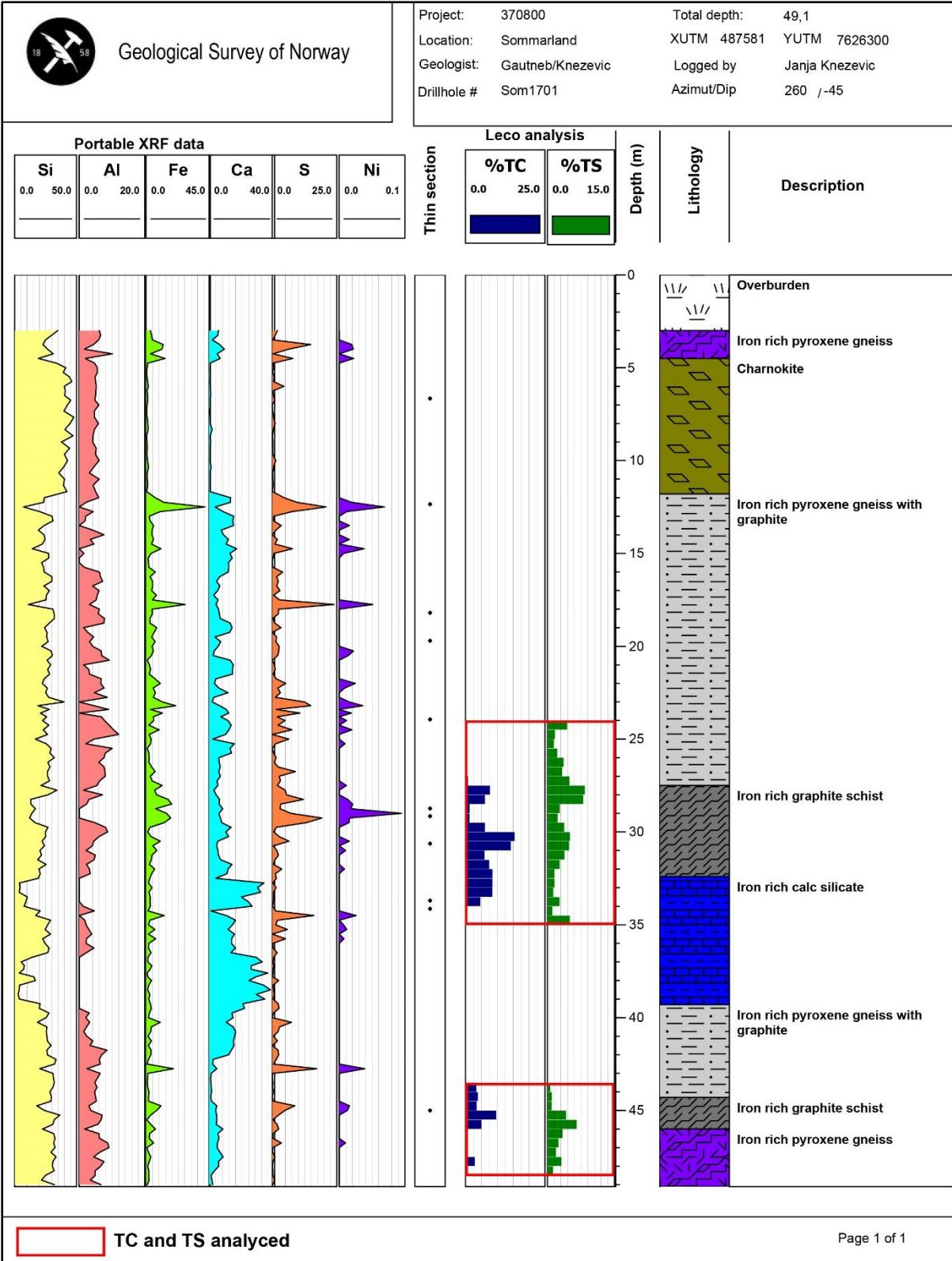


Figure 6.7: Portable XRF analyses of among others Fe-S-Ni, Leco analysis of total carbon (TC) and total sulphur (TS) in addition to the lithological log from drill hole Som1701.

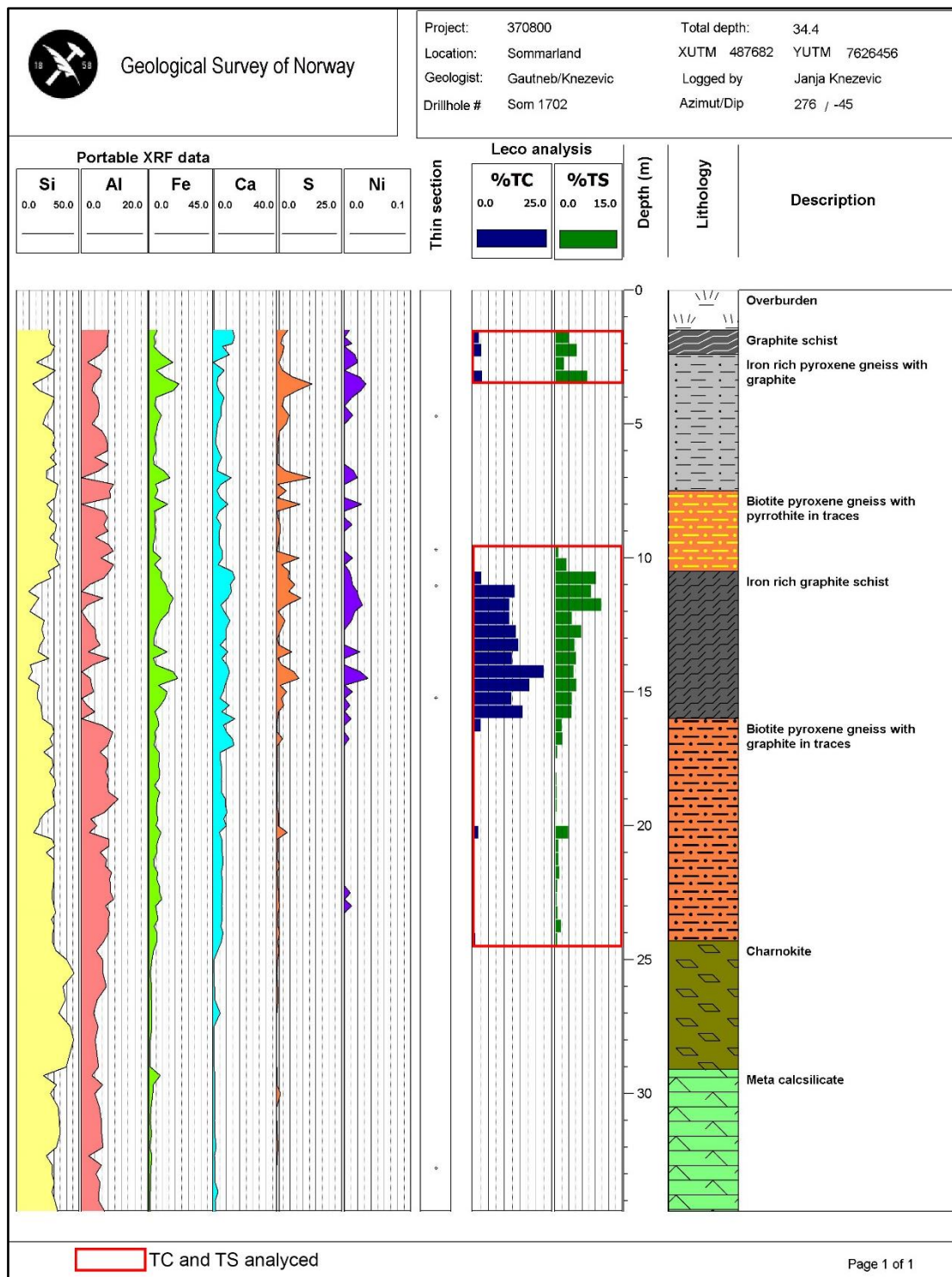


Figure 6.8: Portable XRF analyses of, among others Fe-S-Ni, Leco analysis of total carbon (TC) and total sulphur (TS) together with the lithological log from bore hole Som1702.

The portable XRF analyses (figures 6.7 and 6.8) show that there is a correlation between Fe, S and Ni. This probably demonstrates that the main Fe and S bearing mineral is dominantly pyrrhotite. This is also confirmed by the XRD analyses.

The host rock comprises of a pyroxene and plagioclase-rich rock with abundant iron sulphides together with mafic layers or veins rich in mica. Variable amount of pyrrhotite, pyrite, graphite, magnetite, amphibole, biotite and clay minerals are also

observed. In the drill hole Som1701 the graphite schist occurs with a calc-silicate rock in the foot wall (figure 6.9). In both drill holes at Sommarland younger intrusions of the 1800 Ma AMCG suite are observed (see Chapter2) (figures 6.6, 6.7 and 6.8).

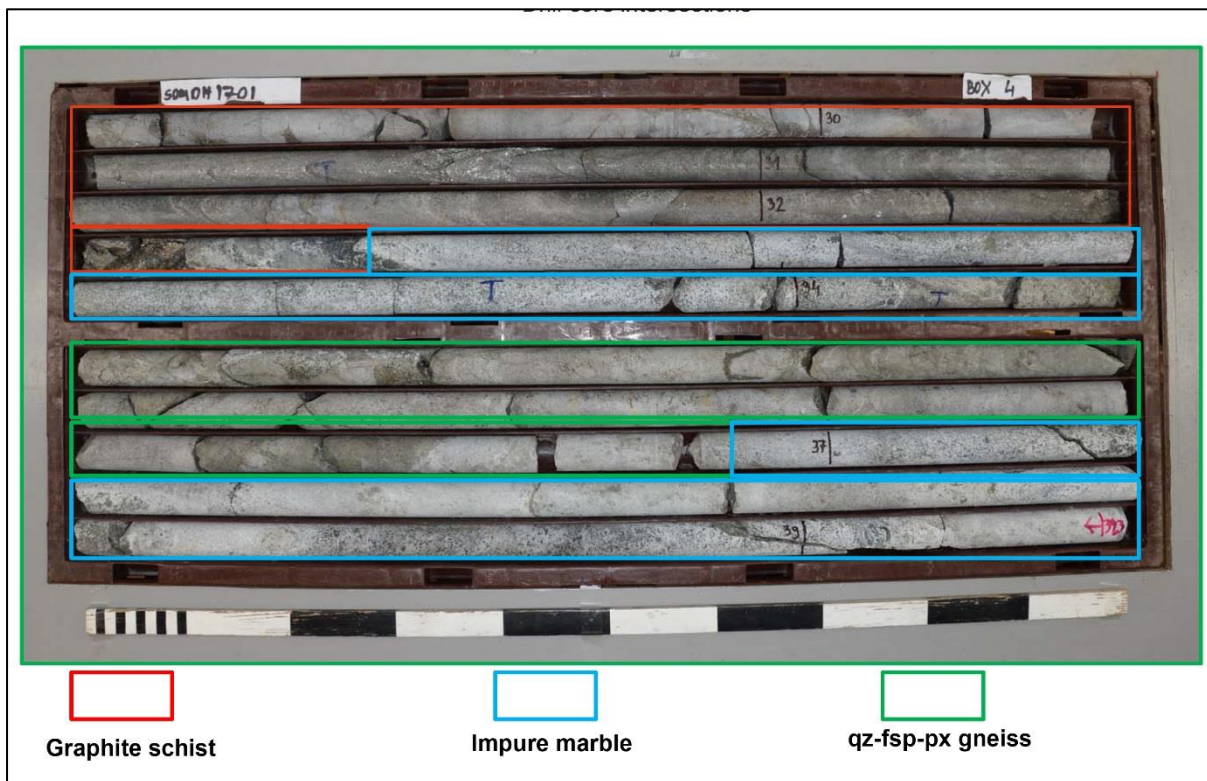


Figure 6.9: Part of drill core (dry upper and wet lower picture) showing a sequence with graphite schist, impure marble (calc-silicate rock) and quartz-feldspar-pyroxene gneiss. Appendix 3 show pictures of all drill cores from 2017 drilling.

In drill hole Som1701, the graphite schist occurs with an iron rich pyroxene gneiss with graphite in the hanging wall and a calc-silicate rock in the footwall. This is one of the few complete sections where the contact between graphite schist and calc-silicate rock can be observed (figures 6.9 and 6.10).

### 6.3.2 Mineralogy from thin sections

The following mineralogical description is based on analysis of thin sections from the drill cores (see figures 6.10 to 6.15).

A thin section of the calc-silicate host rock (impure marble) is shown in figure 6.10. Crystals of calcite and serpentine are shown.

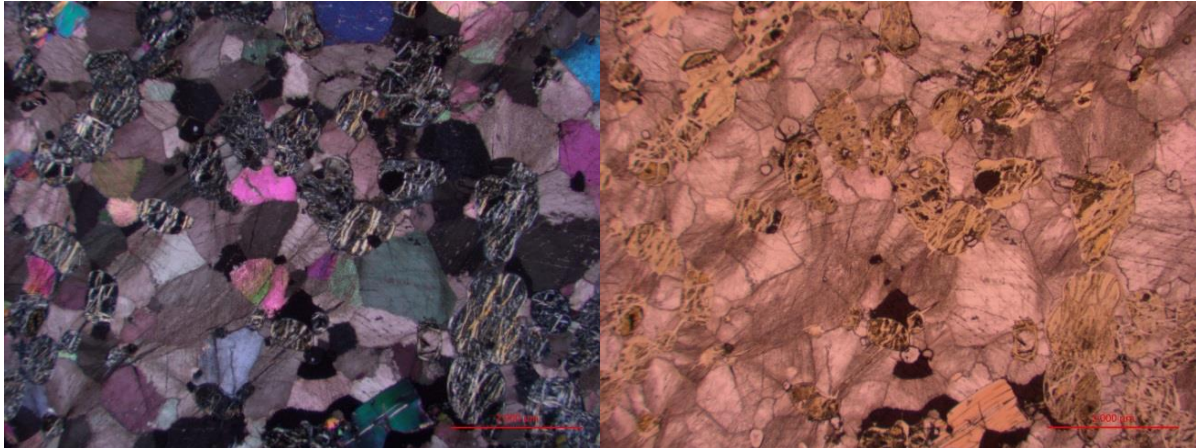


**Figure 6.10:** Thin section of calc-silicate rock show crystals of calcite and serpentine. Thin section HG-DhSom1701-33.7.

The pyroxene gneisses can in places contain patches of graphite without having the features of a typical graphite schist. The accessory minerals observed are titanite, zircon, rutile, chlorite, apatite and secondary clay minerals. The intervals with the most visible graphite were sampled. A thin section of a representative graphite schist is shown in figure 6.11.

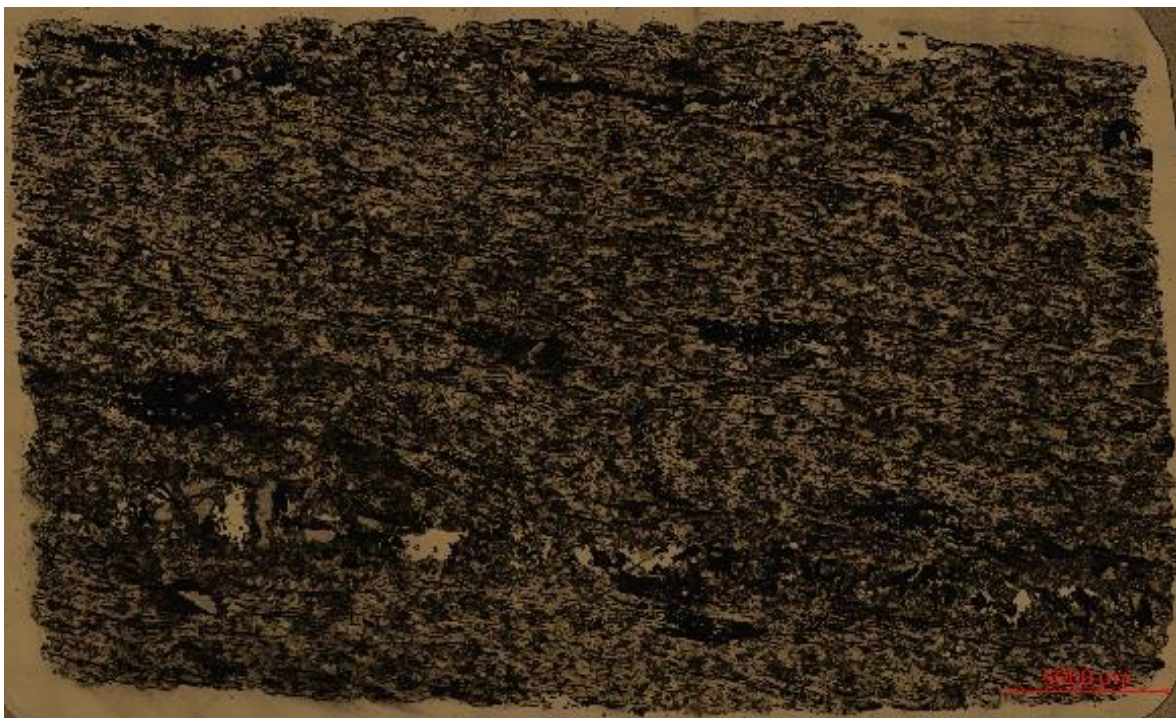


**Figure 6.11:** Iron rich graphite schist (transmitted light) TC 14,3%, TS 4,88% (30,5-31m). Thin section HG-DhSom1701-30.63.

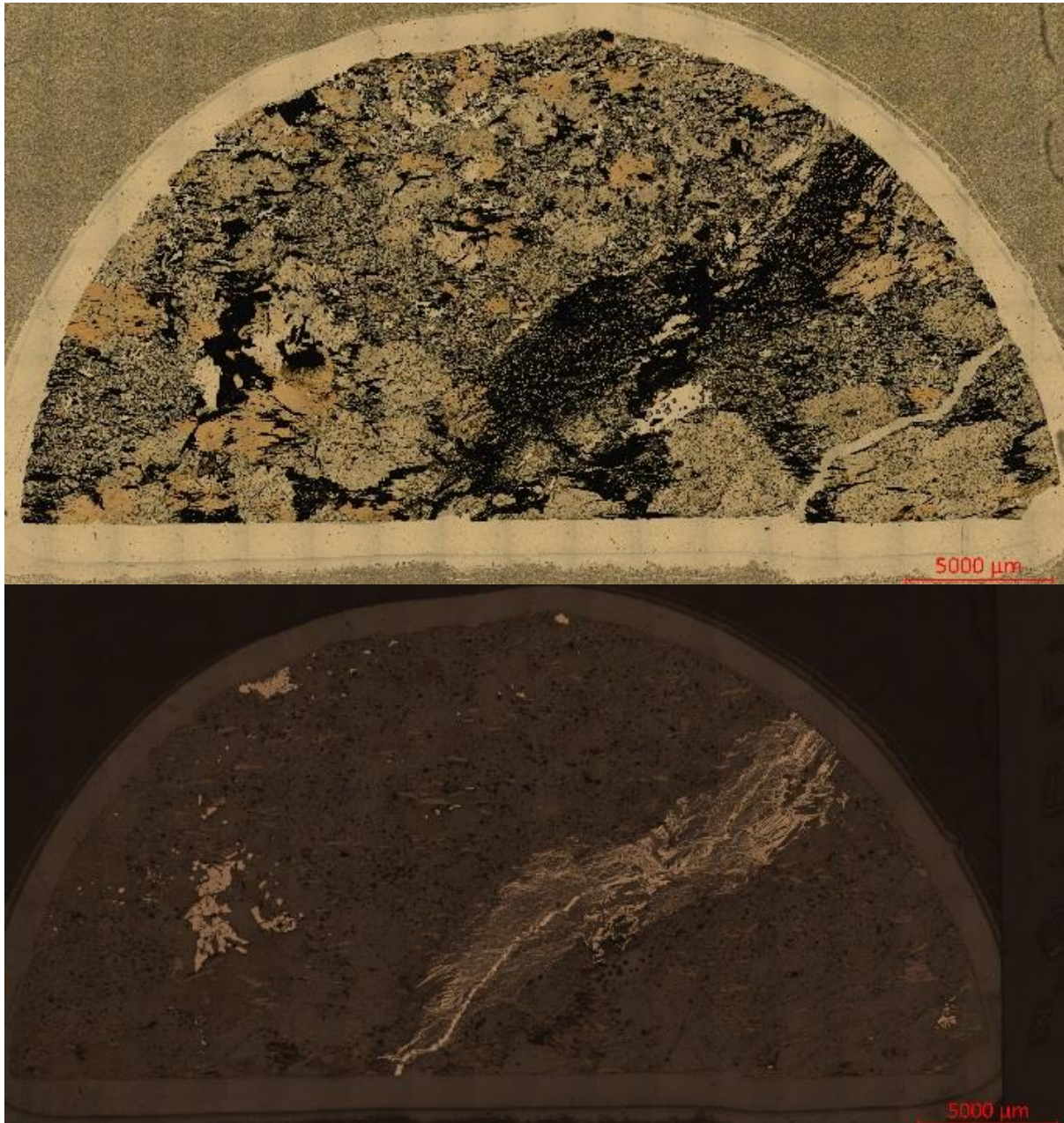


Figure 6.12: Thin section HG-DhSom1701-30.63, iron rich graphite schist in reflected light, TC 14.3 %, TS 4.88 % (30,5-31m).



Figure 6.13: Thin section JK-DhSom1701-19.7, host rock that contain graphite in veins and disseminated thin long graphite flakes and abundant iron sulphides.

In addition to the sampled graphite-rich zones, graphite is also present in traces amount almost along the whole drill core and occurs mainly as disseminated graphite and in mafic veins together with biotite, pyrrhotite, pyrite, mica and other minerals (figure 6.13).



**Figure 6.14: Thin section (JK-DhSom1-29.15) showing disseminated graphite with pyrrhotite vein, TC = 1,31% and TS = 2,32%( 29-29,5m)**

The richest graphite interval is 5 m long (DhSom1702, 11-16m) with an average TC of 12.4 % (figure 6.15).

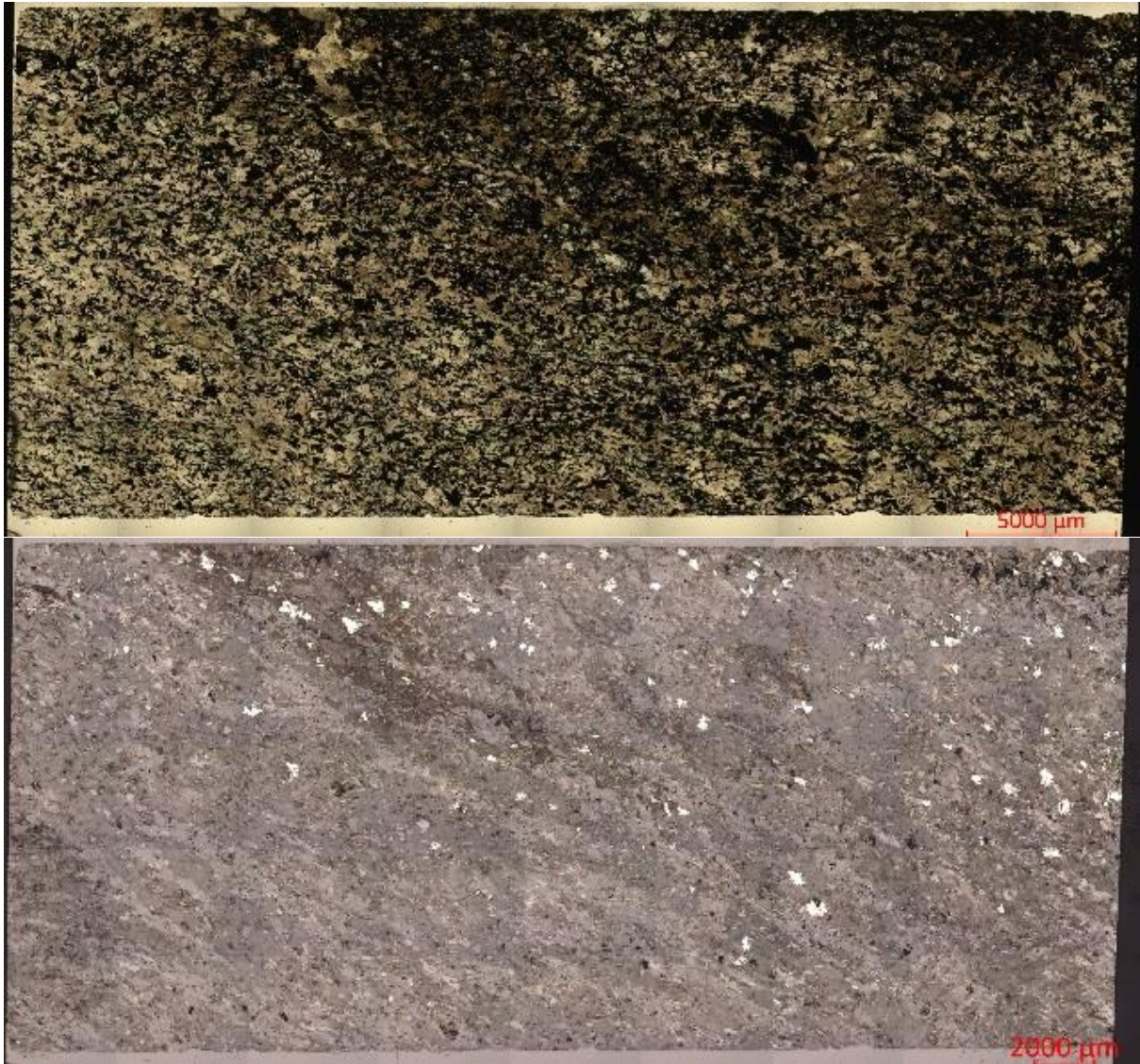


Figure 6.15: Thin section (Hg-DhSom1702-15.22) of the richest graphite interval, iron rich graphite schist with TC12,4%, TS 3,83% (15-15,5m).

### 6.3.3 Quality of the graphite at Sommarland

Samples from the drill holes were analysed for total carbon (TC) and total sulphur (TS) using a Leco SC-632 analyser at the NGU-lab. Analysed sections are shown in figure 6.14 and 6.15. All analyses are shown in Appendix 2.

The analyses of graphite bearing sections are summarized below. In Table 6.3 we have compiled sections of the different drill core with a graphite cut off 1 % and 3 % TC respectively.

**Table 6.3: Intervals and % TC at 1% and 3 % cut off in the drill hole at Sommarland.**

Drill hole	Cut off %	Interval from	Interval to	Interval length (m)	Average TC %
Som1701	1	27.5	34	6.5	7.4
Som1701	1	43	46	3	5.13
Som1702	1	1.5	2.5	1	2.56
Som1702	1	3	3.5	0.5	3.25
Som1702	1	10.5	16.5	6	12.72
Som1702	1	20	20.5	0.5	2
All average >1%				2.91	5.31
Som1701	3	27	28.5	1.5	6.96
Som1701	3	29	34	5	8.58
Som1701	3	43.5	46	2.5	5.13
Som1702	3	3	3.5	0.5	3.25
Som1702	3	11	16	5	14.7
All average >3%				2.9	7.72

The highest carbon content of 12.7 % and 14.7% are in sections of 6 and 5 metres respectively in drill hole Som1702 using a cut-off grade of 1% and 3%. Using the same cut-off grade, the average TC for all these zones are 5.31 % and 7.72 % for these two bore holes at Sommarland.

The graphite at Sommarland is of a type the graphite industry classifies as flake graphite (as in all graphite in Norway).

The field sampling, core logging and thin section images show that the graphite ore is a very inhomogeneous rock purely based on percentage of graphite. The flake size between several thin sections is also very variable. This means that grain size measurements of graphite flake size based on thin section image processing may not be representative.

The flake size distribution of graphite flakes after crushing and flotation is critical for the graphite industry. Gautneb et al. (2017) report the results of a bench scale trials using graphite ore that is similar to the Sommarland graphite and from a nearby locality (Møklund). The results show that the graphite ore can be upgraded using standard methods to qualities similar to what is sold on the market today. Similar results were reported by Øzmerih (1991) from beneficiation trials of graphite from Lille Hornvann in the Jennestad area.

## 6.4 Geophysics Kråkberget, Sommarland East and Sommarland South

At **Kråkberget**, 1.5 km north of Sommarland, some SP and EM31 measurements have been performed (Figure 6.2 and Figure 6.16). The area is surrounded by seawater on three sides and as a result the apparent resistivity from helicopter-borne EM measurements is partly censored. The EM31 measurements (Figure 6.16) show several high apparent conductivity values. Apparent conductivity higher than 200 mS/m (apparent resistivity  $< 5 \Omega\text{m}$ ,) indicates graphite mineralisation. SP (Figure 6.2) shows one anomaly  $> 500$  mV, and this coincide with high apparent electric conductivity from EM31 measurements. The anomalous readings at both EM31 and SP indicate graphite. The abandoned Kråkberget graphite mine is found adjacent to these anomalies. Unfortunately, the strike length is  $< 150$  m and the potential for interesting graphite is limited. Despite the very low resistivity from helicopter-borne EM measurements, the ground follow-up study does not show graphite. The low apparent resistivity measured from helicopter appears to be an effect of saline water in soil and bedrock.

The **Sommarland East area** lies ca. 1 km east of Central Sommarland on both sides of the main road in the area (Jørlandsveien). EM31 measurements are performed in two areas (Figure 6.17). Apparent conductivity in both areas are limited to a maximum of 50 mS/m (apparent resistivity  $> 20 \Omega\text{m}$ ). Although the apparent conductivity is low, graphite of good quality cannot be excluded since low electric conductivity might be caused by the thickness of the soil. From helicopter-borne EM data, the total length along the strike of the northern possible mineralisation can be interpreted to be ca. 800 m while the length of the southern structure is interpreted to be  $< 500$  m. To obtain information on the type of mineralisation and quality, trenching or core drilling is necessary.

The **Sommarland South** area lies ca. 2 km south-west of Central Sommarland. EM31 measurements are performed in a triangle (Figure 6.18). Apparent conductivity higher than 100 mS/m (apparent resistivity  $< 10 \Omega\text{m}$ ) was measured at three locations and these anomalies indicates graphite mineralisation. From the helicopter-borne EM measurements, a strike length of ca. 1 km is interpreted, and it is likely that the mineralisation continues under the lake in the area. The half peak value width of the EM31 anomalies (see section 6.2.1) varies from ca. 10 m up to 20 m, which indicates that graphite may have a considerably thickness. However, this thickness might also be the result of several thinner graphite structures. To obtain information on the type of mineralisation and quality, trenching or core drilling is necessary.

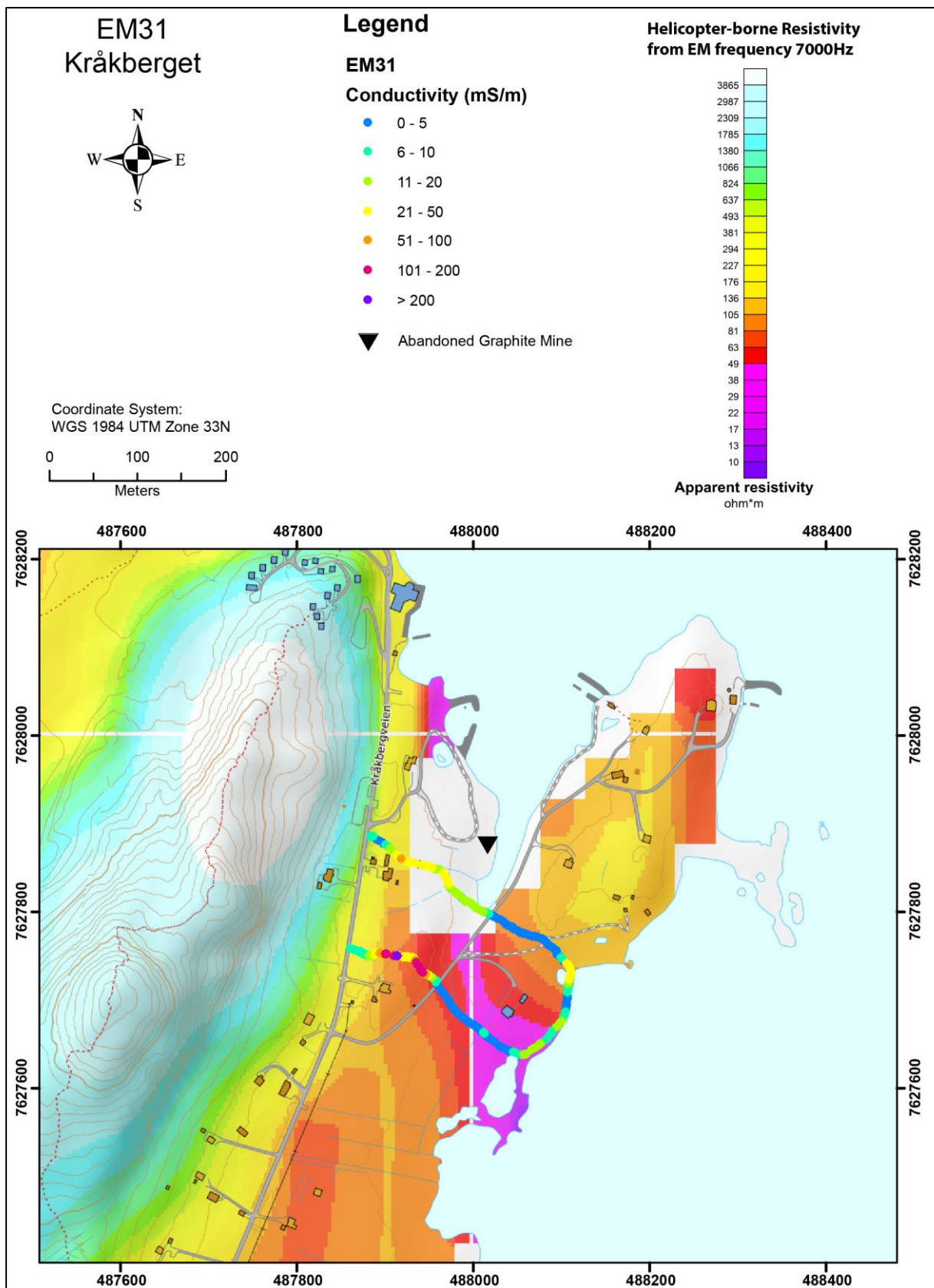


Figure 6.16: Kråkberget north of Sommarland. Results from EM31 measurements overlain on top of helicopter-borne measurements of apparent resistivity from EM 7000 Hz coaxial coil configuration.

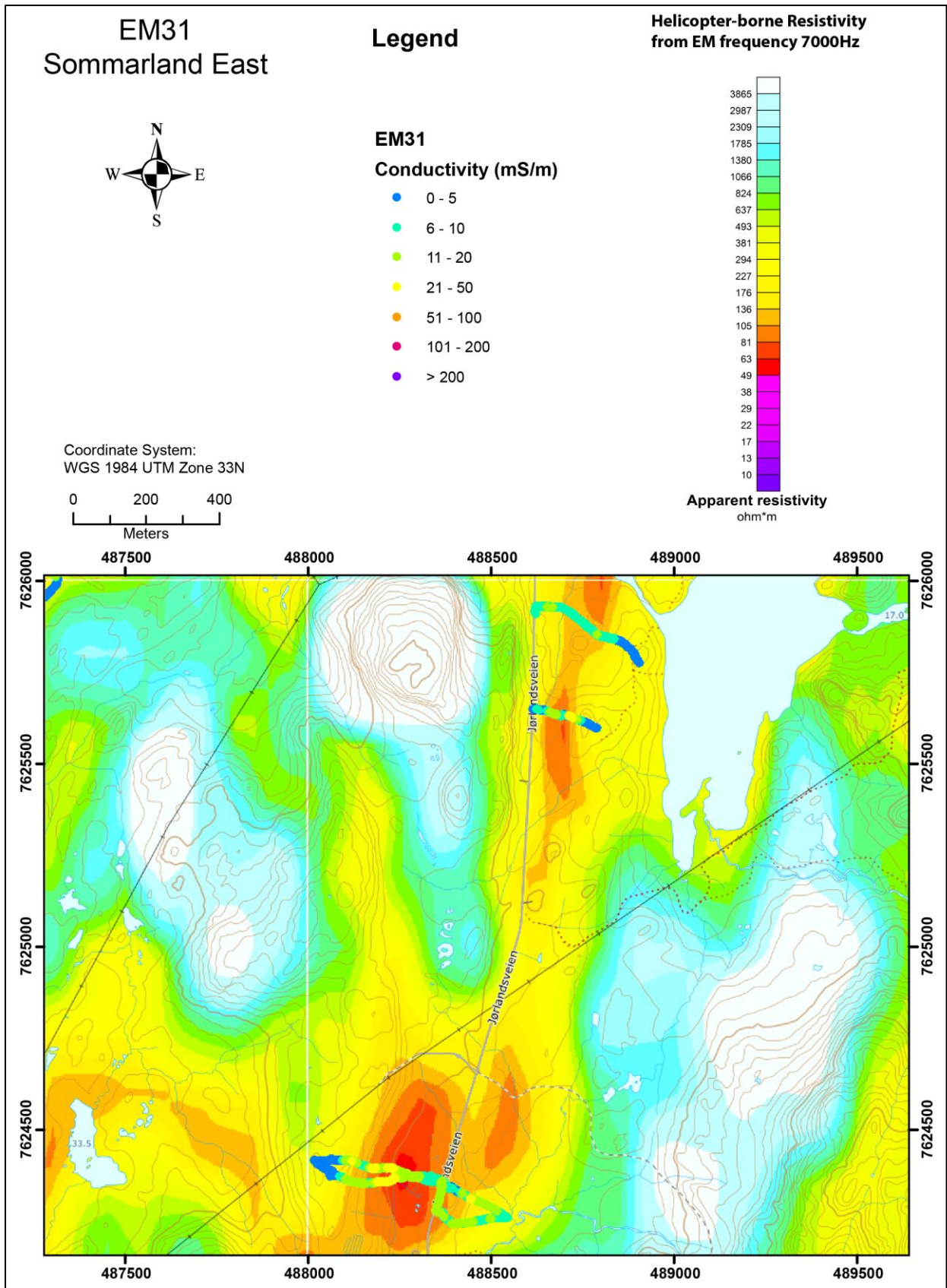


Figure 6.17: Sommarland East. Results from EM31 measurements overlain on top of helicopter-borne measurements of apparent resistivity from EM 7000 Hz coaxial coil configuration.

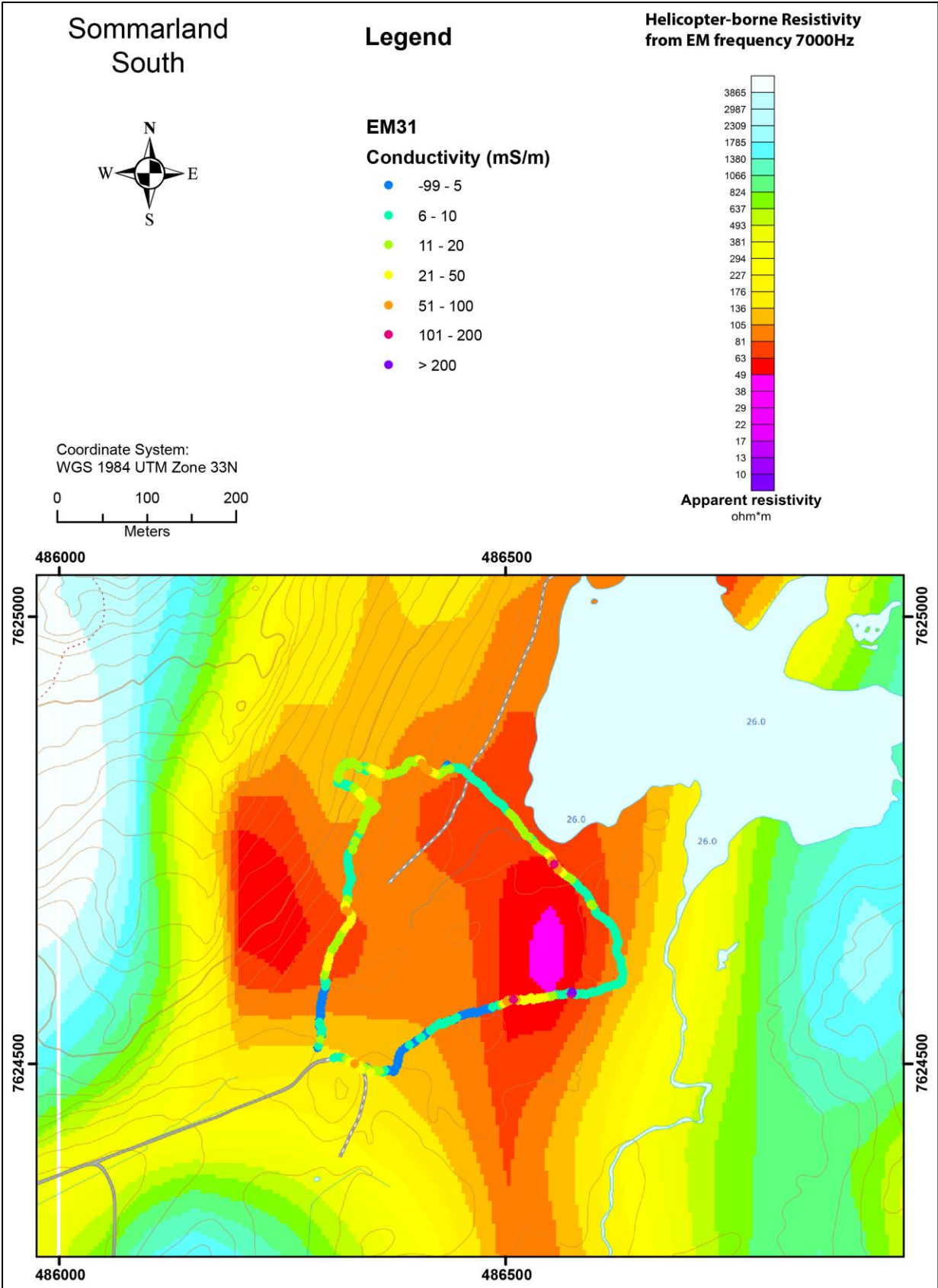


Figure 6.18: Sommarland South. Results from EM31 measurements overlain on top of helicopter-borne measurements of apparent resistivity from EM 7000 Hz coaxial coil configuration.

## 6.5 Sommarland summary

A summary of the results from the investigations at the Sommarland area is given in table 6.4. Interpreted potential graphite structures from the Central Sommarland area are shown in Figure 6.19. For details, see the text for the different areas.

**Table 6.4: Interpreted length, width, mean Total Carbon (TC) analyses in ground samples and in drill holes for the individual zones at Sommarland.**

Area / zone	Ca. length (m)	Ca. width (m)	Mean TC ground (%)	Mean TC Core drilling (%)	Comment
Sommarland A	< 100	Som1702 4	15.2	See Table 6.3 14.7	Cut by Som1702
Sommarland B	400	Som1701 4	?	See Table 6.3 8.6	Cut by Som1701
Sommarland C	300		Unknown		Not exposed graphite
Sommarland D	< 100		14.20 %		
Sommarland E	< 100?		7.74		
Kråkberget	< 150?		18.0 old data		
Sommarland East	800 < 500		Unknown		Not exposed graphite
Sommarland South	1000		Unknown		Not exposed graphite

The total length of graphite structures in the Central Sommarland area is ca. 1000 m and the average width of these may be up to ca. 4 m (confirmed in two drill holes). The full width half maximum (FWHM) of the EM31 anomalies (see section 6.2.1) varies from ca. 2 m up to 20 m, which indicates that graphite is irregular but might have a considerably thickness.

Assuming the mineralisation can be continuous down to 100 m, the total volume of the graphite mineralisation is ca. 400,000 m<sup>3</sup>. Assuming an average total carbon (TC) concentration from the two drill holes and surface samples (12 %), the tonnage of flake graphite is ca. 100,000 tons (graphite density 2.2 t/m<sup>3</sup>).

The Kråkberget abandoned graphite mine appears to have a strike length which is too limited to be of economic interest. However, the depth penetration with the EM31 measurements is relatively shallow and this could mean there is more, undetected graphite at depth.

The Sommarland East area does not show conductivity values that can be associated with graphite, but this can also be the result of thick soil cover. If this is the case, then further work could be core drilling.

In the Sommarland South area 2 to 3 structures are interpreted with an apparent conductivity that may be caused by graphite. The total length of these can be ca.

1000 m and the thickness might be of economic interest. Further work with EM31 measurements and possible trenching is recommended.

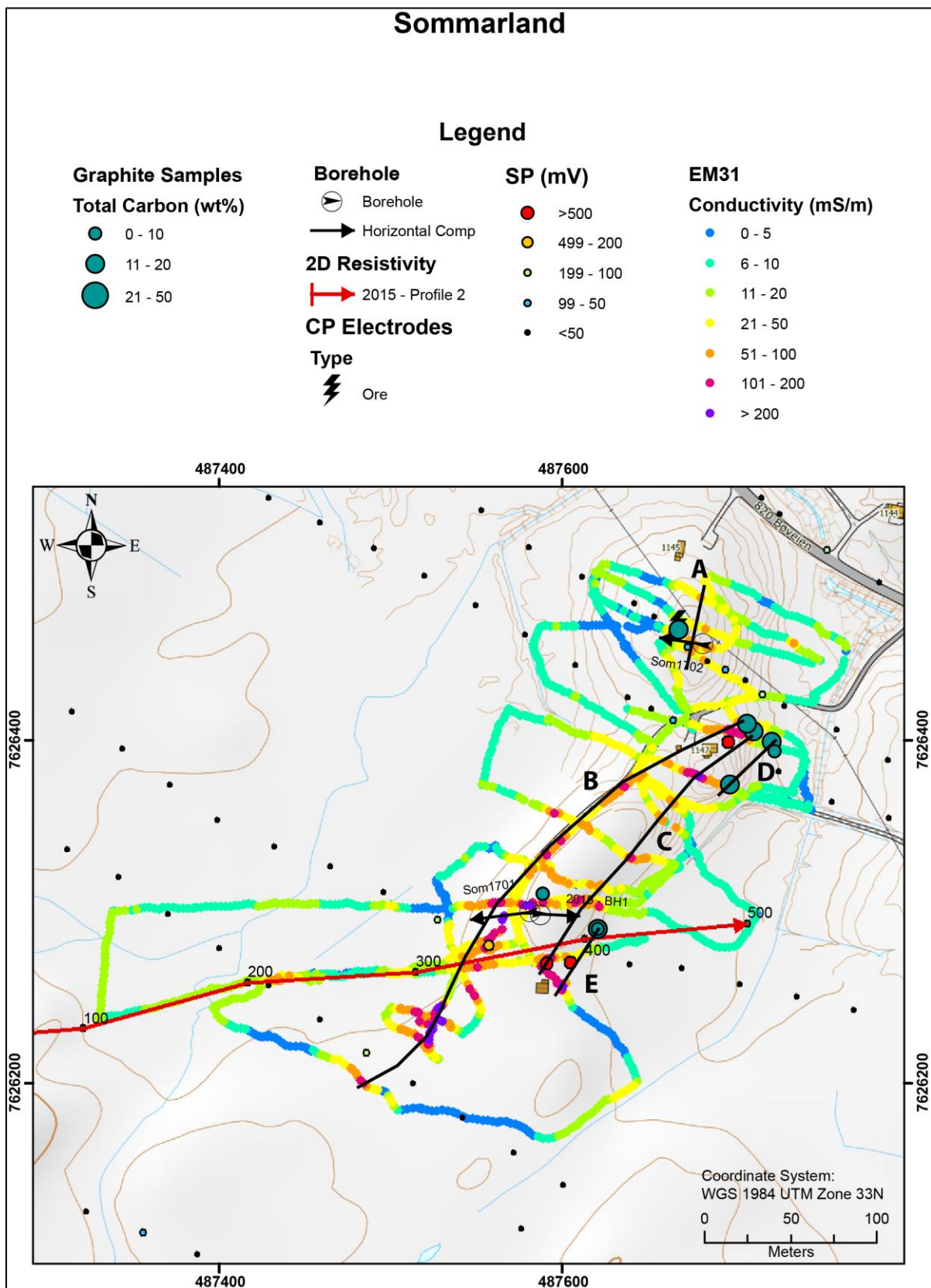


Figure 6.19: Central Sommarland. Interpreted main graphite structures based on EM31, SP and CP data.

## 7. RESULTS OF FOLLOW-UP WORK AT HAUGSNES, BØ MUNICIPALITY

During the field season of 2017, NGU performed geophysical measurements, some geological sampling and core drilling of two short drill holes at Haugsnes.

### 7.1 Geophysics Haugsnes

In the Haugsnes area in Bø municipality some geological and geophysical work has been performed earlier (Neumann 1952, Gautneb et al. 2017 and Rønning et al. 2017). The 2016 investigations in the Haugsnes area can be summarised thus (Rønning et al. 2017):

*Graphite analyses on 11 samples from an outcrop at Haugsnes show an average graphitic carbon content of 19.3 % and a maximum value as high as 33.8 %. This, in combination with a ca. 2 km long EM anomaly from helicopter measurements, and possible graphite mineralisation in a width of up to 80 m, makes this area of special interest. Although this area is populated, NGU aims to do more work on this location: EM31 profiling, possible drilling, trenching, sampling and chemical analysis. Combined CP/SP measurements are also of interest.*

In 2017, NGU performed extensive measurements with EM31, Self Potential (SP) and Charged potential (CP) with one grounding electrode. In addition, core drilling of two bore holes was carried out.

The results from **EM31** measurements at **Haugsnes** are presented in figure 7.1 (northern part) and Figure 7.2 (southern part) integrated with apparent resistivity from helicopter-borne EM measurements with 7000 Hz coaxial coils. This coil configuration favours vertically conducting structures. A large number of anomalous apparent conductivity readings  $> 50$  mS/m (apparent resistivity  $< 20$   $\Omega$ m) are shown. Partly, the apparent conductivity is  $> 200$  mS/m (apparent resistivity  $< 5$   $\Omega$ m) indicating graphite. Graphite is exposed along some of the conducting structures and it is reasonable to believe that all the conducting structures represent graphite.

**SP data** for the whole Haugsnes area is presented in figure 7.3. Several SP anomalies, some of them  $> 500$  mV, are mapped. Anomalies  $> 500$  mV are more frequent in the southern part of the Haugsnes area. As we shall see in the summary, these coincide with high apparent conductivity from EM31 measurements, and it is reasonable to believe that they are caused by graphite.

**CP data** for the whole of the Haugsnes area is presented in figure 7.4. The contact with graphite was established in a showing at coordinate 488355 - 7619264 and the remote electrode was placed at coordinate 488890 - 7619577 (UTM Zone 33). The total variations in CP is as low as ca. 18 mV while at Sommarland the top potential was ca. 1000 mV. This is a strong indication of electric contact with seawater and current leakage. Higher potential in the northern part of the area is consistent with seawater contact. Apart from this, no additional information can be extracted from the CP results.

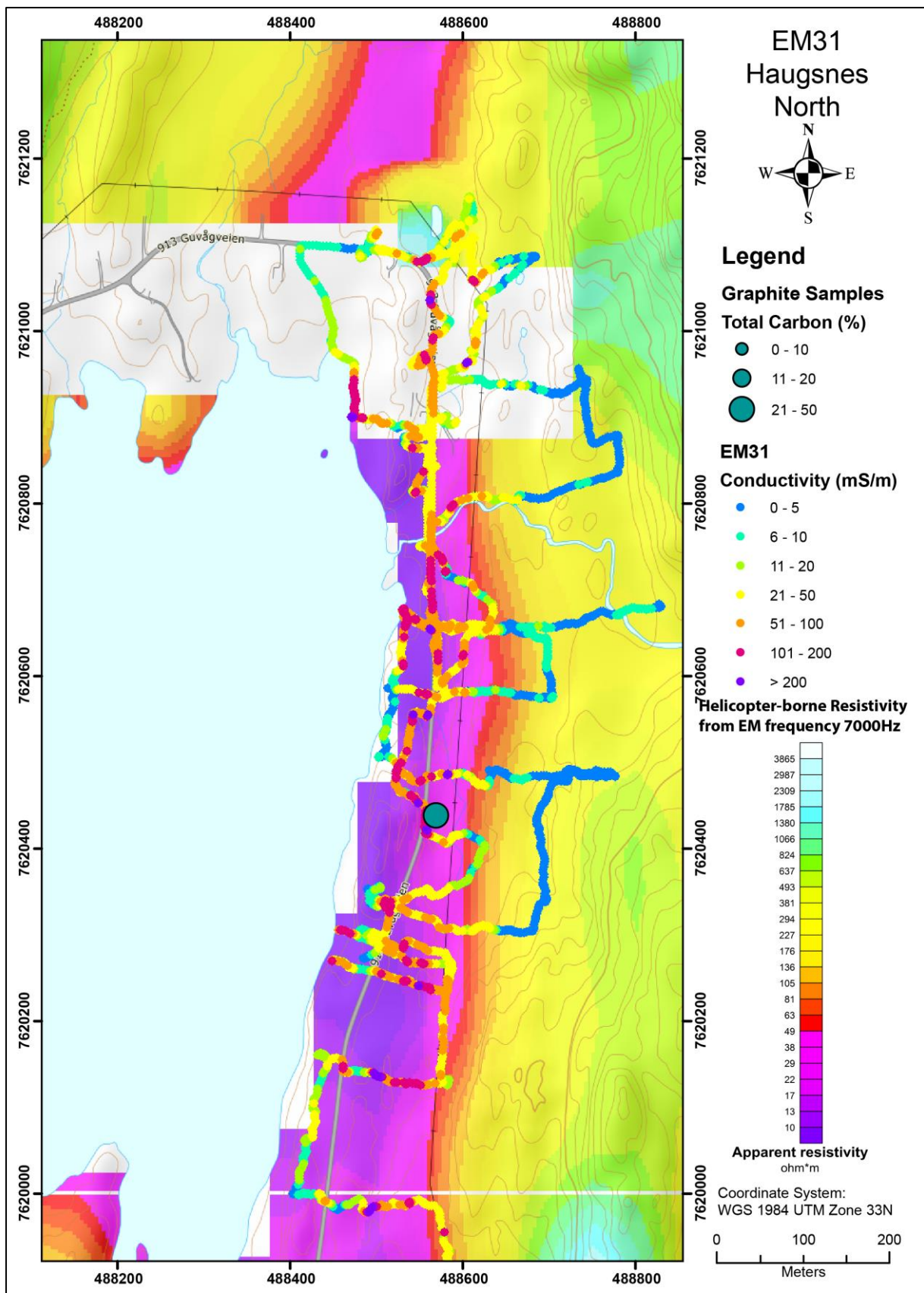


Figure 7.1: The northern part of Haugsnes. Results from EM31 measurements overlay on top of helicopter-borne measurements of apparent resistivity from EM 7000 Hz coaxial coil configuration.

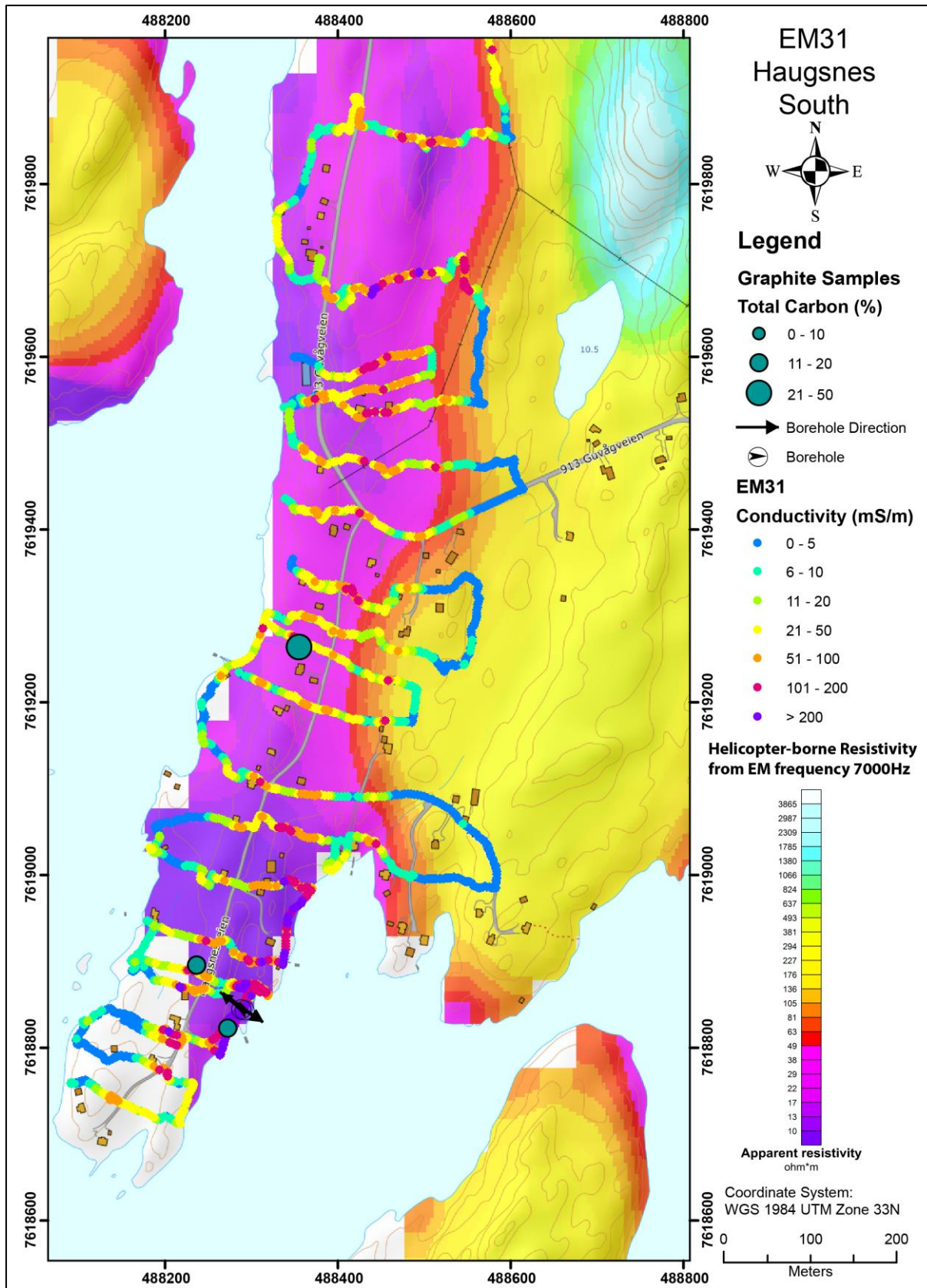


Figure 7.2: The southern part of Haugsnes. Results from EM31 measurements overlain on top of helicopter-borne measurements of apparent resistivity from EM 7000 Hz coaxial coil configuration.

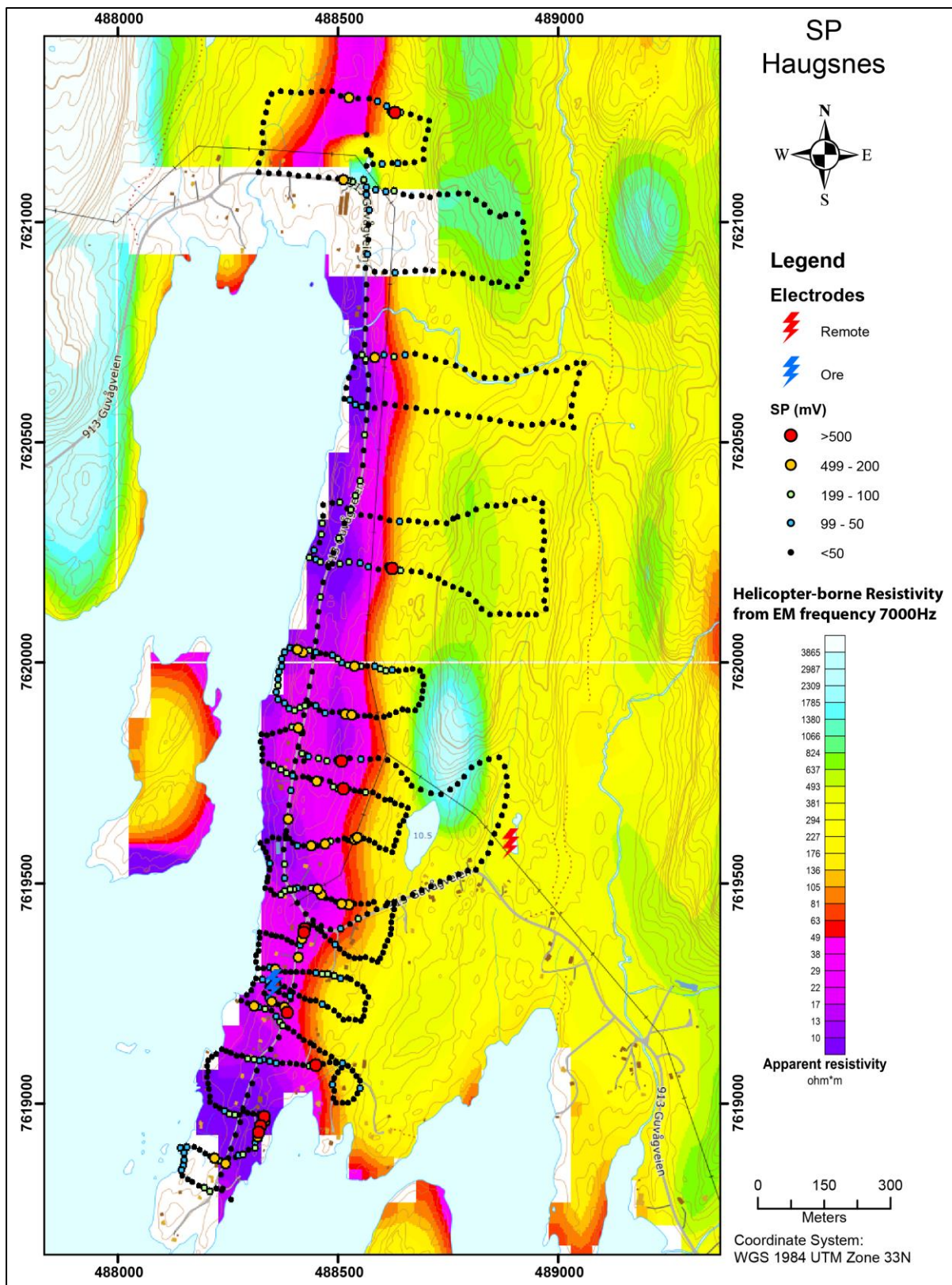


Figure 7.3: Results from SP measurements at Haugsnes overlain on top of helicopter-borne measurements of apparent resistivity from EM 7000 Hz coaxial coil configuration.

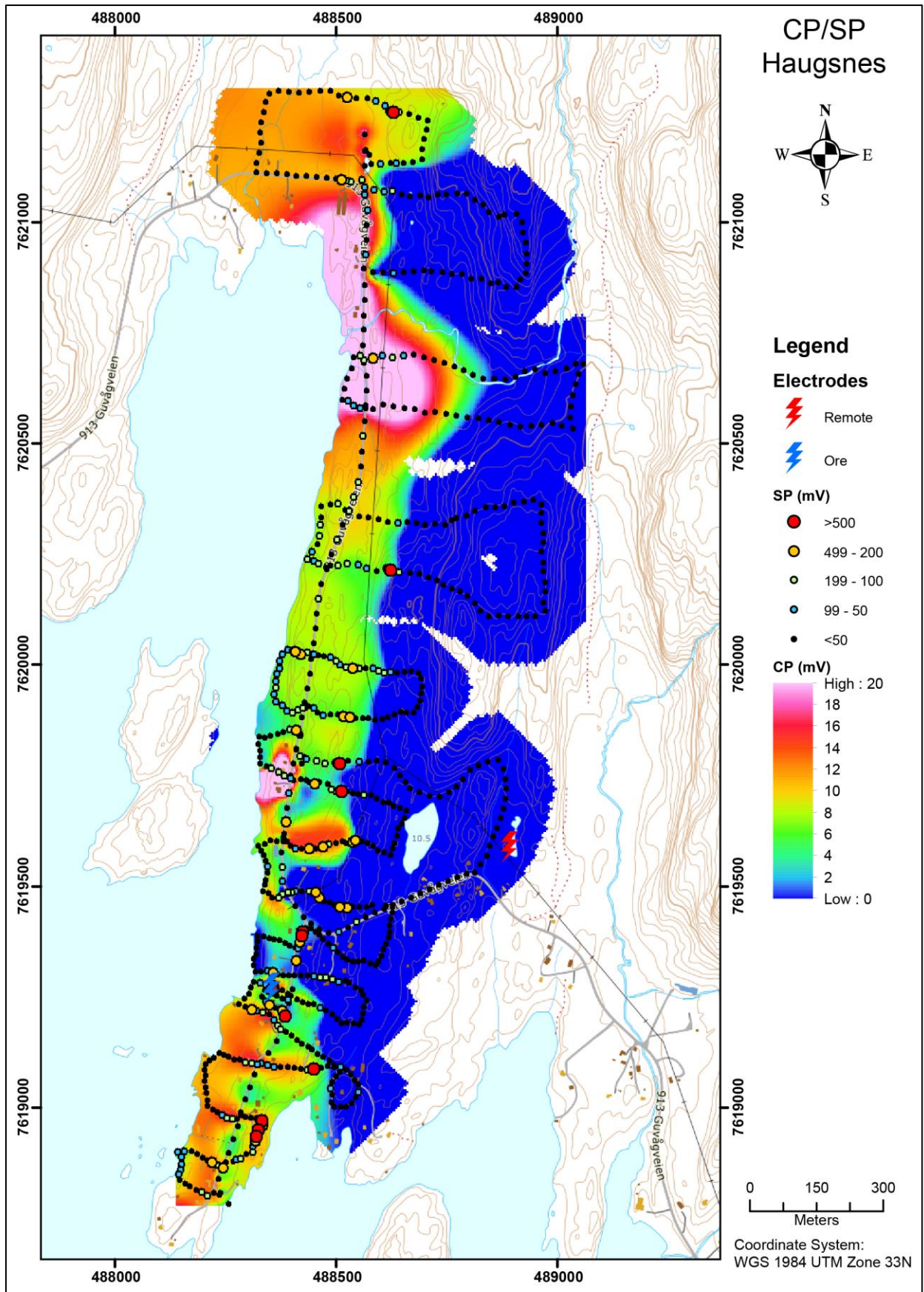


Figure 7.4: Results from CP measurements at Haugsnes

## 7.2 Core drilling at Haugsnes

Based on results from 2016 (Gautneb et al. 2017 and Rønning et al. 2017), NGU core-drilled two drill holes from the same locality at Haugsnes with the truck mounted equipment (Figure 4.5) in 2017. Technical details of these two drill holes are given in table 7.1. The location of the drilling at Haugsnes is shown in figure 7.5 together with results from SP and EM31 measurements.

**Table 7.1: Technical data for core drilling at Haugsnes.**

Bore hole	UTM Easting	UTM Northing	Azimuth (°)	Dip (°)	Length (m)
Haug1701	488288	7618844	310	-45	32,4
Haug1702	488293	8718843	123	-60	50,3

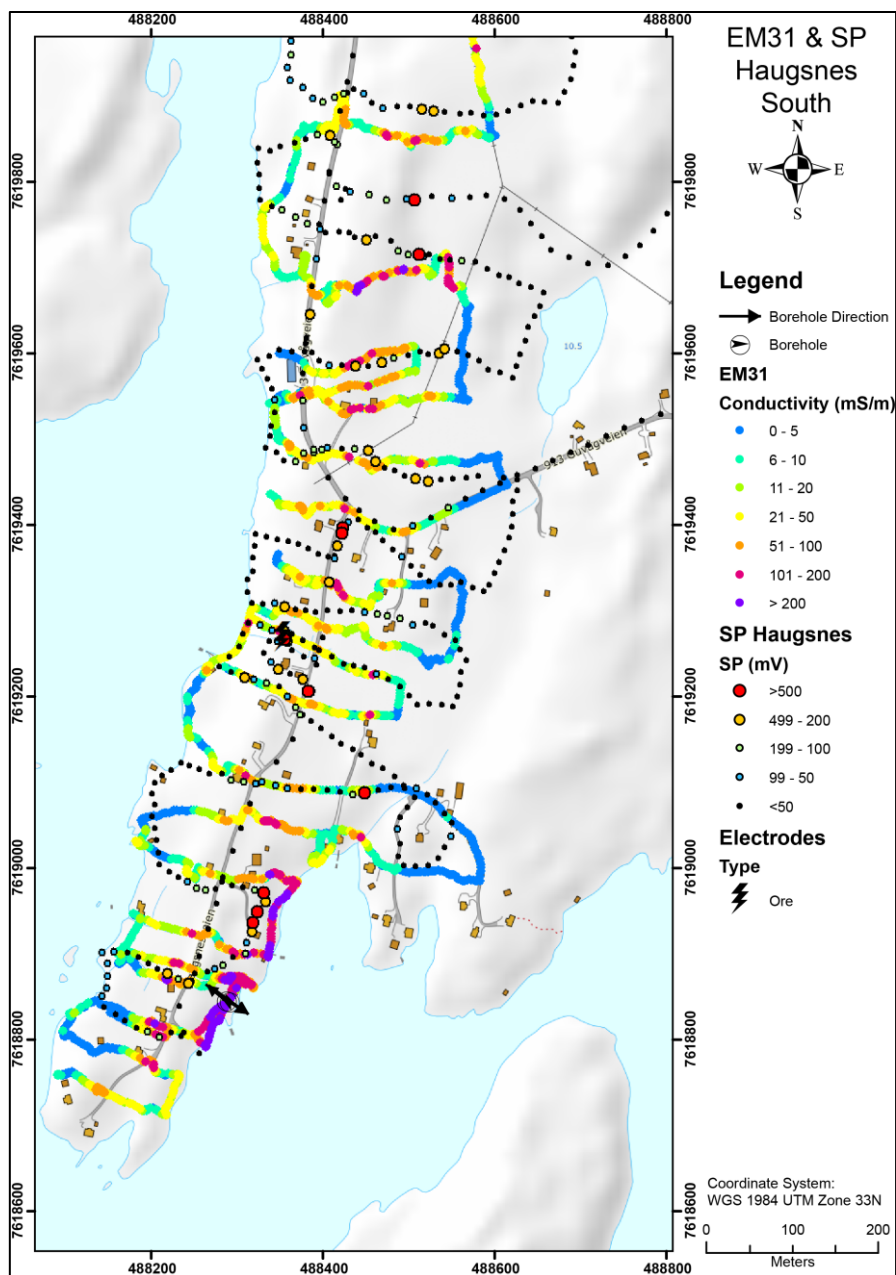


**Figure 7.5: The southern part of Haugsnes. Location of core drilling and detailed results from SP and EM31 measurements.**

## 7.2.1 Geological core logging

The EW section in figure 7.6. and in figures 7.7 and 7.8 shows lithological logs from the 2017 drill holes as well as portable XRF analyses (of among others Fe-S-Ni), Leco analysis of total carbon (TC) and total sulphur (TS). All TC and TS analyses are given in Appendix 2. Images of all drill cores are shown in Appendix 3. Portable XRF analysis are shown in Appendix 4.

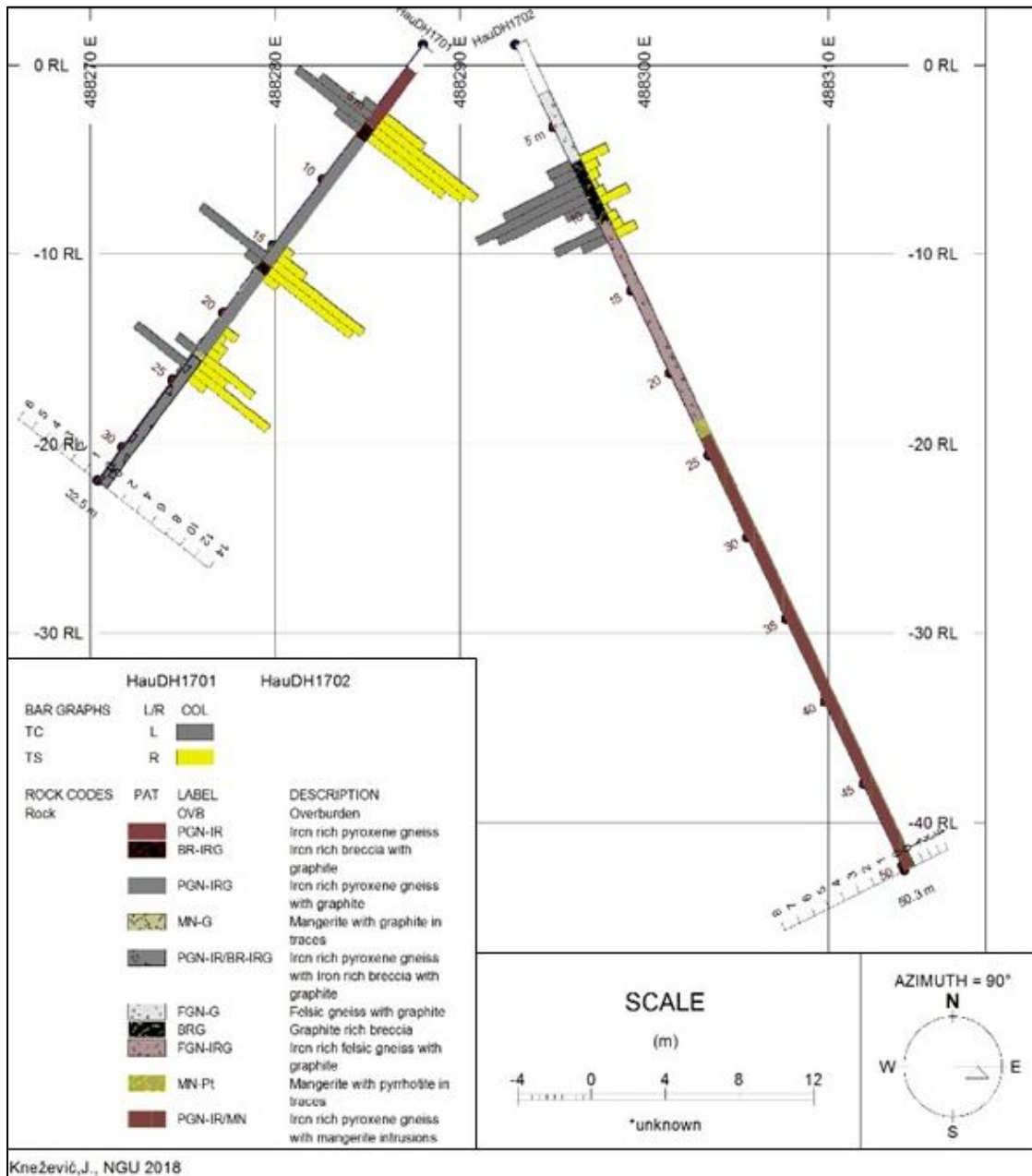


Figure 7.6: Lithological log and a graphical display of Total Carbon (TC in %) and Total Sulphur (TS in %) for the two drill holes at Haugsnes undertaken in 2017 (Haug1701 and Haug1702). View from the south.

Petrophysical data from the Haugsnes drill holes are discussed in chapter 12.2.

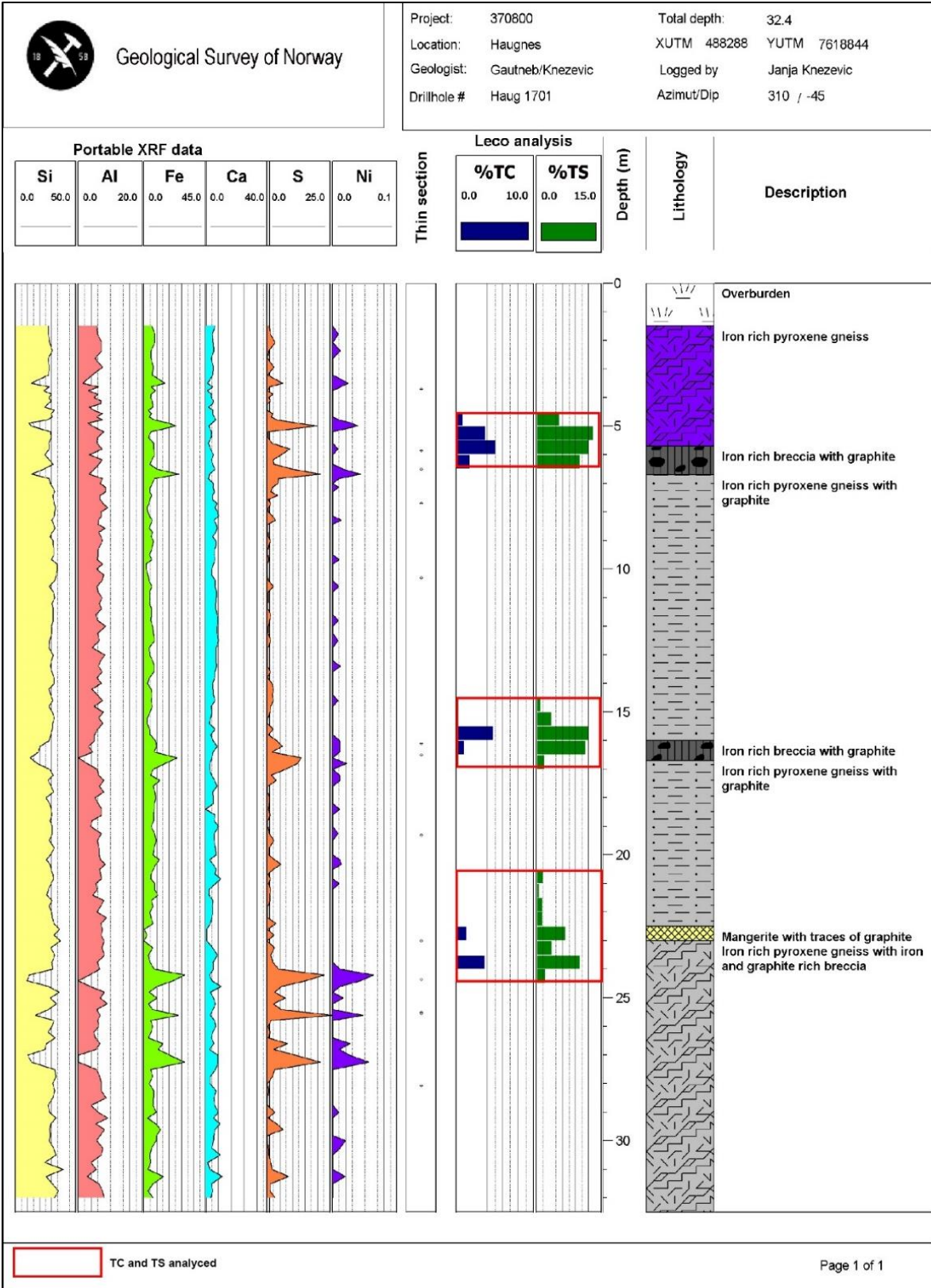


Figure 7.7: Portable XRF analyses of among others Fe-S-Ni, Leco analysis of total carbon (TC) and total sulphur (TS) together with lithological log from drill hole Haug1701.

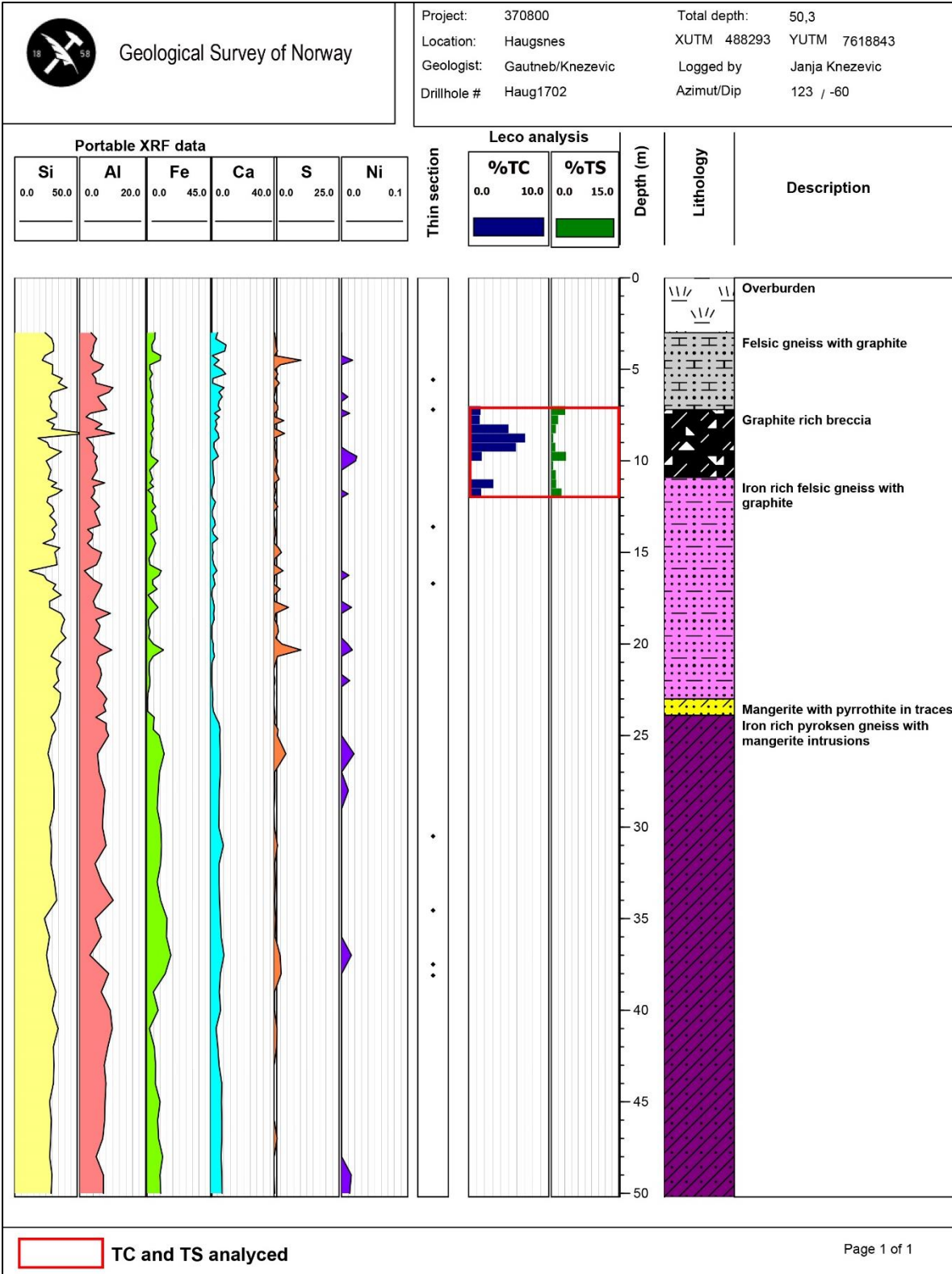


Figure 7.8: Portable XRF analyses of among others Fe-S-Ni, Leco analysis of total carbon (TC) and total sulphur (TS) together with lithological log from drill hole Haug1702.

At Haugsnes, the portable XRF analysis also shows that there is a co-occurrence of Fe, S and Ni showing that the main Fe and S bearing mineral is pyrrhotite. The host rock comprise pyroxene, plagioclase gneiss, rich in iron sulphides, that also contains abundant graphite as observed at Sommarland. The logs demonstrate a difference in the proportion of pyroxene, quartz, feldspar combined with a different deformation

history. In the host rock it is common to find abundant iron with regular mica veins and irregular scattered mafic veins enriched in pyrrhotite, pyrite, magnetite, graphite, and disseminated biotite.

### 7.2.2 Mineralogy from thin sections

The following mineralogical description is based on analysis of thin sections from the drill cores (see figures 7.9 to 7.12).

The graphite occurs in iron and graphite rich breccia together with large amounts of pyrrhotite. Pyrrhotite is a mineral that is ductile and very easily deformed. The resultant breccia type is of a texture with a groundmass of pyrrhotite containing fragments of silicate minerals which contain flakes of graphite (see figures 7.9 and 7.10).

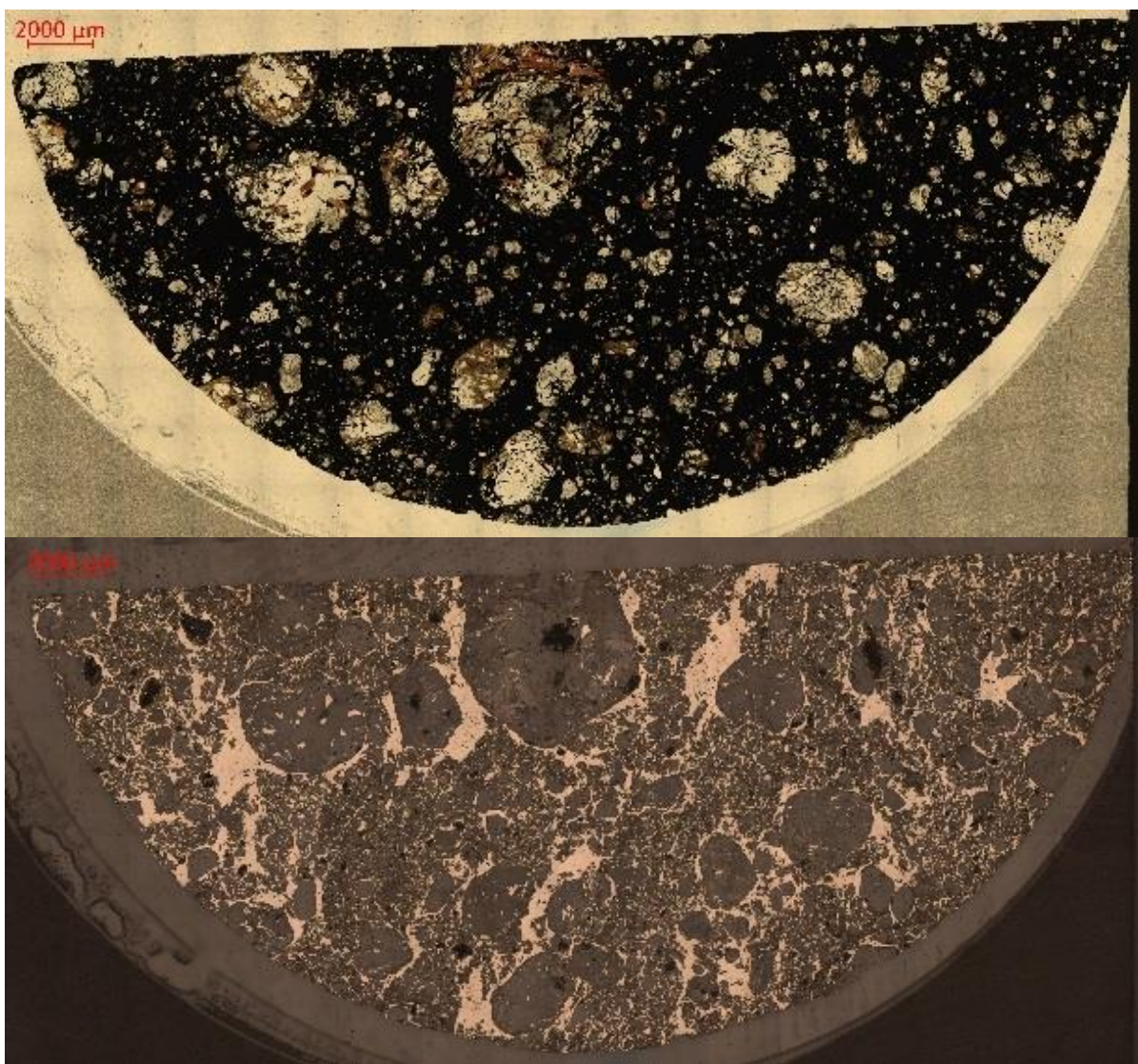


**Figure 7.9: Iron rich breccia with graphite, pyrrhotite rich matrix with fragments of silicate minerals that contain graphite flakes. Thin section JK-DhHau1701-16.5 (transmitted and reflected light respectively).**



Figure 7.10: Left: Brecciated rock-type with fragments of silicate minerals (feldspars, quartz, pyroxene) with graphite in a groundmass of pyrrhotite. Right: Example where the proportion of silicates is higher and less brecciated. Graphite occurs both in pyrrhotite and in silicates. Thin section HG-DhHau1701-6.5 and JK-DhHau22.55 (combined reflected and polarized light).

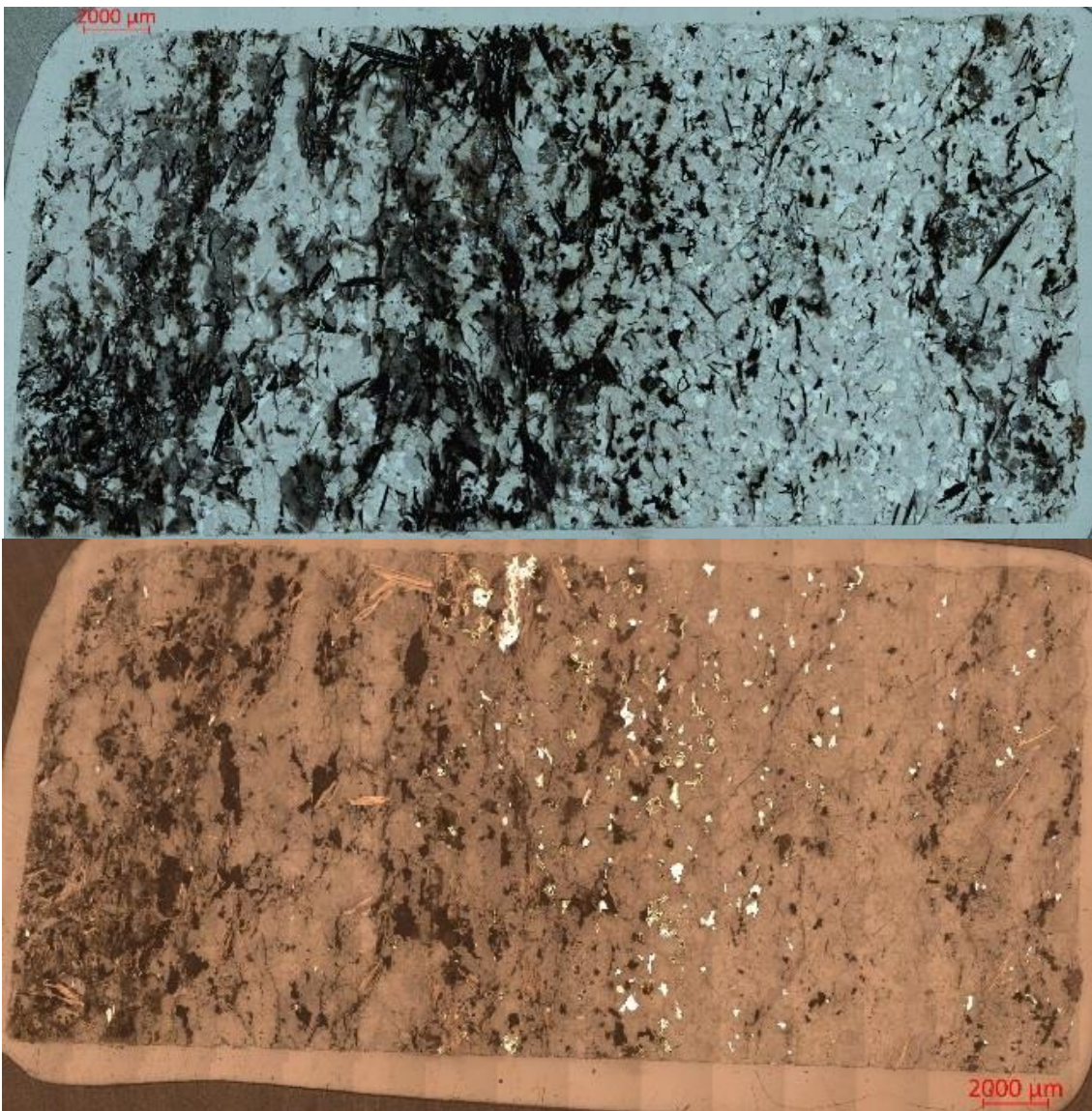


Figure 7.11: Gneiss with graphite flakes up to 2 mm and spotted pyrrhotite and pyrite in thin section JK-DhHau1702-5.57, (upper picture transmitted light, lower picture reflected light).

Graphite is present in many places in the host rock in low grade, as a disseminated mass and as in veins as observed at Sommarland. Flakes of graphite vary in size but can be up to ca. 2 mm and are easily visible with the naked eye as long thin sharp flakes (Figures 7.11 and 7.12).

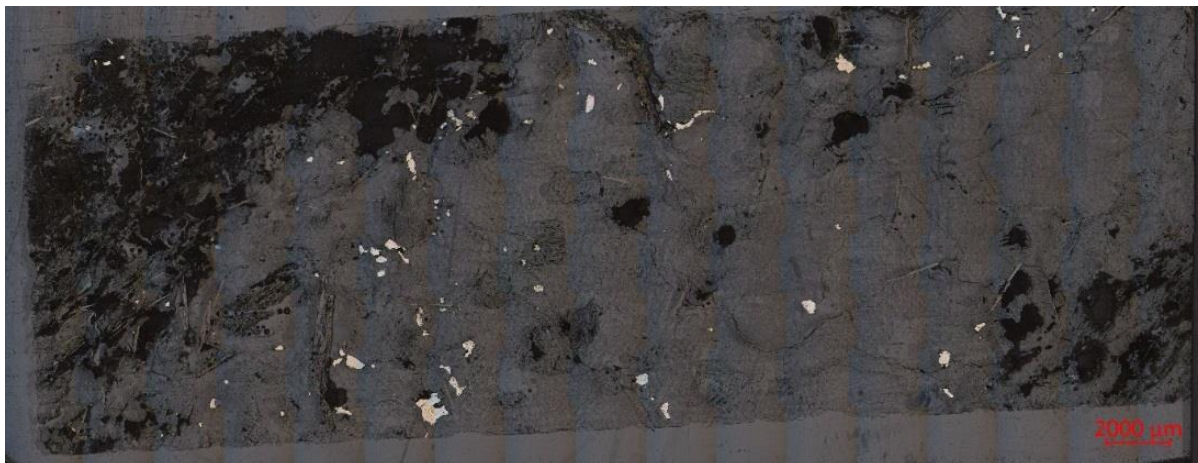


Figure 7.12: Mafic vein with graphite and pyrrhotite and partly disseminated graphite, thin section JK-DhHau1701-13.6.

### 7.2.3 Quality of graphite at Haugsnes

Samples from the drill cores at Haugsnes were analysed for total carbon (TC) and total sulphur (TS) using a Leco SC-632 analyser at NGU-lab. The analysed sections are presented in figures 7.7 and 7.8. All analyses are shown in Appendix 2.

The analyses of graphite-bearing sections are summarised in Table 7.1 below. Sections of the different drill core have been compiled with a cut off 1 % and 3 % TC.

Table 7.1: Haugsnes sections in the different drill core with TC > 1% and 3% and their length and average TC

Drill hole	Cut off %	Interval from	Interval to	Interval length	Average TC %
Haug1701	1	5	6.5	1.5	3.58
Haug1701	1	15.5	16.5	1	2.93
Haug1701	1	22.5	23	0.5	1.34
Haug1701	1	23.5	24	0.5	3.74
Haug1702	1	7	10	3	3.76
Haug1702	1	11	12	1	2.34
<b>All average &gt;1%</b>				<b>1.25</b>	<b>2.94</b>
Haug1701	3	5	6	1	4.46
Haug1701	3	15.5	16	0.5	4.84
Haug1701	3	23.5	24	0.5	3.11
Haug1702	3	8	9.5	1.5	5.99
Haug1702	3	11	11.5	0.5	3.11
<b>All average &gt;3%</b>				<b>0.8</b>	<b>4.3</b>

The graphite at Haugsnes appears as flake graphite. The grain size is very inhomogeneous but individual grains can have a length of up to 2 mm.

The ore sections are thinner and the carbon content lower at Haugsnes than at Sommarland. Figures 7.14 and 7.15 show an interpretation of the ground geophysics at the northern and southern parts of Haugsnes. Several conducting structures are indicated, and the drilling at Haugsnes shows that the graphite layers are repeated in a more detailed scale in the drill holes. This may indicate that the Haugsnes area is less interesting from an economical point of view. However, the drilling was localized on one small area whereas the total length of the Haugsnes area is approximately 2 km.

Petrophysical measurements on the drill cores are discussed in chapter 12.2.

### 7.3 Haugsnes summary

Helicopter-borne EM measurements show good electrical conductivity in a total strike length of ca. 2 km in the Haugsnes area. Combined 2D Resistivity/IP measurements indicate graphite structures in a total width of ca. 80 m (Rønning et al. 2017). Detailed geophysical measurements indicate that this may consist of 5 – 6, or possibly more, individual thinner structures. Graphite is exposed at several of these structures and it is likely that all of the geophysical anomalies are a result of graphite. Figures 7.13 and 7.14 show one possible interpretation of graphite structures at Haugsnes. However, the long distance between these measured profiles means that other interpretations are also likely.

The graphite at Haugsnes appear as flake graphite with a grain size of up to 2 mm.

Chemical analyses of 11 surface samples showed an average total carbon content (TC) of 19,3 % (Table 7.2 and Gautneb et al. 2017). Cores from two drill holes undertaken in 2017 intersect several graphite structures, each of them with a thickness of < 2 m. The average total carbon content of these mineralisation is < 5 % TC.

There is a potential for extensive graphite structures in the Haugsnes area, but their thickness and the total carbon content observed in the drill holes is not of economic interest today. However, graphite content of economically interesting thicknesses cannot be ruled out in other parts of the mineralised area at Haugsnes.

**Table 7.2: Total Carbon (TC) analyses of surface samples from Haugsnes.**

Province/area/locality	N	Average % TC	Max % TC	Min of % TC	StdDv TC
<b>Vesterålen</b>					
Haugsnes	11	19.3	33.8	10.6	9.44

The total strike length of potential graphite structures may be as much as 9000 m. Assuming an average width of 2 m and a depth extent of 100 m, a potential volume of 1.8 mill m<sup>3</sup> is estimated. If we assume that the average TC equals 19.3 % and the density is 2.2 t/m<sup>3</sup> an optimistic estimate would give 760,000 tonnes of flake graphite.

However, if we assume the average TC from the drilling (ca. 5%) this gives an estimate of 200,000 tonnes.

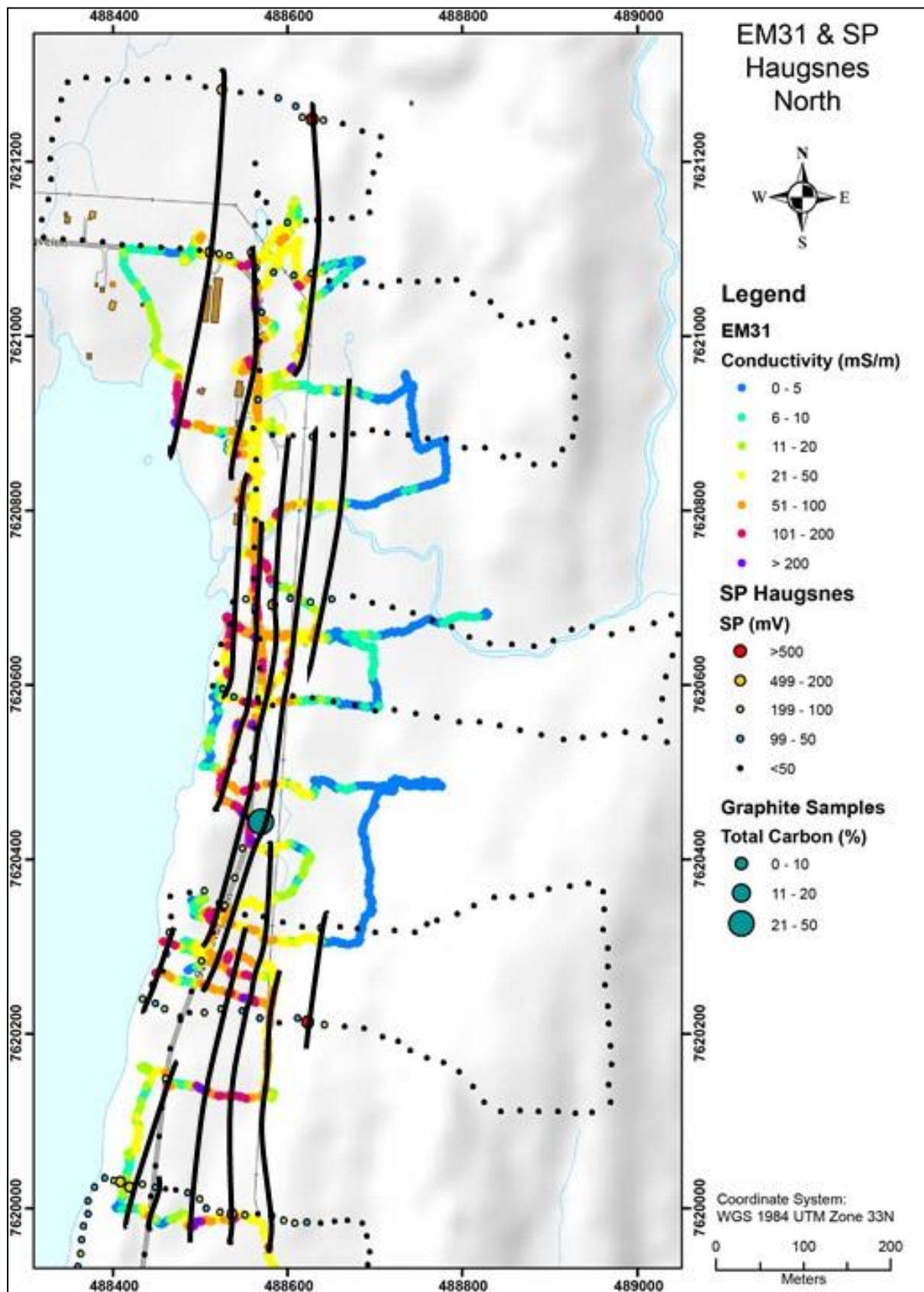


Figure 7.13: The northern part of Haugsnes. The interpreted main graphite structures based on exposed graphite, EM31 and SP data.

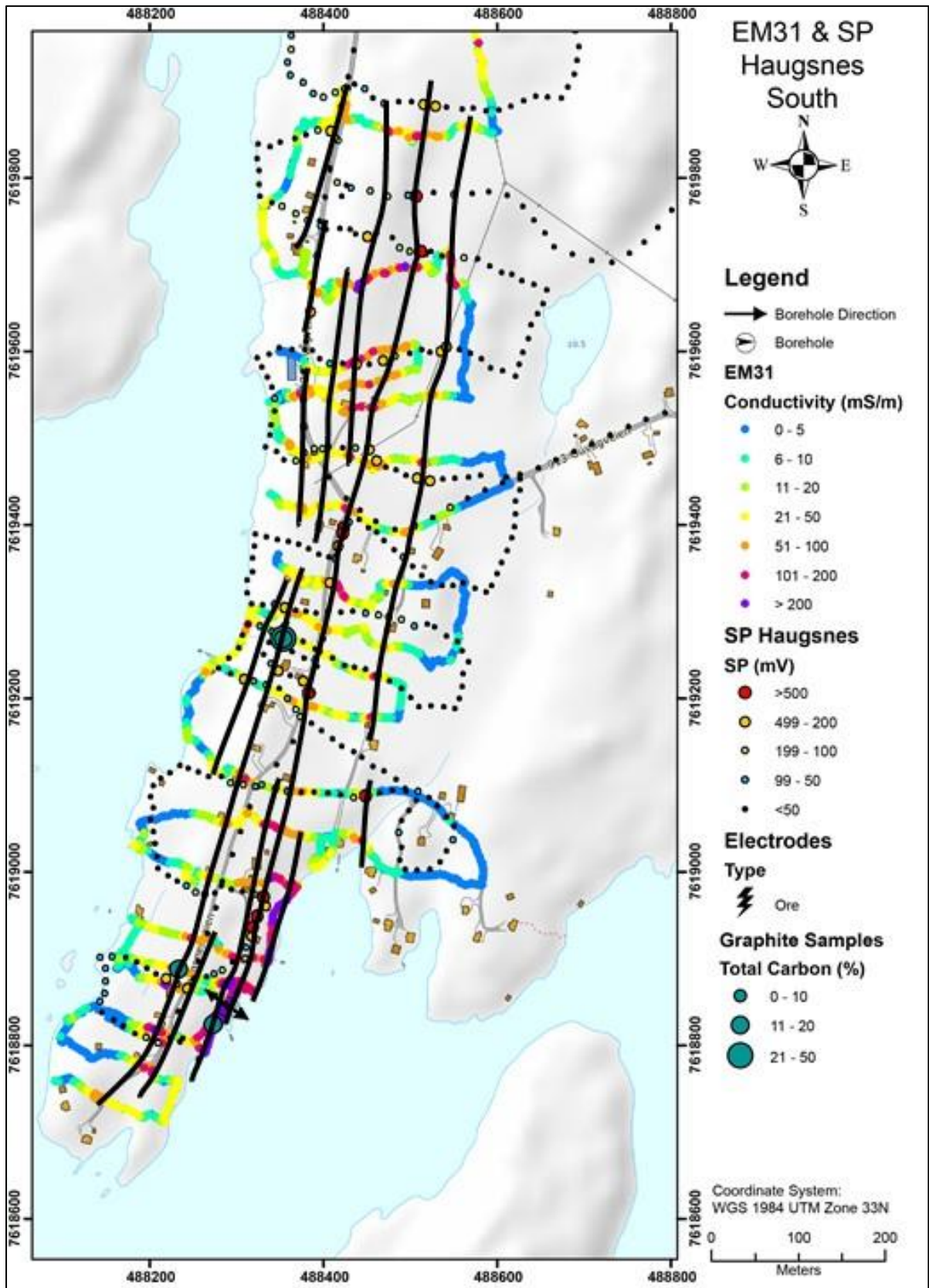


Figure 7.14: The southern part of Haugsnes. The interpreted main graphite structures based on exposed graphite, EM31 and SP data.

## 8. RESULTS OF THE FOLLOW-UP WORK IN OTHER AREAS, BØ MUNICIPALITY

In addition to Sommarland and Haugsnes, some geophysical work was performed at Husvågen – Rise and in the southern part of the Møkland area in 2017.

### 8.1 Husvågen – Rise

In the Husvågen and Rise areas adjacent to Straume in Bø municipality, a circular structure of potential graphite mineralisation is observed at the helicopter-borne EM-measurements (see figure 5.5). No previous studies were performed in this area. In 2017, some EM31 measurements were carried out in the northern part of this structure (see figure 8.1).

At **Husvågen** two high electrical conductivity structures were observed east and south of Gjødalsvatnet (Figure 8.1). Apparent conductivity is between 101 and 200 mS/m (apparent resistivity between 10 and 5  $\Omega$ m) which may be a result of the presence of graphite. The thickness of these two structures from EM31 measurements appears to be > 10m, and the strike length from helicopter-borne EM data is more than 1 km. The area is 100 % covered with soil and no outcrops were observed. To map these structures and verify possible graphite, follow-up EM31 measurements and a profile with 2D Resistivity/IP is recommended to verify graphite-bearing structures. Core drilling should also be considered.

In the **Rise** area, ca. 2 km east of Husvågen, a conductive structure with a total strike length of nearly 1 km is inferred from the helicopter-borne EM (see Figure 8.1). EM31 measurements show apparent conductivity between 10 and 50 mS/m (apparent resistivity 100 to 20  $\Omega$ m) distributed over the whole area. These are not typical values for graphite of good quality. However, the soil cover in this area may be too thick such that the EM31 measurements do not penetrate down to the graphite layers. Geophysical measurements that can achieve a deeper penetration are necessary. A profile of 2D resistivity/IP is recommended. Core drilling should also be considered at this locality.

Follow up with EM31 measurements and a 2D Resistivity/IP profile is also recommended in the southern part of this area (see figure 5.5).

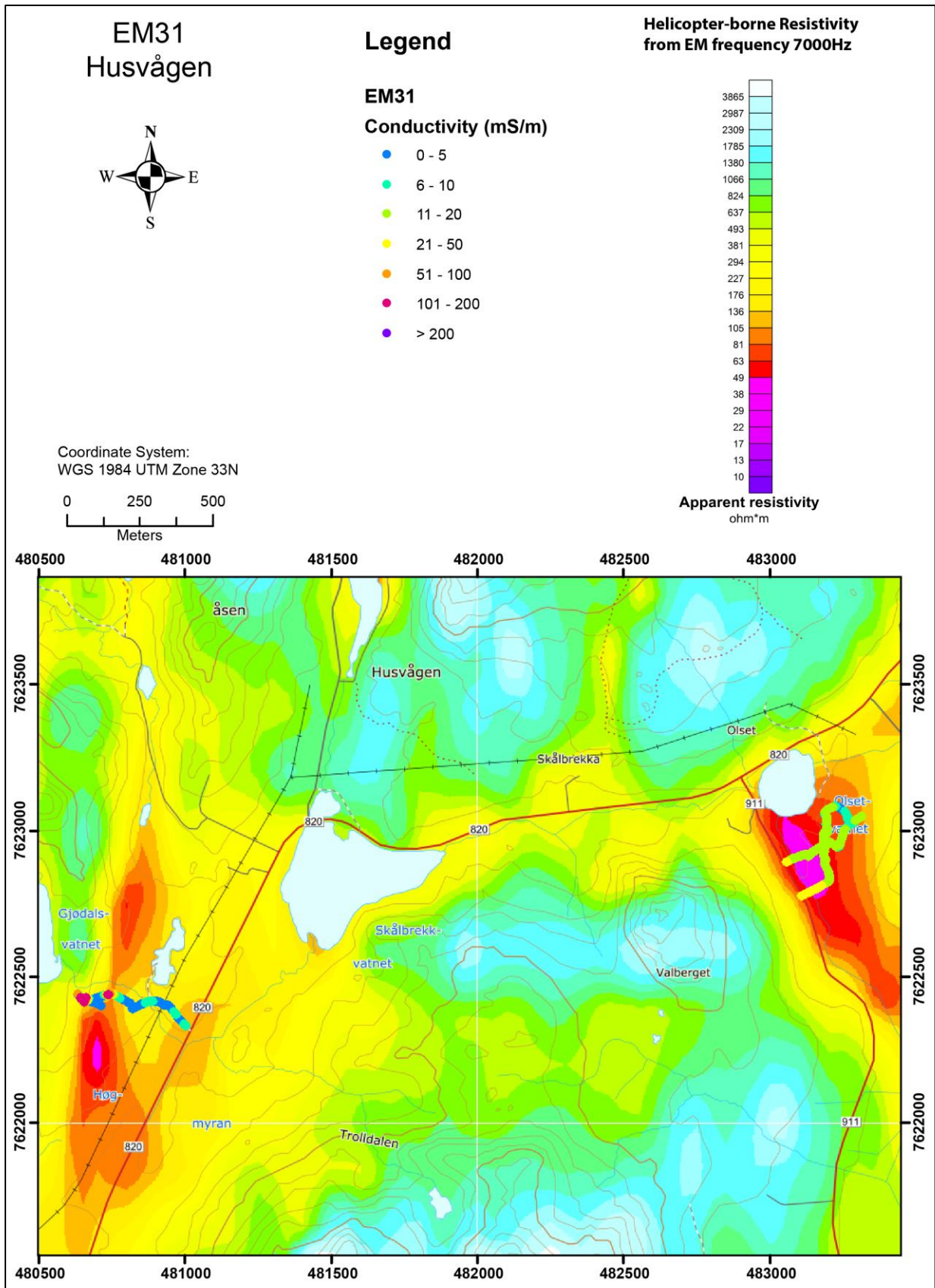


Figure 8.1: The Husvågen area is shown to the left and the Rise area is shown to the right. Results from the EM31 measurements are overlain on top of the helicopter-borne measurements of apparent resistivity from EM 7000 Hz coaxial coil configuration.

## 8.2 Møkland south

The northern part of the **Møkland** area was investigated during the years 2014, 2015 and 2016 (Gautneb et al. 2017, Rønning et al. 2017). Graphite deposits of a relatively good quality but with limited strike length were discovered. Results from the helicopter-borne EM measurements indicate a continuation of the anomalies to the south, and that the apparent resistivity is higher in this area (see figures 5.2 and 5.6).

EM31 measurements in the southern part of the Møkland area were performed in 2017. In Figure 8.2 results are presented together with apparent resistivity from helicopter-borne EM measurements. The latter shows apparent resistivity in some places less than 100  $\Omega\text{m}$ . A conductive structure has been mapped over more than 400 m strike length from coordinate 486080 - 7627400 in the north to 486400 – 762700 in the south. This structure may also continue southwards. The apparent conductivity is as high as > 200 mS/m (apparent resistivity < 5  $\Omega\text{m}$ ). Since this anomaly forms the continuation of the proven graphite layers further to the north, we assume that this anomaly also represents graphite.

The EM31 measurements are limited in the southern part of this deposit (figure 8.2). To gain a more continuous image of potential graphite mineralisation, additional EM31 measurements are recommended. A 2D Resistivity/IP profile along one of the roads in the area is also recommended.

The area is 100 % covered with soil, and no exposures are available for geological mapping. To obtain information concerning the quality of potential graphite in this area, trenching or core drilling is necessary.

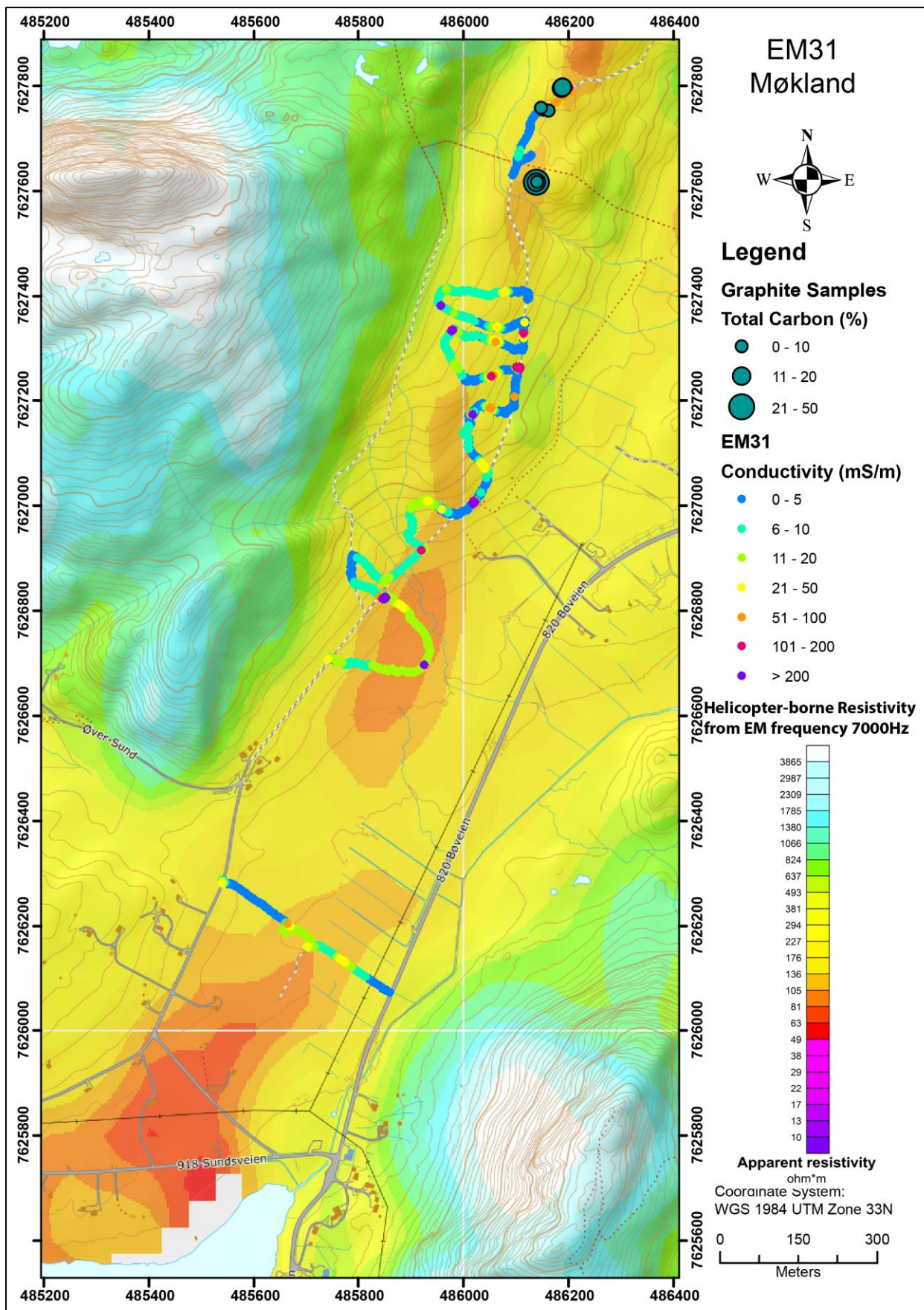


Figure 8.2: The southern part of the Møkland area. Results from EM31 measurements overlain on top of helicopter-borne measurements of apparent resistivity from EM 7000 Hz coaxial coil configuration.

## 9. RESULTS FROM THE FOLLOW-UP WORK AT ØKSNES MUNICIPALITY

During the 2017 field season, NGU performed geophysical measurements and some geological sampling. This was done at three localities in the Øksnes municipality; Smines, East of Myre and at Raudhammaren south-east of Myre.

### 9.1 Follow-up work at Smines

Some geological and geophysical work has been performed at Smines, Øksnes municipality, in 2015 and 2016 (Gautneb et al. 2017 and Rønning et al. 2017) which can be summarised thus (Rønning et al. 2017):

*The graphite occurrence at Smines was discovered when the 2013 airborne geophysical data were available. Apart from some small seaside exposures, the graphite bearing-rocks are completely covered by soil and vegetation. EM 31 traversing indicated several graphite-bearing conductors under thin cover and a trench was made in the area that was most accessible. Several zones of graphite mineralisation were revealed: The aggregated width of individual graphite zones are about 6 meter (Gautneb et al. 2017). CP measurements showed that also this mineralisation has a limited length along strike.*

*Eleven samples from the trench show an average grade of 7.7 % Cg (graphite carbon) with a maximum of 17.1 %.*

*EM31 and SP measurements gave indications of graphite south of the exposure in the trench. However, due to limited time for field work, large areas showing very low resistivity at helicopter-borne EM data were not included in the follow-up work yet, and the area covered by ground measurements at Smines should be extended.*

#### 9.1.1 Geophysical measurements

In 2017 NGU performed some additional EM31 measurement. CP/SP measurements were planned but not performed because of limited time and budget constraints for field work.

New **EM31 results from Smines** are presented in Figure 9.1. The helicopter-borne EM measurements show an ca. 1 km long zone of low resistivity ( $< 40 \Omega\text{m}$ ) from Middagsdalen to Rødbergan in the eastern part (Figure 9.1). In this area, EM31 measurements show a number of apparent conductivity readings  $> 10 \text{ mS/m}$  (apparent resistivity  $< 10 \Omega\text{m}$ .) and conducting material appears partly in a width of 40 – 60 m. This is most likely the result of graphite mineralisation. Two graphite showings are already mapped. In the central part, between Rotdalen and Vikelva (see Figure 9.1), the EM31 anomalies are not particularly high despite the relatively low apparent resistivity in the helicopter-borne EM data. The presence of graphite in this area cannot be excluded since a thicker soil cover may reduce the EM31 anomalies. In the western part the helicopter EM data suggests a new low resistivity anomaly up to ca. 200 m in strike length. In this area, high apparent electrical conductivity is mapped, and graphite is exposed.

The electrical properties in the Smines area indicate the presence of graphite mineralisation and graphite is indeed found at 7 locations. A ca. 1 km long conducting structure is partly followed up with EM31 measurements, but this work has not been completed. Additional geophysical measurements are recommended, and since the terrain in the area is a challenge, this work should be undertaken with combined CP/SP measurements.

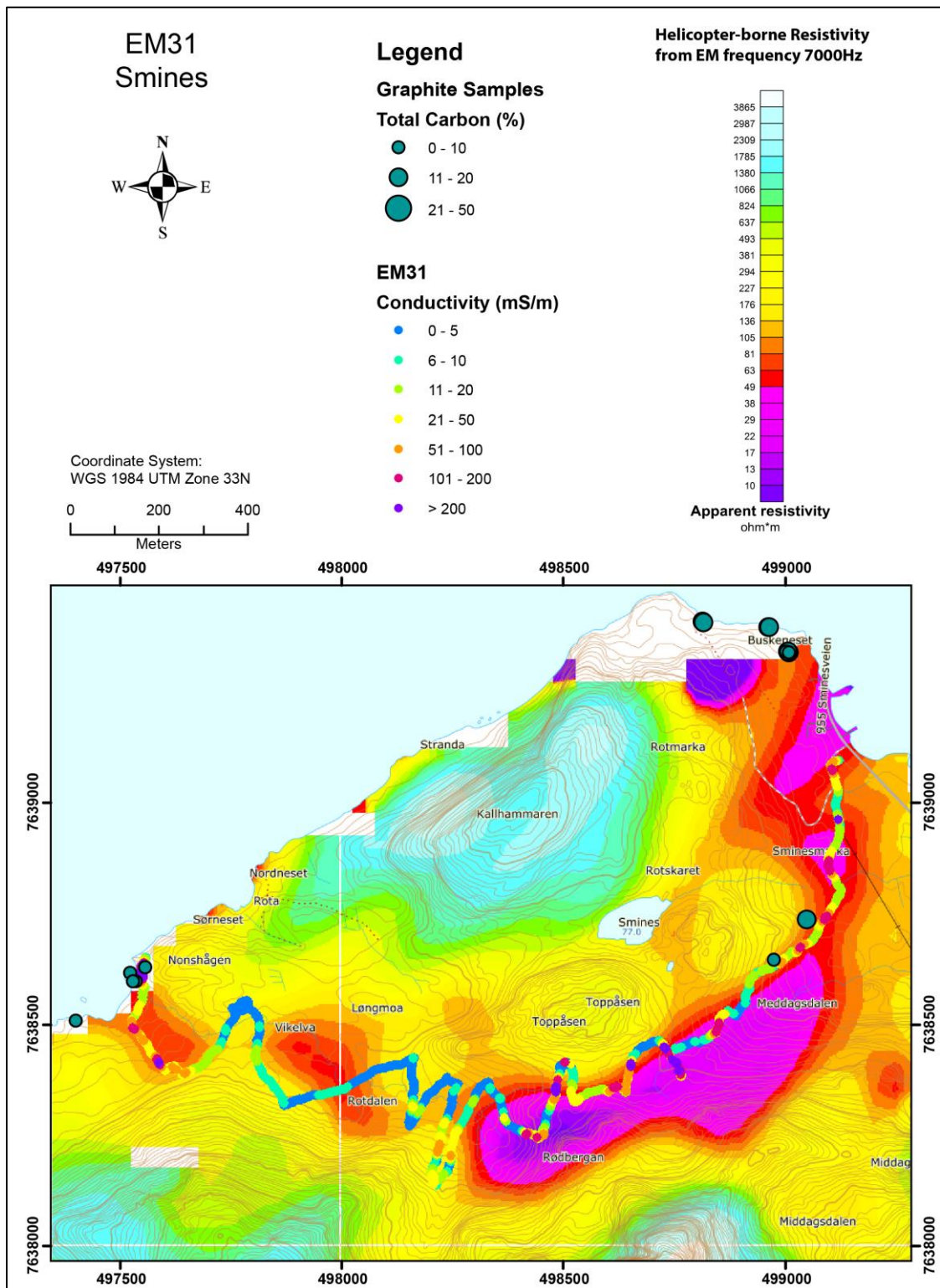


Figure 9.1: Results of EM31 measurements from the Smines area overlain on top of helicopter-borne measurements of apparent resistivity from EM 7000 Hz coaxial coil configuration.

### 9.1.2 Geological update on outcrops and analysis

The Smines area is very poorly exposed and apart from the outcrops along the shore at Buskeneset in the NE and Nonshågen in the SW (Figure 9.1) there is almost no outcrop of graphite schist in the central area. In 2017 sampling was carried out of the host rock for petrophysical analyses and the presence of graphite. One new outcrop of graphite schist was found just north of Middagsdalen (Figure 9.1). This outcrop consists of a medium rich graphite schist and could be a suitable place for future grounding point for CP measurements (Figure 9.2).



Figure 9.2: Graphite outcrop with TC 13,2% TS 0,33%, sample JK-291517-9

In Table 9.1 we have compiled all existing analyses from the Smines area.

Table 9.1: Total Carbon (TC) analysis from the Smines area

Locality	N	Average (TC%)	Max (TC%)	Min (TC%)	Stdv
Smines, all samples	19	8.32	17.30	0.37	5.67

19 analyses have an average TC of 8.32 % and represent both new individual point samples and trench samples from 2016, the latter described in Gautneb et al. 2017 and Rønning et al. (2017).

To make an estimate of graphite volume and tonnage, more data is needed.

## 9.2 Geophysics at Myre east

East of Myre in the Øksnes municipality, an extensive area of low resistivity is observed on the helicopter-borne EM data (Figures 5.2 and 9.3). This anomalous area was also observed in previous helicopter-borne EM measurements (Mogaard et al. 1988). One EM31 profile was measured north of the anomalous area previously (Gautneb & Tveten 1992). No follow-up work has been performed in the best conducting area, probably due to the lack of exposures. Adjacent to the town of Myre, several graphite showings are registered, and in the combined magnetic and resistivity interpretation (Figure 5.6), this area is indicative of a potential for graphite mineralisation.

To evaluate the EM anomalies from helicopter-borne EM measurements east of Myre, two combined 2D Resistivity and Induced Polarisation (IP) profiles were measured in 2017. Their locations are shown in Figure 9.3 and the inverted true resistivity and IP effect are shown in Figures 9.4 and 9.5.

The Resistivity/IP **Profile 4** is measured along a road (Figure 9.3). The resistivity section (Figure 9.4) shows an approximately 5 to 10 m thick high resistive layer ( $> 350 \Omega\text{m}$ ) that can be interpreted as soil (road material, peat and possibly moraine). Marine clay can be excluded. Below this layer, the resistivity is general low, mostly in the interval between 30 and 100  $\Omega\text{m}$  which is not representative for the host rock in the area. Locally, the resistivity is  $< 10 \Omega\text{m}$  and this may be a result of graphite or sulphide. Underneath the soil cover, high IP effects appear along the entire profile. This is probably an indication of disseminated graphite or sulphide.

The resistivity along **Profile 5** (Figure 9.5) demonstrates different characteristics. This profile was measured partly in open land and cultivated ground. The ca. 3 to 15 m thick top layer resistivity is ca. 100 to 500  $\Omega\text{m}$  and can be interpreted as peat or possibly moraine. Marine clay can be excluded as a reason for the helicopter-borne EM resistivity anomalies here. Underneath the top layer the resistivity is partly less than 5  $\Omega\text{m}$  indicating massive graphite or sulphide. IP effects in parts of the profile are an indication of disseminated graphite/sulphide.

The two resistivity/IP profiles east of Myre indicate graphite or sulphide mineralisation. The soil is too thick for trenching (5 to 15 m), and core drilling is the only method to obtain information on the type of mineralisation and quality. The soil is somewhat thick for EM31 measurements, and further geophysical measurements should be undertaken with 2D Resistivity/IP or deeper penetrating EM equipment.

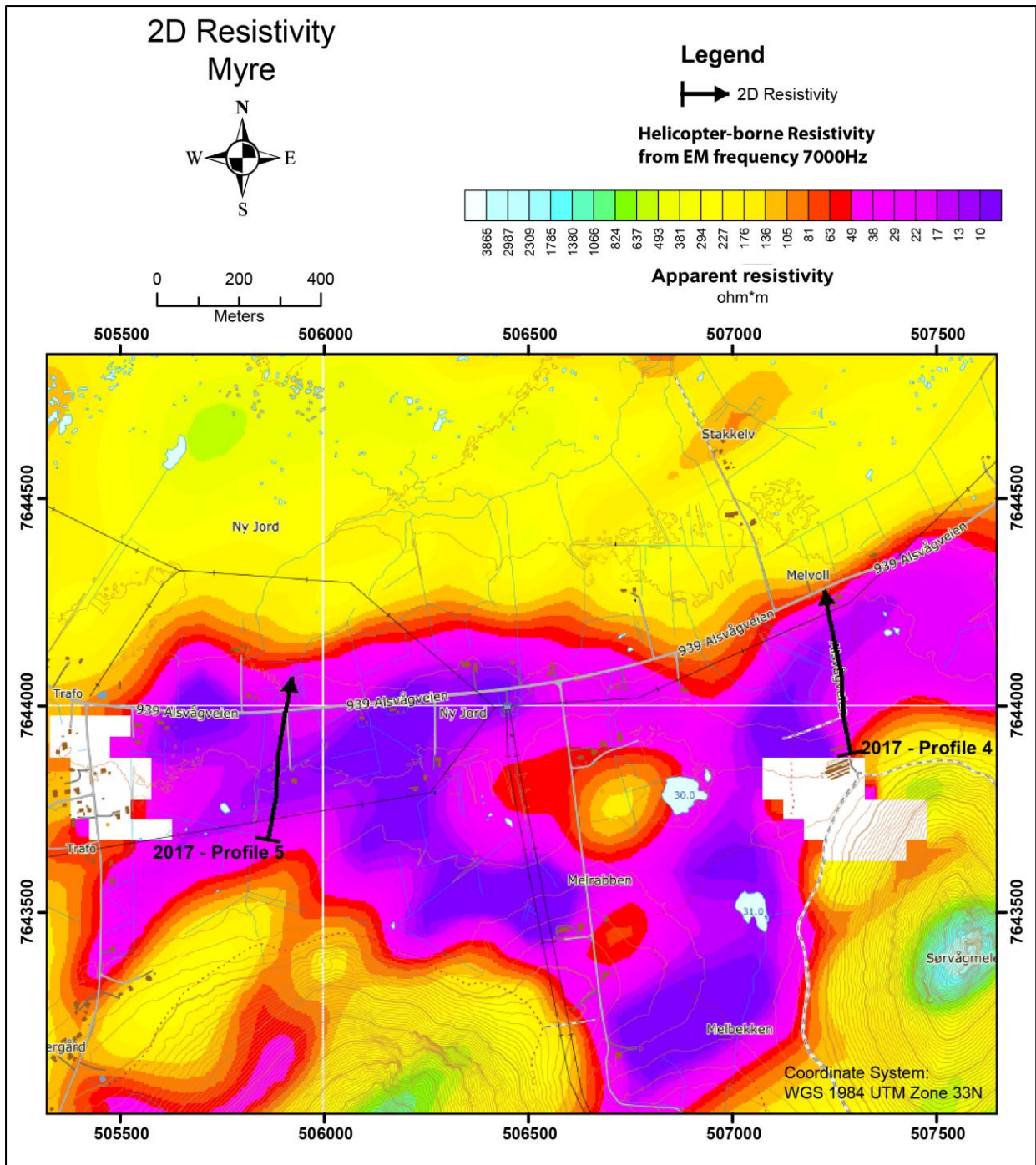


Figure 9.3: The area east of Myre. The location of 2D Resistivity/IP profiles overlain on top of helicopter-borne measurements of apparent resistivity from EM 7000 Hz coaxial coil configuration.

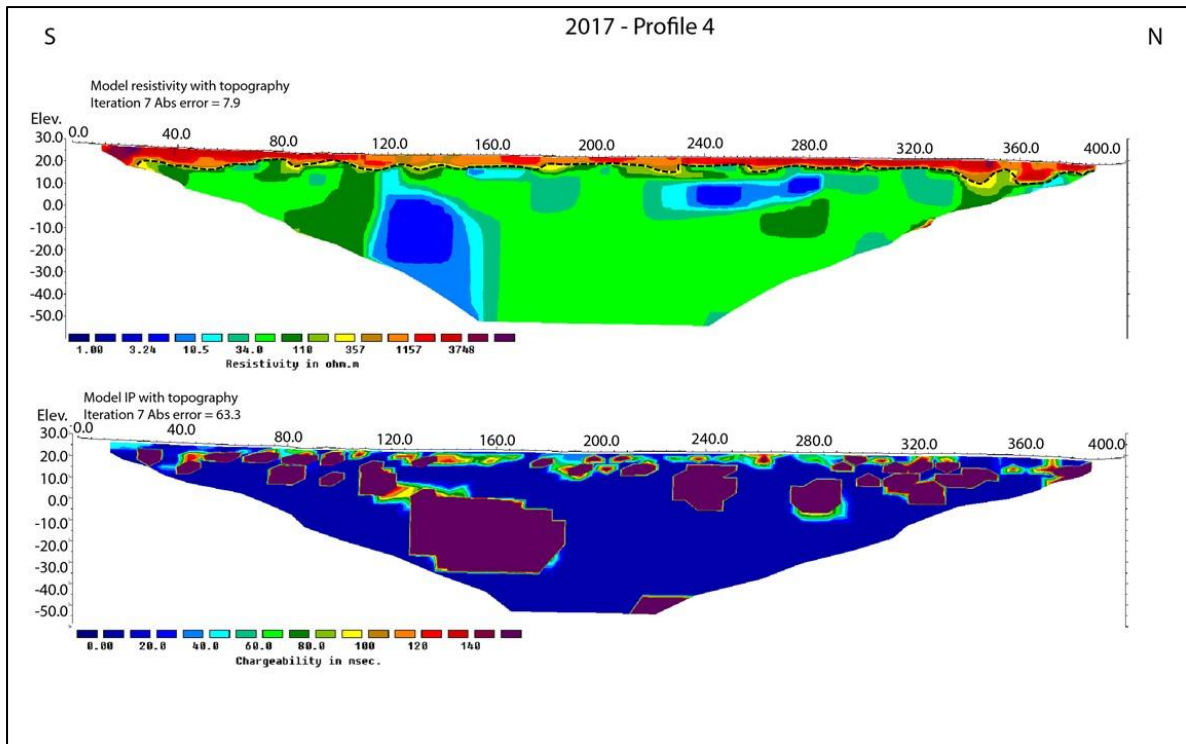


Figure 9.4: The area east of Myre. The results from 2D Resistivity and Induced Polarisation measurements along profile 2017-4. The interpreted soil-bedrock interface is shown as a dotted black line.

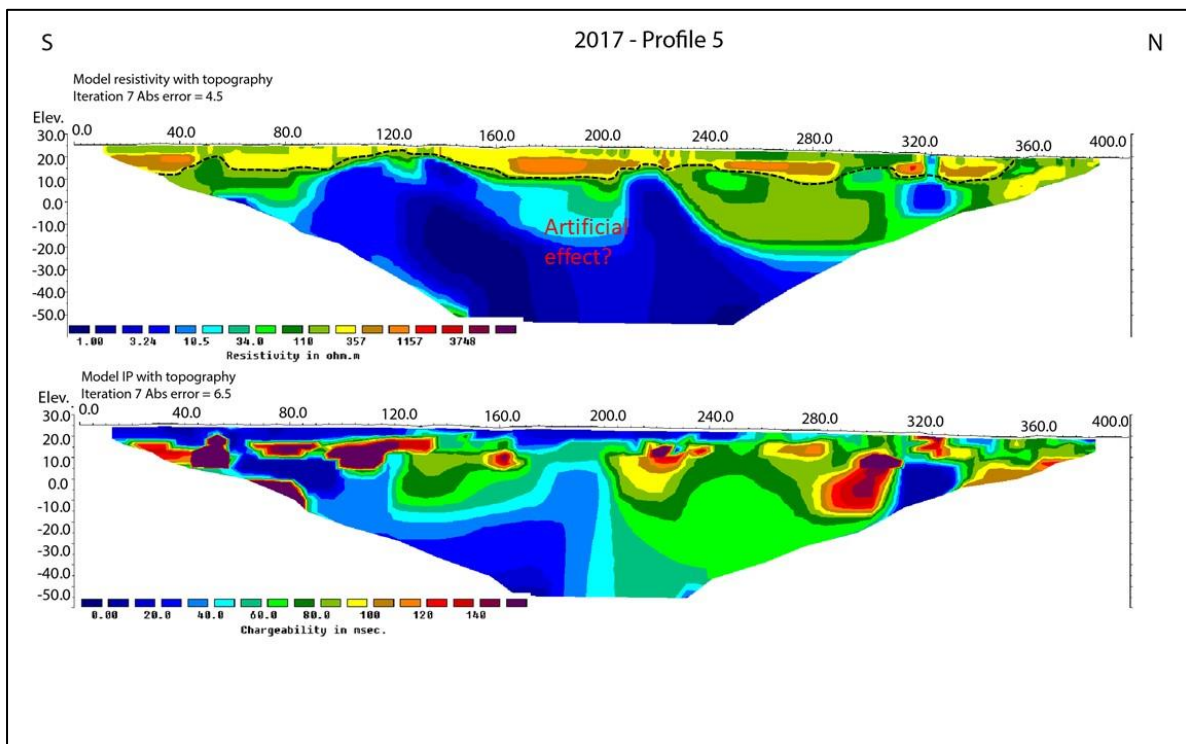


Figure 9.5: The area east of Myre. The results from 2D Resistivity and Induced Polarisation measurements along profile 2017-5. The interpreted soil-bedrock interface is shown as a dotted black line.

### 9.3 Geophysics and sampling at Raudhammaren

Graphite mineralisation next to the Raudhammaren area was previously briefly described by Gautneb & Tveten (1992). Geological reconnaissance work was performed in 2016 (Gautneb et al. 2017). The area is completely covered with soil, but graphite-bearing loose boulders were found on the western side of the mountain. In 2017, this area was followed up with EM31 measurements and some new boulder sampling was performed.

Results of the EM31 measurements are presented in figure 9.6. In figure 9.7, a possible interpretation of graphite structures is presented.

The **EM31** measurements (Figure 9.6) show several readings of very high apparent electric conductivity ( $> 200$  mS/m, apparent resistivity  $< 5 \Omega\text{m}$ ). It is likely that all of these are caused by graphite mineralisation. The width of the individual conducting structures can be estimated from the EM31 measurements to be tens of metres.

Five new samples of loose graphite schist boulders in the scree on the western side of Raudhammaren were collected in 2017. The total number of samples from this locality is presently 14 (Table 9.2). The sample localities are shown in figure 9.7 and coordinates are given in Appendix 5.

**Table 9.2: TC analysis from Raudhammaren**

Locality	N	Average TC (%)	Max TC (%)	Min TC (%)	Stdv
Raudhammaren, All samples	14	14.82	25.90	6.71	6.50

Since this locality is completely covered by quaternary material, graphite outcrops have not been found. However, graphite boulders are found over an area of approximately 300 x 200 meters, possibly indicating the presence of graphite at depth over a considerable area. This supports the interpretation of the combined airborne and ground geophysics shown in Figure 9.6.

An interpretation of potential graphite structures is shown in figure 9.7. Due to the irregular line distribution and a confusing squared image from the helicopter-borne EM, there might be other connections between the different EM31 anomalies. Therefore, this interpretation is only one possible solution. The total length of interpreted graphite structures in this area is ca. 2 km. With an average width of 20 m (EM31 readings), a depth extent of 100 m and an average Total Carbon (TC) content of 14.8 % and a graphite density of 2.2 t/m<sup>3</sup> this would give ca. 320,000 tonnes of flake graphite. This should be regarded as an optimistic estimate.

Since this is a remote area without access for NGU's truck mounted drilling rig, no further work is planned at the moment.

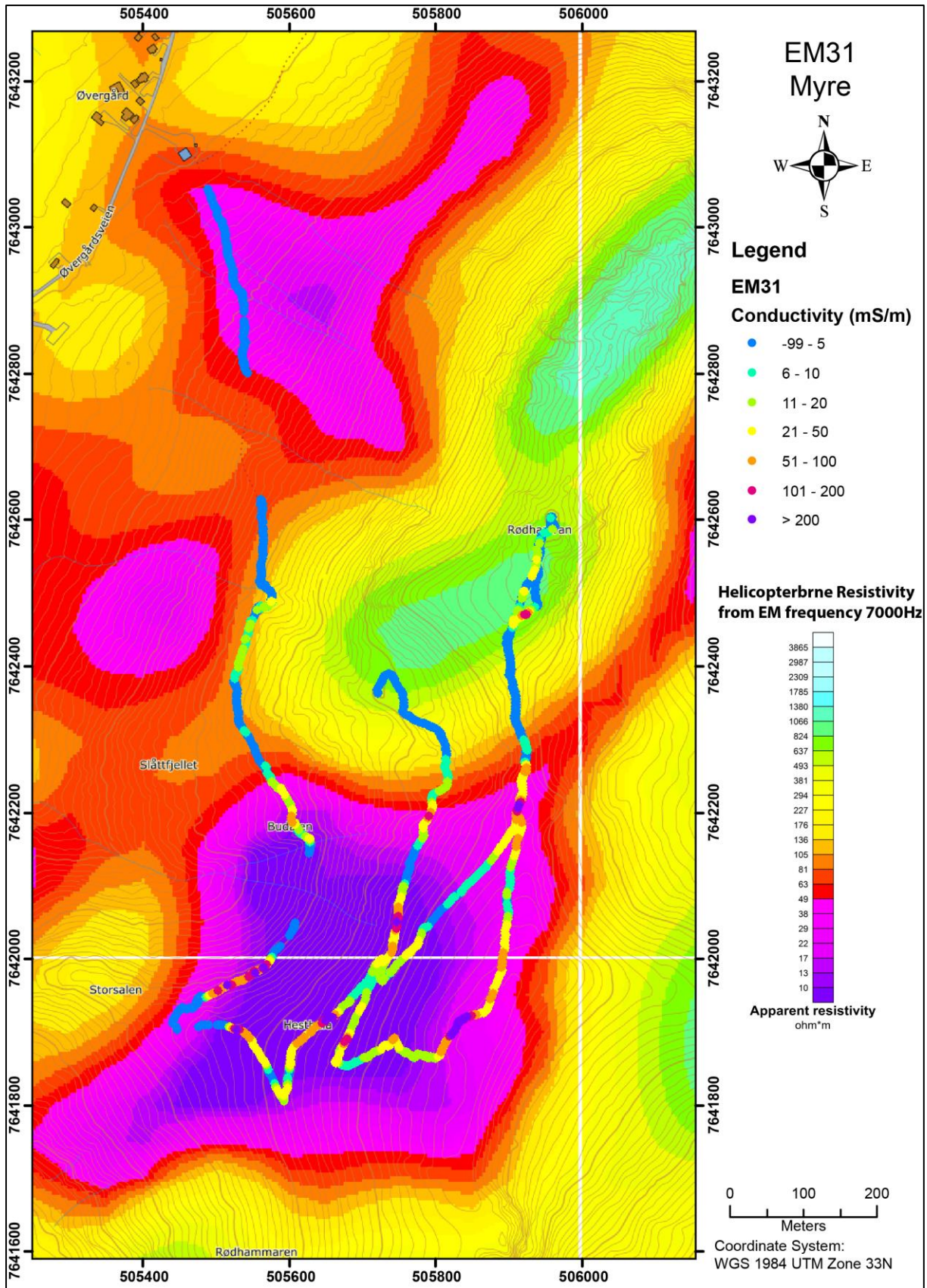


Figure 9.6: The Raudhammaren area, south-east of Myre. The results from EM31 measurements overlain on top of helicopter-borne measurements of apparent resistivity from EM 7000 Hz coaxial coil configuration.

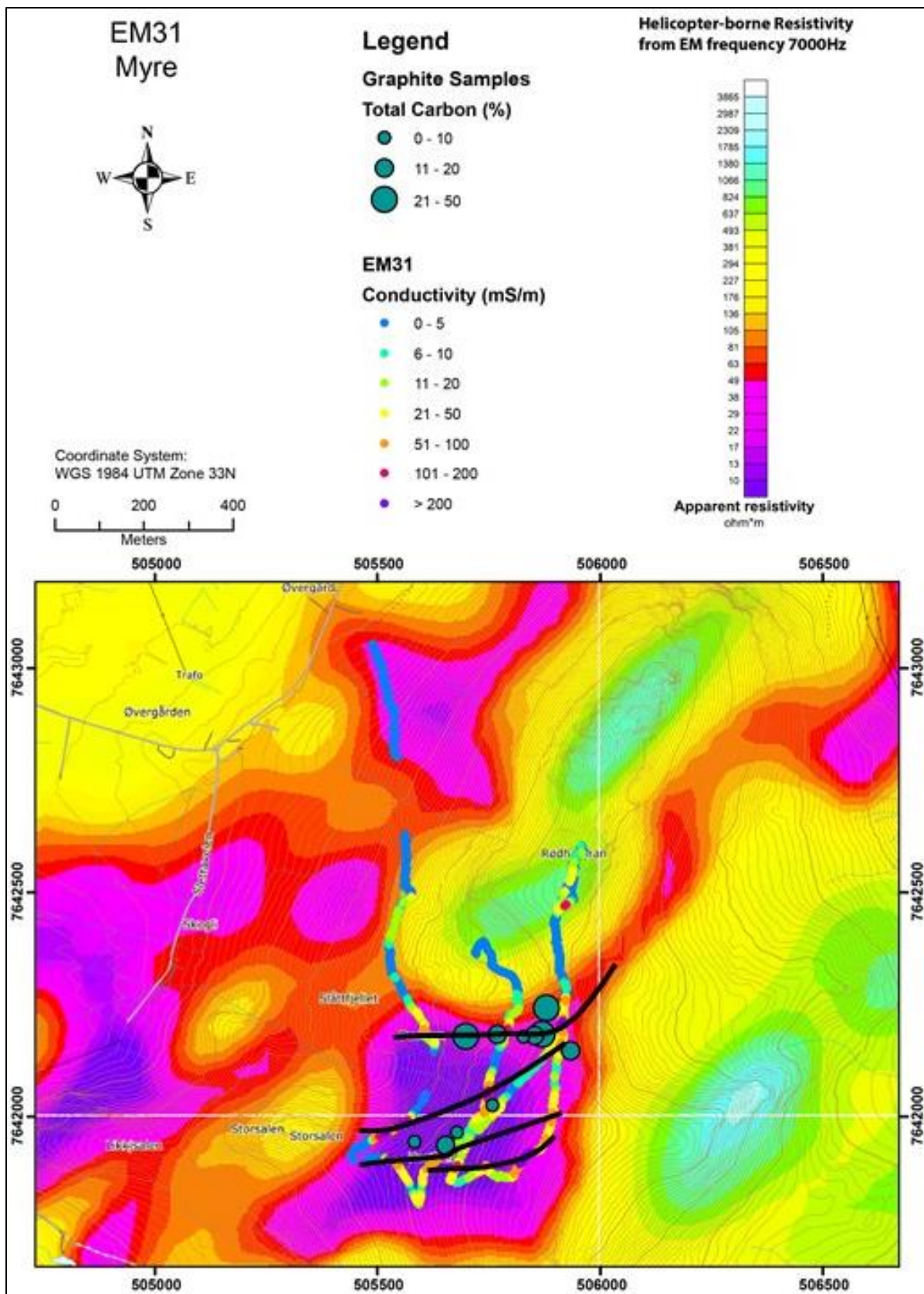


Figure 9.7: The Raudhamaren area, south-east of Myre. The results from EM31 measurements, the location of graphite bearing loose boulders and an interpretation of potential graphite structures overlain on top of helicopter-borne measurements of apparent resistivity from EM 7000 Hz coaxial coil configuration.

## 10. RESULTS OF FOLLOW-UP WORK, SORTLAND MUNICIPALITY

During the field season of 2017, NGU performed geophysical measurements, some geological observations and sampling at three localities in the Sortland municipality; Romsetfjord, Vikeid and Brenna.

### 10.1 Geophysics and geology at Romsetfjord

As a result of the 2013 helicopter-borne EM measurements (Rodionov et al. 2013a), graphite mineralisation was discovered at Romsetfjord in 2015 and 2016. The combined low resistivity and low magnetic field analysis (Figure 5.6) means that this is a target area for follow-up studies. The average concentration of graphitic carbon in 6 samples was 12.4 % (Gautneb et al. 2017). In 2017 some follow-up work with EM31 and additional sampling were performed.

In figure 10.1, the results from the **EM31** measurements and graphite showings are presented overlain on top of apparent resistivity from 7000 Hz coaxial coil configuration measurements. Only a few irregular EM31 lines were measured, and some of these show apparent conductivity values  $> 100$  mS/m (apparent resistivity  $< 10$   $\Omega$ m). In one location north-west of the farm Romset (west of Massvika, see figure 10.1), high conductivity is coincident with a graphite mineralisation.

Several graphite showings were discovered in the area, but the line spacing of the EM31 measurements are inadequate for a detailed interpretation. Systematic measurements with EM31 are recommended from the farm Romset and towards Melkarneset in the north.

To make an estimate of graphite volume and tonnage at this locality, more data is needed.

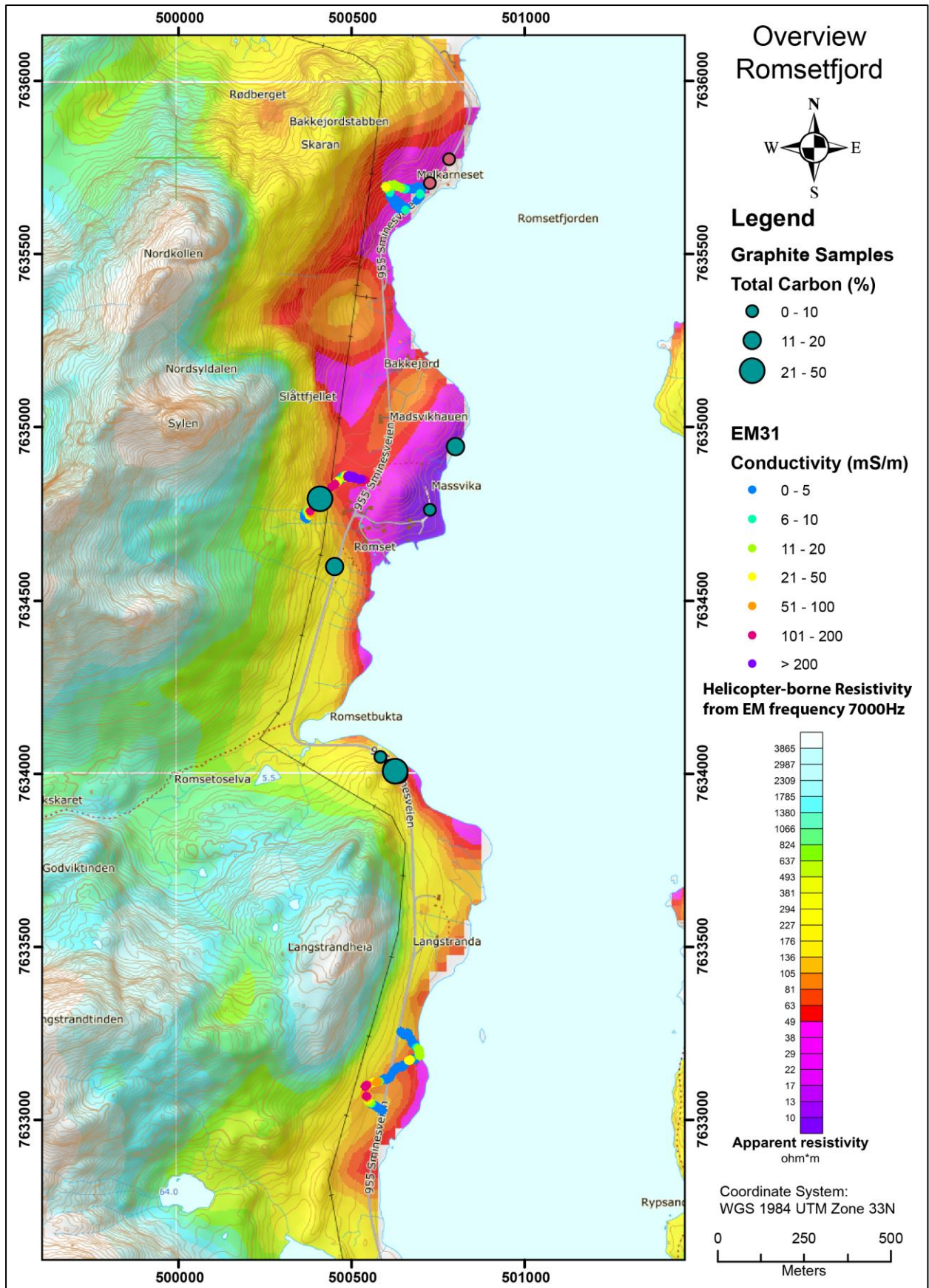


Figure 10.1: Results from EM31 measurements along Romsetfjord and graphite showings overlain on top of helicopter-borne measurements of apparent resistivity from EM 7000 Hz coaxial coil configuration.

## 10.2 Geophysics and geology at Vikeid

Graphite mineralisation in the vicinity of the Vikeid area was previously described by Gautneb & Tveten (1992). As follow-up work of the 1988 helicopter-borne EM measurements (Mogaard et al. 1988), potential graphite mineralisation was mapped using EM31. Thin graphite structures (1 – 2 m) were observed in 6 trenches. The graphitic carbon content varied from < 1% to a maximum value of 24.2 % (Gautneb & Tveten 1992).

The new helicopter-borne EM data indicates graphite can be present in the area outside the trenches from the 1992 investigations. The combined interpretation of helicopter-borne EM and magnetic data show a strong indication of interesting graphite in the area (see Figure 5.6). Some profiling with EM31 was therefore carried out; three lines with 2D Resistivity/IP and some sampling for petrophysical analysis in 2017.

The new **EM31** data is presented in Figure 10.2 together with the location of graphite samples. The location of 2D Resistivity/IP profiles is shown in Figure 10.3 and the inverted resistivity/IP sections are presented in Figures 10.4, 10.5 and 10.6.

The **EM 31** profiles (figure 10.2) show that conductors with > 200 mS/m occur along an NE-SW trending geophysical anomaly. Gautneb & Tveten (1992) found graphite schist in 3 (out of 6) trenches in this area. The samples show graphite content that varies from ca. 5 % to ca. 44 %. The area is almost completely covered by quaternary deposits and no evidence of the previous investigations is visible at the present day (see Gautneb & Tveten 1992 for details).

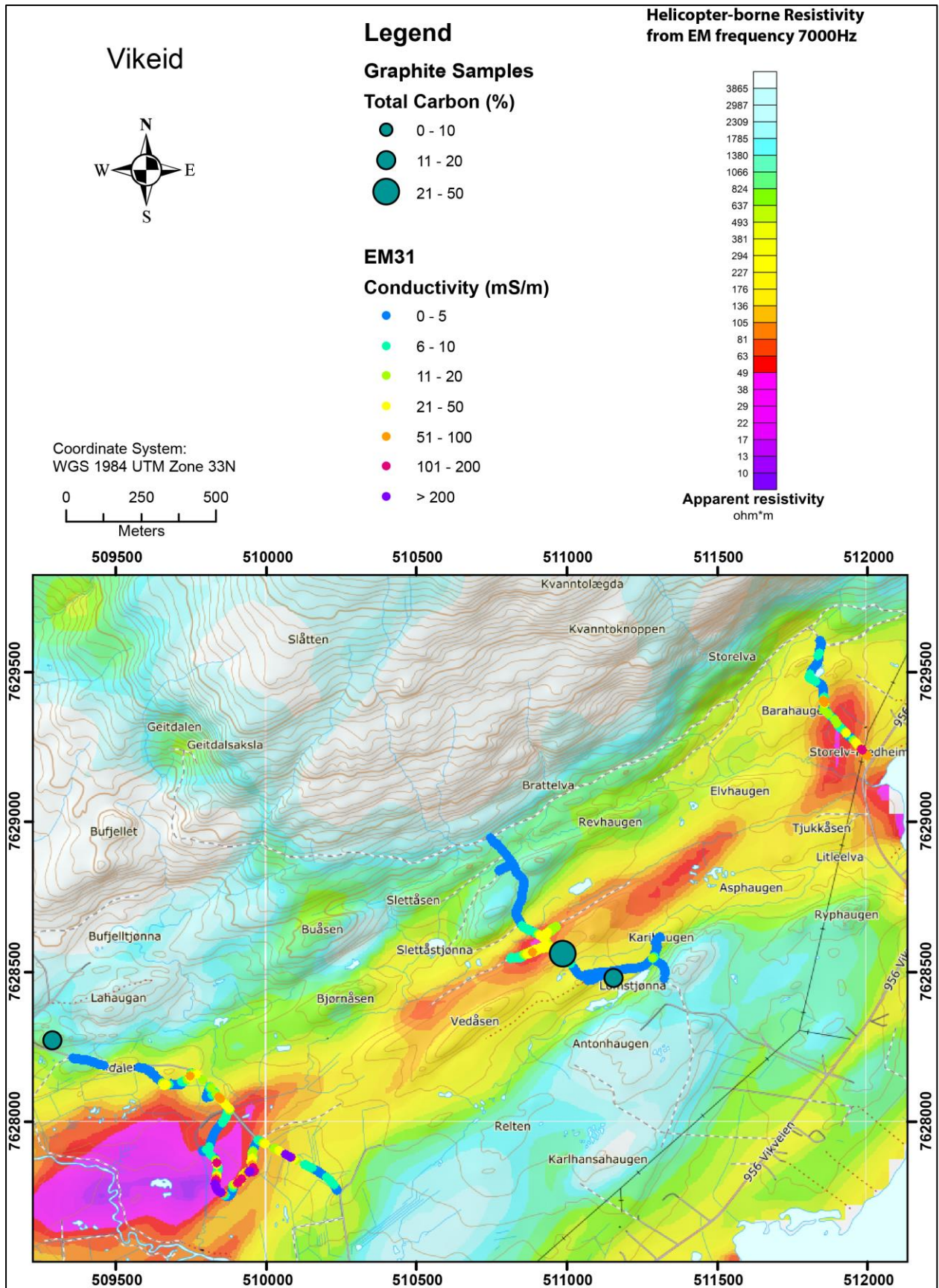


Figure 10.2: Results from EM31 measurements at Vikeid and graphite showings overlain on top of helicopter-borne measurements of apparent resistivity from EM 7000 Hz coaxial coil configuration.

The **2D Resistivity/IP profile 1** is located at the eastern flank of the most conductive structure in the Vikeid area (see Figure 10.3). The resistivity section (Figure 10.4) shows a deep quaternary cover up to 10 m thick. Underneath this cover, a ca. 120 m wide zone is observed (position 60 to position 185) with resistivity  $< 10 \Omega\text{m}$ , partly  $< 3 \Omega\text{m}$ . South of this zone (position 185 to 250) the resistivity is also anomalous low, between  $10 \Omega\text{m}$  and  $350 \Omega\text{m}$ . Further south the resistivity is normal for the host rock in the area ( $> 700 \Omega\text{m}$ ). Induced polarisation shows locally high values in the two most conductive zones indicating electronic conducting minerals (graphite or sulphide). The zone with the lowest resistivity may represent horizons of massive graphite/sulphide while the moderate resistivity can be due to dissemination of the same minerals. Modelling has shown that the continuous low resistivity zone may consist of several conducting zones, potentially graphite (Rønning et al. 2014).

The **2D Resistivity/IP profile 2** is located north-west of Lomstjønnna in the central part of the Vikeid area (see Figure 10.3). The resistivity section (Figure 10.5) is located in an area with 2-10 m thick quaternary cover. Underneath this cover, a ca. 150 m wide conducting zone is observed (position 40 to position 190). The resistivity is  $< 10 \Omega\text{m}$ , partly  $< 3 \Omega\text{m}$ . South of this zone, (position 190 to 250) the resistivity is also anomalous low, between  $10 \Omega\text{m}$  and  $350 \Omega\text{m}$ , the same as in profile 2. Further to the south, the resistivity is back to normal for the host rock in the area ( $> 700 \Omega\text{m}$ ). Induced polarisation shows locally high values in the two most conductive zones indicating electronic conductive minerals, graphite or sulphide. The zone with the lowest resistivity may represent horizons of massive graphite/sulphide while the moderate resistivity are potentially disseminations of the same minerals. Modelling has shown that the continuous low resistivity zone may consist of potentially several conducting graphite horizons (Rønning et al. 2014).

The **2D Resistivity/IP profile 7** intersects a ca. 150 m wide low resistive zone observed from helicopter-borne EM data north-west of Storelvbugta in the Vikeid area (see Figure 10.3). The thickness of the cover on this resistivity section (Figure 10.6) is from ca. 2-3 m to 15 m. The resistivity in this material is somewhat high ( $< 1200 \Omega\text{m}$ ). This may represent more coarse grained dry soil, but an interpretation of bedrock without mineralisation cannot be excluded.

Underneath this cover, along the entire profile of 300 m, a resistivity of  $< 10 \Omega\text{m}$ , and partly  $< 3 \Omega\text{m}$  is found. Induced polarisation shows locally high values which indicates disseminated electronic conducting minerals, graphite of sulphite. Modelling has shown that the continuous low resistivity zone potentially consists of several conducting graphite horizons (Rønning et al. 2014).

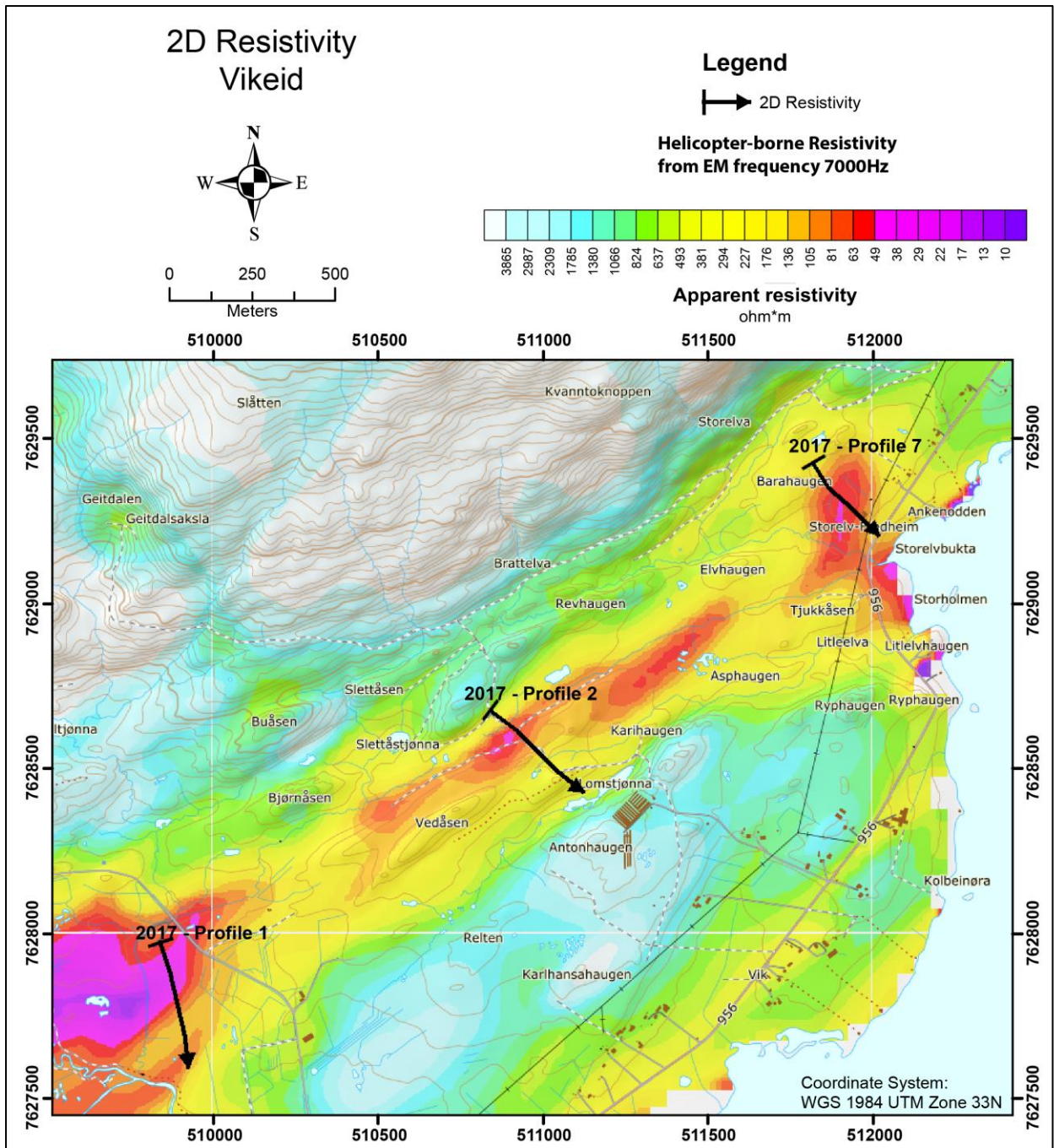


Figure 10.3: The Vikeid area. The location of the 2D Resistivity/IP profiles overlain on top of helicopter-borne measurements of apparent resistivity from EM 7000 Hz coaxial coil configuration.

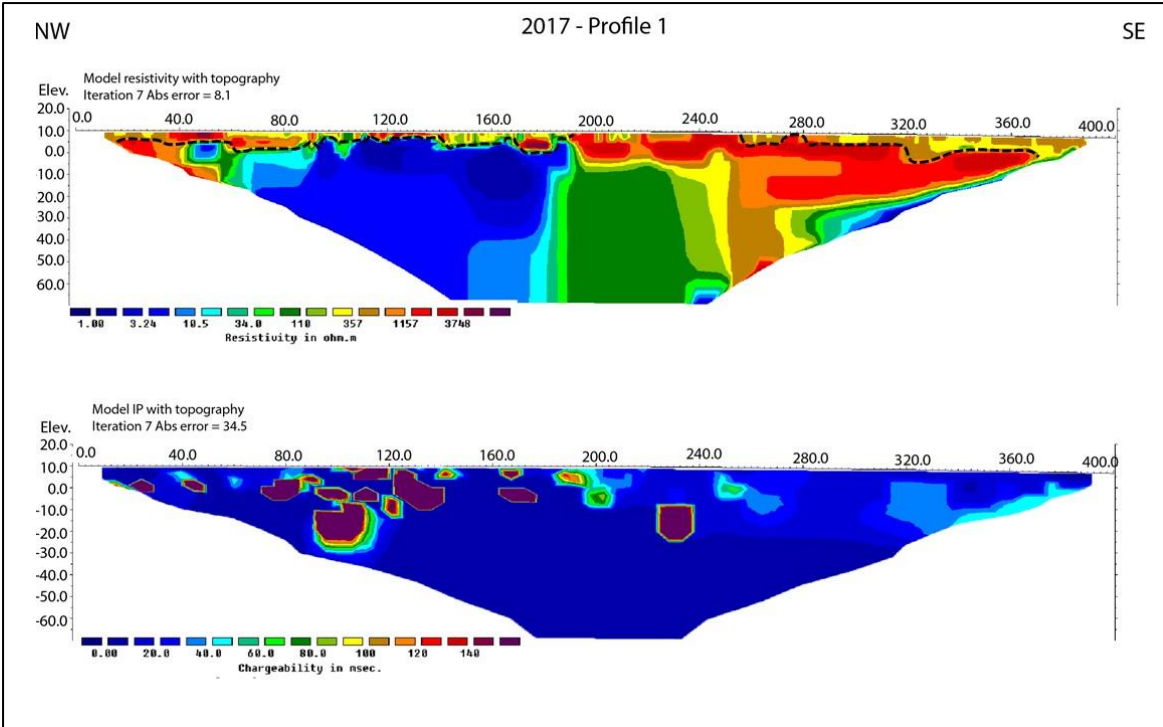


Figure 10.4: The Vikeid area. The results of the 2D Resistivity and Induced Polarisation measurements along profile 2017-1. The interpreted soil-bedrock interface as dotted black line.

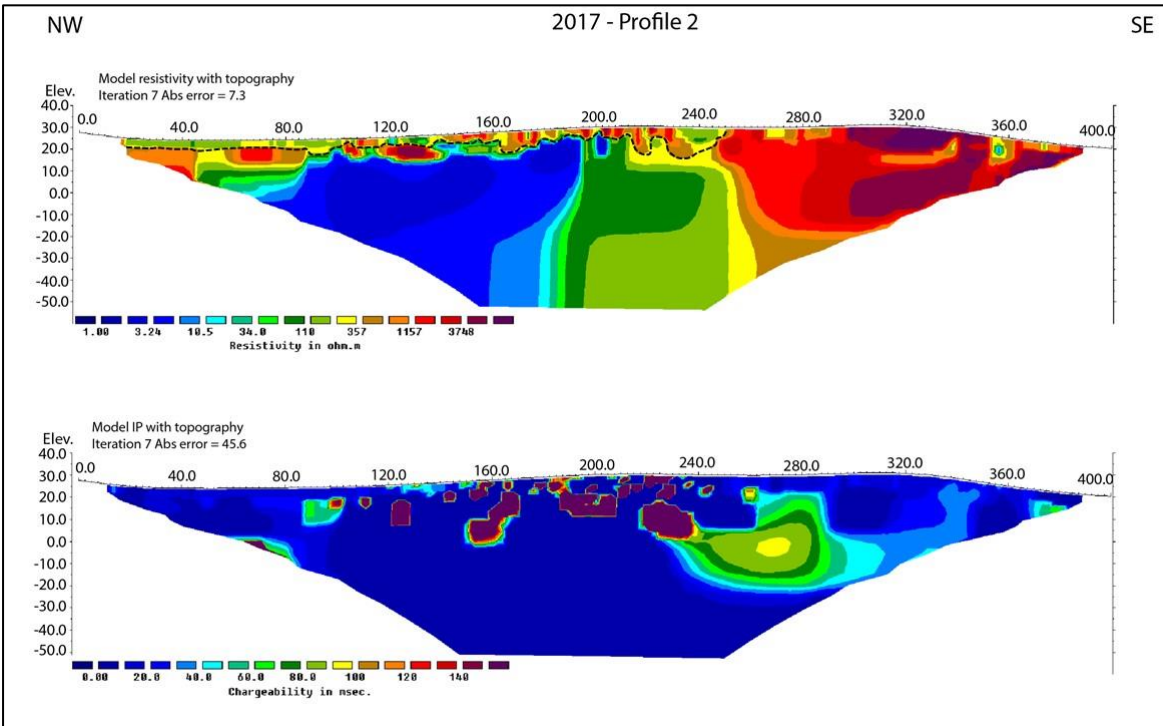


Figure 10.5: The Vikeid area. The results of the 2D Resistivity and Induced Polarisation measurements along profile 2017-2. The interpreted soil-bedrock interface as dotted black line.

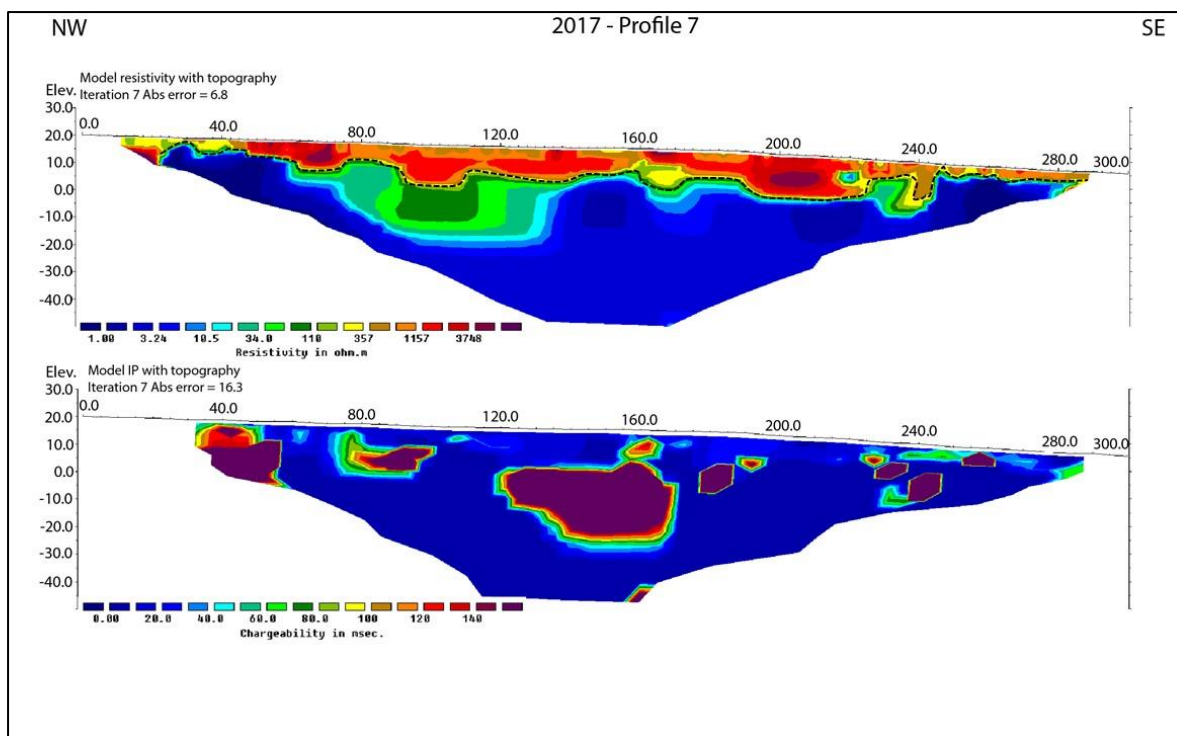


Figure 10.6: The Vikeid area. The results of the 2D Resistivity and Induced Polarisation measurements along profile 2017-7. The interpreted soil-bedrock interface as dotted black line.

### Summary of the Vikeid area.

The Vikeid area was previously investigated in 1992 (Gautneb & Tveten 1992). New 2D resistivity/IP measurements were performed in 2017 and indicate that graphite is more prevalent than in the six trenches investigated in 1992. To obtain information concerning the mineralogy and the quality of the graphite horizons detailed geophysics with subsequent core drilling is necessary. The geometrical size of the individual structures may be mapped by Charged Potential (CP) measurements.

To make an estimate of graphite volume and tonnage, more data is needed.

### 10.3 Geophysics and geology at Brenna

In the Brenne area (previously called Grønjordå) west of Frøskeland in the Sortland municipality, graphite mineralisation was discovered in roadcuts (Gautneb et al. 2017). Average total carbon content (TC) was 6.9 % and the maximum value 9.9 %. In the 2017 study, EM31 measurements and two 2D Resistivity /IP profiles were undertaken.

The **EM31 data** is presented in Figure 10.7, together with graphite showings integrated with apparent resistivity calculated from helicopter-borne EM measurements with 7000Hz coaxial coils. Several high conductive anomalies (apparent conductivity > 100 mS/m, apparent resistivity < 10  $\Omega$ m) were mapped, partly where exposed graphite mineralisation occurred.

The location of the two **resistivity/IP profiles** is shown in Figure 10.8. Profile 3 intersects the EM anomalies perpendicularly. The soil cover is interpreted to be ca. 2 to 8 m thick (Figure 10.9). Underneath this top layer, resistivity values of less than 10  $\Omega$ m and partly less than 3  $\Omega$ m appear along nearly the entire profile. As discussed earlier, this may be an artificial effect of several approximately vertical conducting structures. This is especially observed between position 120 and 220, where moderate resistivity values are bending down. This can be a shielding effect of two conductors located at the two positions (see modelling in Rønning et al. 2014).

**The Resistivity profile 6**, presented in figure 10.10, is parallel to the strike direction of the graphite mineralisation. The IP data is affected by a lot of noise and therefore these data are not presented. Low resistivity values (< 10  $\Omega$ m) are observed along almost the entire profile, indicating the presence of graphite. Between the positions 100 and 150 the graphite appears to be outcropping or nearly outcropping. In other areas the soil cover can be as much as ca. 10 m.

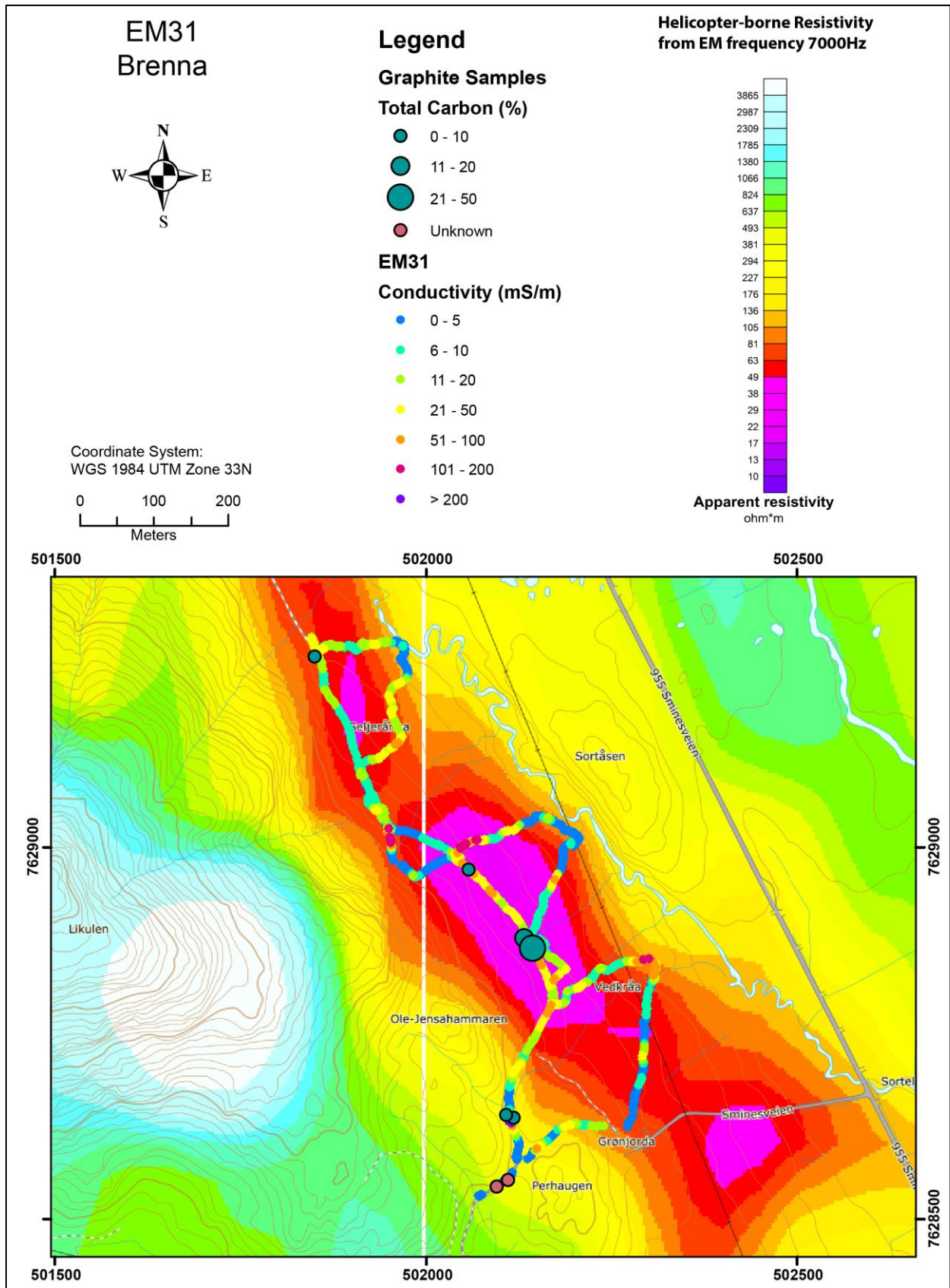


Figure 10.7: The Brenna area. The results from the EM31 measurements and graphite showings overlay on top of helicopter-borne measurements of apparent resistivity from EM 7000 Hz coaxial coil configuration.

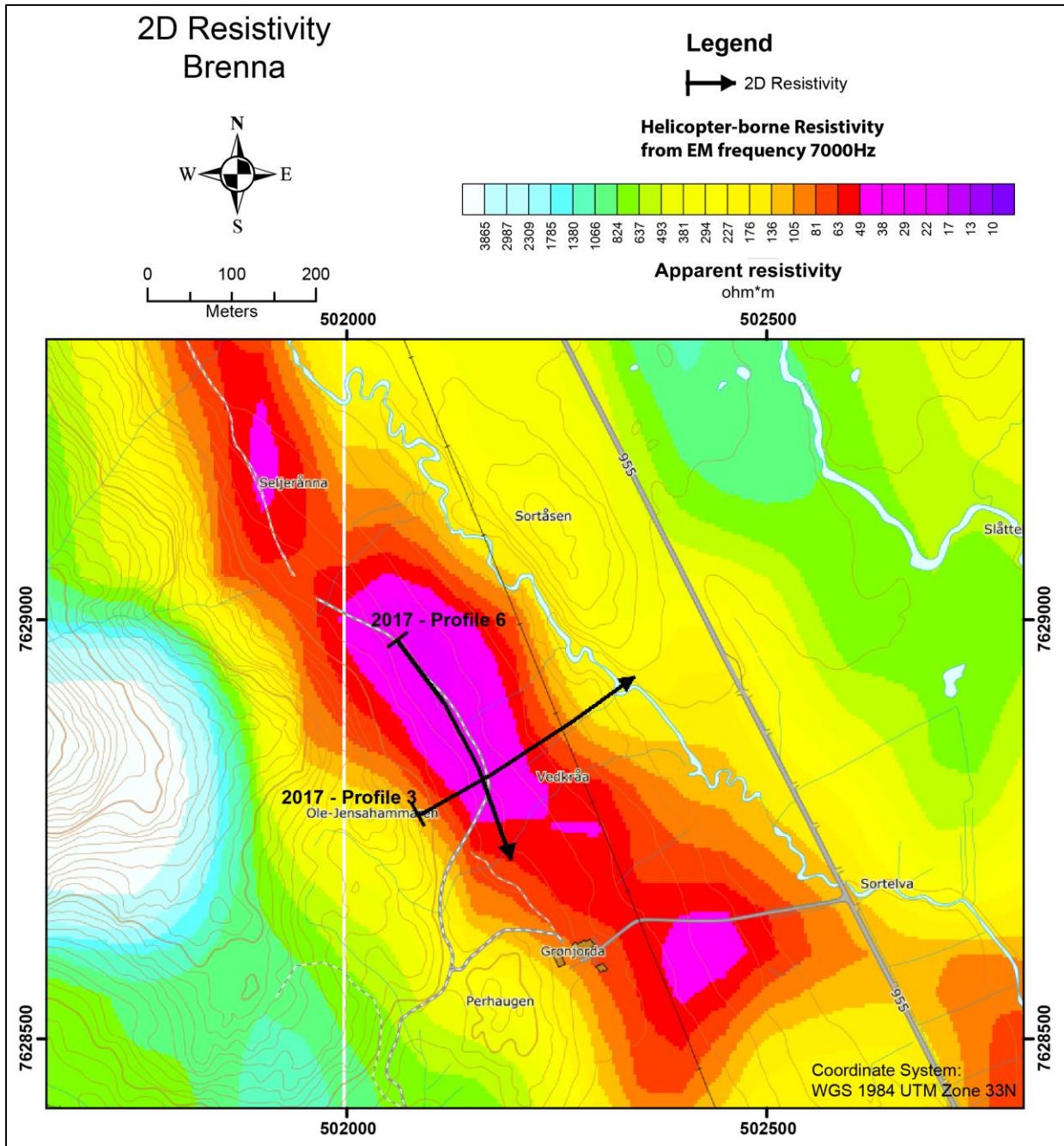


Figure 10.8: The Brenna area. The location of the 2D Resistivity/IP profile overlain on top of helicopter-borne measurements of apparent resistivity from EM 7000 Hz coaxial coil configuration.

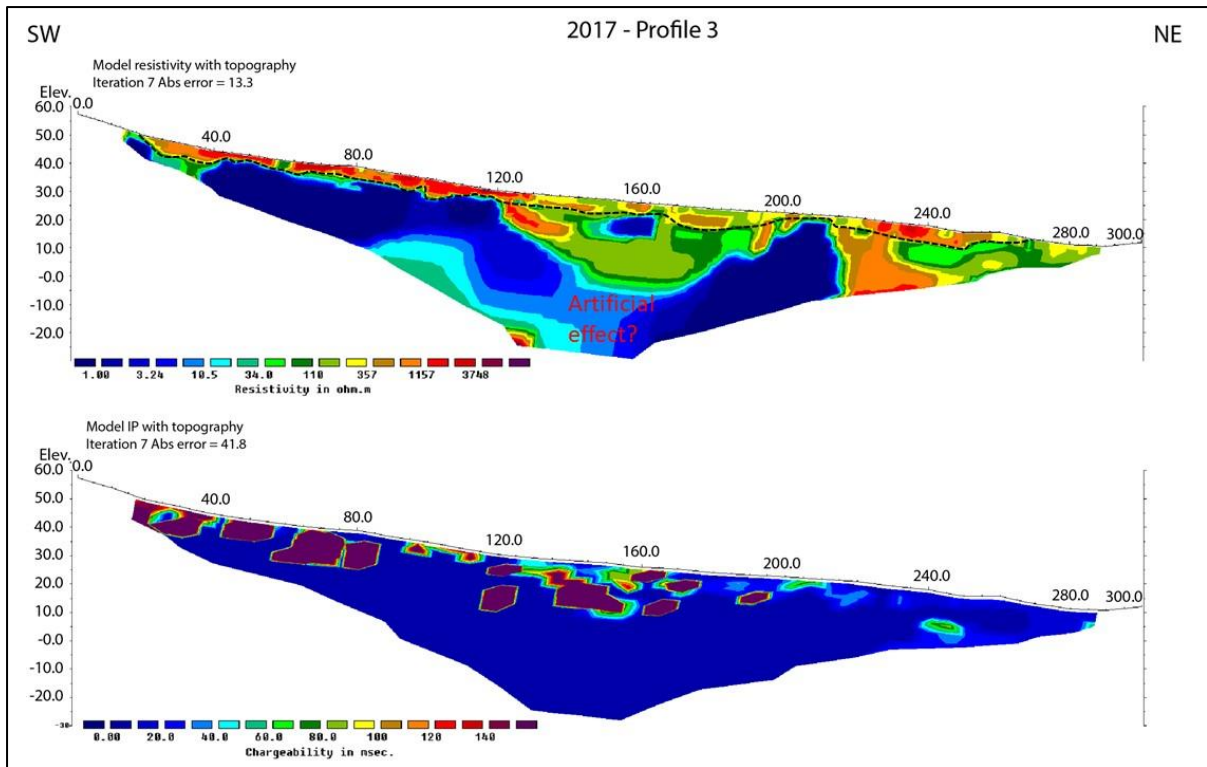


Figure 10.9: The Brenna area. The results from the 2D Resistivity and Induced Polarisation measurements along profile 2017-3. The interpreted soil-bedrock interface is shown as a dotted black line.

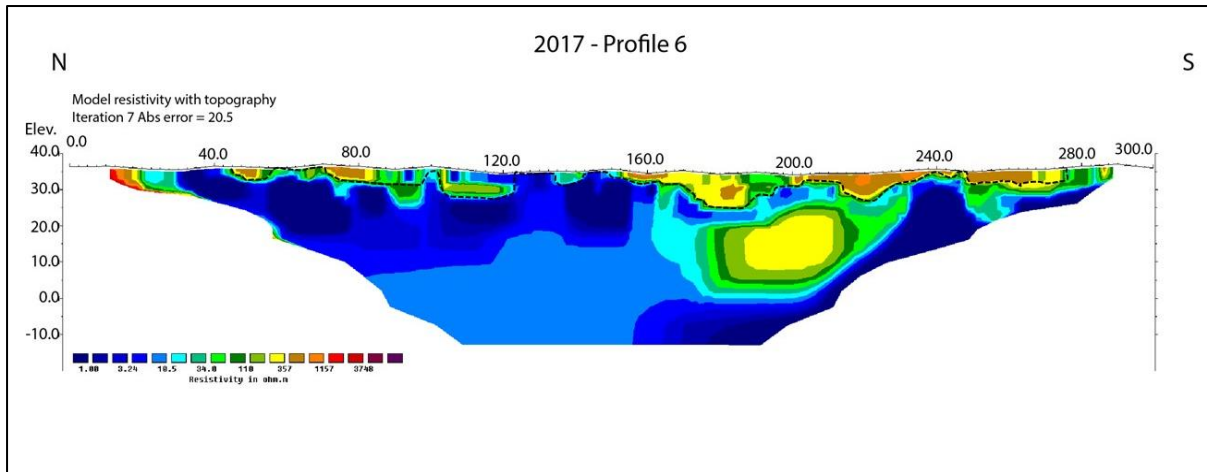


Figure 10.10: The Brenna area. The results from the 2D Resistivity measurements along profile 2017-6. The interpreted soil-bedrock interface is shown as a dotted black line.

### Brenna summary.

EM31 and 2D Resistivity/IP measurements has increased the knowledge of the graphite mineralisation at Brenna. In figure 10.11, an interpretation of individual structures is presented. The total length of these are ca. 1200 m and widths are in average ca. 5 m (estimated from EM31 data). A depth extent of 100 m will give an estimated total volume of 600000 m<sup>3</sup>.

The graphitic content of carbon (TC) from 6 samples shows an average value of 11.4 % and a maximum value of 30.4 %. If this is representative for the entire graphite structures, a total graphite tonnage in the Brenna area can be estimated to ca. 150,000 tonnes (graphite density equal 2.2 t/m<sup>3</sup>). As in other areas, the quality of the graphite is good (flake graphite).

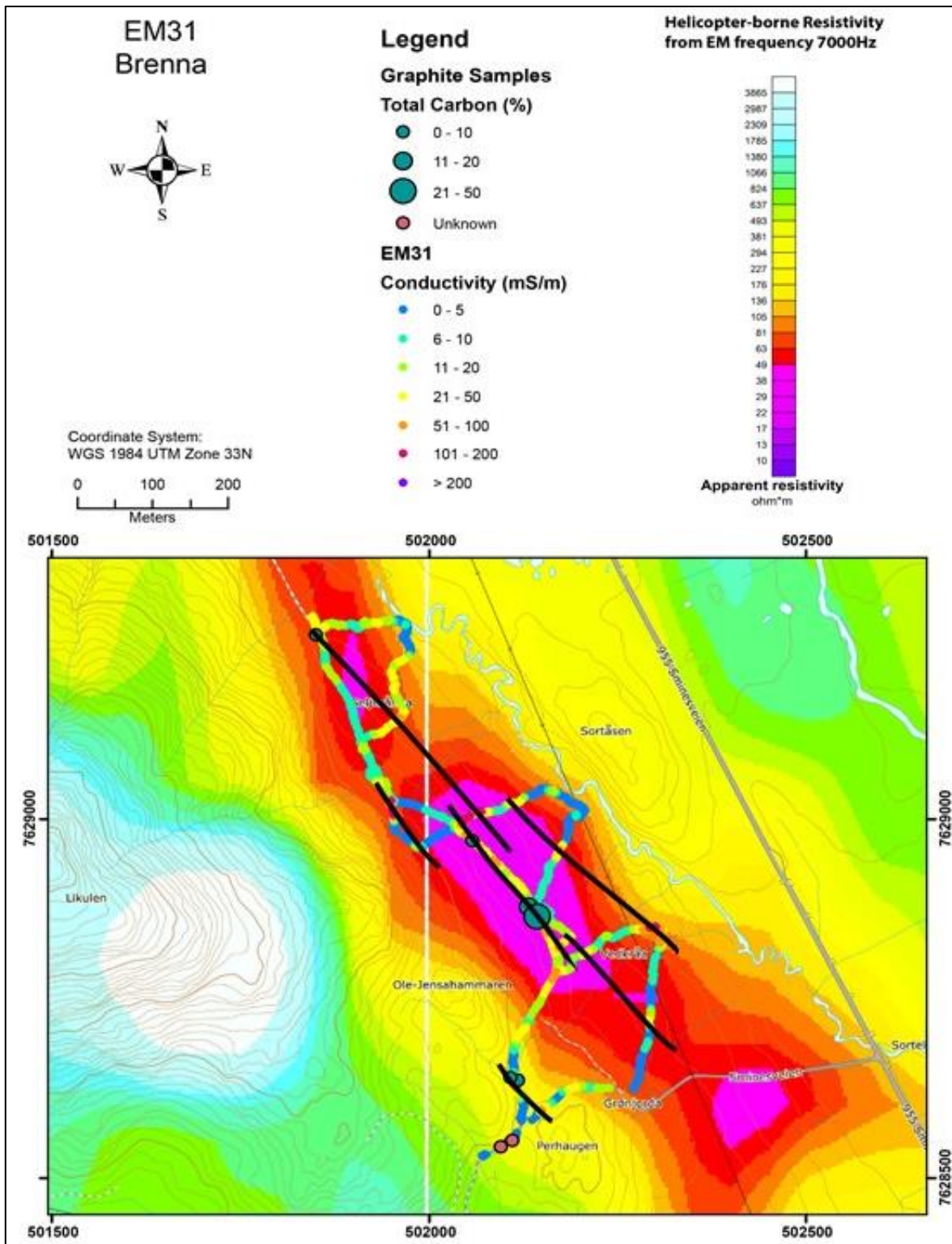


Figure 10.11: The Brenna area. The interpreted graphite structures based on EM31 and helicopter-borne EM data are shown as black lines.

## 11. RESULTS OF THE FOLLOW-UP WORK IN HADSEL MUNICIPALITY

During the field season of 2017, NGU performed geophysical measurements, some geological observations and sampling at three localities in the Hadsel municipality; Morfjord abandoned mine, Sommarhus and Sellåter.

### 11.1 Morfjord south (abandoned old mine)

In the Morfjord abandoned mine a ca. 30 m long adit can be followed showing a ca. 2 m thick vertical graphite body. The combined magnetic and electromagnetic analysis (figure 5.10) suggests that this is an interesting area for graphite. Analysis of three samples from the area show an average graphitic carbon content of 18.5 % with a maximum value of 19.7 % (Gautneb et al. 2017).

In 2017 NGU performed additional EM31 measurements. The results are presented in figure 11.1. Several high conductive anomalies (apparent conductivity > 100 mS/m, apparent resistivity < 10  $\Omega$ m) are shown. The mineralisation can be followed for a strike length of ca. 600 m and is observed to truncate against a charnockite body in the south.

Interpreted connections between the different conductive anomalies are shown in figure 11.2. Graphite is interpreted in a total strike length of ca. 1300 m delineated into four structures. Assuming an average width of ca. 2 m, as in the abandoned mine, and a depth extend of 100 m, this represents a total volume of 260,000 m<sup>3</sup>. Using the average carbon content of 18.5 %, the graphite tonnage is estimated to ca. 100,000 tonnes.

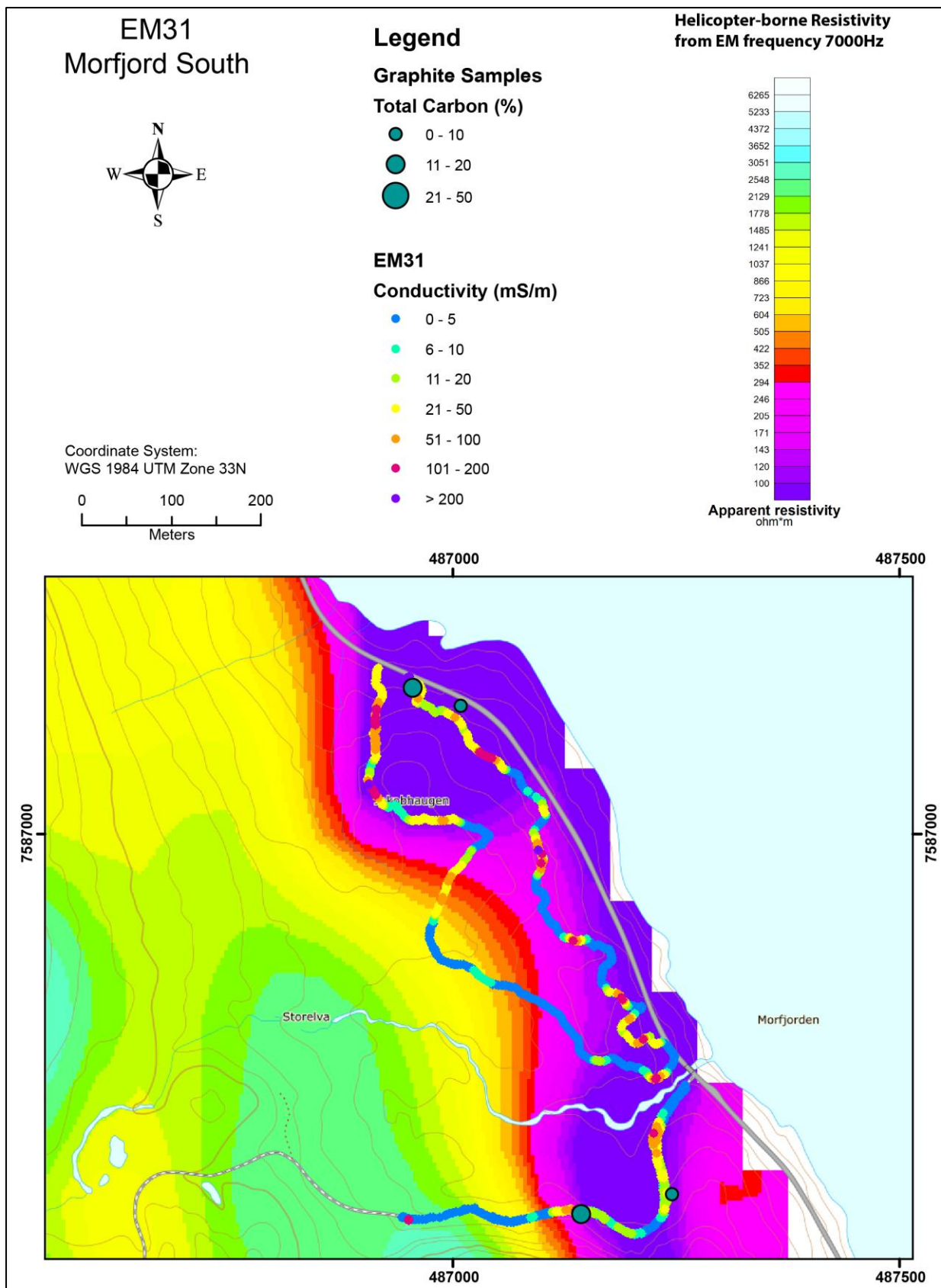


Figure 11.1: The Morfjord abandoned graphite mine. The results from the EM31 measurements and graphite showings overlain on top of helicopter-borne measurements of apparent resistivity from EM 7000 Hz coaxial coil configuration.

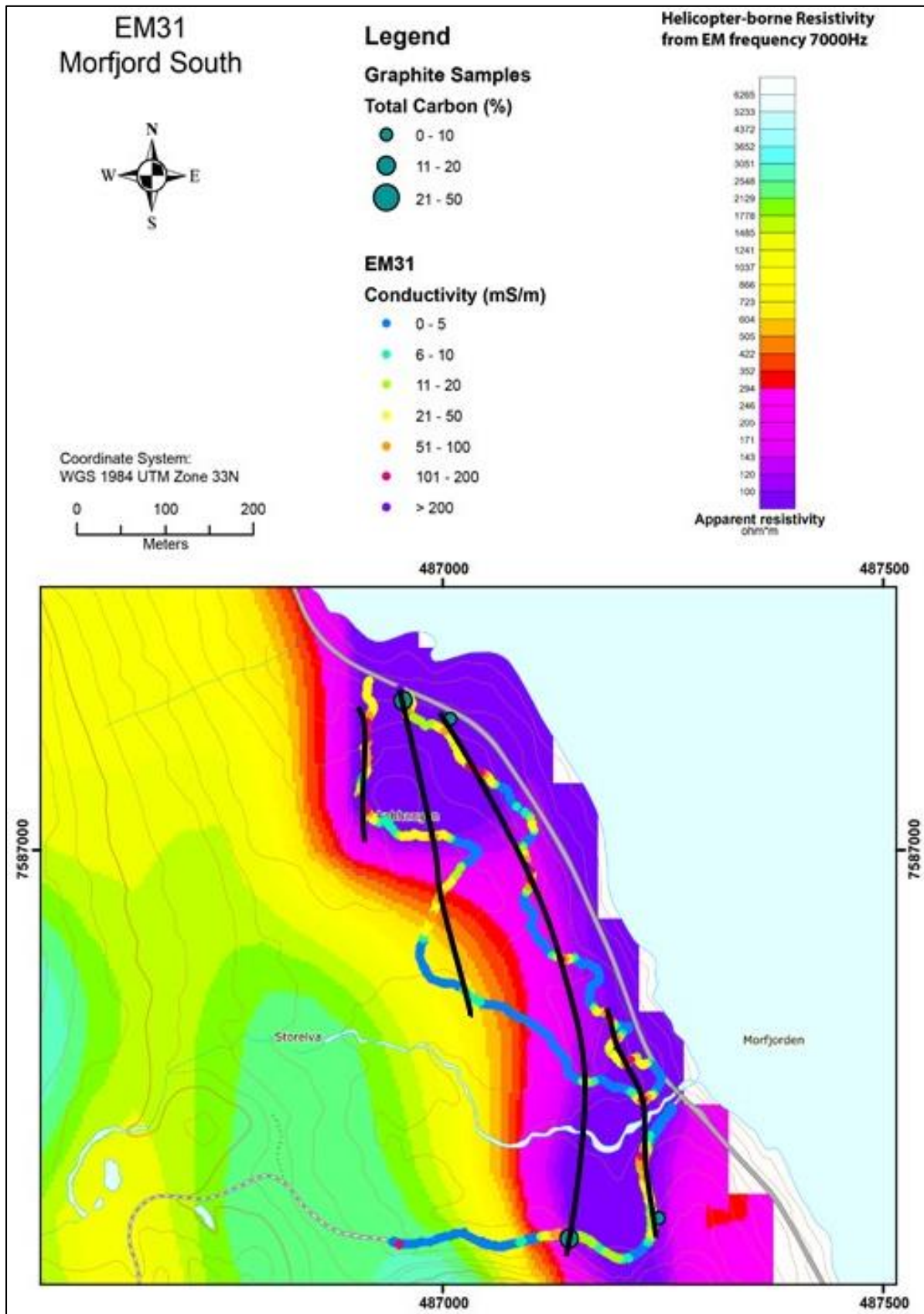


Figure 11.2: The Morfjord abandoned graphite mine. The interpreted graphite structures based on EM31 and helicopter-borne EM data are shown as black lines.

## 11.2 Geophysics and geology at Sommarhus and Sellåter

The two areas of Sommarhus and Sellåter have not been investigated before. The area shows up as interesting for graphite in the combined magnetic and electromagnetic analysis presented in figure 5.10. In 2017, NGU performed EM31 measurements and sampling/analyses.

**The EM31** results are presented in figure 11.3. At Sommarhus, several readings of high electric conductivity (apparent conductivity > 200 mS/m, apparent resistivity < 5  $\Omega$ m) are noticed. These high values may represent graphite, and graphite was discovered at two locations (see figure 11.3). There is insufficient EM31 measurements to give a complete image of the graphite structures, but there is a possibility that the graphite continues under the sea towards the old Morfjord mine in the south.

At Sellåter, on the other side of the fjord, the EM31 data shows similar conductivity values. Graphite is also observed here but is not mapped in detail.

Analysis of the total carbon (TC) content from the three areas are summarised in table 11.1. Sommarhus shows the most interesting total carbon (TC) values. In both areas, further EM31 measurements are recommended to map the graphite structures.

**Table 11.1: The number of samples and analysed graphite content (TC) in samples from the Sommarhus and Sellåter areas.**

Province/area/locality	N	Average %TC	Max % TC	Min of % TC	StdDv TC
Morfjord	3	18.45	19.70	16.80	1.49
Sellåter	7	6.30	9.72	3.30	2.02
Sommarhus	7	24.07	37.70	11.30	9.75
<b>Morfjord, all samples</b>	<b>17</b>	<b>15.76</b>	<b>37.70</b>	<b>3.30</b>	<b>10.40</b>

Most likely the graphite occurrence at Sommarhus is situated along strike from the Morfjord mine and is part of the same zone, but the presence of seawater masks their presence in the geophysical data. It is also possible that the Sellåter occurrence is connected to Sommarhus under the Morfjord fjord. Given the occurrence of graphite on shoreline of the Morfjord fjord one can even speculate that the central part of the Morfjord fjord consists of graphite schist and associated rocks that have been removed by weathering and ice erosion. The graphite occurrences in the Morfjord mine, Sommarhus and Sellåter can be a part of the same mineralised zone where the majority of the deposit is now under sea level.

Additional EM31 measurements at Sommarhus and Sellåter are recommended to make a continuous image of the mineralisation.

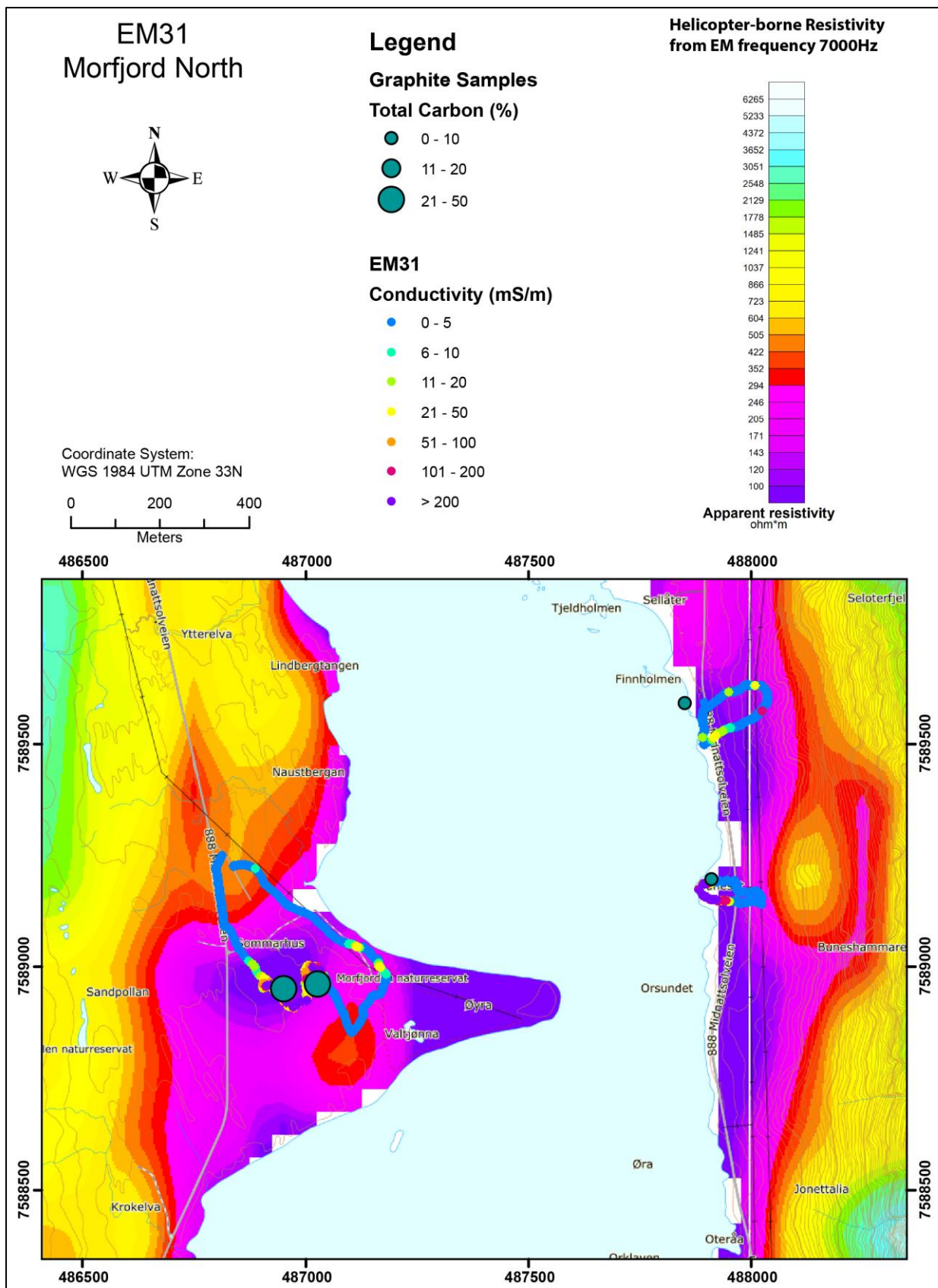


Figure 11.3: The Sommarhus and Sellåter areas. The results from the EM31 measurements and graphite showings overlay on top of helicopter-borne measurements of apparent resistivity from EM 7000 Hz coaxial coil configuration.

## 12. ADDITIONAL OBSERVATIONS AND DATA

In this chapter we present the petrography and petrophysics of the graphite schist and associated rocks.

### 12.1 Petrography of the graphite schist and associated rocks

Gautneb et al. (2017) gave a brief review of the petrography and mineralogy of the graphite schists using Raudhammaren as an example. In this study the understanding of the mineralogy, its variation and its complexity have been improved as a result of drilling at Sommarland and Haugsnes (Chapter 6 and 7). In this section descriptions are limited to the petrography and mineralogy of the graphite bearing units and to describe their typical variations. The description of the petrography is based on selected thin sections. A complete list of thin sections from the 2017 drilling is shown in Appendix 1.

#### 12.1.1 Examples of thin sections

The graphite schist has been shown to be a mineralogically variable rock. The silicate minerals are dominantly quartz, feldspar and pyroxene with variable amounts of mica, orto- and clino-pyroxene and in some cases also clinozoisite (figure 12.1). Figures 12.2 to 12.6 show features that are typical for graphite schist. Figure 12.3 shows that the graphite flakes are approximately 3000 to 4000  $\mu\text{m}$  and in some cases even larger. Graphite crystals occur very irregularly distributed in the rock, and there is a large variation both in grain size distribution and in area percentage of graphite within a small area, even on the thin section scale.

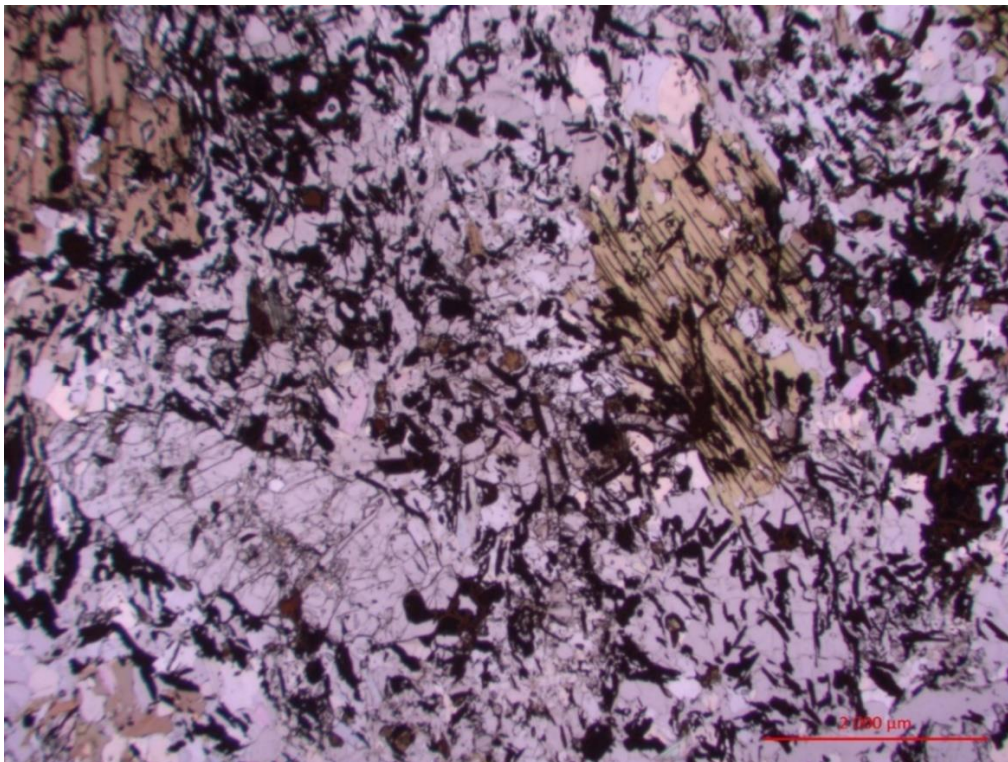


Figure 12.1: Thin section of graphite schist with a large crystal of clinozoisite in the lower left corner (Hg11-17).



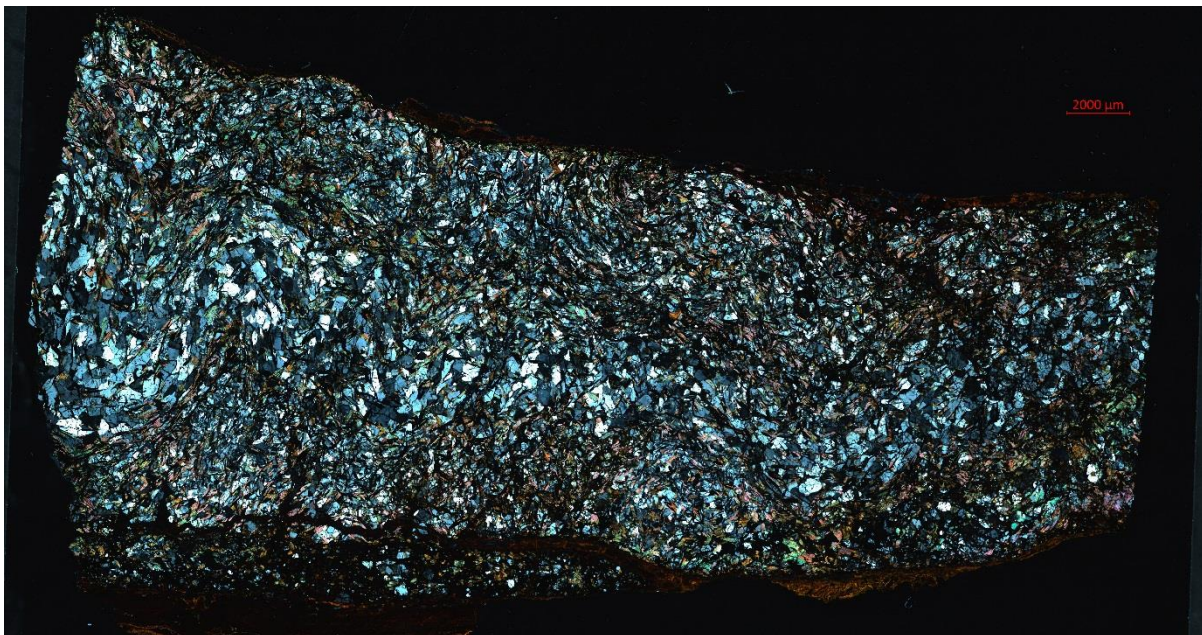
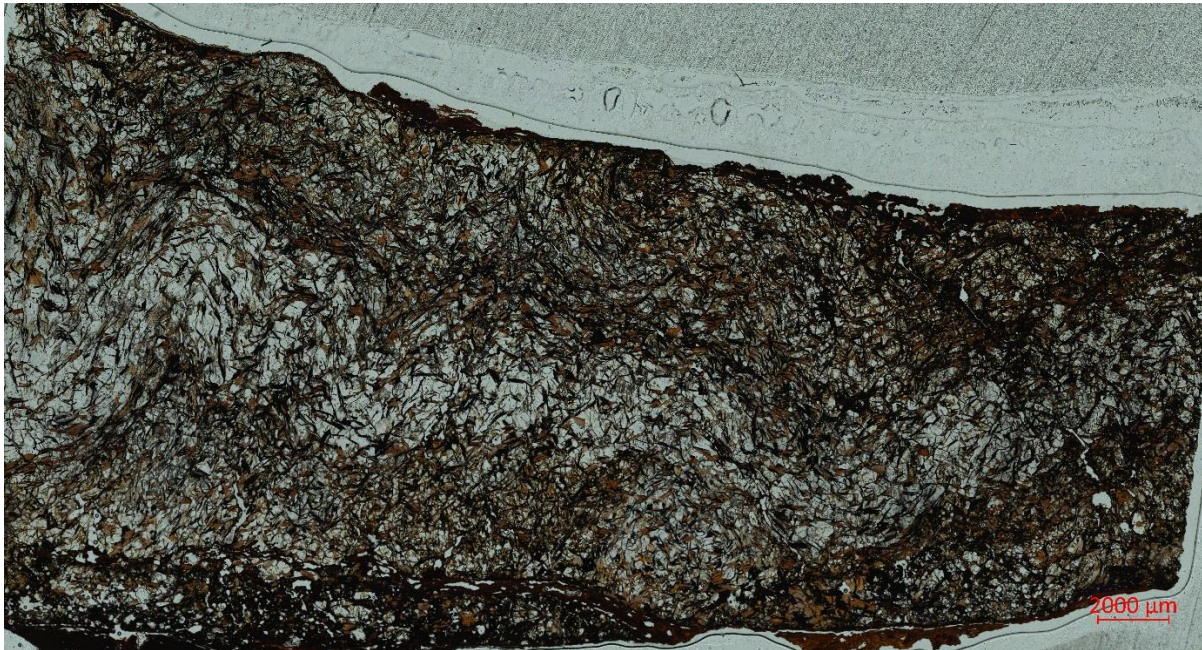
Figure 12.2: The graphite seen in reflected light showing large variations in the distribution and grain size of graphite flakes (thin section JK-2617-2-Sommarhus- 24,7%TC).



Figure 12.3: Thin section of graphite bearing rock showing large variations in both grain size and amount of graphite crystals over short distances (thin section JK6617-2).

We believe that this small scale variation is a common feature. The spatial variation of the amount of graphite in a thin section is also repeated on different scales from drill core, individual outcrops and on a large scale in areas such as Haugsnes (Chapter 7).

Often, but not always, the graphite schist is very schistose and strong foliation is visible from a macro- to micro-scale (figure 12.4).



**Figure 12.4:** Thin section showing an example of a strongly foliated and folded graphite schist, Transmitted light upper, polarised light lower (thin section JK291517-9).

Particularly rich graphite schists are commonly also rich in pyrrhotite. Pyrrhotite is a very ductile mineral that commonly deforms easier than the surrounding silicate minerals. The result is a rock with a breccia type of texture (figure 12.5) where fragments of silicates, often with crystals of graphite “float” in a matrix of pyrrhotite. This schist texture varies greatly with the proportion between sulphides and silicates combined with the degree of deformation.

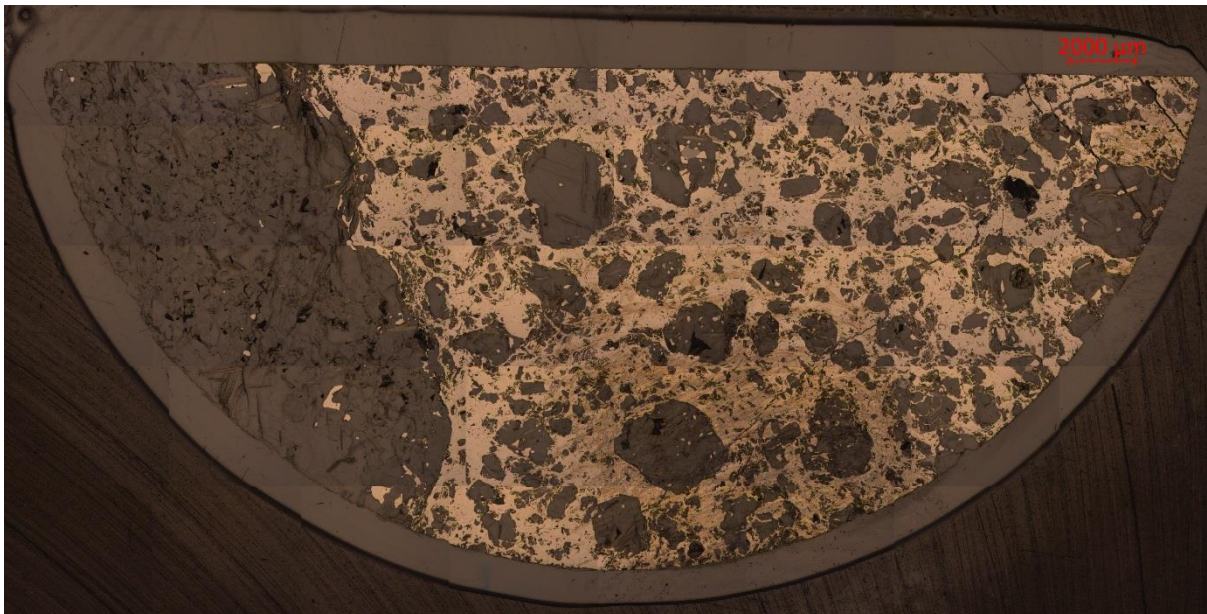


Figure 12.5: Thin section from half of a drill core, showing brecciation of the rock in areas with a high content of pyrrhotite combined with strong deformation, Transmitted light upper and reflected light lower (thin section HG-DhHau1701-6.5).

Typically, the host rock comprises rocks with variable content of feldspars, pyroxene and often with abundant biotite (figure 12.6).

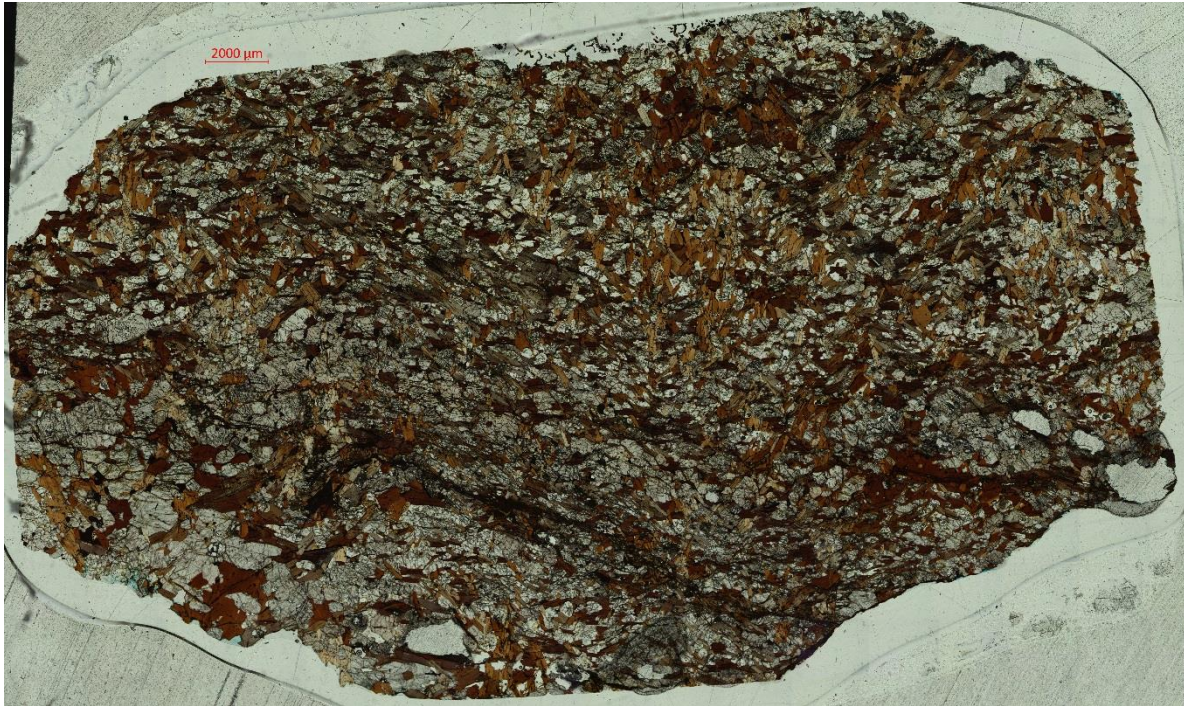


Figure 12.6: Biotite gneiss with graphite in traces, thin section JK-29517-pf7

### 12.1.2 Particle analysis of graphite crystals

To determine the flake graphite grain size, image processing of selected thin sections was performed. We selected one thin section from a sample with one of the highest levels of total carbon. An image of the measured thin section (HG-Dh Som1702 15.22) is shown in Figure 6.15.

#### **Method**

The measurements were undertaken using the following steps:

- a) A photomosaic of the whole thin section (about 3.5 cm<sup>2</sup>) was recorded, in reflected, transmitted and polarized light.
- b) Using the ZEN software from Carl Zeiss, colours corresponding to graphite crystals were selected, taking care that a majority of the selected areas actually represent graphite. The program then calculates automatically the graphite volume (area) in % and a number of form parameters such as *Area*, *Feret maximum* and *Feret minimum* etc for each particle. The most useful parameter is *Diameter*, which represent the calculated diameter of a circle with the same area as the measured particle and is the same as what is reported using other methods like sieving or coulter/sedigraph.

#### **Limitations and errors**

The biggest limitation of these measurements is that they represent an in situ measurement of the rock before crushing and beneficiation. The grain size of the rock would therefore be very different from a finished crushed product. There is also a limitation related to the pixel size of the image. In this case the pixel size is 9.08 microns corresponding to an area of 82.44 micron<sup>2</sup>. This is the limit of the minimum

particle size that can be measured. In addition, every image contains a certain amount of “noise” such as dust and other minor particles that are excluded prior to measurement. In a beneficiation process, the smallest particles will follow the tailing and lack of information from particles below 82 microns and removal of “dust” and “noise” are believed therefore not to create error but to increase the robustness of the measurements.

The measurements also have a number of geological related errors listed below (with decreasing importance):

Graphite crystals that touch each other are measured as a single large grain. Our results should therefore be regarded as maximum values. In particular, the biggest crystals measured represent aggregates of what would be regarded as several individual smaller crystals.

- A) Since the thickness of a thin section (30 microns) has a small but not insignificant variation in the Z axis when studied under the microscope, graphite crystals just below the surface of the thin section are also measured. They should ideally have been excluded. This error also contributes to overestimate the maximum values.
- B) In transmitted light other opaque minerals or minerals that are indistinguishable from graphite would also be recorded as graphite. This is particularly the case for sulphides and iron oxides. The amount of these minerals is low and measurements of the amount of sulphides using the same method as for graphite show that the area percentage of sulphide in our case is 0.67 %. This does not represent a significant error.

## Results

The grain size distribution is shown in Figure 12.7 and shows a very skewed distribution. but also shows features that are very characteristic for the graphite schist in this area (and in general). Most of the graphite crystals have a grain size of approximately 200 - to 300 microns. Above 800 micron the rock consists of a number of large individual graphite crystals up to a maximum grain size of about 3200 microns. These large grains represent aggregates of graphite crystals. They also make up the bulk of the areal percentage of graphite. The total areal percentage is 29.03%. This sample is a thin section from 15.22 metres in the drill hole Som1702. The interval from 14-16 metres in this drill hole shows an average TC content of 17.22 %. Area (volume) percentage as measured by image processing from a thin section and weight percentage from a bulk rock analysis, are not directly comparable. Theoretically for graphite,

$$\text{Volume \%} = \text{Weight \%} \times 1.7 \quad (\text{Hutchison 1975}).$$

The average TC content of 17.22 % multiplied by 1.7 gives 29.3 %. This is almost equal to the measured areal percentage of 29.0 %.

Such results are correct with the limits and errors described above. However, if one wants a practical usable understanding of the graphite flake size distribution, a mineral liberation study (MLA) should be performed.

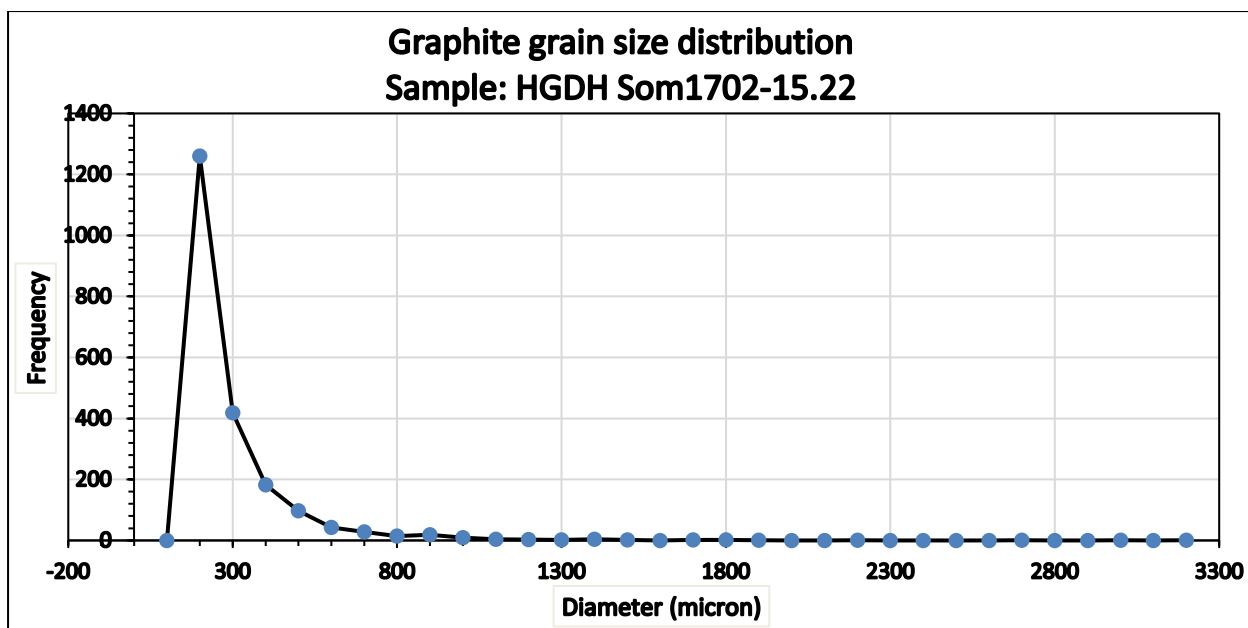


Figure 12.7: The grain size distribution of graphite crystals in sample HG-DhSom1702 15.22.

## 12.2 Petrophysical data from the drill cores

The core was sampled for petrophysical measurements at selected intervals. This was usually at the same levels along the cores where thin sections were taken. The following analyses: were recorded:

- Density,
- Magnetic susceptibility
- Magnetic remanence
- Heath conductivity
- Specific heath capacity.

In addition, the resistivity was qualitative recorded.

The drill holes were not available for resistivity logging. Instead, the resistivity was recorded continuously along the drill cores, using an ohm meter. Points or areas where the current was short-circuited were observed and recorded. If a short-circuit was observed at an individual point (1-2 cm distance) the relative value of 1 was recorded for this interval indicating disseminated graphite (or other electronic conducting minerals). If a short-circuit was observed over a longer distance (usually > 5 cm), this suggests that a considerable part of the drill core is electronic conductive. A relative value of 2 was recorded for this interval as an indicator of massive graphite.

Logs showing the variation in the petrophysical parameters along the drill cores are shown in figures 12.8 to 12.11. Measured petrophysical data are shown in Appendix 7.

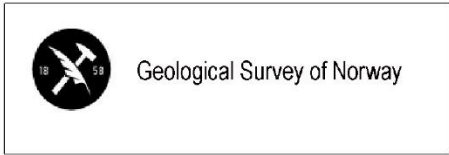
The magnetic susceptibility and the magnetic remanence show a very large variation from  $606 \cdot 10^{-6}$  SI to  $251581 \cdot 10^{-6} \cdot$ SI and from 9 to 1122286 mA/m respectively. The

magnetic susceptibility is measured with an electromagnetic method, and for electrical conductive graphite, this data is not reliable.

The density of the rock is less variable and is usually between 2.3 and 3.0 t/m<sup>3</sup>. This variation is controlled by the amount of graphite and other minerals. According to the literature, the density of pure graphite is 1.9 – 2.3 t/m<sup>3</sup> (Telford et al. 1976).

Of particular interest is the variation in observed resistivity. In general, and as expected, the graphite rich parts show low resistivity and a current short-circuit is observed in these intervals. However, all drill cores show scattered places where a current short-circuit is observed over distances of > 5 cm but < 0.5 m. In addition, there are a number of places where points with close to zero resistivity are observed. These points coincide with disseminated graphite grains.

This behaviour of the resistivity can be explained and is in agreement with what is observed visually in the cores and in thin sections. Patches, veins and small local enrichment in graphite and/or iron-oxides and sulphides occur scattered in many of the rock types and result in local resistivity close to zero. This type of mineralisation is what causes the Induced Polarisation (IP) effect.



Project: 370800 Total depth: 49,1  
 Location: Sommarland XUTM 487581 YUTM 7626300  
 Geologist: Gautneb/Knezevic Logged by: Janja Knezevic  
 Drillhole # Som1701 Azimut/Dip 260 / -45

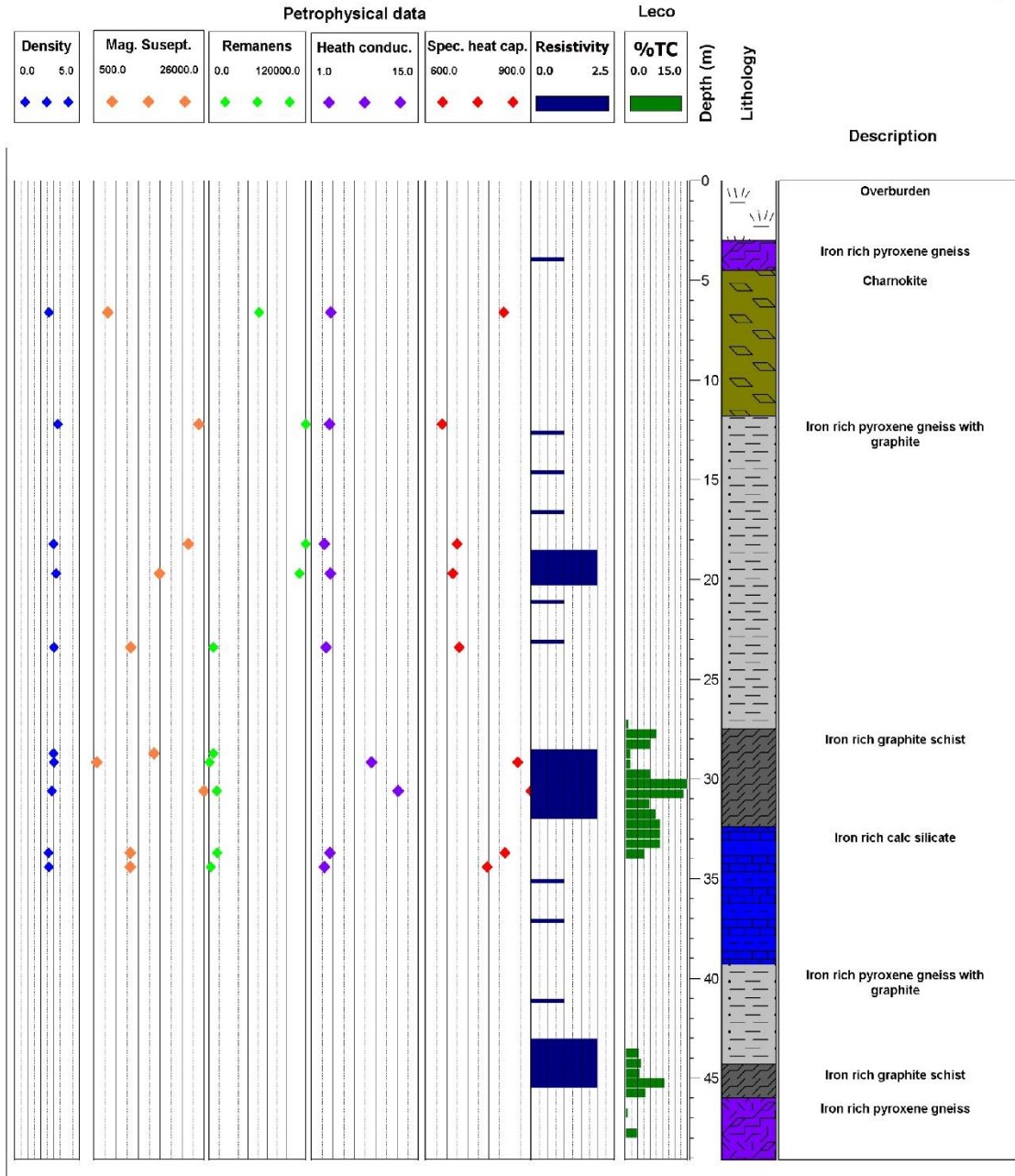


Figure 12.8: The petrophysical data and lithological log of the SOM1701 drill cores.

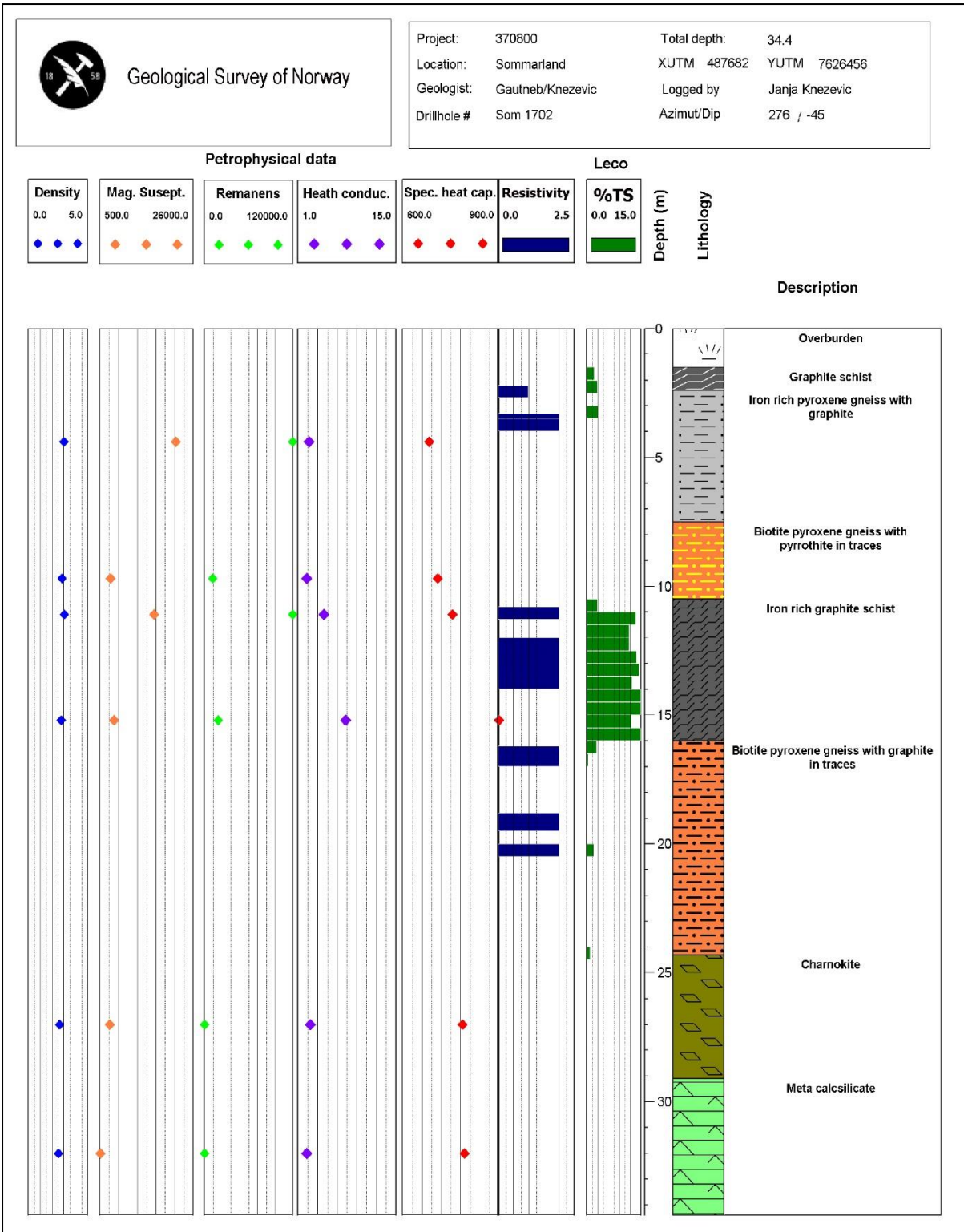


Figure 12.9: The petrophysical data and lithological log of the SOM1702 drill cores.

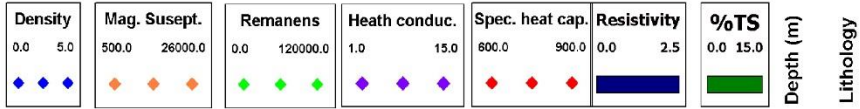


Geological Survey of Norway

Project: 370800      Total depth: 32.4  
Location: Hauges      XUTM 488288      YUTM 7618844  
Geologist: Gautneb/Knezevic      Logged by: Janja Knezevic  
Drillhole #: Haug 1701      Azimut/Dip: 310 / -45

Petrophysical data

Leco



Description

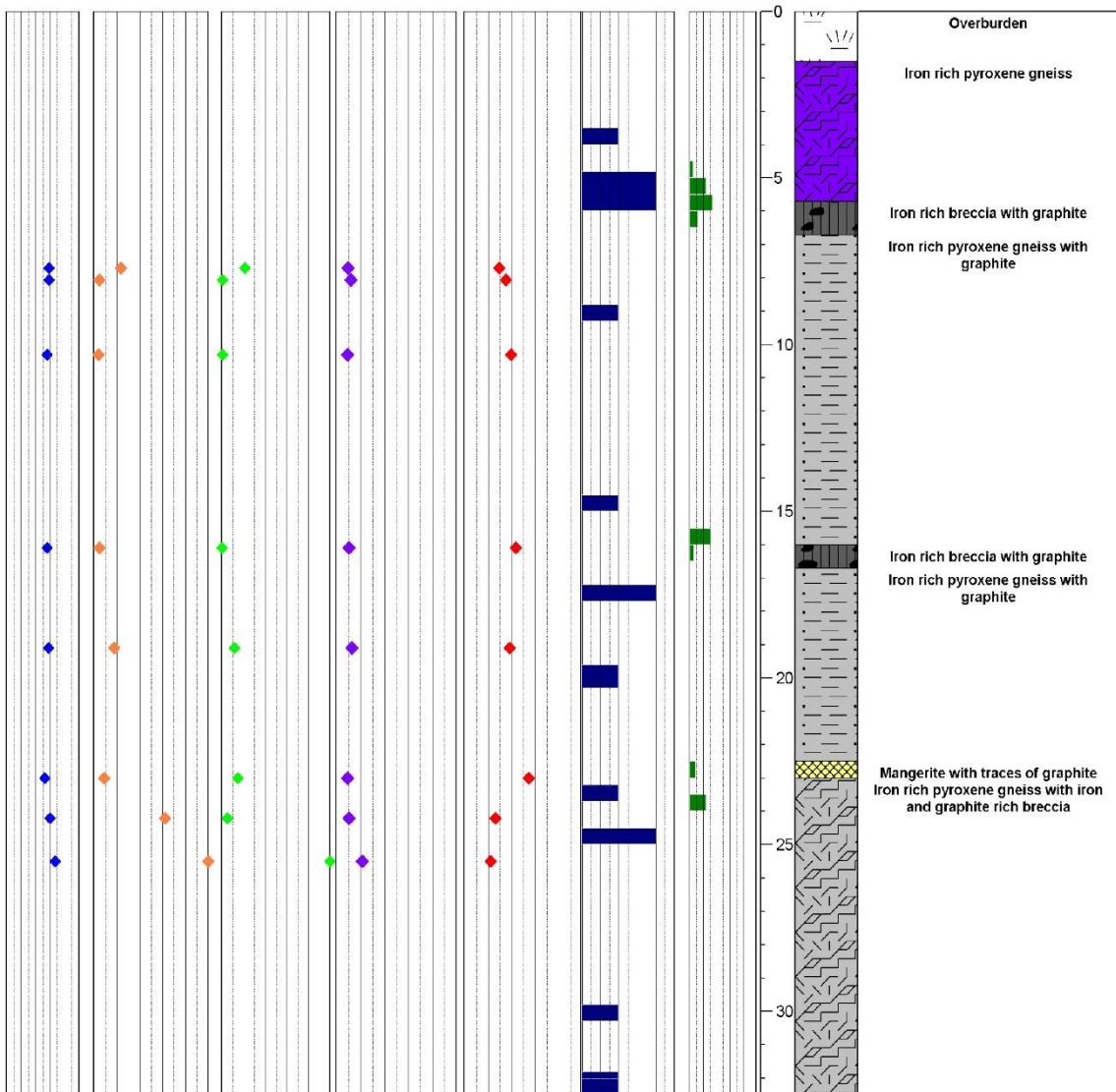


Figure 12.10: The petrophysical data and lithological log of the Haug1701 drill cores.



## 13. SUMMARY AND CONCLUSIONS

In the following chapter the total potential volume and tonnage of graphite is evaluated, where this is possible.

### 13.1 Summary of geometric information

For some selected localities a reasonable understanding of the number of graphite bearing zones and their strike length has been established. This has been achieved through trenching, EM31 profiles and core drilling at two localities. Reasonable interpretations have been made on the thickness of the graphite bearing zones. Assuming a mineable depth of 100 m allows an estimation of the total volume of graphite ore at different localities using the relationship below (Table 13.1):

$$\text{Volume (m}^3\text{)} = \text{Estimated total strike length (m)} \times \text{average width (m)} \times 100 \text{ (m)}$$

**Table 13.1: Estimation of volume of graphite bearing rocks from some selected localities.**

Locality	No. of zones	Total strike length (m)	Depth extent (m)	Average width (m)	Estimated volume (m <sup>3</sup> )
Sommarland	5	1000	100	4	400,000
Haugnes	11	8900	100	2	1,780,000
Raudhammaren	4	2000	100	4	800,000
Brenna	5	1200	100	5	600,000
Morfjord mine	4	1300	100	2	260,000

All of the calculations in Table 13.1 are by their nature uncertain. The total strike length is estimated from the surface SP and EM31 measurements and this data may be underestimated in cases where the graphite zones are not fully mapped. The depth extent of 100 m is a standard value and represents a depth that can easily be mined. In this study it has not been possible to evaluate the depth of the individual zones in any area, and therefore an assumed depth of 100 m may be too high. The average width of the graphite zones is established partly from core drilling (Sommarland and Haugnes) and may in fact be a good thickness estimate in these areas. In other areas, we have used the EM31 measurements to interpret the width of the mineralised zones. As was established from the drill cores, the quality of the graphite can vary markedly within individual zones. The volume of graphite is therefore an estimate which can be used for individual evaluation, but further investigations are needed to establish a more realistic resource knowledge.

A similar kind of volume estimation will be performed in other areas when more data becomes available in the future.

## 13.2 Summary of tonnage estimates

Based on the estimated volume of graphite in the investigated areas and what is known about the Total carbon (TC) content, an estimate of the graphite tonnage can be made.

**Table 13.2: Estimation of the tonnage of graphite from some selected localities.**

Locality	Estimated volume (m <sup>3</sup> )	Average TC (%)	Tonnage of flake graphite (t)	Comment
Sommarland	400,000	12.1	106,000	Surface samples
Sommarland	400,000	11.6	102,000	Drill cores
Haugnes	1,780,000	19.3	755,000	Surface samples
Haugnes	1,780,000	5.2	204,000	Drill cores
Raudhammaren	800,000	14.8	260,000	Surface samples
Brenna	600,000	11.4	150,000	Surface samples
Morfjord mine	260,000	15.8	90,000	Surface samples

As already discussed above, the volume of estimated graphite is uncertain. In addition, the uncertainty in the graphite tonnage is increased due to uncertainty in the total carbon content (TC). At Sommarland (Table 13.2), the average TC from surface samples is almost the same as the average from drill cores, thereby reducing the uncertainty. At Haugnes, the average TC from surface samples is 19.3 % while the average from the two drill holes is only 5.2 %. In addition, the individual thickness at Haugnes is sub-economical as established from the core drilling. The tonnage values in Table 14.2 are therefore an indication of how much graphite the different areas may contain.

## 13.3 Summary of carbon analysis, updated table

Gautneb et al. (2017), gives an overview of available analyses of total carbon (TC) from all investigated occurrences from 1990 until 2016. In Table 13.3 below, this overview has been updated with samples from 2017. Samples from the drill cores are not included in Table 14.3. They are discussed in chapters 6.3 and 7.2. The analyses are separated into areas and localities. Individual areas usually contain several localities, that can be individual sample localities along strike of a larger body or as several unrelated sampling points in a restricted geographical area. The table below also includes a few localities that are not discussed in this or earlier reports. All samples with coordinates are presented in Appendix 5.

In total 318 samples have been documented for the whole Vesterålen province with a grand total of an average 16.30 % TC. However, there is a large variation in TC from -0.06 % (the detection limit for the analyses) to 44.31 %. Certain localities, particularly in the trenches, sampling was done more or less continuously along the length of the trench. Since the graphite most often occurs very irregularly, the batch of samples from trenches may include rock samples that are not graphite schist. These samples

may contain no graphite and have a TC value that are very low or equal to the detection limit. In such cases the average % TC are believed to be realistic for the whole locality.

**Table 13.3: An upgraded overview of all available analysis of total carbon (TC) from investigated occurrences in Lofoten and Vesterålen from 1990 until 2016.**

Province/area/locality	N	Average TC (%)	Max TC (%)	Min of TC (%)	StdDv TC
<b>Vesterålen</b>					
<b>Andøya</b>					
Saura	1	2.26	2.26	2.26	
<b>Andøya All samples</b>	<b>1</b>	<b>2.26</b>	<b>2.26</b>	<b>2.26</b>	
<b>Brenna</b>					
Grønjordå	6	11.43	30.40	3.89	9.67
<b>Brenna, All samples</b>	<b>6</b>	<b>11.43</b>	<b>30.40</b>	<b>3.89</b>	<b>9.67</b>
<b>Hinnøya</b>					
Storå	1	10.50	10.50	10.50	
<b>Hinnøya, All samples</b>	<b>1</b>	<b>10.50</b>	<b>10.50</b>	<b>10.50</b>	
<b>Jennestad</b>					
Golia	8	17.60	32.78	5.69	11.16
Græva	20	29.52	39.65	1.30	12.25
Hornvann	71	22.07	44.31	0.06	12.55
Jennestad	4	9.21	15.20	3.53	5.00
Koven	10	15.16	26.13	0.85	8.97
Larmark gruve	5	9.72	12.74	3.18	4.11
Lille Hornvann	39	14.04	33.07	4.65	6.88
Vedåsen	4	14.16	16.66	11.50	2.13
Vikeid	1	21.70	21.70	21.70	
<b>Jennestad, All samples</b>	<b>162</b>	<b>19.51</b>	<b>44.31</b>	<b>0.06</b>	<b>11.77</b>
<b>Jørlandsvatnet</b>					
Jørlandsvatnet	1	14.20	14.20	14.20	
<b>Jørlandsvatnet, All samples</b>	<b>1</b>	<b>14.20</b>	<b>14.20</b>	<b>14.20</b>	
<b>Kvern fjord-Haugnes</b>					
Haugneset	11	19.30	33.82	10.60	9.44
Kvern fjordalen	5	6.06	13.70	0.12	6.32
<b>Kvern fjord-Haugnes, All samples</b>	<b>16</b>	<b>15.16</b>	<b>33.82</b>	<b>0.12</b>	<b>10.50</b>
<b>Kveøya</b>					
Øynes	2	18.75	20.60	16.90	2.62
<b>Kveøya, All samples</b>	<b>2</b>	<b>18.75</b>	<b>20.60</b>	<b>16.90</b>	<b>2.62</b>
<b>Morfjord</b>					
Morfjord	3	18.45	19.70	16.80	1.49
Sellåter	7	6.30	9.72	3.30	2.02
Sommarhus	7	24.07	37.70	11.30	9.75
<b>Morfjord, All samples</b>	<b>17</b>	<b>15.76</b>	<b>37.70</b>	<b>3.30</b>	<b>10.40</b>

<b>Møkland</b>					
Møkland trench 3 2015	5	9.32	18.30	0.03	8.61
Møkland trench 3 2015	2	9.22	18.10	0.35	12.55
Møkland trench 1 2015	7	0.08	0.17	0.03	0.05
Møkland trench 1 2016	6	6.72	14.50	0.47	6.06
Møkland trench 2 2015	7	12.03	21.10	1.13	7.85
Møkland trench 2 2016	1	-0.06	-0.06	-0.06	
Møkland trench 3 2016	8	13.98	22.30	5.76	5.70
Møkland trench 2 2015	2	20.90	25.70	16.10	6.79
<b>Møkland, All samples</b>	<b>38</b>	<b>9.04</b>	<b>25.70</b>	<b>-0.06</b>	<b>8.22</b>
<b>Raudhammaren</b>					
Raudhammaren	14	14.82	25.90	6.71	6.50
<b>Raudhammaren, All samples</b>	<b>14</b>	<b>14.82</b>	<b>25.90</b>	<b>6.71</b>	<b>6.50</b>
<b>Romsetfjord</b>					
Langstrand	12	14.48	31.00	3.62	8.21
<b>Romsetfjord, All samples</b>	<b>12</b>	<b>14.48</b>	<b>31.00</b>	<b>3.62</b>	<b>8.21</b>
<b>Skogsøya</b>					
Skalvneset	4	31.43	34.90	27.80	3.55
Skogsøya	10	19.29	34.20	0.40	11.43
Svinøya	2	23.35	24.90	21.80	2.19
<b>Skogsøya, All samples</b>	<b>16</b>	<b>19.26</b>	<b>34.90</b>	<b>0.40</b>	<b>11.10</b>
<b>Smines</b>					
Kaldhammaren	4	11.39	16.30	3.44	5.93
Rota	1	2.65	2.65	2.65	
Smines	14	7.85	17.30	0.37	5.55
<b>Smines, All samples</b>	<b>19</b>	<b>8.32</b>	<b>17.30</b>	<b>0.37</b>	<b>5.67</b>
<b>Sommarland</b>					
Central Sommarland	13	12.10	18.20	2.83	5.53
<b>Sommarland Total</b>	<b>13</b>	<b>12.10</b>	<b>18.20</b>	<b>2.83</b>	<b>5.53</b>
<b>Vesterålen, All samples</b>	<b>318</b>	<b>16.30</b>	<b>44.31</b>	<b>-0.06</b>	<b>11.05</b>
<b>Grand Total</b>	<b>318</b>	<b>16.30</b>	<b>44.31</b>	<b>-0.06</b>	<b>11.05</b>

## 14. REFERENCES

- AarhusInv, 2013: *Manual for Iversion software ver 6.1*, Aarhus, Denmark: Hydro Geophysics Group (HGG), University of Aarhus.  
[http://www.hgg.geo.au.dk/HGGsoftware/em1dinv/em1dinv\\_manual.pdf](http://www.hgg.geo.au.dk/HGGsoftware/em1dinv/em1dinv_manual.pdf) .
- ABEM, 2012: *ABEM Terrameter LS. Instruction Manual, release 1.11*, Sundbyberg: ABEM Instrument AB, Sweden.
- Corfu, F. 2004: U-Pb age, setting and tectonic significance of the anorthosite-mangerite-charnockite -Granite suite, Lofoten-Vesterålen, Norway. *Journal of Petrology*, 45, 1799-1819.
- Corfu, F. 2007: Multistage metamorphic evolution and nature of the amphibolite–granulite facies transition in Lofoten–Vesterålen, Norway, revealed by U–Pb in accessory minerals. *Chemical Geology*, 241, 108-128.
- Dahlin, T., 1993: *On the automation of 2D resistivity surveying for engineering and environmental applications..* Lund: Department of Engineering Geology, Lund Institute of Technology, Lund University. 187pp, ISBN 91-628-1032-4.
- Dahlin, T. & Zhou, B., 2006: Multiple-gradient array measurements for multichannel 2D. *Near Surface Geophysics, Vol 4, No 2*, April, pp. 113-123.
- Dalsegg, E., 1994: *CP-, SP- og ledningsevne målinger ved grafittundersøkelser ved Hornvannet, Sortland, Nordland*, Trondheim: NGU Report 94.003.
- Davidson, B. & Skår, Ø. 2004: Lofoten and Vesterålen: A Precambrian puzzle. (Abstract). The 26<sup>th</sup> Nordic Geological Winter Meeting, January 6<sup>th</sup> – 9<sup>th</sup> 2004, Uppsala, Sweden. *Geologiske Förenings Föreläsningar*. Vol 126, 20-21.
- Engvik, A.K., Davidson B., Coint, N., Lutro, O., Tveten, E. and Schiellerup, H. 2016: High-grade metamorphism of the Archean to Palaeoproterozoic gneiss complex in Vesterålen, North Norway. (Abstract) 32<sup>nd</sup> Geological Winter Meeting Helsinki, *Bulletin of the Geological Society of Finland*, special issue, 153-154
- Gautneb, H. & Tveten, E. 1992: *Grafittundersøkelser og geologisk kartlegging på Langøya, Sortland Kommune Nordland*. NGU report 92.155.
- Gautneb, H. 1992: *Grafittundersøkelser i Hornvannområdet, Sortland, Sortland Kommune Nordland*. NGU report 92.293.
- Gautneb H. 1993: *Grafittundersøkelser i Hornvannområdet, Sortland, Sortland Kommune Nordland*. NGU report 93.134
- Gautneb H. 1995: *Grafittundersøkelser Hornvann 1994, Sortland Kommune Nordland*. NGU report 95.076.
- Gautneb, H. & Tveten, E. 2000: The geology, exploration and characterization of graphite deposits in the Jennestad area, Vesterålen area northern Norway. *Norges geologiske undersøkelse Bulletin*. 436, 67-74.
- Gautneb, H., Knezevic, J., Johannesen, N.E., Wanvik, J.E., Engvik, A., Davidson, B., Rønning, J.S. 2017: Geological and ore dressing investigations of graphite occurrences in Bø, Sortland, Hadsel and Øksnes municipalities, Vesterålen, Nordland County, Northern Norway 2015 – 2016. NGU Report 2017.015 (70pp.).
- Geosoft 1997: *HEM System (Helicopter Electromagnetic data Processing, Analysis and Presentation System*, Toronto, Ontario Canada: Geosoft.
- Geonics 1984: *Operating manual EM31-D Non-contacting terrain conductivity meter*. Revised June 1984, Mississauga, Ontario Canada: Geonics LTD.
- Geotech 1997: *Hummingbird Electromagnetic System, User manual*, s.l.: Geotech Ltd.

- Griffin, W.L., Taylor, P.N., Hakkinen, J.W., Heier, K.S., Iden, I., Krogh, E.-J., Malm, O., Olsen, K.I., Ormåsén D.E. & Tveten, E. 1978: Archean and Proterozoic crustal evolution in Lofoten-Vesterålen N Norway. *Journal of the Geological Society of London* 135, 629-647.
- Helland A. 1987: Lofoten og Vesterålen. *Norges geologiske undersøkelse*. Vol. 23, 1-246.
- Heier, K.S. 1960: Petrology and geochemistry of high-grade metamorphic and igneous rocks on Langøya Northern Norway. *Norges geologiske undersøkelse bulletin* 207, 1-246.
- Hutchison C.S. 1975: The norm its variation, their calculation and relationships. *Schweizerische Mineralogische und Petrographische Mitteilungen*, 55, 243-256.
- Keilhau, B. M. 1844: Beretning om en geonostisk reise i norlandene i 1855. *Nyt Magazin for naturvidenskabene*. 11, nr.3.
- Kihle, O. & Eidsvig, P. D., 1978: Nye tolkninger for tolkning av CP-målinger, Trondheim: NGU Rapport 1534.(28 s.)..
- Lile, O. B., 1971. CP - Oppladet potensial. Trondheim: Lic.grad avhandling. Universitetet i Trondheim, Norges Tekniske Høgskole, Institutt for gruvedrift.
- Loke, M. H., 2014: Geoelectrical Imaging 2D & 3D. Instruction Manual. Res2DInv ver 4.00. <http://www.geotomosoft.com/>.
- Mogaard; J.O., Olsen, O., Rønning S, Blokkum, O. 1988: Geofysiske undersøkelser fra Helikopter over Langøya, Vesterålen: NGU report 88.151
- Neumann, H. 1952: Dagbok fra Nord-Norge 26.5-19.8 1952 Ba report 7709.
- Reynolds, J. 2011: *An Introduction to Applied and Environmental Geophysics*, 2nd edition. Wiley – Blackwell, Oxford UK.
- Rodinov, A., Ofstad, F., Stampolidis, A. & Tassis G. 2013a: Helicopter-borne magnetic, electromagnetic and radiometric geophysical survey at Langøya in Vesterålen, Nordland. NGU report 2013.044.
- Rodionov, A., Ofstad, F. & Tassis, G. 2013b: Helicopter-borne magnetic, electromagnetic and radiometric geophysical survey in the western part of Austvågøya, Lofoten archipelago, Nordland. NGU Report 2013.045
- Rønning J.S. 1991: CP målinger ved grafittundersøkelser på Vikeid, Sortland kommune Nordland. NGU report 91.262.
- Rønning J.S. 1993: CP og SP målinger ved grafittundersøkelser på Vikeid, Sortland kommune Nordland. NGU report 93.018.
- Rønning, J.S., Rodionov, a., Ofstad, F., Lylum R. 2012: Elektromagnetiske, magnetiske, og radiometriske målinger fra helikopter i området Skaland - Trælen på Senja. NGU report 2012.061.
- Rønning, J. S., Gautneb, H., Dalsegg, E., Larsen, B.E. & Rodionov, A. 2014: Oppfølgende grafittundersøkelser i Meløy og Rødøy kommuner, Nordland, Trondheim: NGU. Report nr 2014.046.
- Rønning, J.S., Larsen, B.E., Elvebakk, H., Gautneb, H., Ofstad, F. & Knežević, J. 2017: Geophysical investigations of graphite occurrences in Bø and Øksnes municipalities, Vesterålen, Nordland County, Northern Norway 2015-2016. NGU Report 2017.044 (50 pp.).
- Sato, M. & Mooney, H. M., 1960: The electrochemical mechanism of sulfide self-potentials. *Geophysics*, Volume 25, pp. 226-249.
- UBC, 2000: Manual for EM1DFM., Vancouver, Canada: UBC - Geophysical Inversion facility, Department of Earth and Ocean Sciences, University of British Columbia.

Skjeseth S. 1952: Foreløpig rapport fra geologiske undersøkelser av Jennestad grafitt-felt. Report BA5232, Norges geologiske undersøkelse.

Vokes F.M. 1954: Rapport over befarings av Jennestad grafitt-felt. Report BA5340 Norges geologiske undersøkelse.

Telford, W.M., Geldart, L.P., Sheriff, R.E. & Keys, D.A. 1976: Applied Geophysics. Cambridge University Press. Cambridge UK.

Tveten, E. 1978: Berggrunnskart over Norge; Svolve 1:250.000. Norges geologiske undersøkelse.

Tveten, E. & Henningsen, T. 1998: Berggrunnskart over Norge; 1:250.000 Andøy. Norges geologiske undersøkelse.

Øzmerih, L. 1991: Graphite beneficiation from Jennestad ore. SINTEF report STF F91059, 21p

## **Appendixes**

**Appendix 1: List of thin sections from the drill cores**

**Appendix 2: TS and TC analysis of drill cores**

**Appendix 3: Pictures of drill cores**

**Appendix 4: Portable XRF analysis of drill cores.**

**Appendix 5: Complete list of analysed samples for TS, TC and TOC from 1990-2017**

**Appendix 6: Samples analysed for total carbon, total sulphur and petrophysics**

**Appendix 7: Petrophysics of drill core samples**

All data exist in excel format, that can be provided upon request.

## Appendix 1: List of thin sections from the drill cores

The samples were collected by Janja Knezevic (JK) and Håvard Gautneb (HG). Additional information is available upon request. The thin sections are available for inspection for visitors to NGU.

Drill core id	som1701			Drill core id	som1702
Sample id	Depth			Sample id	Depth
HG-DHSom1701-6,65	6.66			HG-DHSom1702-4,7	4.7
HG-DHSom1701-12,35	12.35			JK-DHSom1702-9,65	9.68
JK-DHSom1701-18,2	18.2			HG-DHSom1702-11,04	11.04
JK-DHSom1701-19,7	19.7			HG-DHSom1702-15,22	15.22
JK-DHSom1701-23,94	23.94			JK-DHSom1702-32,78	32.78
HG-DHSom1701-28,74	28.74				
JK-DHSom1701-29,15	29.15				
HG-DHSom1701-30,63	30.63				
HG-DHSom1701-33,7	33.7				
HG-DHSom1701-45	45				
Drill core id	hau1701			Drill core id	hau1702
Sample id	Depth			Sample id	Depth
HG-DHHau1701-3,7	3.7			JK-DHHau1702-5,57	5.57
HG-DHHau1701-5,85	5.85			JK-DHHau1702-7,2	7.2
HG-DHHau1701-6,5	6.5			JK-DHHau1702-13,6	13.6
JK-DHHau1701-10,3	10.3			JK-DHHau1702-16,7	16.7
JK-DHHau1701-16,5	16.5			JK-DHHau1702-30,5	30.5
JK-DHHau1701-19,3	19.3			JK-DHHau1702-34,55	34.55
JK-DHHau1701-23	23			JK-DHHau1702-38,1	38.1
JK-DHHau1701-25,55	25.55				
JK-DHHau1701-28,06	28.06				

## Appendix 2: TS and TC analysis of drill cores

See text for description of methods.

ID	Sample_no	From	To	TS (%)	TC (%)
189043	Som1701-42	24	24.5	4.42	0.08
189044	Som1701-43	24.5	25	1.70	0.11
189045	Som1701-44	25	25.5	1.46	0.07
189046	Som1701-45	25.5	26	2.21	0.15
189047	Som1701-46	26	26.5	3.64	0.11
189048	Som1701-47	26.5	27	3.31	0.13
189049	Som1701-48	27	27.5	4.96	0.82
189050	Som1701-49	27.5	28	8.40	7.74
189051	Som1701-50	28	28.5	8.05	6.18
189052	Som1701-51	28.5	29	2.79	1.33
189053	Som1701-52	29	29.5	2.32	1.31
189054	Som1701-53	29.5	30	3.78	6.17
189055	Som1701-54	30	30.5	5.06	15.5
189056	Som1701-55	30.5	31	4.88	14.3
189057	Som1701-56	31	31.5	3.85	6.00
189058	Som1701-57	31.5	32	2.76	7.48
189059	Som1701-58	32	32.5	1.57	8.51
189060	Som1701-59	32.5	33	1.58	8.51
189061	Som1701-60	33	33.5	1.32	8.50
189062	Som1701-61	33.5	34	2.72	4.68
189063	Som1701-62	34	34.5	1.11	0.16
189064	Som1701-63	34.5	35	5.04	0.18
189079	Som1701-75	43.5	44	0.64	3.42
189080	Som1701-76	44	44.5	1.00	3.93
189081	Som1701-77	44.5	45	0.96	3.54
189082	Som1701-78	45	45.5	4.17	9.70
189084	Som1701-79	45.5	46	6.58	5.07
189085	Som1701-80	46	46.5	3.42	0.10
189086	Som1701-81	46.5	47	2.49	0.70
189087	Som1701-82	47	47.5	1.92	0.07
189088	Som1701-83	47.5	48	3.13	0.03
189089	Som1701-84	48	48.5	1.27	0.03
189101	Som1702-1	1.5	2	3.23	2.12
189102	Som1702-2	2	2.5	4.95	2.99
189103	Som1702-3	2.5	3	2.11	0.08
189104	Som1702-4	3	3.5	7.30	3.25
189117	Som1702-17	9.5	10	0.79	0.03
189118	Som1702-18	10	10.5	2.65	0.12
189119	Som1702-19	10.5	11	9.26	2.96
189120	Som1702-20	11	11.5	8.11	13.5

189121	Som1702-21	11.5	12	10.4	11.8
189122	Som1702-22	12	12.5	3.80	11.8
189123	Som1702-23	12.5	13	5.99	13.8
189124	Som1702-23b	13	13.5	4.43	14.6
189125	Som1702-24	13.5	14	4.72	12.5
189126	Som1702-25	14	14.5	4.20	22.5
189127	Som1702-26	14.5	15	4.88	18.1
189128	Som1702-27	15	15.5	3.83	12.4
189129	Som1702-28	15.5	16	3.77	15.9
189130	Som1702-29	16	16.5	1.53	2.82
189131	Som1702-30	16.5	17	1.76	0.42
189132	Som1702-31	17	17.5	0.55	0.21
189133	Som1702-32	17.5	18	0.19	0.06
189134	Som1702-33	18	18.5	0.38	0.10
189135	Som1702-34	18.5	19	0.42	0.03
189136	Som1702-35	19	19.5	0.46	0.14
189137	Som1702-36	19.5	20	0.24	0.14
189138	Som1702-37	20	20.5	3.00	2.0
189139	Som1702-37b	20.5	21	0.84	0.03
189140	Som1702-38	21	21.5	0.82	0.03
189141	Som1702-38b	21.5	22	1.04	0.03
189142	Som1702-40	22	22.5	0.52	0.03
189143	Som1702-41	22.5	23	0.48	0.06
189144	Som1702-42	23	23.5	0.61	0.08
189145	Som1702-43	23.5	24	1.38	0.03
189146	Som1702-44	24	24.5	0.57	1.00
189159	Haug1701-6b	4.5	5	5.34	0.89
189160	Haug1701-7	5	5.5	13.2	3.77
189161	Haug1701-8	5.5	6	12.2	5.14
189162	Haug1701-9	6	6.5	10.1	1.82
189179	Haug1701-26	14.5	15	1.00	0.03
189180	Haug1701-27	15	15.5	3.47	0.13
189181	Haug1701-28	15.5	16	12.1	4.84
189182	Haug1701-29	16	16.5	11.3	1.01
189183	Haug1701-30	16.5	17	1.79	0.11
189191	Haug1701-38	20.5	21	1.56	0.08
189192	Haug1701-39	21	21.5	0.68	0.03
189193	Haug1701-40	21.5	22	1.43	0.06
189194	Haug1701-41	22	22.5	1.40	0.140
189195	Haug1701-42	22.5	23	6.66	1.34
189196	Haug1701-43	23	23.5	3.60	0.09
189197	Haug1701-44	23.5	24	10.1	3.74
189198	Haug1701-45	24	24.5	2.12	0.137

189220	Haug1702-9	7	7.5	3.09	1.50
189221	Haug1702-10	7.5	8	1.51	1.40
189222	Haug1702-11	8	8.5	1.05	4.98
189223	Haug1702-12	8.5	9	0.45	7.08
189224	Haug1702-13	9	9.5	0.90	5.92
189225	Haug1702-14	9.5	10	3.29	1.65
189226	Haug1702-15	10	10.5	0.43	0.31
189227	Haug1702-16	10.5	11	1.03	0.20
189228	Haug1702-17	11	11.5	1.12	3.11
189229	Haug1702-18	11.5	12	2.32	1.57
<b>average</b>				<b>3.39</b>	<b>3.67</b>
<b>max</b>				<b>13.20</b>	<b>22.50</b>
<b>min</b>				<b>0.19</b>	<b>0.03</b>

### Appendix 3: Pictures of drill cores

Som1701 & Som1702 = Sommarland drilling in 2017, Haug1701 & Haug1702 Haugsnes drilling in 2017.



Som1701 Box 1, 0 – 10 m.



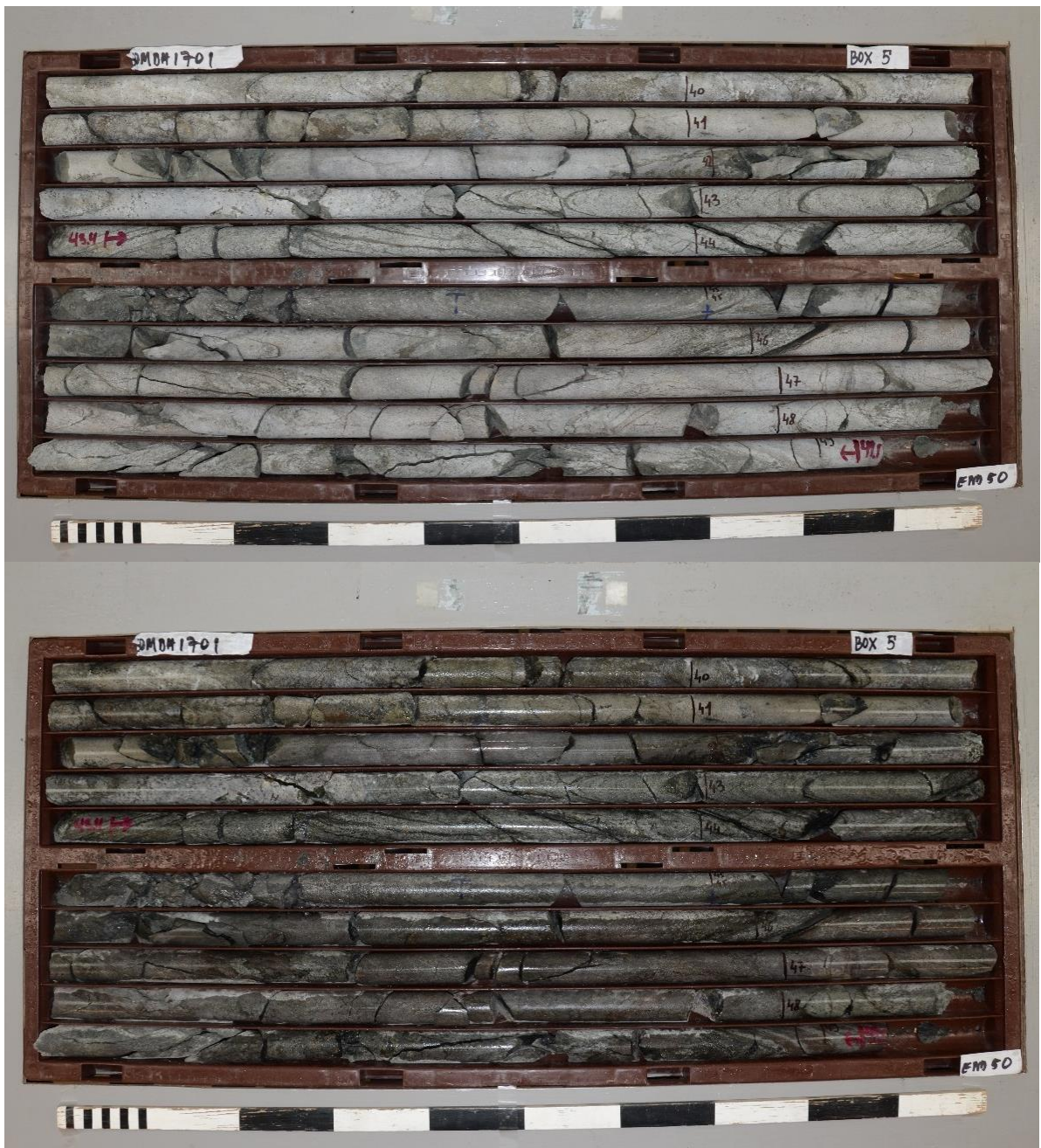
Som1701 Box 2, 10 – 20 m.



Som1701 Box 3, 20 – 30 m.



Som1701 Box 4, 30 – 40 m.



Som1701 Box 5, 40 – 50 m.



Som1702 Box1, 0 – 10 m.



Som1702 Box 2, 10 – 20 m.



Som1702 Box 3, 20 – 30 m.



Som1702 Box 4, 30 – 35,5 m.



Haug1701 Box 1, 0 – 10 m.



Haug1701 Box 2, 10 – 20 m.



Haug1701 Box 3, 20 – 30 m.



Haug1701 Box 4, 30 – 33 m.



Haug1702 Box 1, 0 – 10 m



Haug1702 Box 2, 10 – 20 m.



Haug1702 Box 3, 20 – 30 m.



Haug1702 Box 4, 30 – 40 m



Haug1702 Box 5, 40 – 50 m.

#### Appendix 4: Portable XRF analysis of drill cores.

The drill core where analysed by a Niton portable XRF, using standard methods, counting time per point was 20 seconds. There were usually 4 points analysed per metre core. Additional information is available upon request. All values are in %.

Drill hole	Depth (m)	Al	Ca	Fe	Ni	S	Si
Som1701	3	6.1	5.7	3.0	-	2.0	34.7
Som1701	3.25	6.6	5.4	3.9	-	1.1	29.9
Som1701	3.5	5.9	1.9	4.4	-	0.2	24.8
Som1701	3.75	4.4	6.4	11.9	0.0	14.9	22.8
Som1701	4	1.6	9.2	11.1	0.0	6.4	26.5
Som1701	4.25	10.1	4.9	3.0	-	0.3	31.1
Som1701	4.5	1.8	6.8	13.3	0.0	8.0	19.1
Som1701	4.75	4.6	0.6	1.1	-	0.3	33.7
Som1701	5	5.5	0.5	0.7	-	0.4	41.2
Som1701	5.25	5.6	0.5	0.4	-	0.1	39.3
Som1701	5.5	4.8	0.6	0.7	-	0.8	44.3
Som1701	5.75	5.0	0.4	1.0	-	0.5	46.2
Som1701	6	5.2	0.6	1.6	-	4.5	40.1
Som1701	6.25	5.1	0.9	0.6	-	0.2	40.9
Som1701	6.5	5.0	0.9	1.0	-	0.4	40.4
Som1701	6.75	4.7	0.6	1.1	-	1.0	45.3
Som1701	7	6.0	0.8	0.7	-	-	42.8
Som1701	7.33	4.6	0.3	0.4	-	0.2	39.8
Som1701	7.67	4.7	0.5	0.7	-	0.5	47.8
Som1701	8	5.9	0.6	1.2	-	1.1	44.8
Som1701	8.33	4.6	1.8	1.4	-	0.4	40.6
Som1701	8.67	4.2	0.6	0.3	-	0.1	47.2
Som1701	9	4.1	0.9	0.7	-	0.2	37.7
Som1701	9.33	5.1	0.5	0.8	-	0.2	44.4
Som1701	9.67	5.0	0.6	0.6	-	0.2	40.2
Som1701	10	6.1	0.5	1.0	-	1.4	42.7
Som1701	10.33	4.5	1.1	1.7	-	0.5	39.8
Som1701	10.67	3.1	0.7	0.8	-	0.2	35.6
Som1701	11	6.1	0.6	0.8	-	0.2	40.3
Som1701	11.33	4.2	0.6	1.1	-	0.3	39.4
Som1701	11.67	5.0	0.5	0.5	-	0.1	42.3
Som1701	12	5.9	13.0	6.3	-	4.5	23.9
Som1701	12.25	2.1	13.0	12.4	0.0	9.6	23.4
Som1701	12.5	-	3.7	41.2	0.1	20.9	7.1
Som1701	12.75	4.3	8.5	9.8	0.0	7.7	20.2
Som1701	13	2.0	15.0	2.2	-	0.6	30.3
Som1701	13.25	1.8	14.4	2.9	-	0.5	30.9
Som1701	13.5	-	14.9	5.2	0.0	3.4	23.8
Som1701	13.75	4.2	7.3	4.1	-	1.4	19.1

Som1701	14	7.5	8.7	4.1	-	-	23.7
Som1701	14.25	3.4	11.7	5.2	0.0	1.9	24.5
Som1701	14.5	4.5	10.4	3.7	-	1.0	22.3
Som1701	14.75	-	16.8	10.4	0.0	7.8	14.3
Som1701	15	1.4	12.7	3.5	0.0	0.6	27.5
Som1701	15.25	-	14.1	1.5	-	0.3	27.5
Som1701	15.5	-	11.9	1.6	-	-	21.8
Som1701	15.75	1.5	11.9	1.9	-	0.2	23.3
Som1701	16	6.2	11.6	6.4	-	4.0	23.8
Som1701	16.25	6.5	6.4	2.7	-	1.7	30.1
Som1701	16.5	7.1	4.5	4.5	-	2.3	30.0
Som1701	16.75	4.1	6.6	4.6	-	1.7	23.5
Som1701	17	6.1	5.2	3.9	-	3.0	28.0
Som1701	17.25	5.5	2.7	7.2	-	0.5	25.6
Som1701	17.5	5.2	5.4	4.4	-	2.8	25.4
Som1701	17.75	3.1	4.2	27.4	0.1	24.0	11.0
Som1701	18	6.2	5.7	4.2	-	2.5	30.9
Som1701	18.25	5.8	6.2	4.3	-	2.4	31.8
Som1701	18.5	7.7	6.7	2.7	-	0.2	32.1
Som1701	18.75	7.6	12.8	2.7	-	1.0	28.0
Som1701	19	1.4	14.0	7.5	-	3.4	24.1
Som1701	19.25	2.6	12.5	5.6	-	-	26.2
Som1701	19.5	4.4	3.5	3.9	-	1.7	25.9
Som1701	19.75	3.1	7.0	6.3	-	1.4	26.9
Som1701	20	4.1	5.5	4.2	-	2.7	21.9
Som1701	20.25	6.7	3.1	5.1	0.0	2.5	29.5
Som1701	20.5	6.9	2.5	3.7	0.0	2.1	30.5
Som1701	20.75	9.2	12.9	0.8	-	-	26.2
Som1701	21	1.3	14.7	2.3	-	0.8	29.1
Som1701	21.25	2.9	14.2	3.1	-	1.1	26.6
Som1701	21.5	3.2	14.2	2.2	-	0.4	28.3
Som1701	21.75	6.7	4.2	6.2	-	1.5	23.8
Som1701	22	6.6	3.2	9.9	0.0	5.2	22.3
Som1701	22.25	7.6	5.9	5.0	0.0	2.1	26.3
Som1701	22.5	4.6	11.5	6.5	-	3.1	25.1
Som1701	22.75	8.6	2.8	5.0	-	1.2	27.5
Som1701	23	-	1.9	11.4	0.0	12.5	40.0
Som1701	23.2	4.5	6.4	20.7	0.0	14.9	18.7
Som1701	23.4	9.0	10.4	3.2	-	1.5	28.0
Som1701	23.6	-	12.0	11.4	0.0	10.7	20.8
Som1701	23.8	6.8	7.1	5.0	-	1.9	25.8
Som1701	24	7.7	11.5	5.4	0.0	5.0	22.4
Som1701	24.25	9.1	13.4	1.9	-	2.2	27.6
Som1701	24.5	10.5	12.1	9.1	0.0	7.6	23.1
Som1701	24.75	12.1	10.0	2.1	-	-	26.6

Som1701	25	4.5	2.2	3.5	-	6.4	16.7
Som1701	25.25	2.0	15.3	3.1	0.0	1.3	25.5
Som1701	25.5	10.1	12.8	0.8	-	-	29.4
Som1701	25.75	8.0	13.7	2.0	-	0.5	28.4
Som1701	26	7.6	5.9	2.2	-	1.5	32.0
Som1701	26.25	6.0	6.2	2.0	-	0.8	26.8
Som1701	26.5	7.6	6.8	3.9	-	2.2	28.5
Som1701	26.75	7.9	5.9	6.3	-	9.0	26.5
Som1701	27	7.9	6.8	2.9	-	2.7	26.6
Som1701	27.25	6.2	4.8	4.2	-	3.2	28.1
Som1701	27.5	5.4	5.3	11.1	0.0	2.0	21.3
Som1701	27.75	1.3	2.8	6.0	-	5.0	34.2
Som1701	28	7.1	4.3	7.3	-	5.4	26.9
Som1701	28.25	3.0	6.3	15.4	0.0	12.1	12.9
Som1701	28.5	2.3	6.1	17.9	0.0	3.3	13.1
Som1701	28.75	-	8.3	6.7	0.0	3.0	16.8
Som1701	29	-	6.0	14.3	0.1	7.3	13.8
Som1701	29.25	-	6.9	17.2	0.0	19.3	12.0
Som1701	29.5	4.7	7.6	12.7	0.0	13.2	16.4
Som1701	29.75	8.0	13.4	2.8	-	1.6	26.9
Som1701	30	8.7	10.1	1.2	-	0.6	24.9
Som1701	30.25	6.0	11.9	3.4	-	2.6	25.1
Som1701	30.5	4.5	5.3	9.9	0.0	6.5	22.2
Som1701	30.75	4.0	4.5	4.7	-	0.4	24.0
Som1701	31	2.1	5.4	7.5	0.0	1.7	20.4
Som1701	31.25	4.9	5.7	4.1	-	2.4	21.6
Som1701	31.5	4.5	7.1	3.6	-	1.1	18.6
Som1701	31.75	2.2	13.9	2.3	-	0.4	25.4
Som1701	32	3.1	11.6	5.9	0.0	3.7	19.6
Som1701	32.25	3.3	10.8	3.8	-	1.2	20.7
Som1701	32.5	-	4.0	2.6	-	1.6	19.1
Som1701	32.75	-	33.5	1.6	-	0.2	3.8
Som1701	33	-	29.5	4.1	-	1.5	4.2
Som1701	33.25	-	31.4	2.0	-	0.5	3.6
Som1701	33.5	-	19.7	2.9	-	0.5	10.2
Som1701	33.75	-	23.9	2.7	-	0.4	9.0
Som1701	34	1.2	26.1	3.0	-	0.2	7.6
Som1701	34.25	4.6	1.0	1.3	-	1.3	20.6
Som1701	34.5	-	10.5	12.6	0.0	16.1	17.0
Som1701	34.75	1.7	16.1	2.7	-	2.0	29.0
Som1701	35	2.1	14.2	1.7	0.0	1.3	26.6
Som1701	35.25	2.9	11.6	6.1	0.0	5.8	24.6
Som1701	35.5	3.8	15.5	1.5	-	-	28.9
Som1701	35.75	2.2	13.7	6.7	0.0	5.1	22.6
Som1701	36	2.1	13.6	1.9	-	0.2	24.5

Som1701	36.25	4.5	16.1	1.6	-	0.3	27.8
Som1701	36.5	2.2	13.2	3.5	-	1.9	26.7
Som1701	36.75	-	28.7	1.3	-	0.5	14.0
Som1701	37	-	32.3	1.3	-	0.2	5.2
Som1701	37.2	-	25.7	4.0	-	0.6	7.9
Som1701	37.4	-	25.7	2.8	-	0.3	7.2
Som1701	37.6	-	35.8	0.7	-	0.3	3.6
Som1701	37.8	-	28.6	1.1	-	0.2	15.4
Som1701	38	-	24.3	3.7	-	2.5	16.7
Som1701	38.25	-	33.2	1.8	-	0.3	3.9
Som1701	38.5	-	37.4	1.1	-	0.5	3.6
Som1701	38.75	-	28.8	2.6	-	0.8	2.8
Som1701	39	-	34.0	1.9	-	0.3	3.9
Som1701	39.25	-	20.6	3.0	-	2.3	20.6
Som1701	39.5	-	21.6	3.7	-	2.6	19.9
Som1701	39.75	3.0	13.9	2.4	-	0.4	27.7
Som1701	40	2.0	14.6	1.6	-	-	25.4
Som1701	40.25	3.2	10.5	9.9	-	7.4	18.3
Som1701	40.5	2.2	14.7	3.6	-	2.8	26.1
Som1701	40.75	1.4	16.2	3.2	-	2.3	25.5
Som1701	41	2.3	15.6	1.3	-	0.5	26.1
Som1701	41.25	4.1	14.8	3.7	-	2.0	26.3
Som1701	41.5	3.3	15.2	1.6	-	-	29.4
Som1701	41.75	8.5	13.6	3.5	-	2.2	26.0
Som1701	42	6.9	11.9	3.3	-	2.5	26.4
Som1701	42.25	6.1	2.5	1.7	-	1.5	33.4
Som1701	42.5	6.5	2.1	0.5	-	0.5	32.2
Som1701	42.75	2.4	4.7	19.2	0.0	17.3	20.3
Som1701	43	6.4	1.2	1.2	-	0.1	30.8
Som1701	43.25	5.6	0.9	1.0	-	0.1	31.4
Som1701	43.5	4.8	1.0	0.8	-	0.3	32.0
Som1701	43.75	5.4	1.3	1.1	-	0.2	30.9
Som1701	44	4.7	1.5	2.0	-	0.4	28.4
Som1701	44.25	5.0	0.9	1.7	-	-	29.7
Som1701	44.5	5.2	1.5	1.7	-	0.4	29.4
Som1701	44.75	2.9	4.6	10.4	0.0	8.7	17.8
Som1701	45	3.5	4.0	7.4	0.0	4.9	24.1
Som1701	45.25	7.0	4.6	3.2	-	2.4	36.4
Som1701	45.5	6.7	4.6	0.5	-	0.3	32.0
Som1701	45.75	5.6	4.4	3.3	-	1.9	30.8
Som1701	46	1.7	8.4	6.5	-	2.5	22.5
Som1701	46.25	6.1	5.3	2.4	-	0.3	31.6
Som1701	46.5	6.2	6.0	2.2	-	0.3	32.6
Som1701	46.75	8.7	5.1	5.2	0.0	3.5	31.5
Som1701	47	9.1	4.8	0.6	-	0.2	32.6

Som1701	47.25	6.3	6.6	1.7	-	0.2	29.3
Som1701	47.5	4.5	8.6	3.3	-	1.0	33.4
Som1701	47.75	7.5	5.7	2.2	-	0.3	30.8
Som1701	48	6.6	5.8	1.1	-	0.1	30.5
Som1701	48.25	4.9	3.2	1.9	-	0.2	31.9
Som1701	48.5	4.9	1.2	1.9	-	0.2	24.9
Som1701	48.75	3.4	1.8	2.1	-	1.0	21.6
Som1701	49	6.6	2.2	0.8	-	0.2	32.2
Som1702	3	6.1	5.7	3.0	-	2.0	34.7
Som1702	3.25	6.6	5.4	3.9	-	1.1	29.9
Som1702	3.5	5.9	1.9	4.4	-	0.2	24.8
Som1702	3.75	4.4	6.4	11.9	0.0	14.9	22.8
Som1702	4	1.6	9.2	11.1	0.0	6.4	26.5
Som1702	4.25	10.1	4.9	3.0	-	0.3	31.1
Som1702	4.5	1.8	6.8	13.3	0.0	8.0	19.1
Som1702	4.75	4.6	0.6	1.1	-	0.3	33.7
Som1702	5	5.5	0.5	0.7	-	0.4	41.2
Som1702	5.25	5.6	0.5	0.4	-	0.1	39.3
Som1702	5.5	4.8	0.6	0.7	-	0.8	44.3
Som1702	5.75	5.0	0.4	1.0	-	0.5	46.2
Som1702	6	5.2	0.6	1.6	-	4.5	40.1
Som1702	6.25	5.1	0.9	0.6	-	0.2	40.9
Som1702	6.5	5.0	0.9	1.0	-	0.4	40.4
Som1702	6.75	4.7	0.6	1.1	-	1.0	45.3
Som1702	7	6.0	0.8	0.7	-	-	42.8
Som1702	7.33	4.6	0.3	0.4	-	0.2	39.8
Som1702	7.67	4.7	0.5	0.7	-	0.5	47.8
Som1702	8	5.9	0.6	1.2	-	1.1	44.8
Som1702	8.33	4.6	1.8	1.4	-	0.4	40.6
Som1702	8.67	4.2	0.6	0.3	-	0.1	47.2
Som1702	9	4.1	0.9	0.7	-	0.2	37.7
Som1702	9.33	5.1	0.5	0.8	-	0.2	44.4
Som1702	9.67	5.0	0.6	0.6	-	0.2	40.2
Som1702	10	6.1	0.5	1.0	-	1.4	42.7
Som1702	10.33	4.5	1.1	1.7	-	0.5	39.8
Som1702	10.67	3.1	0.7	0.8	-	0.2	35.6
Som1702	11	6.1	0.6	0.8	-	0.2	40.3
Som1702	11.33	4.2	0.6	1.1	-	0.3	39.4
Som1702	11.67	5.0	0.5	0.5	-	0.1	42.3
Som1702	12	5.9	13.0	6.3	-	4.5	23.9
Som1702	12.25	2.1	13.0	12.4	0.0	9.6	23.4
Som1702	12.5	-	3.7	41.2	0.1	20.9	7.1
Som1702	12.75	4.3	8.5	9.8	0.0	7.7	20.2
Som1702	13	2.0	15.0	2.2	-	0.6	30.3
Som1702	13.25	1.8	14.4	2.9	-	0.5	30.9

Som1702	13.5	-	14.9	5.2	0.0	3.4	23.8
Som1702	13.75	4.2	7.3	4.1	-	1.4	19.1
Som1702	14	7.5	8.7	4.1	-	-	23.7
Som1702	14.25	3.4	11.7	5.2	0.0	1.9	24.5
Som1702	14.5	4.5	10.4	3.7	-	1.0	22.3
Som1702	14.75	-	16.8	10.4	0.0	7.8	14.3
Som1702	15	1.4	12.7	3.5	0.0	0.6	27.5
Som1702	15.25	-	14.1	1.5	-	0.3	27.5
Som1702	15.5	-	11.9	1.6	-	-	21.8
Som1702	15.75	1.5	11.9	1.9	-	0.2	23.3
Som1702	16	6.2	11.6	6.4	-	4.0	23.8
Som1702	16.25	6.5	6.4	2.7	-	1.7	30.1
Som1702	16.5	7.1	4.5	4.5	-	2.3	30.0
Som1702	16.75	4.1	6.6	4.6	-	1.7	23.5
Som1702	17	6.1	5.2	3.9	-	3.0	28.0
Som1702	17.25	5.5	2.7	7.2	-	0.5	25.6
Som1702	17.5	5.2	5.4	4.4	-	2.8	25.4
Som1702	17.75	3.1	4.2	27.4	0.1	24.0	11.0
Som1702	18	6.2	5.7	4.2	-	2.5	30.9
Som1702	18.25	5.8	6.2	4.3	-	2.4	31.8
Som1702	18.5	7.7	6.7	2.7	-	0.2	32.1
Som1702	18.75	7.6	12.8	2.7	-	1.0	28.0
Som1702	19	1.4	14.0	7.5	-	3.4	24.1
Som1702	19.25	2.6	12.5	5.6	-	-	26.2
Som1702	19.5	4.4	3.5	3.9	-	1.7	25.9
Som1702	19.75	3.1	7.0	6.3	-	1.4	26.9
Som1702	20	4.1	5.5	4.2	-	2.7	21.9
Som1702	20.25	6.7	3.1	5.1	0.0	2.5	29.5
Som1702	20.5	6.9	2.5	3.7	0.0	2.1	30.5
Som1702	20.75	9.2	12.9	0.8	-	-	26.2
Som1702	21	1.3	14.7	2.3	-	0.8	29.1
Som1702	21.25	2.9	14.2	3.1	-	1.1	26.6
Som1702	21.5	3.2	14.2	2.2	-	0.4	28.3
Som1702	21.75	6.7	4.2	6.2	-	1.5	23.8
Som1702	22	6.6	3.2	9.9	0.0	5.2	22.3
Som1702	22.25	7.6	5.9	5.0	0.0	2.1	26.3
Som1702	22.5	4.6	11.5	6.5	-	3.1	25.1
Som1702	22.75	8.6	2.8	5.0	-	1.2	27.5
Som1702	23	-	1.9	11.4	0.0	12.5	40.0
Som1702	23.2	4.5	6.4	20.7	0.0	14.9	18.7
Som1702	23.4	9.0	10.4	3.2	-	1.5	28.0
Som1702	23.6	-	12.0	11.4	0.0	10.7	20.8
Som1702	23.8	6.8	7.1	5.0	-	1.9	25.8
Som1702	24	7.7	11.5	5.4	0.0	5.0	22.4
Som1702	24.25	9.1	13.4	1.9	-	2.2	27.6

Som1702	24.5	10.5	12.1	9.1	0.0	7.6	23.1
Som1702	24.75	12.1	10.0	2.1	-	-	26.6
Som1702	25	4.5	2.2	3.5	-	6.4	16.7
Som1702	25.25	2.0	15.3	3.1	0.0	1.3	25.5
Som1702	25.5	10.1	12.8	0.8	-	-	29.4
Som1702	25.75	8.0	13.7	2.0	-	0.5	28.4
Som1702	26	7.6	5.9	2.2	-	1.5	32.0
Som1702	26.25	6.0	6.2	2.0	-	0.8	26.8
Som1702	26.5	7.6	6.8	3.9	-	2.2	28.5
Som1702	26.75	7.9	5.9	6.3	-	9.0	26.5
Som1702	27	7.9	6.8	2.9	-	2.7	26.6
Som1702	27.25	6.2	4.8	4.2	-	3.2	28.1
Som1702	27.5	5.4	5.3	11.1	0.0	2.0	21.3
Som1702	27.75	1.3	2.8	6.0	-	5.0	34.2
Som1702	28	7.1	4.3	7.3	-	5.4	26.9
Som1702	28.25	3.0	6.3	15.4	0.0	12.1	12.9
Som1702	28.5	2.3	6.1	17.9	0.0	3.3	13.1
Som1702	28.75	-	8.3	6.7	0.0	3.0	16.8
Som1702	29	-	6.0	14.3	0.1	7.3	13.8
Som1702	29.25	-	6.9	17.2	0.0	19.3	12.0
Som1702	29.5	4.7	7.6	12.7	0.0	13.2	16.4
Som1702	29.75	8.0	13.4	2.8	-	1.6	26.9
Som1702	30	8.7	10.1	1.2	-	0.6	24.9
Som1702	30.25	6.0	11.9	3.4	-	2.6	25.1
Som1702	30.5	4.5	5.3	9.9	0.0	6.5	22.2
Som1702	30.75	4.0	4.5	4.7	-	0.4	24.0
Som1702	31	2.1	5.4	7.5	0.0	1.7	20.4
Som1702	31.25	4.9	5.7	4.1	-	2.4	21.6
Som1702	31.5	4.5	7.1	3.6	-	1.1	18.6
Som1702	31.75	2.2	13.9	2.3	-	0.4	25.4
Som1702	32	3.1	11.6	5.9	0.0	3.7	19.6
Som1702	32.25	3.3	10.8	3.8	-	1.2	20.7
Som1702	32.5	-	4.0	2.6	-	1.6	19.1
Som1702	32.75	-	33.5	1.6	-	0.2	3.8
Som1702	33	-	29.5	4.1	-	1.5	4.2
Som1702	33.25	-	31.4	2.0	-	0.5	3.6
Som1702	33.5	-	19.7	2.9	-	0.5	10.2
Som1702	33.75	-	23.9	2.7	-	0.4	9.0
Som1702	34	1.2	26.1	3.0	-	0.2	7.6
Som1702	34.25	4.6	1.0	1.3	-	1.3	20.6
Som1702	34.5	-	10.5	12.6	0.0	16.1	17.0
Som1702	34.75	1.7	16.1	2.7	-	2.0	29.0
Som1702	35	2.1	14.2	1.7	0.0	1.3	26.6
Som1702	35.25	2.9	11.6	6.1	0.0	5.8	24.6
Som1702	35.5	3.8	15.5	1.5	-	-	28.9

Som1702	35.75	2.2	13.7	6.7	0.0	5.1	22.6
Som1702	36	2.1	13.6	1.9	-	0.2	24.5
Som1702	36.25	4.5	16.1	1.6	-	0.3	27.8
Som1702	36.5	2.2	13.2	3.5	-	1.9	26.7
Som1702	36.75	-	28.7	1.3	-	0.5	14.0
Som1702	37	-	32.3	1.3	-	0.2	5.2
Som1702	37.2	-	25.7	4.0	-	0.6	7.9
Som1702	37.4	-	25.7	2.8	-	0.3	7.2
Som1702	37.6	-	35.8	0.7	-	0.3	3.6
Som1702	37.8	-	28.6	1.1	-	0.2	15.4
Som1702	38	-	24.3	3.7	-	2.5	16.7
Som1702	38.25	-	33.2	1.8	-	0.3	3.9
Som1702	38.5	-	37.4	1.1	-	0.5	3.6
Som1702	38.75	-	28.8	2.6	-	0.8	2.8
Som1702	39	-	34.0	1.9	-	0.3	3.9
Som1702	39.25	-	20.6	3.0	-	2.3	20.6
Som1702	39.5	-	21.6	3.7	-	2.6	19.9
Som1702	39.75	3.0	13.9	2.4	-	0.4	27.7
Som1702	40	2.0	14.6	1.6	-	-	25.4
Som1702	40.25	3.2	10.5	9.9	-	7.4	18.3
Som1702	40.5	2.2	14.7	3.6	-	2.8	26.1
Som1702	40.75	1.4	16.2	3.2	-	2.3	25.5
Som1702	41	2.3	15.6	1.3	-	0.5	26.1
Som1702	41.25	4.1	14.8	3.7	-	2.0	26.3
Som1702	41.5	3.3	15.2	1.6	-	-	29.4
Som1702	41.75	8.5	13.6	3.5	-	2.2	26.0
Som1702	42	6.9	11.9	3.3	-	2.5	26.4
Som1702	42.25	6.1	2.5	1.7	-	1.5	33.4
Som1702	42.5	6.5	2.1	0.5	-	0.5	32.2
Som1702	42.75	2.4	4.7	19.2	0.0	17.3	20.3
Som1702	43	6.4	1.2	1.2	-	0.1	30.8
Som1702	43.25	5.6	0.9	1.0	-	0.1	31.4
Som1702	43.5	4.8	1.0	0.8	-	0.3	32.0
Som1702	43.75	5.4	1.3	1.1	-	0.2	30.9
Som1702	44	4.7	1.5	2.0	-	0.4	28.4
Som1702	44.25	5.0	0.9	1.7	-	-	29.7
Som1702	44.5	5.2	1.5	1.7	-	0.4	29.4
Som1702	44.75	2.9	4.6	10.4	0.0	8.7	17.8
Som1702	45	3.5	4.0	7.4	0.0	4.9	24.1
Som1702	45.25	7.0	4.6	3.2	-	2.4	36.4
Som1702	45.5	6.7	4.6	0.5	-	0.3	32.0
Som1702	45.75	5.6	4.4	3.3	-	1.9	30.8
Som1702	46	1.7	8.4	6.5	-	2.5	22.5
Som1702	46.25	6.1	5.3	2.4	-	0.3	31.6
Som1702	46.5	6.2	6.0	2.2	-	0.3	32.6

Som1702	46.75	8.7	5.1	5.2	0.0	3.5	31.5
Som1702	47	9.1	4.8	0.6	-	0.2	32.6
Som1702	47.25	6.3	6.6	1.7	-	0.2	29.3
Som1702	47.5	4.5	8.6	3.3	-	1.0	33.4
Som1702	47.75	7.5	5.7	2.2	-	0.3	30.8
Som1702	48	6.6	5.8	1.1	-	0.1	30.5
Som1702	48.25	4.9	3.2	1.9	-	0.2	31.9
Som1702	48.5	4.9	1.2	1.9	-	0.2	24.9
Som1702	48.75	3.4	1.8	2.1	-	1.0	21.6
Som1702	49	6.6	2.2	0.8	-	0.2	32.2
Haug1701	1.5	5.7	5.9	5.8	-	0.8	27.2
Haug1701	1.79	6.1	4.3	8.1	0.0	1.3	27.4
Haug1701	2.07	7.3	4.8	7.9	-	3.1	28.4
Haug1701	2.36	7.3	5.2	5.3	0.0	0.6	30.7
Haug1701	2.64	5.2	3.4	5.2	-	0.2	26.8
Haug1701	2.93	7.5	5.0	7.0	-	2.7	28.0
Haug1701	3.21	4.3	4.4	5.9	-	0.2	27.3
Haug1701	3.5	1.4	1.3	15.0	0.0	6.1	13.0
Haug1701	3.63	6.2	4.3	5.2	0.0	1.0	27.9
Haug1701	3.75	3.1	1.1	8.2	-	0.2	23.4
Haug1701	3.88	6.1	3.6	5.2	-	2.2	30.1
Haug1701	4	5.0	3.7	4.9	-	0.6	27.5
Haug1701	4.11	7.1	5.0	5.9	-	1.3	29.6
Haug1701	4.22	6.9	4.5	6.3	-	0.2	27.1
Haug1701	4.33	3.4	1.8	6.7	-	0.1	24.4
Haug1701	4.44	4.8	4.6	3.2	-	-	32.1
Haug1701	4.56	7.5	4.5	5.5	-	2.2	29.5
Haug1701	4.67	5.7	5.5	3.6	-	1.5	30.5
Haug1701	4.78	7.5	6.5	7.5	0.0	3.8	26.5
Haug1701	4.89	2.9	3.9	17.5	0.0	11.7	11.2
Haug1701	5	4.3	1.9	23.1	0.0	19.8	12.8
Haug1701	5.2	7.9	3.6	5.1	-	0.4	29.0
Haug1701	5.4	6.0	3.4	3.1	-	0.3	29.7
Haug1701	5.6	5.7	1.8	7.1	-	1.8	27.8
Haug1701	5.8	7.4	3.3	7.2	0.0	8.9	27.8
Haug1701	6	3.5	5.0	7.6	-	5.7	24.4
Haug1701	6.17	7.4	3.8	5.7	-	2.4	27.8
Haug1701	6.33	6.4	4.6	4.2	-	2.7	31.3
Haug1701	6.5	4.9	5.9	9.5	0.0	10.1	23.3
Haug1701	6.67	3.3	2.5	25.2	0.1	21.2	13.5
Haug1701	6.83	7.6	1.7	7.8	0.0	4.5	28.0
Haug1701	7	6.8	4.9	6.1	-	4.3	28.9
Haug1701	7.14	8.6	4.6	4.6	0.0	2.1	31.0
Haug1701	7.29	8.5	5.5	4.1	-	1.4	32.6
Haug1701	7.43	6.8	4.5	5.4	-	4.2	30.9

Haug1701	7.57	6.8	4.5	4.2	-	0.4	31.6
Haug1701	7.71	7.8	7.0	3.8	-	1.3	32.4
Haug1701	7.86	9.1	6.0	2.2	-	0.5	33.2
Haug1701	8	7.1	7.5	2.9	-	0.5	32.5
Haug1701	8.14	7.2	8.0	3.8	-	2.0	32.2
Haug1701	8.29	6.3	5.5	5.9	0.0	3.3	30.2
Haug1701	8.43	6.2	6.7	4.9	-	0.3	31.4
Haug1701	8.57	8.4	7.2	3.8	-	0.3	32.8
Haug1701	8.71	6.3	6.5	6.3	-	0.3	30.7
Haug1701	8.86	7.0	4.5	5.1	-	0.4	28.5
Haug1701	9	7.5	6.5	6.8	-	1.3	31.1
Haug1701	9.17	6.8	6.6	6.1	-	0.6	31.2
Haug1701	9.33	6.1	5.7	5.4	-	0.3	32.0
Haug1701	9.5	6.2	5.3	4.1	-	0.4	31.8
Haug1701	9.67	5.9	6.0	5.8	0.0	0.7	29.9
Haug1701	9.83	7.5	4.9	1.4	-	0.1	34.7
Haug1701	10	5.7	4.1	1.6	-	0.2	34.7
Haug1701	10.2	7.9	3.8	2.9	-	0.2	33.9
Haug1701	10.4	7.4	6.3	3.6	-	0.5	32.7
Haug1701	10.6	5.8	5.9	5.7	0.0	2.5	28.0
Haug1701	10.8	6.2	6.9	4.0	-	0.3	31.4
Haug1701	11	7.4	6.6	4.3	-	0.4	32.5
Haug1701	11.2	6.6	6.5	4.0	-	0.4	30.3
Haug1701	11.4	7.2	6.5	5.5	-	0.4	31.2
Haug1701	11.6	5.4	7.1	5.5	-	1.4	31.3
Haug1701	11.8	6.1	8.0	4.9	0.0	1.0	31.1
Haug1701	12	8.5	7.1	6.4	-	0.5	30.0
Haug1701	12.25	6.1	7.0	6.9	-	0.3	30.2
Haug1701	12.5	6.5	8.2	7.7	0.0	1.5	28.4
Haug1701	12.75	4.3	6.7	3.7	-	0.3	27.5
Haug1701	13	8.2	6.6	4.3	-	0.3	31.3
Haug1701	13.2	7.0	6.3	6.3	-	0.3	30.0
Haug1701	13.4	6.3	6.8	7.3	0.0	0.2	28.9
Haug1701	13.6	7.4	5.9	7.2	-	1.2	30.1
Haug1701	13.8	5.8	5.7	4.1	-	0.2	31.9
Haug1701	14	7.1	4.4	2.6	-	1.9	32.1
Haug1701	14.2	4.2	4.6	5.2	-	2.6	27.6
Haug1701	14.4	6.0	4.9	5.7	-	2.1	29.4
Haug1701	14.6	7.5	5.9	5.0	0.0	2.4	30.9
Haug1701	14.8	4.9	3.6	6.1	-	1.4	27.5
Haug1701	15	7.7	3.9	4.3	-	1.1	30.7
Haug1701	15.2	6.2	3.3	2.5	-	0.4	32.2
Haug1701	15.4	7.7	2.2	2.3	-	-	31.1
Haug1701	15.6	6.1	5.8	4.1	-	2.3	30.7
Haug1701	15.8	5.1	3.3	4.5	-	0.4	29.4

Haug1701	16	5.1	4.7	8.1	0.0	3.8	28.1
Haug1701	16.2	3.2	7.3	9.0	0.0	5.9	20.3
Haug1701	16.4	4.4	4.6	7.5	0.0	1.9	18.9
Haug1701	16.6	-	4.1	24.0	-	13.6	12.2
Haug1701	16.8	2.7	2.8	15.0	0.0	11.9	18.1
Haug1701	17	6.0	2.5	6.5	-	7.3	28.3
Haug1701	17.2	6.3	3.8	4.7	0.0	1.6	31.1
Haug1701	17.4	7.9	5.7	11.5	0.0	3.6	27.0
Haug1701	17.6	6.5	7.1	6.5	-	0.3	29.7
Haug1701	17.8	7.9	4.4	7.9	-	0.2	31.5
Haug1701	18	5.2	4.8	8.4	-	0.9	25.5
Haug1701	18.2	6.2	5.0	7.6	-	0.7	28.3
Haug1701	18.4	7.2	-	7.3	0.0	0.5	29.5
Haug1701	18.6	7.3	5.9	6.9	-	1.1	30.4
Haug1701	18.8	4.3	5.5	7.1	-	0.3	28.6
Haug1701	19	3.9	8.1	5.3	-	0.3	30.5
Haug1701	19.25	7.2	5.6	7.6	0.0	0.7	30.7
Haug1701	19.5	5.9	5.4	8.8	-	2.6	28.1
Haug1701	19.75	6.4	6.2	7.4	-	0.8	32.2
Haug1701	20	6.6	6.7	6.5	-	0.6	28.9
Haug1701	20.17	6.9	2.5	11.1	0.0	3.0	25.7
Haug1701	20.33	8.4	4.8	8.5	0.0	5.5	28.8
Haug1701	20.5	6.7	6.6	6.8	-	2.3	29.6
Haug1701	20.67	6.9	5.9	5.1	-	0.3	31.0
Haug1701	20.83	7.1	9.4	4.7	-	1.3	31.5
Haug1701	21	5.5	6.1	7.9	0.0	0.4	29.5
Haug1701	21.2	5.9	2.3	7.6	-	1.4	27.3
Haug1701	21.4	4.4	1.9	9.8	-	1.0	25.9
Haug1701	21.6	7.9	4.7	5.4	-	1.1	30.3
Haug1701	21.8	6.9	4.1	6.5	-	0.3	28.1
Haug1701	22	5.8	4.3	4.1	-	0.3	30.0
Haug1701	22.2	8.7	4.0	5.1	-	0.2	30.5
Haug1701	22.4	7.0	3.0	6.6	-	3.4	31.8
Haug1701	22.6	7.6	0.8	0.4	-	0.2	36.7
Haug1701	22.8	7.2	0.7	2.4	-	2.7	31.9
Haug1701	23	8.0	0.7	0.1	-	-	37.2
Haug1701	23.25	7.4	4.5	6.3	-	2.8	29.3
Haug1701	23.5	8.1	7.5	3.1	-	1.5	32.5
Haug1701	23.75	5.9	4.6	4.3	-	2.1	30.2
Haug1701	24	6.7	4.8	7.4	0.0	4.6	30.8
Haug1701	24.2	3.4	2.5	29.3	0.1	22.6	11.5
Haug1701	24.4	-	4.0	21.2	0.1	15.4	9.4
Haug1701	24.6	3.8	9.6	9.3	0.0	5.6	27.2
Haug1701	24.8	8.2	3.0	3.7	-	3.1	36.1
Haug1701	25	6.8	4.9	9.3	0.0	7.0	29.1

Haug1701	25.2	9.0	6.1	3.1	-	2.5	33.9
Haug1701	25.4	5.6	4.7	6.2	-	5.5	27.3
Haug1701	25.6	6.8	3.0	24.7	0.1	25.6	16.3
Haug1701	25.8	6.1	5.6	4.9	-	1.5	32.1
Haug1701	26	6.4	6.4	6.3	-	0.3	30.2
Haug1701	26.2	4.8	4.4	5.2	-	1.0	27.0
Haug1701	26.4	5.3	3.8	3.1	-	0.4	32.8
Haug1701	26.6	6.8	5.1	13.8	0.0	8.2	25.6
Haug1701	26.8	5.4	2.5	10.3	0.0	2.6	24.4
Haug1701	27	-	7.6	18.5	0.0	11.2	10.1
Haug1701	27.25	-	7.9	29.1	0.1	21.1	13.2
Haug1701	27.5	5.6	6.3	5.0	-	2.9	32.7
Haug1701	27.75	6.7	3.0	6.3	-	2.0	33.5
Haug1701	28	7.2	2.6	3.7	-	0.2	31.1
Haug1701	28.25	7.2	6.6	7.3	-	0.7	32.6
Haug1701	28.5	8.6	5.3	6.8	-	0.2	31.0
Haug1701	28.75	4.0	5.7	6.6	-	0.2	26.9
Haug1701	29	6.2	8.0	8.7	0.0	3.0	28.2
Haug1701	29.2	9.2	4.9	2.5	-	0.3	33.7
Haug1701	29.4	5.4	8.9	8.7	-	3.8	29.3
Haug1701	29.6	8.2	5.8	11.8	-	6.3	28.2
Haug1701	29.8	6.8	5.1	9.0	-	0.1	28.8
Haug1701	30	5.7	4.9	8.9	0.0	0.2	28.1
Haug1701	30.25	7.6	4.0	5.3	0.0	0.4	31.7
Haug1701	30.5	7.2	9.2	4.2	-	0.6	33.7
Haug1701	30.75	4.0	1.2	4.8	-	1.3	24.4
Haug1701	31	5.6	2.6	3.0	-	1.8	39.9
Haug1701	31.25	2.7	10.3	14.0	0.0	8.6	25.3
Haug1701	31.5	6.4	3.6	6.6	-	1.2	30.4
Haug1701	31.75	7.6	4.4	2.8	-	1.1	35.4
Haug1701	32	8.0	3.2	6.4	-	3.1	32.2
Haug1702	3	3.4	4.2	5.5	-	0.1	24.4
Haug1702	3.33	5.1	3.1	5.4	-	0.5	29.7
Haug1702	3.67	4.2	9.4	3.2	-	0.6	31.2
Haug1702	4	4.0	8.6	3.7	-	1.2	31.0
Haug1702	4.25	3.3	1.0	9.5	-	0.2	24.3
Haug1702	4.5	4.0	5.1	9.0	0.0	10.4	22.1
Haug1702	4.75	7.1	2.0	2.0	-	2.3	30.3
Haug1702	5	6.2	6.8	2.0	-	0.3	30.5
Haug1702	5.25	3.8	9.1	3.7	-	1.4	30.0
Haug1702	5.5	4.8	1.4	1.9	-	0.4	38.1
Haug1702	5.75	4.9	1.3	2.6	-	2.0	35.1
Haug1702	6	10.1	8.1	2.4	-	0.5	42.0
Haug1702	6.25	8.8	5.0	3.3	-	0.4	30.2
Haug1702	6.5	5.5	7.0	4.1	0.0	-	27.6

Haug1702	6.75	6.3	5.0	2.6	-	0.2	29.4
Haug1702	7	7.6	4.7	3.8	-	1.4	28.5
Haug1702	7.2	8.2	5.9	3.4	-	1.4	29.8
Haug1702	7.4	3.1	2.3	3.2	0.0	0.3	33.7
Haug1702	7.6	1.9	5.4	4.2	-	0.3	33.4
Haug1702	7.8	4.5	2.9	4.5	-	3.7	25.7
Haug1702	8	6.7	3.8	3.6	-	0.3	31.8
Haug1702	8.25	4.7	2.6	4.3	-	0.3	29.5
Haug1702	8.5	10.5	4.6	2.5	-	4.0	57.0
Haug1702	8.75	2.1	5.0	3.8	-	-	18.7
Haug1702	9	3.4	2.0	3.3	-	0.4	26.2
Haug1702	9.25	4.3	2.0	3.1	-	0.2	27.8
Haug1702	9.5	4.1	3.3	2.2	0.0	0.6	37.5
Haug1702	9.75	5.3	4.7	3.1	0.0	0.6	31.4
Haug1702	10	4.6	1.3	7.7	0.0	1.4	25.2
Haug1702	10.5	5.3	1.5	1.8	-	0.4	29.0
Haug1702	11	3.7	2.1	3.8	-	1.9	26.8
Haug1702	11.2	7.6	2.1	1.9	-	0.3	33.6
Haug1702	11.4	4.0	1.3	4.4	-	0.1	29.4
Haug1702	11.6	4.6	0.7	0.6	-	0.6	38.0
Haug1702	11.8	4.3	0.7	3.2	0.0	0.3	33.6
Haug1702	12	3.5	1.1	4.0	-	-	26.8
Haug1702	12.25	4.9	2.9	3.9	-	0.4	25.9
Haug1702	12.5	6.0	1.9	6.0	-	1.3	30.3
Haug1702	12.75	4.5	1.0	3.0	-	-	31.4
Haug1702	13	5.0	1.1	5.6	-	-	28.1
Haug1702	13.25	5.6	2.4	5.9	-	0.3	32.0
Haug1702	13.5	6.2	2.8	6.6	-	0.2	33.5
Haug1702	13.75	2.4	1.1	6.9	-	0.5	29.8
Haug1702	14	3.9	1.8	2.5	-	0.6	32.3
Haug1702	14.25	3.7	4.3	4.6	-	0.1	31.1
Haug1702	14.5	2.3	1.1	5.8	-	0.1	22.6
Haug1702	14.75	3.8	1.0	4.6	-	1.7	36.1
Haug1702	15	6.6	1.5	3.4	-	2.8	32.1
Haug1702	15.33	6.0	1.1	1.2	-	0.4	33.3
Haug1702	15.67	5.1	2.0	1.9	-	0.1	34.0
Haug1702	16	1.4	3.8	9.7	-	3.4	11.7
Haug1702	16.25	2.7	1.5	8.3	0.0	0.2	23.3
Haug1702	16.5	4.2	2.1	3.8	-	0.2	25.7
Haug1702	16.75	6.7	2.7	3.9	-	-	32.9
Haug1702	17	6.1	1.0	7.0	-	2.3	30.6
Haug1702	17.33	5.1	0.6	0.7	-	0.1	37.2
Haug1702	17.67	4.1	1.6	4.1	-	0.2	27.8
Haug1702	18	4.8	2.3	7.6	0.0	5.5	28.0
Haug1702	18.33	9.3	1.8	3.4	-	0.6	37.1

Haug1702	18.67	4.9	2.1	1.0	-	0.3	40.0
Haug1702	19	6.1	0.8	1.1	-	1.3	38.1
Haug1702	19.33	5.6	0.7	2.1	-	1.6	37.2
Haug1702	19.67	4.4	0.7	1.1	-	0.6	41.0
Haug1702	20	6.2	1.6	4.3	0.0	2.9	35.7
Haug1702	20.33	9.7	1.5	11.4	0.0	10.3	31.7
Haug1702	20.67	5.7	2.3	4.2	-	1.3	29.1
Haug1702	21	5.2	1.0	1.6	-	0.6	36.9
Haug1702	21.33	6.2	0.7	1.4	-	-	33.6
Haug1702	21.67	6.6	0.6	1.5	-	-	33.9
Haug1702	22	6.0	0.6	2.0	0.0	0.3	35.4
Haug1702	22.33	5.2	0.9	1.7	-	-	31.0
Haug1702	22.67	6.9	1.2	0.7	-	0.1	36.7
Haug1702	23	8.2	1.3	0.3	-	-	36.5
Haug1702	23.33	7.2	1.2	0.3	-	-	35.4
Haug1702	23.67	7.9	1.7	0.3	-	0.1	33.1
Haug1702	24	4.9	3.2	4.9	-	0.4	29.1
Haug1702	24.33	8.0	5.1	4.5	-	0.2	31.7
Haug1702	24.67	8.0	5.7	4.3	-	1.5	32.9
Haug1702	25	8.8	5.6	8.5	-	1.2	30.0
Haug1702	26	5.4	5.8	11.8	0.0	4.5	26.6
Haug1702	27	5.9	5.9	8.6	-	0.2	30.7
Haug1702	28	7.6	5.3	7.7	0.0	0.3	31.5
Haug1702	29	7.2	5.2	7.0	-	-	31.4
Haug1702	30	6.9	5.0	9.5	-	0.1	28.2
Haug1702	31	8.0	7.7	9.9	-	1.2	29.5
Haug1702	32	4.6	5.2	9.4	-	0.2	29.0
Haug1702	33	6.6	5.2	7.0	-	0.5	31.9
Haug1702	34	10.1	5.4	9.3	-	0.2	33.6
Haug1702	35	4.7	5.9	13.8	-	0.6	23.8
Haug1702	36	6.5	6.4	13.4	-	0.4	27.9
Haug1702	37	3.1	8.1	16.5	0.0	2.3	25.5
Haug1702	38	8.8	5.9	12.6	-	2.7	28.0
Haug1702	39	6.5	5.3	4.3	-	0.1	33.0
Haug1702	40	9.2	6.0	7.7	-	0.1	30.2
Haug1702	41	9.8	3.3	1.6	-	1.1	34.8
Haug1702	42	8.5	4.4	5.0	-	0.9	30.9
Haug1702	43	7.4	5.1	5.8	-	-	31.4
Haug1702	44	7.9	6.8	5.7	-	-	31.0
Haug1702	45	7.7	6.6	9.0	-	-	28.0
Haug1702	46	7.5	6.8	7.3	-	-	29.3
Haug1702	47	7.0	6.8	7.9	-	1.2	28.9
Haug1702	48	5.0	6.4	10.8	-	-	28.0
Haug1702	49	7.2	6.8	8.9	0.0	-	29.9
Haug1702	50	7.2	7.0	9.5	0.0	0.2	29.2

## Appendix 5: Complete list of analysed samples for TS, TC and TOC from 1990-2017

Data is available in excel format on request.

Blank cell = not analysed. Negative values = below detection limit.

The individual samplers can be contacted for information on their particular set of samples.

Sampler, all at NGU: HG = Håvard Gautneb, JK = Janja Knezevic, BD = Børre Davidsen, NC = Nolwenn Coint, JEW = Jan Egil Wanvik, HS = Henrik Schiellerup

NGU no	Year	Area	so ne	Easting	Northing	Samp ler	Sample no.	Text	TS	TC	TOC
90-5d	1990	Jennestad	33	507225	7625671	HG	90-5d	Graphite schist		39.65	
90-7a	1990	Jennestad	33	507225	7625671	HG	90-7a	Graphite schist		8.50	
90-7b	1990	Jennestad	33	507225	7625671	HG	90-7b	Graphite schist		35.86	
90-7c	1990	Jennestad	33	507225	7625671	HG	90-7c	Graphite schist		36.88	
90-10	1990	Jennestad	33	507570	7625318	HG	90-10	Graphite schist		8.25	
90-8	1990	Jennestad	33	507570	7625318	HG	90-8	Graphite schist		1.71	
90-9a	1990	Jennestad	33	507570	7625318	HG	90-9a	Graphite schist		26.22	
90-9b	1990	Jennestad	33	507570	7625318	HG	90-9b	Graphite schist		37.23	
90-9c	1990	Jennestad	33	507570	7625318	HG	90-9c	Graphite schist		39.23	
90-9d	1990	Jennestad	33	507570	7625318	HG	90-9d	Graphite schist		44.31	
90/20	1990	Jennestad	33	508592	7625860	HG	90/20	Graphite schist		24.25	
90-20a	1990	Jennestad	33	508592	7625860	HG	90-20a	Graphite schist		14.86	
90-21b	1990	Jennestad	33	508592	7625860	HG	90-21b	Graphite schist		16.57	
90-21c	1990	Jennestad	33	508592	7625860	HG	90-21c	Graphite schist		25.77	
LH-1	1990	Jennestad	33	508592	7625860	HG	LH-1	Graphite schist		18.02	
LH-2	1990	Jennestad	33	508592	7625860	HG	LH-2	Graphite schist		18.18	
LH-3	1990	Jennestad	33	508592	7625860	HG	LH-3	Graphite schist		14.79	
LH-4	1990	Jennestad	33	508592	7625860	HG	LH-4	Graphite schist		14.52	
LH-5	1990	Jennestad	33	508592	7625860	HG	LH-5	Graphite schist		11.95	
LH-6	1990	Jennestad	33	508592	7625860	HG	LH-6	Graphite schist		12.22	

LH-7	1990	Jennestad	33	508592	7625860	HG	LH-7	Graphite schist		14.25	
LH-8	1990	Jennestad	33	508592	7625860	HG	LH-8	Graphite schist		17.68	
90-15a	1990	Jennestad	33	508704	7627725	HG	90-15a	Graphite schist		13.88	
La-1	1990	Jennestad	33	510369	7625405	HG	La-1	Graphite schist		12.32	
La-2	1990	Jennestad	33	510369	7625405	HG	La-2	Graphite schist		12.74	
90/19	1990	Jennestad	33	511140	7628483	HG	90/19	Graphite schist		14.61	
90-15b	1990	Jennestad	33	511140	7628483	HG	90-15b	Graphite schist		16.66	
9148	1991	Jennestad	33	507225	7625671	HG	9148	Graphite schist		38.79	
9148	1991	Jennestad	33	507225	7625671	HG	9148	Graphite schist		38.79	
9160	1991	Jennestad	33	507225	7625671	HG	9160	Graphite schist		1.30	
9160	1991	Jennestad	33	507225	7625671	HG	9160	Graphite schist		1.30	
9153a	1991	Jennestad	33	507570	7625318	HG	9153a	Graphite schist		38.42	
9153a	1991	Jennestad	33	507570	7625318	HG	9153a	Graphite schist		38.42	
9126	1991	Jennestad	33	508427	7625680	HG	9126	Graphite schist		9.92	
9129	1991	Jennestad	33	508438	7625617	HG	9129	Graphite schist		10.60	
9128a	1991	Jennestad	33	508438	7625617	HG	9128a	Graphite schist		15.90	
9128b	1991	Jennestad	33	508438	7625617	HG	9128b	Graphite schist		6.62	
9128c	1991	Jennestad	33	508438	7625617	HG	9128c	Graphite schist		7.00	
9128d	1991	Jennestad	33	508438	7625617	HG	9128d	Graphite schist		12.58	
9128e	1991	Jennestad	33	508438	7625617	HG	9128e	Graphite schist		10.55	
9128f	1991	Jennestad	33	508438	7625617	HG	9128f	Graphite schist		6.64	
9128g	1991	Jennestad	33	508438	7625617	HG	9128g	Graphite schist		5.64	
9128h	1991	Jennestad	33	508438	7625617	HG	9128h	Graphite schist		7.81	
9130a	1991	Jennestad	33	508438	7625617	HG	9130a	Graphite schist		9.22	
9130b	1991	Jennestad	33	508438	7625617	HG	9130b	Graphite schist		9.80	
9130c	1991	Jennestad	33	508438	7625617	HG	9130c	Graphite schist		9.27	
9125	1991	Jennestad	33	508448	7625722	HG	9125	Graphite schist		7.80	
9123a	1991	Jennestad	33	508473	7625750	HG	9123a	Graphite schist		21.28	
9123b	1991	Jennestad	33	508473	7625750	HG	9123b	Graphite schist		27.41	

9123c	1991	Jennestad	33	508473	7625750	HG	9123c	Graphite schist		30.46	
9123d	1991	Jennestad	33	508473	7625750	HG	9123d	Graphite schist		33.07	
9122b	1991	Jennestad	33	508545	7625722	HG	9122b	Graphite schist		16.93	
9121a	1991	Jennestad	33	508554	7625752	HG	9121a	Graphite schist		12.80	
9121b	1991	Jennestad	33	508554	7625752	HG	9121b	Graphite schist		4.65	
9121c	1991	Jennestad	33	508554	7625752	HG	9121c	Graphite schist		8.70	
9121d	1991	Jennestad	33	508554	7625752	HG	9121d	Graphite schist		11.00	
9121e	1991	Jennestad	33	508554	7625752	HG	9121e	Graphite schist		9.23	
9111B2	1991	Jennestad	33	508592	7625860	HG	911B2	Graphite schist		18.89	
9159a	1991	Jennestad	33	508592	7625860	HG	9159a	Graphite schist		9.62	
9159b	1991	Jennestad	33	508592	7625860	HG	9159b	Graphite schist		10.93	
9139	1991	Jennestad	33	510079	7625023	HG	9139	Graphite schist		9.16	
9147	1991	Jennestad	33	510079	7625023	HG	9147	Graphite schist		26.13	
9162	1991	Jennestad	33	510369	7625405	HG	9162	Graphite schist		8.13	
9164	1991	Jennestad	33	510369	7625405	HG	9164	Graphite schist		3.18	
9166	1991	Jennestad	33	510369	7625405	HG	9166	Graphite schist		12.23	
9132	1991	Jennestad	33	510980	7625361	HG	9132	Graphite schist		10.20	
9138	1991	Jennestad	33	510980	7625361	HG	9138	Graphite schist		32.60	
9136a	1991	Jennestad	33	510980	7625361	HG	9136a	Graphite schist		32.78	
93-6a	1993	Jennestad	33	507173	7625918	HG	93-6a	Graphite schist	1.16	22.29	
93-6b	1993	Jennestad	33	507173	7625918	HG	93-6b	Graphite schist	1.35	19.52	
93-6c	1993	Jennestad	33	507173	7625918	HG	93-6c	Graphite schist	2.26	19.50	
93-6d	1993	Jennestad	33	507173	7625918	HG	93-6d	Graphite schist	1.67	20.07	
93-6e	1993	Jennestad	33	507173	7625918	HG	93-6e	Graphite schist	1.92	11.65	
93-6f	1993	Jennestad	33	507173	7625918	HG	93-6f	Graphite schist	1.52	17.39	
93-5a	1993	Jennestad	33	507192	7625886	HG	93-5a	Graphite schist	1.57	10.48	
93-5b	1993	Jennestad	33	507192	7625886	HG	93-5b	Graphite schist	1.04	10.54	
93-5c	1993	Jennestad	33	507192	7625886	HG	93-5c	Graphite schist	3.20	8.03	
93-5d	1993	Jennestad	33	507192	7625886	HG	93-5d	Graphite schist	4.91	12.27	

93-5e	1993	Jennestad	33	507192	7625886	HG	93-5e	Graphite schist	0.80	13.05	
93-5f	1993	Jennestad	33	507192	7625886	HG	93-5f	Graphite schist	2.19	6.88	
93-3h	1993	Jennestad	33	507251	7625822	HG	93-3h	Graphite schist	0.22	26.73	
93-4a	1993	Jennestad	33	507251	7625822	HG	93-4a	Graphite schist	0.80	17.42	
93-4b	1993	Jennestad	33	507251	7625822	HG	93-4b	Graphite schist	0.72	29.36	
93-4c	1993	Jennestad	33	507251	7625822	HG	93-4c	Graphite schist	0.79	25.91	
93-4D1	1993	Jennestad	33	507251	7625822	HG	93-4D1	Graphite schist	0.01	14.52	
93-4e	1993	Jennestad	33	507251	7625822	HG	93-4e	Graphite schist	0.20	14.05	
93-4f	1993	Jennestad	33	507251	7625822	HG	93-4f	Graphite schist	0.01	9.00	
9221	1993	Jennestad	33	507271	7625612	HG	9221	Graphite schist	0.09	34.63	
9221b	1993	Jennestad	33	507271	7625612	HG	9221b	Graphite schist	0.01	37.71	
9221c	1993	Jennestad	33	507271	7625612	HG	9221c	Graphite schist	0.51	35.06	
9221d	1993	Jennestad	33	507271	7625612	HG	9221d	Graphite schist	0.01	37.76	
9221e	1993	Jennestad	33	507271	7625612	HG	9221e	Graphite schist	0.22	38.08	
9221f	1993	Jennestad	33	507271	7625612	HG	9221f	Graphite schist	0.15	34.89	
9221g	1993	Jennestad	33	507271	7625612	HG	9221g	Graphite schist	0.01	21.31	
9221h	1993	Jennestad	33	507271	7625612	HG	9221h	Graphite schist	0.01	32.31	
9221i	1993	Jennestad	33	507271	7625612	HG	9221i	Graphite schist	0.06	22.83	
9222A	1993	Jennestad	33	507283	7625602	HG	9222A	Graphite schist	0.01	30.83	
9222b	1993	Jennestad	33	507283	7625602	HG	9222b	Graphite schist	0.02	28.75	
9223	1993	Jennestad	33	507299	7625584	HG	9223	Graphite schist	0.01	35.1	
93-3a	1993	Jennestad	33	507378	7625725	HG	93-3a	Graphite schist	0.18	29.90	
93-3b	1993	Jennestad	33	507378	7625725	HG	93-3b	graphite schist	0.34	21.69	
93-3c	1993	Jennestad	33	507378	7625725	HG	93-3c	Graphite schist	0.28	31.91	
93-3d	1993	Jennestad	33	507378	7625725	HG	93-3d	Graphite schist	0.12	33.48	
93-3e	1993	Jennestad	33	507378	7625725	HG	93-3e	Graphite schist	0.01	29.55	
93-3f	1993	Jennestad	33	507378	7625725	HG	93-3f	Graphite schist	0.21	30.72	
93-3g	1993	Jennestad	33	507378	7625725	HG	93-3g	Graphite schist	0.15	26.44	
93-2a	1993	Jennestad	33	507412	7625699	HG	93-2a	Graphite schist	0.20	13.40	

93-2b	1993	Jennestad	33	507412	7625699	HG	93-2b	Graphite schist	0.20	14.21	
93-2c	1993	Jennestad	33	507412	7625699	HG	93-2c	Graphite schist	0.60	15.53	
93-2d	1993	Jennestad	33	507412	7625699	HG	93-2d	Graphite schist	0.20	9.64	
93-1a	1993	Jennestad	33	507438	7625659	HG	93-1a	Graphite schist	0.58	18.03	
93-1b	1993	Jennestad	33	507438	7625659	HG	93-1b	Graphite schist	0.24	12.26	
93-1c	1993	Jennestad	33	507438	7625659	HG	93-1c	Graphite schist	0.36	12.78	
93-1d	1993	Jennestad	33	507438	7625659	HG	93-1d	Graphite schist	1.30	7.56	
93-1e	1993	Jennestad	33	507438	7625659	HG	93-1e	Graphite schist	0.50	12.18	
93-1f	1993	Jennestad	33	507438	7625659	HG	93-1f	Graphite schist	0.18	14.15	
9224a	1993	Jennestad	33	507447	7625565	HG	9224a	Graphite schist	2.998	0.06	
9224b	1993	Jennestad	33	507447	7625565	HG	9224b	Graphite schist	3.195	7.678	
9224c	1993	Jennestad	33	507447	7625565	HG	9224c	Graphite schist	3.498	9.071	
9225a	1993	Jennestad	33	507448	7625537	HG	9225a	Graphite schist	3.083	7.368	
9225b	1993	Jennestad	33	507448	7625537	HG	9225b	Graphite schist	3.368	7.081	
9225c	1993	Jennestad	33	507448	7625537	HG	9225c	Graphite schist	2.356	2.895	
9226a	1993	Jennestad	33	507453	7625509	HG	9226a	Graphite schist	0.1545	7.801	
9226b	1993	Jennestad	33	507453	7625509	HG	9226b	Graphite schist	0.6637	7.485	
9227a	1993	Jennestad	33	507477	7625456	HG	9227a	Graphite schist	0.7981	37.5	
9227b	1993	Jennestad	33	507477	7625456	HG	9227b	Graphite schist	0.447	33.89	
9227c	1993	Jennestad	33	507477	7625456	HG	9227c	Graphite schist	0.258	40.49	
9227d	1993	Jennestad	33	507477	7625456	HG	9227d	Graphite schist	0.0682	28.67	
9227e	1993	Jennestad	33	507477	7625456	HG	9227e	Graphite schist	0.5395	29.91	
9228a	1993	Jennestad	33	507489	7625440	HG	9228a	Graphite schist	0.3911	38.35	
9228b	1993	Jennestad	33	507489	7625440	HG	9228b	Graphite schist	0.1498	38.23	
9228c	1993	Jennestad	33	507489	7625440	HG	9228c	Graphite schist	0.0902	31.68	
9228d	1993	Jennestad	33	507489	7625440	HG	9228d	Graphite schist	0.0528	39.67	
92229c	1993	Jennestad	33	507521	7625411	HG	92229c	Graphite schist	0.047	32.26	
9229a	1993	Jennestad	33	507521	7625411	HG	9229a	Graphite schist	0.2016	40.73	
9229b	1993	Jennestad	33	507521	7625411	HG	9229b	Graphite schist	0.1146	41.68	

9229d	1993	Jennestad	33	507521	7625411	HG	9229d	Graphite schist	0.2253	42.83	
71992	2012	Morfjord	33	486956	7587163	JEW	JW12-8	Disseminated graphite schist		18.86	
71972	2012	Morfjord	33	487144	7586575	HG	HG22-12	Disseminated graphite schist		16.80	
71973	2012	Morfjord	33	487144	7586575	HG	HG23-12	Disseminated graphite schist		19.70	
71961	2012	Sommarland	33	487589	7626310	HG	HG11-12	graphite schist from various exposures just north of the abandoned house at Sommarland		4.05	
71962	2012	Sommarland	33	487589	7626310	HG	HG12-12	Graphite schist from various exposures just north of the abandoned house at Sommarland		2.83	
71963	2012	Sommarland	33	487589	7626310	HG	HG13-12	Graphite schist from various exposures just north of the abandoned house at Sommarland		5.44	
71959	2012	Sommarland	33	487621	7626290	HG	HG9-12	Graphite schist from various exposures just north of the abandoned house at Sommarland		9.26	
71960	2012	Sommarland	33	487621	7626290	HG	HG10-12	Graphite schist from various exposures just north of the abandoned house at Sommarland		17.13	
71968	2012	Kvern fjord-Haugnes	33	488238	7618895	HG	HG18-12	Massive and high-grade graphite schist		14.21	
71969	2012	Kvern fjord-Haugnes	33	488238	7618895	HG	HG19-12	Massive and high-grade graphite schist		15.17	
71970	2012	Kvern fjord-Haugnes	33	488238	7618895	HG	HG20-12	Massive and high-grade graphite schist		13.73	
71971	2012	Kvern fjord-Haugnes	33	488274	7618822	HG	HG21-12	Massive and high-grade graphite schist		12.36	
71964	2012	Kvern fjord-Haugnes	33	488356	7619263	HG	HG14-12	Massive and high-grade graphite schist		33.82	
71965	2012	Kvern fjord-Haugnes	33	488356	7619263	HG	HG15-12	Massive and high-grade graphite schist		14.71	
71966	2012	Kvern fjord-Haugnes	33	488356	7619263	HG	HG16-12	Massive and high-grade graphite schist		33.68	
71967	2012	Kvern fjord-Haugnes	33	488356	7619263	HG	HG17-12	Massive and high-grade graphite schist		33.71	
71955	2012	Jennestad	33	507225	7625670	HG	HG5-12	High grade graphite schist from the dump outside the showing		39.11	
71956	2012	Jennestad	33	507225	7625670	HG	HG6-12	High grade graphite schist from the dump outside the showing		36.70	
71990	2012	Jennestad	33	507580	7625322	JEW	JW12-6	Massive and high-grade graphite schist		36.68	
71991	2012	Jennestad	33	507580	7625322	JEW	JW12-7	Massive and high-grade graphite schist		28.62	

71957	2012	Jennestad	33	508574	7625822	HG	HG7-12	Graphite schist from the remains at Lille Hornvann	15.57	
71958	2012	Jennestad	33	508574	7625822	HG	HG8-12	Graphite schist from the remains at Lille Hornvann	9.01	
71953	2012	Jennestad	33	510079	7625023	HG	HG3-12	Weathered but coarse flake graphite schist	23.02	
71988	2012	Jennestad	33	510084	7625026	JEW	JW12-4	Weathered but coarse flake graphite schist	21.14	
71989	2012	Jennestad	33	510084	7625026	JEW	JW12-5	Weathered but coarse flake graphite schist	24.03	
71954	2012	Jennestad	33	510102	7625026	HG	HG4-12	Weathered but coarse flake graphite schist	18.89	
71952	2012	Jennestad	33	510785	7625331	HG	HG2-12	High grade graphite schist from bedrock exposure	24.41	
71987	2012	Jennestad	33	510785	7625343	JEW	JW12-3	High grade graphite schist from bedrock exposure	18.37	
71951	2012	Jennestad	33	510982	7625361	HG	HG1-12	Banded graphite schist from the mine entrance	9.33	
71985	2012	Jennestad	33	510982	7625362	JEW	JW12-1	Banded graphite schist from the mine entrance	7.40	
71986	2012	Jennestad	33	510982	7625362	JEW	JW12-2	Banded graphite schist from the mine entrance	5.69	
90448	2014	Møkland	33	486633	7628877	HG	HG46-14	Graphite schist	0.01	16.7
90449	2014	Møkland	33	486633	7628877	HG	HG47-14	Graphite schist	0.01	16.1
90450	2014	Møkland	33	486640	7628864	HG	HG48-14	Graphite schist	0.01	25.7
90451	2014	Møkland	33	486640	7628864	HG	HG49-14	Graphite schist	0.0546	21.1
90445	2014	Kvern fjord- Haugnes	33	488628	7622908	HG	HG43-14	Graphite schist	0.0248	0.122
90446	2014	Kvern fjord- Haugnes	33	488628	7622906	HG	HG44-14	Graphite schist	0.01	0.473
90447	2014	Kvern fjord- Haugnes	33	488628	7622906	HG	HG45-14	Graphite schist	0.01	13.7
90444	2014	Smynes	33	497537	7638596	HG	HG42-14	Graphite schist	0.03	0.56
90439	2014	Skogsøya	33	497813	7640671	HG	HG37-14	Graphite schist	0.51	6.46
90438	2014	Skogsøya	33	498139	7640440	HG	HG36-14	Graphite schist	1.76	26.4
90437	2014	Skogsøya	33	498225	7640414	HG	HG35-14	Graphite schist	0.01	16.7
90436	2014	Skogsøya	33	498267	7640357	HG	HG34-14	Graphite schist	0.01	34.2
90434	2014	Skogsøya	33	498270	7640336	HG	HG32b-14	Graphite schist	0.32	29.1
90435	2014	Skogsøya	33	498270	7640336	HG	HG33-14	Graphite schist	0.06	19

90440	2014	Skogsøya	33	498345	7639890	HG	HG38-14	Graphite schist	0.02	24.9	
90441	2014	Skogsøya	33	498345	7639890	HG	HG39-14	Graphite schist	0.02	21.8	
90442	2014	Smines	33	498966	7639397	HG	HG40-14	Graphite schist	0.86	13.8	
90443	2014	Smines	33	498977	7638646	HG	HG41-14	Graphite schist	0.15	3.92	
90433	2014	Brenna	33	501851	7629256	HG	HG32a-14	Graphite schist	0.01	3.89	
90432	2014	Brenna	33	502109	7628640	HG	HG31b-14	Graphite schist	4.07	9.9	
90457	2015	Møkland	33	486149	7627757	HG	hg2-15	Graphite schist, loose material from road fill løsmaterialet fra veifylling	0.52	1.13	
90458	2015	Møkland	33	486154	7627755	HG	hg3-15	Graphite schist, loose material from road fill	0.05	6.19	
90459	2015	Møkland	33	486163	7627753	HG	hg4-14	Graphite schist, loose material from road fill	0.03	4.48	
90472	2015	Møkland	33	486454	7628298	HG	hg17-15	Coarse, partly amorphous graphite from upper trench	0.14	18.1	
90474	2015	Møkland	33	486456	7628313	HG	hg19 -15	Host rock to graphite schist in upper trench	4.78	0.35	
90476	2015	Møkland	33	486456	7628315	HG	hg21-15	High grade and strongly weathered graphite rock	0.14	13.4	
90471	2015	Møkland	33	486457	7628305	HG	hg16-15	Very coarse flake graphite from upper trench.	0.05	14.7	
90469	2015	Møkland	33	486627	7628843	HG	hg14-15	Graphite schist upper trench	1.53	0.17	
90470	2015	Møkland	33	486627	7628843	HG	hg15-15	Graphite schist upper trench	3.07	0.03	
90484	2015	Møkland	33	486629	7628840	HG	hg29-15	Sample from blasted upper trench Møkland	1.58	0.03	
90486	2015	Møkland	33	486629	7628840	HG	hg31-15	Sample from blasted upper trench Møkland	1.7	0.09	
90461	2015	Møkland	33	486631	7628873	HG	hg6-15	Flake graphite og good quality Møkland	0.03	16.9	
90467	2015	Møkland	33	486631	7628839	HG	hg12-15	Graphite schist upper trench	0.08	0.12	
90478	2015	Kvern fjord-Haugnes	33	488623	7622905	HG	hg23-15	Graphite schist	0.01	10.6	
90463	2015	Smines	33	499004	7639342	HG	hg8-15	Graphite schist Smines	2.39	2.71	
90479	2015	Smines	33	499009	7639339	HG	hg24-15	Sample from blasted material Smines	1.03	12.8	

90480	2015	Smines	33	499009	7639339	HG	hg25-15	Sample from blasted material Smines	0.78	10.6	
90481	2015	Smines	33	499009	7639339	HG	hg26-15	Sample from blasted material Smines	3.05	4.38	
90465	2015	Jennestad	33	510277	7625132	HG	hg10-15	Sample from trench Koven	0.26	12.7	
90475	2015	Møkland	33	486453	7628307	HG	hg20-15	Very coarse flake graphite schist in upper trench	0.04	18.3	
90473	2015	Møkland	33	486454	7628314	HG	hg18-15	qz fsp host rock to graphite schist in upper trench	2.89	0.16	
90477	2015	Møkland	33	486463	7628307	HG	hg22-15	Amphibolitic dark rock type in footwall to graphite schist	0.08	0.03	
90485	2015	Møkland	33	486629	7628840	HG	hg30-15	Sample from blasted material in upper trench Møkland	2.93	0.03	
90468	2015	Møkland	33	486632	7628842	HG	hg13-15	Graphite schist upper trench	3.83	0.11	
90466	2015	Møkland	33	486633	7628873	HG	hg11-15	Rich graphite ore from outcrop	0.01	17.7	
90456	2015	Smines	33	498817	7639406	HG	hg1-15	Flake graphite Smines	1.54	17.3	
90462	2015	Smines	33	499008	7639342	HG	hg7-15	Graphite schist Smines	0.06	10.5	
90482	2015	Smines	33	499009	7639339	HG	hg27-15	Sample from blasted material Smines	3.1	1.46	
90483	2015	Smines	33	499009	7639339	HG	hg28-15	Sample from blasted material Smines	2.15	9.66	
90464	2015	Jennestad	33	510277	7625132	HG	hg9-15	Sample from trench Koven	0.73	13.3	
140104	2016	Møkland	33	486132	7627617	HG	hg4-16	Rotten weathered graphite schist	0.03	10.6	
140103	2016	Møkland	33	486134	7627619	HG	hg3-16	Rotten weathered graphite schist	0.13	16.6	
140127	2016	Møkland	33	486139	7627617	JK	JK-3	Weathered graphite schist	0.03	5.76	
140101	2016	Møkland	33	486140	7627616	HG	hg1-16	Rotten weathered graphite schist	0.04	22.3	
140129	2016	Møkland	33	486141	7627615	JK	JK-5	Weathered graphite schist	0.14	18.1	
140130	2016	Møkland	33	486141	7627615	JK	JK-5(B)	Weathered graphite schist (wall)	0.024	18.1	
140102	2016	Møkland	33	486142	7627618	HG	hg2-16	Rotten weathered graphite schist	0.15	12.4	
140128	2016	Møkland	33	486143	7627615	JK	Jk-4	Weathered graphite schist	0.06	7.97	
140126	2016	Møkland	33	486177	7627634	JK	JK-2	Amphibolite with graphite and sulphides	4.23	-0.06	
140131	2016	Møkland	33	486188	7627795	JK	JK-6	Weathered graphite schist	0.09	2.45	

140141	2016	Møkland	33	486188	7627795	JK	JK-6B	Weathered graphite schist	0.1	14.5	
140107	2016	Kvern fjord- Haugnes	33	486190	7627797	HG	hg7-16	Good quality graphite schist	0.09	11.7	
140125	2016	Møkland	33	486190	7627797	JK	JK-1	Weathered graphite schist	0.17	13.4	
140132	2016	Møkland	33	486190	7627797	JK	JK-7	Weathered graphite schist	0.92	0.47	
140106	2016	Møkland	33	486192	7627796	HG	hg6-16	Good quality graphite schist	0.10	2.16	
140105	2016	Møkland	33	486193	7627799	HG	hg5-16	Rotten weathered graphite schist	0.07	7.32	
140133	2016	Kvern fjord- Haugnes	33	488236	7618894	JK	JK8	Graphite schist	0.09	12.6	
140124	2016	Kvern fjord- Haugnes	33	488563	7620431	HG	hg24-16	Medium grade graphite schist	0.07	17.7	
140108	2016	Kvern fjord- Haugnes	33	488618	7622873	HG	hg8-16	Disseminated graphite schist	0.03	4.28	
97603	2016	Jørlandsvatnet	33	488625	7 622 904	HS	xxxxxxx	Graphite schist	- 0.02	14.2	14.1
82127	2016	Smnes	33	497526	7 638 615	BD	ØKS 1449A	Graphite schist	17.9	2.65	2.70
140114	2016	Skogsøya	33	497840	7640813	HG	hg14-16	Low grade graphite schist	0.08	6.91	
140113	2016	Skogsøya	33	497896	7640656	HG	hg13-16	Low grade graphite schist	2.58	0.40	
140140	2016	Skogsøya	33	498136	7640440	JK	JK-15	Graphite schist, old trench	0.14	29.2	
82185	2016	Skogsøya	33	498180	7640374	BD	ØKS 14128B	Graphite schist	0.54	4.44	4.43
82187	2016	Skogsøya	33	498263	7640351	BD	ØKS 14129A	Graphite schist	0.08	31.6	29.1
82188	2016	Skogsøya	33	498263	7640351	BD	ØKS 14129B	Graphite schist	0.06	34.9	31.2
82189	2016	Skogsøya	33	498263	7640351	BD	ØKS 14129C	Graphite schist	0.17	27.8	25.2
140139	2016	Skogsøya	33	498266	7640354	JK	JK-14	Well exposed graphite outcrop, 348/80E	0.05	24.5	
82120	2016	Smnes	33	498815	7639408	BD	ØKS 1435A	Graphite schist	2.32	3.44	3.32
82121	2016	Smnes	33	498815	7639408	BD	ØKS 1435B	Graphite schist	5.92	16.3	17.1
82075	2016	Smnes	33	498963	7639395	BD	ØKS 1323B-1	Graphite schist	3.05	15.5	

	2016	Smines	33	498963	7639395	BD	ØKS 1323B-2	Graphite schist	0.42	10.3	
092193	2016	Romsetfjord	33	500412	7634791	BD	BD Øks 1602a	Graphite schist	0.03	31.0	30.7
099390	2016	Romsetfjord	33	500454	7634597	BD	BD Øks 1609	Graphite schist	0.06	14.2	14.5
140118	2016	Romsetfjord	33	500587	7634047	HG	hg18-16	Weathered sulphide rich graphite schist	1.33	3.62	
140119	2016	Romsetfjord	33	500587	7634047	HG	hg19-16	Weathered sulphide rich graphite schist	1.62	5.44	
140120	2016	Romsetfjord	33	500620	7634013	HG	hg20-16	Weathered sulphide rich graphite schist	1.2	11.9	
140121	2016	Romsetfjord	33	500622	7634010	HG	hg21-16	Weathered sulphide rich graphite schist	4.03	25.6	
140122	2016	Romsetfjord	33	500625	7634004	HG	hg22-16	Weathered sulphide rich graphite schist	10.9	15.4	
140123	2016	Romsetfjord	33	500634	7633995	HG	hg23-16	Weathered sulphide rich graphite schist	0.16	12.5	
092191	2016	Romsetfjord	33	500639	7 633996	BD	BD Øks 1601a	Graphite schist	0.28	17.3	17.2
092192	2016	Romsetfjord	33	500639	7 633996	BD	BD Øks 1601b	Graphite schist	1.12	18.2	18.7
092198	2016	Romsetfjord	33	500730	7 634761	BD	BD Øks 1605	Graphite schist	0.39	3.92	3.98
092200	2016	Romsetfjord	33	500804	7 634942	BD	BD Øks 1607	Graphite schist	0.52	14.7	14.4
82142	2016	Brenna	33	502119	7 628636	BD	ØKS 1464A	Graphite schist	2.87	8.58	8.77
140109	2016	Raudhammaren	33	505696	7642187	HG	hg9-16	Graphite schists loose bolder	-0.02	25.9	
140110	2016	Raudhammaren	33	505696	7642187	HG	hg10-16	Graphite schists loose bolder	-0.02	17.1	
140111	2016	Raudhammaren	33	505770	7642183	HG	hg11-16	Graphite schists loose bolder	0.09	19.8	
140112	2016	Raudhammaren	33	505770	7642183	HG	hg12-16	Graphite schists loose bolder	0.04	11.7	
140138	2016	Raudhammaren	33	505771	7642181	JK	JK9	Graphite schists loose bolder	0.05	18.8	
140134	2016	Raudhammaren	33	505824	7642184	JK	JK10	Graphite schists loose bolder	0.05	7.77	
140135	2016	Raudhammaren	33	505850	7642189	JK	JK11	Graphite schists loose bolder	0.08	12.3	
140136	2016	Raudhammaren	33	505871	7642194	JK	JK12	Graphite schists loose bolder	0.03	24.1	

140137	2016	Raudhammaren	33	505937	7642166	JK	JK13	Graphite schists loose bolder	0.64	11.2	
140116	2016	Jennestad	33	510039	7624973	HG	hg16-16	Medium grade graphite schist	0.09	0.85	
140117	2016	Jennestad	33	510039	7624973	HG	hg17-16	Medium grade graphite schist	0.06	2.37	
140115	2016	Jennestad	33	510984	7628557	HG	hg15-16	Loose bolder weathered graphite schist	0.03	11.5	
106468	2016	Hinnøya	33	511084	7 594428	NC	RAF10646 8	Graphite schist	5.88	10.5	
92127	2016	Jennestad	33	512657	7 626511	BD	JEN 1454A	Graphite schist	2.22	3.53	
92134	2016	Jennestad	33	512765	7 626502	BD	JEN 1461A	Graphite schist	0.26	10.9	
92132	2016	Jennestad	33	512767	7626493	BD	JEN 1460A	Graphite schist	0.15	15.2	
92135	2016	Jennestad	33	512791	7626512	BD	JEN 1462	Graphite schist	0.46	7.21	
82200	2016	Andøya	33	542110	7670382	BD	AND 1452B	Graphite schist	- 0.02	2.26	1.62
092185	2016	Kveøya	33	543315	7631378	BD	BD Kvæ 1602a	Graphite schist	0.05	16.9	16.6
092186	2016	Kveøya	33	543315	7 631378	BD	BD Kvæ 1602b	Graphite schist	0.03	20.6	20.4
137166	2017	Morfjord	33	486962	7588922	HG	hg14-17	Graphite schist	0.34	33.3	
137167	2017	Morfjord	33	486969	7588919	HG	Hg15-17	Graphite schist	0.48	37.7	
137170	2017	Morfjord	33	486981	7588914	HG	Hg18-17	Graphite schist	0.01	11.3	
137169	2017	Morfjord	33	486985	7588930	HG	hg17-17	Graphite schist	0.08	22.00	
137165	2017	Morfjord	33	487012	7587147	HG	hg12-17	Graphite schist	0.99	9.72	
137171	2017	Morfjord	33	487017	7588984	HG	hg19-17	Graphite schist	0.03	12.9	
137168	2017	Morfjord	33	487019	7588991	HG	Hg16-17	Graphite schist	0.03	26.6	
137184	2017	Morfjord	33	487019	7588991	JK	jk2617-1	From cutting (jk1617-1gps)	0.03	24.7	
137183	2017	Morfjord	33	487246	7586598	JK	JK30517-5	Graphite, Morfjord mine	0.12	3.3	
137157	2017	Sommarland	33	487668	7626464	HG	H3-17	Graphite schist	0.01	17.2	
137158	2017	Sommarland	33	487668	7626464	HG	H4-17	Graphite schist	0.01	12.4	
137159	2017	Sommarland	33	487668	7626464	HG	H5-17	Graphite schist	0.01	16.1	
137178	2017	Sommarland	33	487698	7626374	JK	JK28517-4	Graphite bolder	0.03	16.4	
137177	2017	Sommarland	33	487708	7626409	JK	JK28517-3	Graphite schist-outcrop covered	0.07	11	

137176	2017	Sommarland	33	487712	7626405	JK	jk28517-2	Graphite Schist- outcrop covered	0.02	17.8	
137160	2017	Sommarland	33	487722	7626399	HG	Hg6-17	Graphite schist	0.36	18.2	
137175	2017	Sommarland	33	487724	7626393	JK	JK28517-1	Sommarland 2.-trench loose bolder	0.66	9.48	
137182	2017	Morfjord	33	487853	7589590	JK	JK30517-3	Graphite outcrop-contact zone	0.39	6.29	
137163	2017	Morfjord	33	487894	7589187	HG	Hg10-17	Graphite schist	0.96	7.87	
137161	2017	Morfjord	33	487897	7589189	HG	Hg8-17	Graphite schist	0.69	5.69	
137162	2017	Morfjord	33	487897	7589189	HG	Hg9-17	Graphite schist	0.32	5.83	
137164	2017	Morfjord	33	487898	7589194	HG	Hg11-17	Mafic rock for thin section	3.2	5.38	
137179	2017	Smines	33	497532	7638596	JK	JK29517-8	graphite schist	0.03	8.57	
137180	2017	Smines	33	497558	7638628	JK	JK29517-pf7	Mags10pf7/no grafitt	0.15	0.37	
137181	2017	Smines	33	499051	7638736	JK	JK29517-9	Graphite schist	0.33	13.2	
137174	2017	Brenna	33	502059	7628968	HG	hg22-17	Graphite schist	0.01	5.09	
137173	2017	Brenna	33	502135	7628872	HG	hg21-17	Graphite schist	0.06	10.7	
137172	2017	Brenna	33	502146	7628862	HG	hg20-17	Graphite schist	0.03	30.4	
137189	2017	Raudhammaren	33	505584	7641943	JK	JK3617-7	Graphite schist, Loose bolder	0.06	9.83	
137188	2017	Raudhammaren	33	505653	7641935	JK	JK3617-6	Graphite schist, Loose bolder	0.02	10.1	
137187	2017	Raudhammaren	33	505675	7641959	JK	JK3617-5	Graphite schist, Loose bolder	0.12	6.71	
137186	2017	Raudhammaren	33	505735	7641993	JK	JK3617-3	Graphite schist, Loose bolder	0.07	9.02	
137185	2017	Raudhammaren	33	505880	7642242	JK	JK3617-1	Graphite schist	0.12	23.1	
137190	2017	Jennestad	33	510988	7628559	JK	JK5617-4	Weathered supracrustal mafic gneiss with graphite schist	0.13	21.7	

## Appendix 6: Samples analysed for total carbon and total sulphur and petrophysics

Data is available in excel format on request. (i/a or blank cell = not analysed)

Note: Magnetic susceptibility on electric conductive samples (rich in graphite) is not reliable (marked in red).

NGUnr.	Sample ID	UT M Zone	UTMX	UTMY	Sample description	Density (g/cm <sup>3</sup> )	Porosity (%)	Susceptibility (10 <sup>-6</sup> SI)	Remanens (mA/M)	Heat conduct. k (W/mK)	Heat cap. c <sub>p</sub> (J/kgK)	Total Carbon (% TC)	Total Sulphur (% TS)
71972	HG22-12	33	487144	7586575	Graphite Schist from Morfjord indre	3.00		417	0			16.80	
71973	HG23-12	33	487144	7586575	Graphite Schist from Morfjord indre	2.90		423	17			19.70	
137183	JK30517-5	33	487246	7586598	Graphite schist	2.51	0.06	453	24	3.06	841	3.30	0.12
137165	HG12-17	33	487012	7587147	Graphite Schist	2.39	0.06	1	9	4.17	942	20.20	0.99
71992	JW12-8	33	486956	7587163	Graphite Schist from Morfjord øst	2.68		343	17			18.86	
137170	Hg18-17	33	486981	7588914	Graphite Schist	2.43	0.04	-103	7	10.54	1100	24.20	0.01
137167	Hg15-17	33	486969	7588919	Graphite Schist	2.22	0.06	30	7	11.57	1214	22.20	0.48
137166	HG14-17	33	486962	7588922	Graphite Schist	2.31	0.06	69	6	27.42	1114	21.20	0.34
137171	HG19-17	33	487017	7588984	Graphite Schist	2.53	0.03	-114	3	4.86	916	25.20	0.03
137168	HG16-17	33	487019	7588991	Graphite Schist	2.38	0.05	-211	6	12.6	1140	23.20	0.03
137182	JK30517-3	33	487853	7589590	Graphite schist/contact zone with gneiss	2.44	0.08	511	25	3.37	882	6.29	0.39
71971	HG21-12	33	488274	7618822	Graphite Schist from Haugsnes 3	2.43		-62	10			12.36	
71968	HG18-12	33	488238	7618895	Graphite Schist from Haugsnes 2	2.46		-49	0			14.21	
71969	HG19-12	33	488238	7618895	Graphite Schist from Haugsnet 2	2.40		36	0			15.17	
71970	HG20-12	33	488238	7618895	Graphite Schist from Haugsnes 2	2.41		-42	7			13.73	
71964	HG14-12	33	488356	7619263	Graphite Schist from Haugsnes 1	2.37		-112	0			33.82	
71965	HG15-12	33	488356	7619263	Graphite Schist from Haugsnes 1	2.53		32	10			14.71	
71966	HG16-12	33	488356	7619263	Graphite Schist from Haugsnes 1	2.34		-144	23			33.68	
71967	HG17-12	33	488356	7619263	Graphite Schist from Haugsnes 1	2.26		-89	20			33.71	

140124	HG24-16	33	488563	7620431	Graphite Schist	2.43	0.07	233	7	7.66	1050	37.20	0.07
97603		33	488625	7622904	Graphite schist	2.81		815				14.20	-
90478	HG23-15	33	488623	7622905	Graphite schist	2.71	0.07	899	6	i/a	i/a	10.60	0.01
71959	HG9-12	33	487621	7626290	Graphite Schist from Sommarland	2.48		121	8			9.26	
71960	HG10-12	33	487621	7626290	Graphite Schist from Sommarland	2.30		0	0			17.13	
71961	HG11-12	33	487589	7626310	Graphite Schist from Sommarland	2.67		564	502			4.05	
71962	HG12-12	33	487589	7626310	Graphite Schist from Sommarland	2.65		770	615			2.83	
71963	HG13-12	33	487589	7626310	Graphite Schist from Sommarland	2.52		347	0			5.44	
137160	HG6-17	33	487722	7626399	Graphite Schist	2.41	0.04	-134	9	5.57	995	19.20	0.36
140116	HG16-16	33	510039	7624973	Graphite Schist	2.36	0.09	1181	5	i/a	i/a	0.85	0.09
140117	HG17-16	33	510039	7624973	Graphite Schist	2.62	0.03	481	11	2.69	787	35.20	0.06
137157	H3-17	33	487668	7626464	Graphite Schist	2.4	0.04	-64	19	8.11	1074	17.20	0.01
137159	H5-17	33	487668	7626464	Graphite Schist	2.44	0.04	-127	22	6.66	1019	18.20	0.01
71953	HG3-12	33	510079	7625023	Graphite Schist from Koven	2.37		0	28			23.02	
71988	JW12-4	33	510084	7625026	Graphite Schist from Koven	2.34		21	0			21.14	
71989	JW12-5	33	510084	7625026	Graphite Schist from Koven	2.41		-44	7			24.03	
71954	HG4-12	33	510102	7625026	Graphite Schist from Koven	2.45		16	5			18.89	
90465	HG10-15	33	510277	7625132	Sample from trench Koven	2.81	0.05	645	4	i/a	i/a	12.70	0.26
71990	JW12-6	33	507580	7625322	Graphite Schist from Hornvann østre cutting	2.36		-163	12			36.68	
71991	JW12-7	33	507580	7625322	Graphite Schist from Hornvann østre cutting	2.47		0	31			28.62	
71952	HG2-12	33	510785	7625331	Graphite Schist from Øvre Golia Røsk	2.42		0	0			24.41	
71987	JW12-3	33	510785	7625343	Graphite Schist from Øvre Golia Røsk	2.39		-29	13			18.37	
71951	HG1-12	33	510982	7625361	Graphite Schist from Godlia gruve	2.63		351	0			9.33	
71985	JW12-1	33	510982	7625362	Graphite Schist from Godlia gruve	2.63		291	6			7.40	
71986	JW12-2	33	510982	7625362	Graphite Schist from Godlia gruve	2.53		147	22			5.69	
71955	HG5-12	33	507225	7625670	Graphite Schist from Græva	2.39		-346	0			39.11	

71956	HG6-12	33	507225	7625670	Graphite Schist from Græva	2.41		-239	0			36.70	
71957	HG7-12	33	508574	7625822	Graphite Schist from Lille Hornvann	2.49		105	5			15.57	
71958	HG8-12	33	508574	7625822	Graphite Schist from Lille Hornvann	2.85		281	5			9.01	
140130	JK5 (B)	33	486141	7627615	Graphite Schist	2.35	0.1	61	13	7.41	1079	38.20	0.02
140101	HG1-16	33	486140	7627616	Graphite Schist	1.92	0.12	748	35	i/a	i/a	29.20	0.04
140102	HG2-16	33	486142	7627618	Graphite Schist	2.28	0.1	345	3	4.67	1012	30.20	0.15
90459	HG4-14	33	486163	7627753	Graphite Schist from road fill	2.45	0.07	406	4	i/a	i/a	4.48	0.03
90458	HG3-15	33	486154	7627755	Graphite Schist from road fill	2.39	0.07	449	3	i/a	i/a	6.19	0.05
90457	HG2-15	33	486149	7627757	Graphite Schist from road fill	2.74	0.04	811	21	i/a	i/a	1.13	0.52
140107	HG7-16	33	486190	7627797	Graphite Schist	2.47	0.05	923	19	i/a	i/a	11.70	0.09
140105	HG5-16	33	486193	7627799	Graphite Schist	2.22	0.08	-68	12	2.89	942	31.20	0.07
92132	JEN 1460A	33	512767	7626493	Graphite Schist	2.48		152				15.20	0.15
92134	JEN 1461A	33	512765	7626502	Graphite Schist	2.50		141				10.90	0.26
90472	HG17-15	33	486454	7628298	Coarse, partially amorphous graphite from upper trench	2.35	0.1	466	22	i/a	i/a	18.10	0.14
90471	HG16-15	33	486457	7628305	Very coarse flake graphite from upper trench	2.38	0.09	454	7	i/a	i/a	14.70	0.05
90474	HG19 -15	33	486456	7628313	Host rock to Graphite Schist upper trench	2.75	<0.01	552	6	i/a	i/a	0.35	4.78
90476	HG21-15	33	486456	7628315	High grade and strongly weathered graphite rock	2.24	0.12	539	19	i/a	i/a	13.40	0.14
90467	HG12-15	33	486631	7628839	Graphite Schist upper trench	2.51	0.05	521	21	i/a	i/a	0.12	0.08
90469	HG14-15	33	486627	7628843	Graphite Schist upper trench	2.42	0.08	2507	955	i/a	i/a	0.17	1.53
90470	HG15-15	33	486627	7628843	Graphite Schist upper trench	2.75	0.02	4183	1236	i/a	i/a	0.03	3.07
90461	HG6-15	33	486631	7628873	Flake graphite good quality Møkland	2.36	0.07	373	4	i/a	i/a	16.90	0.03
82142	ØKS 1464A	33	502119	7628636	Graphite Schist	2.69		199				8.58	2.87
137172	HG20-17	33	502146	7628862	Graphite Schist	2.42	0.09	87	6	4.58	948	26.20	0.03
137173	HG21-17	33	502135	7628872	Graphite Schist	2.33	0.07	199	10	i/a	i/a	27.20	0.06
137174	HG22-17	33	502059	7628968	Graphite Schist	2.71	0.05	405	6	3.94	821	28.20	0.01

137190	JK5617-4	33	510988	7628559	Graphite schist	2.23	0.1	631	12	8.46	1163	21.70	0.13
140123	HG23-16	33	500634	7633995	Graphite Schist	2.21	0.09	-90	5	10.05	1202	36.20	0.16
92191	BD Øks 1601a	33	500639	7633996	Graphite Schist	2.33		334				17.30	0.28
92192	BD Øks 1601b	33	500639	7633996	Graphite Schist	2.43		353				18.20	1.12
140122	HG22-16	33	500625	7634004	Graphite Schist	2.9	0.01	952	129	i/a	i/a	15.40	10.90
140120	HG20-16	33	500620	7634013	Graphite Schist	2.62	0.03	1013	10	i/a	i/a	11.90	1.20
140118	HG18-16	33	500587	7634047	Graphite Schist	2.19	0.16	1208	4	i/a	i/a	3.62	1.33
99390	BD Øks 1609	33	500454	7634596	Graphite Schist	2.25		294				14.20	0.06
92198	BD Øks 1605	33	500729	7634760	Graphite Schist	2.63		550				3.92	0.39
92193	BD Øks 1602a	33	500412	7634791	Graphite Schist	2.29		312				31.00	0.03
92200	BD Øks 1607	33	500803	7634941	Graphite Schist	2.56		351				14.70	0.52
137179	JK29517-8	33	497532	7638596	Graphite Schist	2.51	0.02	345		8.93	1042	8.57	0.03
82127	ØKS 1449A	33	497526	7638615	Graphite	2.92		2 292				2.65	17.90
137180	JK29517- pf7	33	497558	7638628	Biotite gneiss	2.8	0.05	1003	23	2.6	733	0.37	0.15
137181	JK29517-9	33	499051	7638736	Graphite schist	2.34	0.07	853	23	5.17	1008	13.20	0.33
90479	HG24-15	33	499009	7639339	Sample from blasted material Smines	2.35	0.05	326	7	i/a	i/a	12.80	1.03
90480	HG25-15	33	499009	7639339	Sample from blasted material Smines	2.61	0.05	581	5	i/a	i/a	10.60	0.78
90481	HG26-15	33	499009	7639339	Sample from blasted material Smines	2.12	0.12	369	4	i/a	i/a	4.38	3.05
82075	ØKS 1323B-1	33	498963	7639395	Graphite schist	2.59		264	15			15.50	3.05
82120	ØKS 1435A	33	498815	7639408	Graphite	3.00		653				3.44	2.32
82121	ØKS 1435B	33	498815	7639408	Graphite	2.80		2 001				16.30	5.92
82189	ØKS 14129C	33	498263	7640351	Graphite	2.37		15				27.80	0.17
140113	HG13-16	33	497896	7640656	Graphite Schist	2.66	<0.01	963	19	i/a	i/a	0.40	2.58

140114	HG14-16	33	497840	7640813	Graphite Schist	2.38	0.08	968	5	i/a	i/a	6.91	0.08
137189	JK3617-7	33	505584	7641943	Graphite schist loose boulder	2.48	0.05	499	9	2.76	836	9.83	0.06
140109	HG9-16	33	505696	7642187	Graphite Schist	2.34	0.06	-55	5	8.59	1111	32.20	-0.02
140110	HG10-16	33	505696	7642187	Graphite Schist	2.3	0.07	-10	7	7.65	1109	33.20	-0.02
140111	HG11-16	33	505770	7642183	Graphite Schist	2.18	0.11	-87	5	6.11	1115	34.20	0.08
140112	HG12-16	33	505770	7642183	Graphite Schist	2.17	0.12	845	3	i/a	i/a	11.70	0.04
137185	JK3617-1	33	505880	7642242	Graphite schist	2.82	0.02	2101	462	2.8	737	23.10	0.12
82282	AND 14113	33	539533	7667765	Sulphide rich black schist	2.75		660				4.87	5.03
82200	AND 1452B	33	542110	7670382	Graphite bearing sediment	2.64		16				2.26	-0.02
82255	AND 1461	33	541920	7670414	Black schist	2.67		224				2.70	0.22
137116	HG40-16	33	609633	7702117	Graphite Schist	2.21	0.11	1019	8			5.51	0.26
137112	HG36-16	33	609368	7702499	Graphite Schist	2.3	0.11	1292	6			3.50	0.74
137117	HG41-16	33	609581	7702693	Graphite Schist	2.44	0.05	1230	24			6.69	0.12
137118	HG42-16	33	609553	7702741	Graphite Schist	2.29	0.1	1162	12			5.76	0.08
137113	HG37-16	33	609245	7702815	Graphite Schist	2.35	0.08	1141	7			7.92	0.10
137114	HG38-16	33	609243	7702817	Graphite Schist	2.32	0.08	993	9			11.64	0.85
137127	HG51-16	33	609089	7702916	Graphite Schist	2.39	0.07	1010	14			1.94	0.55
137126	HG50-16	33	609078	7702923	Graphite Schist	2.3	0.09	1076	14			5.73	0.16
137144	HG68-16	33	617637	7702330	Graphite Schist	2.74	0.02	10199	1367			4.94	5.00
137145	HG69-16	33	617697	7702362	Graphite Schist	2.39	0.07	839	13			8.46	0.85
137138	HG62-16	33	608096	7704677	Graphite Schist	2.12	0.12	1035	4			6.50	0.22
137139	HG63-16	33	608092	7704682	Graphite Schist	2.18	0.12	973	7			6.56	0.34
137137	HG61-16	33	608085	7704848	Graphite Schist	2.22	0.1	1150	3			5.34	0.42
137136	HG60-16	33	608063	7704863	Graphite Schist	2.25	0.1	903	13			9.48	0.12
137105	HG29-16	33	607940	7704925	Graphite Schist	2.34	0.1	1138	2			9.11	0.58
137142	HG66-16	33	607208	7705023	Graphite Schist	2.35	0.08	1131	5			5.43	0.38
137141	HG65-16	33	607228	7705022	Graphite Schist	2.36	0.08	933	3			4.56	0.09

137120	HG44-16	33	607410	7705025	Graphite Schist	2.41	0.08	1146	16			7.08	0.36
137106	HG30-16	33	608092	7704991	Graphite Schist	2.27	0.1	911	10			10.38	0.30
137135	HG59-16	33	608095	7704991	Graphite Schist	2.15	0.14	1095	6			9.48	0.48
137124	HG48-16	33	607620	7705036	Graphite Schist	2.26	0.11	950	4			5.76	0.30
137104	HG28-16	33	607618	7705037	Graphite Schist	2.31	0.08	1103	5			5.57	0.47
137122	HG46-16	33	607421	7705060	Graphite Schist	2.29	0.08	950	8			40.30	0.06
137119	HG43-16	33	607397	7705070	Graphite Schist	2.39	0.07	963	10			7.07	0.26
137123	HG47-16	33	607569	7705058	Graphite Schist	2.44	0.06	1002	21			6.12	0.14
137129	HG53-16	33	607423	7705078	Graphite Schist	2.45	0.06	1156	8			9.54	0.66
137108	HG32-16	33	607993	7705036	Graphite Schist	2.36	0.12	1308	6			8.36	0.12
137134	HG58-16	33	607972	7705045	Graphite Schist	2.43	0.1	944	7			31.35	0.02
137107	HG31-16	33	607993	7705045	Graphite Schist	2.42	0.11	740	25			6.77	0.03
137110	HG34-16	33	608002	7705049	Graphite Schist	2.22	0.1	862	6			12.60	0.21
137143	HG67-16	33	607364	7705122	Graphite Schist	2.42	0.06	955	7			3.99	0.20
137133	HG57-16	33	607911	7705081	Graphite Schist	2.36	0.09	1254	13			10.98	0.17
137132	HG56-16	33	607903	7705096	Graphite Schist	2.28	0.1	1049	95			9.98	0.13
137103	HG27-16	33	607857	7705123	Graphite Schist	2.29	0.11	1002	8			6.86	0.38
137102	HG26-16	33	607861	7705123	Graphite Schist	2.4	0.06	1027	6			4.77	0.41
137140	HG64-16	33	607583	7705249	Graphite Schist	2.43	0.08	1126	6			1.12	0.18
137131	HG55-16	33	607823	7705245	Graphite Schist	2.5	0.08	1458	6			6.53	0.03
137130	HG54-16	33	607727	7705409	Graphite Schist	2.31	0.08	1058	7			5.48	0.34

## Appendix 7: Petrophysics of drill core samples

Sample id show drill core number and core depth.

Note: Magnetic susceptibility on electric conductive samples (rich in graphite) is not reliable (marked in red).

NGU_NO	Sample ID	UTM Zone	UTM East	UTM North	Volume (cm <sup>3</sup> )	Density (g/cm <sup>3</sup> )	Pore volume (cm <sup>3</sup> )	Porosity (%)	Susceptibility (10 <sup>-6</sup> SI)	Remanens (mA/M)	Heath conductivity, k (W/mK)	Specific heath capacity (J/kgK)
189266	Som1701-6.6	33	487581	7626300	57.72	2.64	0.26	<0.01	3607	61846	3.51	822
189267	Som1701-12.2	33	487581	7626300	36.68	3.32	0.27	<0.01	24827	461715	3.33	647
189268	Som1701-18.2	33	487581	7626300	54.66	2.98	0.57	0.01	22347	159473	2.64	690
189269	Som1701-19.7	33	487581	7626300	50.22	3.19	0.77	0.02	15690	112052	3.45	678
189270	Som1701-23.4	33	487581	7626300	36.4	3.01	0.06	<0.01	8925	4702	2.9	695
189271	Som1701-28.7	33	487581	7626300	40.36	3.00	2.05	0.05	14423	4561	i/a	i/a
189272	Som1701-29.15	33	487581	7626300	50.98	3.03	1.14	0.02	1057	258	8.82	862
189273	Som1701-30.6	33	487581	7626300	43.73	2.87	0.8	0.02	31795	9183	12.31	943
189274	Som1701-33.7	33	487581	7626300	39.86	2.61	0.91	0.02	8861	9650	3.4	826
189275	Som1701-34.4	33	487581	7626300	41.85	2.64	0.65	0.02	8824	1811	2.69	776
189276	Som1701-45	33	487581	7626300	54.29	2.72	1.93	0.04	631	9	10.83	978
189277	Som1702-4.4	33	487682	7626456	57.34	3.00	0.3	<0.01	21191	194735	2.55	682
189278	Som1702-9.7	33	487682	7626456	58.73	2.83	0.2	<0.01	3387	10906	2.24	709
189279	Som1702-11.1	33	487682	7626456	41.51	3.04	0.36	<0.01	15237	127994	4.66	755
189280	Som1702-15.2	33	487682	7626456	35.57	2.77	0.88	0.02	4277	18368	7.79	915
189282	Som1702-27	33	487682	7626456	46.31	2.63	0.41	<0.01	3189	45	2.71	786
189283	Som1702-32	33	487682	7626456	58.91	2.53	2.7	0.05	606	14	2.21	792
189285	Haug1701-5.8	33	488288	7618844	31.65	3.46	0.27	<0.01	73938	290827	6.08	706
189286	Haug1701-6.5	33	488288	7618844	33.89	3.45	0.22	<0.01	66601	1122286	6.82	718
189287	Haug1701-7.7	33	488288	7618844	52.72	2.92	0.24	<0.01	6401	25346	2.32	688
189288	Haug1701-10.3	33	488288	7618844	31.88	2.80	0.24	<0.01	1409	283	2.3	719
189289	Haug1701-16.1	33	488288	7618844	49.02	2.78	0.82	0.02	1674	254	2.44	731

189290	Haug1701-19.1	33	488288	7618844	42.75	2.90	1.11	0.03	4944	13593	2.77	715
189291	Haug1701-23	33	488288	7618844	46.23	2.64	0.19	<0.01	2766	17510	2.3	763
189292	Haug1701-24.2	33	488288	7618844	37.45	2.99	0.18	<0.01	16311	5902	2.44	679
189293	Haug1701-25.5	33	488288	7618844	49.86	3.34	0.32	<0.01	69953	255697	3.98	666
189294	Haug1701-28.1	33	488288	7618844	56.35	2.92	0.52	<0.01	1628	616	2.66	705
189295	Haug1702-5.5	33	488293	7618843	55.27	2.49	3.27	0.06	1872	223	3.92	892
189296	Haug1702-7.2	33	488293	7618843	27.48	2.54	0.65	0.02	962	42	4.98	921
189297	Haug1702-13.6	33	488293	7618843	38.32	2.62	1.3	0.03	3679	2106	3.03	805
189298	Haug1702-16.7	33	488293	7618843	34.08	2.48	2.64	0.08	936	63	i/a	i/a
189299	Haug1702-30.5	33	488293	7618843	97.75	2.97	0.33	<0.01	13859	1155	2.54	689
189300	Haug1702-34.5	33	488293	7618843	48.34	3.15	0.17	<0.01	251581	11516	2.79	659
189301	Haug1702-37.5	33	488293	7618843	41.2	3.12	0.33	<0.01	177095	10827	2.85	668
189302	Haug1702-38.1	33	488293	7618843	29.83	2.97	0.27	<0.01	5421	808	2.77	698



GEOLOGICAL  
SURVEY OF  
NORWAY

· NGU ·

Geological Survey of Norway  
PO Box 6315, Sluppen  
N-7491 Trondheim, Norway

Visitor address  
Leiv Eirikssons vei 39  
7040 Trondheim

Tel (+ 47) 73 90 40 00  
E-mail [ngu@ngu.no](mailto:ngu@ngu.no)  
Web [www.ngu.no/en-gb/](http://www.ngu.no/en-gb/)